

OPTICAL AND REDOX STUDIES ON MODIFIED
TRANSITION METAL BIPYRIDYL COMPLEXES

ALAN J. MACKENZIE

Ph.D. Thesis

University of Edinburgh

1987



To my parents

Acknowledgements

I am greatly indebted to Dr. G.A. Heath for his constant help and enthusiasm throughout this study.

I am also particularly grateful to Dr. L.J. Yellowlees for her invaluable assistance during this project.

I also thank Drs. D. Reed, I.H. Sadler and R.W. Cockman for collecting n.m.r. data reported in chapters 3 and 4 and Miss L. Baxter, Miss F. Kelly and Miss L. Wallace who were involved in the initial preparation and study of many of the complexes examined.

I am also grateful to Napier College and Aberdeen University and Dr. A. Forth of the Department of Electrical Engineering at the University of Edinburgh for access to their spectrophotometer facilities.

I also thank the Science and Engineering Research Council for financial assistance and the University of Edinburgh for the use of their facilities.

I thank my parents and friends for their support throughout my studies and in particular during the preparation of this manuscript.

Finally I thank Mrs. C. Ranken who typed the manuscript.

Abstract

This thesis is devoted to a study of a range of transition metal bipyridyl complexes which have been much discussed as possible pigments in solar energy conversion systems. We have primarily been concerned with investigations into the electronic structure of each system through detailed examination of the electrochemical behaviour and absorption spectrum of each complex. We have collected the absorption spectrum of the electrogenerated reduced and oxidised analogues of each complex using in situ techniques as described in chapter 2.

The relationship between the electrochemical behaviour and the absorption spectrum exhibited by a given complex is also discussed as we illustrate how we may predict the energies of anticipated optical transitions using the electrochemical data collected.

Previous studies have shown that the electrochemically reduced analogues of $[\text{Ru}(\text{bipy})_3]^{2+}$ and $[\text{Ir}(\text{bipy})_3]^{3+}$ are best understood in terms of a ligand localised model i.e. the resting oxidation state complex should be formulated as $[\text{M}(\text{Z})(\text{bipy}^{\text{O}})_3]^{z+}$ and the one-electron reduced product as $[\text{M}(\text{Z})(\text{bipy}^{\text{O}})_2(\text{bipy}^-)]^{(z-1)+}$. Contrastingly we have examined the complex $[\text{Cr}(\text{bipy})_3]^{3+}$ and shown this system undergoes three metal-based reductions followed by three ligand-based reductions.

We also investigate a range of modified transition metal bipyridyl systems and report further evidence for ligand-localised reduction. A series of electrode-catalysed substitution reactions involving these complexes are also described.

CONTENTS

	<u>Page</u>
Dedication	i
Declaration	ii
Acknowledgements	iii
Abstract	iv
Contents	v
List of Tables	viii
List of Figures and Schemes	xiii

Chapter 1

INTRODUCTORY REMARKS: Transition metal bipyridyl complexes as solar energy dyes; correlation of optical and electrochemical data in such bipyridyl systems; electrochemical reduction in $[M(bipy)_3]^{n+}$ systems in terms of a localised model	1
References	30

Chapter 2

Electrochemical and absorption spectral studies of cis-bis-2,2'-bipyridyl carbonyl complexes of Ruthenium(II)	37
cis-Carbonylchlorobis(bipyridyl) ruthenium(II)	47
cis-Acetonitrilecarbonylbis(bipyridyl) ruthenium(II)	64
cis-Carbonylpyridinebis(bipyridyl) ruthenium(II)	73

	<u>Page</u>
cis-Bis(carbonyl)bis(bipyridyl)ruthenium(II)	82
cis-Carbonylhydridobis(bipyridyl)ruthenium(II)	85
Experimental	92
References	94

Chapter 3

Further spectroelectrochemical studies on reduction of contrasting iridium(III) and chromium(III) bipyridyl complexes	97
Experimental	129
References	130

Chapter 4

C-Metallated analogues to 2,2'-bipyridyl complexes. N.m.r. and spectroelectrochemical studies of (2,2'-bipyridyl-C ³ ,N ¹)bis(2,2'- bipyridine-N,N')iridium(III) hydrate and [Ru(bipy) ₂ (phpy)] ⁺	132
Experimental	169
References	170

Chapter 5

Spectroelectrochemical characterisation of the complexes $[\text{Ru}(\text{bipy})_n(\text{biq})_{3-n}]^{2+}$ ($n = 0, 1, 2, 3$). Examination of the apparent anomalous metal-to-ligand charge-transfer behaviour	172
Experimental	208
References	209

Appendix 1

Near infra-red ($3\,500 - 7\,000\text{ cm}^{-1}$) studies on reduced transition metal bipyridyl complexes	211
Experimental	219
References	220

Appendix 2

List of Abbreviations used	222
List of Courses attended	224

List of TablesPageChapter 1

1.	Pertinent Electrochemical Data for $[\text{Ru}(\text{bipy})_3]^{2+/3+}$ and $[\text{Ru}(\text{bipy})_2\text{Cl}_2]^{0/+}$	8
2.	Predicted transitions for $[\text{Ru}(\text{bipy})_3]^{2+/3+}$ and $[\text{Ru}(\text{bipy})_2\text{Cl}_2]^{0/+}$	11
3.	Assignment of the absorption bands in $[\text{Ru}(\text{bipy})_3]^{2+/3+}$ and $[\text{Ru}(\text{bipy})_2\text{Cl}_2]^{0/+}$	14
4.	Formulation of $[\text{Ru}(\text{bipy})_3]^{2+/+/0/-}$	17
5.	Formulation of $[\text{Ir}(\text{bipy})_3]^{3+/2+/+/0}$	21

Chapter 2

1.	Electrochemical results for ruthenium- bipyridyl systems	41
2.	Correlation of electrochemical and spectro- scopic data for ruthenium-bipyridyl complexes	45
3.	Assignment of the absorption bands in $[\text{Ru}(\text{bipy})_3]^{3+}$ and $[\text{Ru}(\text{bipy})_2\text{Cl}_2]^+$	51
4.	Assignment of the absorption bands in $[\text{Ru}(\text{bipy})_2\text{CO.Cl}]^{+/2+}$	53
5.	Assignment of the absorption bands in $[\text{Ru}(\text{bipy})_2\text{CO.Cl}]^{+/0/-}$	58
6.	Formulation of reduced complexes of $[\text{Ru}(\text{bipy})_2\text{CO.Cl}]^+$	59

	<u>Page</u>
7. Absorption bands in $[\text{Ru}(\text{bipy})_2\text{CO.MeCN}]^{2+}$ and $[\text{Ru}(\text{bipy})_2(\text{MeCN})_2]^{2+/3+}$	67
8. Assignment of the absorption bands in $[\text{Ru}(\text{bipy})_2\text{CO.MeCN}]^{2+/+}$	68
9. Absorption bands in $[\text{Ru}(\text{bipy})_2\text{CO.py}]^{2+}$	74
10. Assignment of absorption bands in $[\text{Ru}(\text{bipy})_2\text{py.MeCN}]^{2+/3+}$	78
11. Absorption bands in $[\text{Ru}(\text{bipy})_2\text{CO.py}]^{+/0}$	81
12. Formulation of the reduced complexes of $[\text{Ru}(\text{bipy})_2\text{CO.py}]^{2+}$	79
13. Absorption bands in $[\text{Ru}(\text{bipy})_2(\text{CO})_2]^{2+}$	83
14. Formulation of the reduced complex $[\text{Ru}(\text{bipy})_2(\text{CO})_2]^+$	85
15. Assignment of the absorption bands in $[\text{Ru}(\text{bipy})_2\text{CO.H}]^+$	86

Chapter 3

1. Assignment of the absorption bands in $[\text{Ir}(\text{bipy})_2\text{Cl}_2]^{+/0/-}$	105
2. Reduction potentials for a series of iridium Complexes	107
3. ^{19}F n.m.r. data for $[\text{Ir}(\text{bipy})_2(\text{CF}_3\text{SO}_3)_2]$ (CF_3SO_3)	108
4. Assignment of the absorption bands in $[\text{Ir}(\text{bipy})_2(\text{CF}_3\text{SO}_3)_2]^{+/0/-}$	111

5.	Assignment of the absorption bands in $[\text{Ir}(\text{bipy})_3]^{3+/2+/+/0}$	114
6.	Electrode potentials for $[\text{Cr}(\text{bipy})_3]^{3+/2+/+/0}$	117
7.	Assignment of the absorption bands in $[\text{Cr}(\text{bipy})_3]^{3+/2+/+/0}$	125
8.	Absorption bands in $[\text{Cr}(\text{bipy})_3]^-$	127

Chapter 4

1.	Assignment of absorption bands in $[\text{Ir}(\text{bipy})_2\text{OH}(\text{bipy}')]^{2+/+/0}$	139
2.	^1H n.m.r. assignments for C-metallated ring	145
3.	Coupling constants between protons in the C-metallated ring	146
4.	Voltammetric data for $[\text{Ru}(\text{bipy})_2(\text{phpy})]^+$ and some related complexes	153
5.	Voltammetric data for phenylpyridine and bipyridine	154
6.	Correlation of electrochemical and spectro- scopic data for $[\text{Ru}(\text{bipy})_2(\text{phpy})]^+$	160
7.	Absorption bands observed for $[\text{Ru}(\text{bipy})_2(\text{phpy})]^{+/2+}$	164
8.	Absorption bands for $[\text{Ru}(\text{bipy})_2(\text{phpy})]^{0/-}$	168

Chapter 5

1.	Absorption bands in ruthenium bipy/py and ruthenium bipy/biq complexes	178
2.	Electrochemical data for the series $[\text{Ru}(\text{bipy})_n(\text{biq})_{3-n}]^{2+}$ ($n = 0$ to 3)	179
3.	Modelling of the lowest energy MLCT transition using electrochemical data for the complexes $[\text{Ru}(\text{bipy})_n(\text{biq})_{3-n}]^{2+}$ ($n = 0$ to 3)	182
4.	Electrochemical separation between the $[\text{Ru}(\text{II/III})]$ and the final $\text{bipy}^{0/-}$ couple in the series $[\text{Ru}(\text{bipy})_n(\text{biq})_{3-n}]^{2+}$ ($n = 0$ to 3)	182
5.	Electrochemical behaviour of bipyridine and biquinoline	183
6.	Absorption bands in $[\text{Ru}(\text{bipy})_2(\text{biq})]^{2+/3+}$	188
7.	Assignment of the absorption bands in $[\text{Ru}(\text{bipy})_2(\text{biq})]^{2+}$	189
8.	Assignment of the absorption bands in $[\text{Ru}(\text{bipy})_2(\text{biq})]^{3+}$	189
9.	Assignment of the absorption bands in $[\text{Ru}(\text{bipy})_2(\text{biq})]^+$	193
10.	Assignment of the absorption bands in $[\text{Ru}(\text{bipy})(\text{biq})_2]^{2+/3+}$	197
11.	Assignment of the absorption bands in $[\text{Ru}(\text{bipy})(\text{biq})_2]^{+/0}$	202

Appendix 1

- | | | |
|----|--|-----|
| 1. | Near infra-red absorption bands in reduced | 215 |
| | transition-metal bipyridyl systems | |

List of FiguresPageChapter 1

1.	Conversion of light into chemical energy by $[\text{Ru}(\text{bipy})_3]^{2+}$	2
2.	Splitting of water by $[\text{Ru}(\text{bipy})_3]^{2+}$	3
3.	Absorption spectra of $[\text{Ru}(\text{bipy})_3]^{2+/3+}$ in dichloromethane	12
4.	Absorption spectra of $[\text{Ru}(\text{bipy})_2\text{Cl}_2]^{0/+}$ in dichloromethane	13
5.	Schematic energy level scheme for $[\text{Ru}(\text{bipy})_3]^{2+/3+}$ and $[\text{Ru}(\text{bipy})_2\text{Cl}_2]^{0/+}$	15
6.	Absorption spectra of $[\text{Ru}(\text{bipy})_3]^{2+/+/0/-}$ in dimethylsulphoxide	19
7.	Absorption spectra of $[\text{Ir}(\text{bipy})_3]^{3+/2+/+/0}$ in acetonitrile	22

Chapter 2

1.	Schematic representation of O.T.T.L.E.	39
2.	Schematic energy level scheme for a series of complexes $[\text{Ru}(\text{bipy})_2(\text{X})(\text{Y})]^{n+}$	43
3.	Spectral/electrochemical correlation of the frontier orbitals in ruthenium(II) bipyridine complexes	44
4.	Cyclic voltammogram of $[\text{Ru}(\text{bipy})_2\text{CO.Cl}]^+$ in dichloromethane at room temperature	48

5.	Absorption spectra of $[\text{Ru}(\text{bipy})_2\text{CO}.\text{Cl}]^{+/2+}$ in dichloromethane at room temperature	49
6.	Schematic energy level scheme for $[\text{Ru}(\text{bipy})_2\text{CO}.\text{Cl}]^{+/2+}$	54
7.	Absorption spectra of $[\text{Ru}(\text{bipy})_2\text{CO}.\text{Cl}]^{+/o/-}$ in dichloromethane at -40°C	56
8.	Absorption spectrum of Li^+bipy^-	57
9.	Absorption spectra recorded during the conversion of $[\text{Ru}(\text{bipy})_2\text{CO}.\text{Cl}]^+$ to $[\text{Ru}(\text{bipy})_2\text{Cl}_2]$	62
10.	The behaviour of $\text{cis}-[\text{Ru}(\text{bipy})_2\text{CO}.\text{Cl}]^+$ in its reduced and oxidised states	63
11.	Absorption spectra of $[\text{Ru}(\text{bipy})_2\text{CO}.\text{MeCN}]^{2+}$ and $[\text{Ru}(\text{bipy})_2(\text{MeCN})_2]^{2+/3+}$ in acetonitrile at room temperature	66
12.	Absorption spectra of $[\text{Ru}(\text{bipy})_2\text{CO}.\text{MeCN}]^{2+/+}$ in acetonitrile at -35°C	69
13.	Absorption spectra recorded during the reductive electrolysis of $[\text{Ru}(\text{bipy})_2\text{CO}.\text{MeCN}]^{2+}$ in the presence of perchlorate salts	71
14.	The substitution reactions of $[\text{Ru}(\text{bipy})_2\text{CO}.\text{MeCN}]^{2+}$	72
15.	Cyclic voltammogram of $[\text{Ru}(\text{bipy})_2\text{CO}.\text{py}]^{2+}$ recorded in acetonitrile and pyridine	75
16.	Absorption spectra of $[\text{Ru}(\text{bipy})_2\text{CO}.\text{ph}]^{2+}$ and $[\text{Ru}(\text{bipy})_2\text{py}.\text{MeCN}]^{2+/3+}$ in acetonitrile	77
17.	Absorption spectra of $[\text{Ru}(\text{bipy})_2\text{CO}.\text{py}]^{2+/+/o}$ in pyridine	80

18.	Absorption spectra of $[\text{Ru}(\text{bipy})_2(\text{CO})_2]^{2+/+}$ in dichloromethane at -40°C	84
19.	Schematic energy level scheme for $[\text{Ru}(\text{bipy})_2\text{CO.H}]^+$	87
20.	Absorption spectrum of $[\text{Ru}(\text{bipy})_2\text{CO.H}]^+$ in dichloromethane at room temperature	88
21.	Cyclic voltammogram of $[\text{Ru}(\text{bipy})_2\text{CO.H}]^+$ in dichloromethane at room temperature	89
22.	Substitution reactions of $\text{cis-}[\text{Ru}(\text{bipy})_2\text{CO.H}]^+$	91

Chapter 3

1.	A.C. polarogram of $[\text{Ir}(\text{bipy})_2\text{Cl}_2]\text{Cl}$ in acetonitrile at -30°C	101
2.	A.C. polarogram of $[\text{Ir}(\text{bipy})_2\text{Cl}_2](\text{CF}_3\text{SO}_3)$ in acetonitrile at -30°C	102
3.	Absorption spectra of $[\text{Ir}(\text{bipy})_2\text{Cl}_2]^{+/o/-}$ in acetonitrile at -30°C	104
4.	A.C. polarogram of $[\text{Ir}(\text{bipy})_2(\text{CF}_3\text{SO}_3)_2]$ (CF_3SO_3) in dichloromethane at -30°C ; also in the presence of excess $\text{TBA}^+\text{CF}_3\text{SO}_3^-$	109
5.	Absorption spectra of $[\text{Ir}(\text{bipy})_2(\text{CF}_3\text{SO}_3)_2]^{+/o/-}$ in dichloromethane at -30°C in the presence of excess $\text{TBA}^+\text{CF}_3\text{SO}_3^-$	110
6.	Absorption spectra of $[\text{Ir}(\text{bipy})_3]^{3+/2+/+/-o}$ in dichloromethane at room temperature	113
7.	Cyclic voltammograms of $[\text{Ir}(\text{bipy})_3]^{3+}$ and $[\text{Cr}(\text{bipy})_3]^{3+}$ in acetonitrile	115

8.	Ultra-violet spectra of $[\text{Cr}(\text{bipy})_3]^{3+/2+}$ in acetonitrile at room temperature	119
9.	Near infra-red/visible spectra of $[\text{Cr}(\text{bipy})_3]^{3+/2+/+/o}$ in acetonitrile at -30°C in the presence of excess bipyridine	120
10.	Schematic energy level scheme for $[\text{Cr}(\text{bipy})_3]^{3+/2+/+/o}$	122
11.	Absorption spectra of $[\text{Cr}(\text{bipy})_3]^{o/-}$ in tetrahydrofuran at -30°C in the presence of excess bipyridine	126

Chapter 4

1.	Reductive electrode potentials for [$[\text{Ir}(\text{bipy})_3]^{3+}$, $[\text{Ir}(\text{bipy})_2\text{Cl}_2]^+$ and " $[\text{Ir}(\text{bipy})_3 \cdot \text{H}_2\text{O}]^{3+}$ "	136
2.	Absorption spectra of $[\text{Ir}(\text{bipy})_2(\text{bipy}')]^{2+/+/o}$ in acetonitrile at room temperature	138
3.	^1H n.m.r. spectrum of $[\text{Ir}(\text{bipy})_2(\text{bipy}')]^{2+}$ in MeOH-d^4	141
4.	^1H n.m.r. spectrum of $[\text{Ir}(\text{bipy})_2(\text{bipy}')]^{2+}$ in $(\text{Me})_2\text{CO-d}^6$	142
5.	^1H n.m.r. spectrum of $[\text{Ir}(\text{bipy})_2(\text{bipy}')]^{2+}$ in $(\text{Me})_2\text{SO-d}^6$	143
6.	^{13}C n.m.r. spectrum of $[\text{Ir}(\text{bipy})_2(\text{bipy}')]^{2+}$ in $(\text{Me})_2\text{SO-d}^6$	148
7.	Cyclic voltammogram of $[\text{Ru}(\text{bipy})_2(\text{phpy})]^+$ in dichloromethane at room temperature	152

8.	Absorption spectra of bipyridine and phenylpyridine in dichloromethane at room temperature	156
9.	Visible absorption spectra of $[\text{Ru}(\text{bipy})_3]^{2+}$ and $[\text{Ru}(\text{bipy})_2(\text{phpy})]^+$ in acetonitrile at room temperature	158
10.	Comparative energy level scheme for $[\text{Ru}(\text{bipy})_3]^{2+}$ and $[\text{Ru}(\text{bipy})_2(\text{phpy})]^+$	159
11.	Schematic energy level scheme for $[\text{Ru}(\text{bipy})_2(\text{phpy})]^+$	162
12.	Absorption spectra of $[\text{Ru}(\text{bipy})_2(\text{phpy})]^{+/2+}$ in acetonitrile at room temperature	163
13.	Absorption spectra of $[\text{Ru}(\text{bipy})_2(\text{phpy})]^{+/0/-}$ in acetonitrile at room temperature	167

Chapter 5

1.	Absorption spectra of $[\text{Ru}(\text{bipy})_n(\text{biq})_{3-n}]^{2+}$ ($n = 0$ to 3) in acetonitrile at room temperature	175
2.	Absorption spectra of $[\text{Ru}(\text{bipy})_n(\text{py})_{6-2n}]^{2+}$ ($n = 1$ to 3)	176
3.	Comparative energy level scheme for $[\text{Ru}(\text{bipy})_n(\text{biq})_{3-n}]^{2+}$ ($n = 1$ to 3)	181
4.	Absorption spectra of bipyridine and biquinoline in dichloromethane at room temperature	184

	<u>Page</u>
5. Absorption spectrum of Li^+biq^-	186
6. Absorption spectra of $[\text{Ru}(\text{bipy})_2(\text{biq})]^{2+/3+}$ in dichloromethane at room temperature	187
7. Schematic energy level scheme for $[\text{Ru}(\text{bipy})_2(\text{biq})]^{2+/3+}$	191
8. Absorption spectra of $[\text{Ru}(\text{bipy})_2(\text{biq})]^{2+/+}$ in dichloromethane at room temperature	194
9. Absorption spectra of $[\text{Ru}(\text{bipy})(\text{biq})_2]^{2+/3+}$ in dichloromethane at room temperature	196
10. Schematic energy level scheme for $[\text{Ru}(\text{bipy})(\text{biq})_2]^{2+/3+}$	198
11. Cyclic voltammogram of $[\text{Ru}(\text{bipy})(\text{biq})_2]^{2+}$ in dichloromethane at room temperature	200
12. Absorption spectra of $[\text{Ru}(\text{bipy})(\text{biq})_2]^{2+/+/o}$ in dichloromethane at -30°C	201
13. Absorption spectra of $[\text{Ru}(\text{bipy})(\text{biq})_2]^{0/-}$ in tetrahydrofuran at -30°C in the presence of excess bipyridine	204
14. Absorption spectra of $[\text{Ru}(\text{biq})_3]^{2+/+/o/-}$ in acetonitrile	206

Appendix 1

1. Distortion coordinate - energy diagram applicable for valence interchange	214
2. Near infra-red spectrum of $[\text{Ir}(\text{bipy})_3]^{3+/2+}$ in $0.1\text{M TBABF}_4/\text{CH}_3\text{CN}$	217

3.	Near infra-red spectrum of $[\text{Ir}(\text{bipy})_3]^{3+/2+}$ with electrolyte/solvent contributions subtracted	218
----	---	-----

SchemeChapter 3

1.	Preparation of $[\text{Ir}(\text{bipy})_3]^{3+}$	99
----	--	----

Chapter 1

Introductory remarks: Transition metal bipyridyl complexes as solar energy dyes;
Correlation of optical and electrochemical data in such bipyridyl systems;
Electrochemical reduction in $[M(bipy)_3]^{n+}$ systems in terms of a ligand localised model.

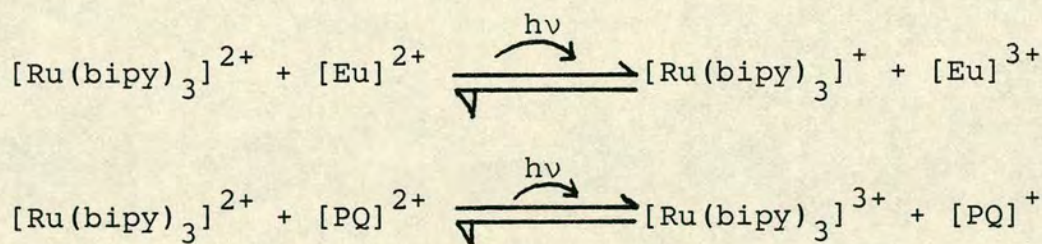
In recent years the photochemical, photophysical and luminescent properties of the tris-bipyridine ruthenium(II) cation, $[Ru(bipy)_3]^{2+}$, I, have been much studied.¹⁻¹⁴ This complex possesses a low-lying relatively long-lived photo-excited state which has led to much discussion of $[Ru(bipy)_3]^{2+}$ as a prototype pigment for use in solar energy conversion systems.¹⁴⁻²¹

The excited state species, $^*[Ru(bipy)_3]^{2+}$, which for example has a lifetime of 5.7 μ secs at 77K in a methanol: ethanol glass (4:1 v/v),⁴ is formed on the absorption of visible light, $\lambda_{max} \sim 582nm$. For many years formation of this excited species was assumed to involve the transfer of an electron from the ruthenium(II) core to an acceptor orbital which is delocalised over all three bipyridine ligands.^{3,22-24} Indeed examination of the Raman^{25,26} and absorption spectra of the excited species provides evidence for such an electron transfer to the bipyridyl ligands.

However further studies of the resonance Raman²⁸ and absorption spectra²⁹ of $^*[Ru(bipy)_3]^{2+}$ have established that the excited species should be interpreted in terms of a localised model. In other words, the promoted electron enters an acceptor orbital which is localised on one bipyridine ligand and I^* is best formulated as $[Ru(III)-(bipy^0)_2(bipy^-)]^{2+}$.

It may be noted that the photo-excited species is a strong oxidising agent, due to the hole in the metal valence core, and also a strong reducing agent because of the promoted electron. This dual nature can only arise in electronically excited systems. Thus I^* can react with a suitable quencher such as europium(II), $[Eu]^{2+}$, to give reactive intermediates $[Ru(bipy)_3]^+$ and $[Eu]^{3+}$ ^{30,31} or equally, the excited species may be oxidatively quenched by, for example, paraquat,^{32,33} $[PQ]^{2+}$, as shown in figure 1.

Figure 1: Conversion of Light into Chemical Energy
by $[Ru(bipy)_3]^{2+}$

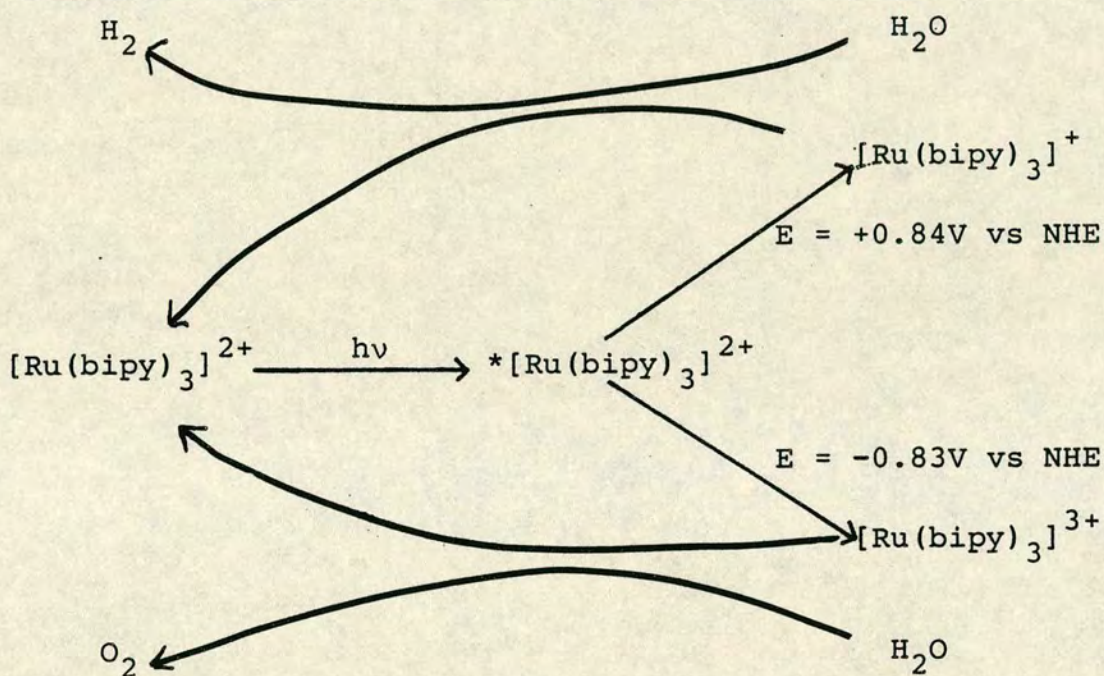


It is apparent that in each case the absorption of light has shifted the system from equilibrium and in the process converted light into chemical energy. It is

possible to devise a cell to harvest this energy.

Another potentially important property of $[\text{Ru}(\text{bipy})_3]^{2+}$ is that the excited state species is thermodynamically capable of splitting water as shown in figure 2.¹⁶

Figure 2: Splitting of Water by $[\text{Ru}(\text{bipy})_3]^{2+}$ ¹⁶



Disproportionation of the excited species gives $[\text{Ru}(\text{bipy})_3]^+$ and $[\text{Ru}(\text{bipy})_3]^{3+}$ which may then reduce or oxidise water to give dihydrogen and dioxygen respectively. However, this process, though thermodynamically feasible, is not efficient kinetically³⁵ since it can only proceed by successive one-electron steps requiring catalysts.³⁶⁻³⁸

A large part of this thesis is devoted to the study

of further Ru(II) and Ir(III) systems which are closely related to $[\text{Ru}(\text{bipy})_3]^{2+}$. The electronic structures of these complexes and their redox and spectroscopic properties are of considerable relevance and intrinsic interest.

For polypyridyl transition-metal complexes, as for other molecules, electronic structure is conventionally expressed in terms of a model embracing a series of two-electron orbitals. The successive filling of these orbitals by the appropriate complement of electrons then leads to the complete description of the ground state configuration of each system. The frontier orbitals (the highest occupied (HOMO) and lowest unoccupied (LUMO) molecular orbitals) of the system are of particular significance in determining optical and redox properties and reactivity. In particular, the existence of strictly defined (quantised) occupied and unoccupied levels implies the possibility of specific electronic transitions which should occur at discrete excitation energies. Nevertheless the full assignment of the bands observed in the absorption spectrum of transition-metal complexes is often extremely difficult. The deduction of electronic structure from the observed spectrum is even more difficult since its entire complexity is not revealed. Many of the anticipated transitions occur at similar energies therefore in the observed spectrum the less intense bands will be obscured. Therefore, only rarely can a unique electronic model be determined from the available data.

Fortunately, for transition metal polypyridyl complexes

it is possible to categorise the nature of the anticipated prominent electronic excitations. These fall into three general types, ligand-based, metal-based and those which involve a transfer of charge.

A ligand-based transition then involves molecular orbitals localised on the ligand itself and in practice the ones normally observed are $\pi\pi^*$ transitions. Likewise transitions involving orbitals localised on the metal centre are said to be metal-based and are named d-d (or ligand-field) transitions.

In contrast a charge-transfer (C.T.) excitation involves electron transfer between contrasting molecular orbitals, one of which is based on the metal centre and the other on the ligand. A charge-transfer band could thus involve a displacement of negative charge from the metal to the ligand (MLCT) or from the ligand to the metal (LMCT).³⁹

The intensity of a band is determined by quantum mechanical selection rules; transitions which are both orbitally- and spin-allowed are naturally the most intense. Therefore, ligand-field (d-d) transitions, which are orbitally forbidden, are orders of magnitude less intense than charge-transfer and intraligand bands. Generally ligand-field transitions are very difficult to observe in transition-metal bipyridyl complexes due to the overlap of more intense charge-transfer bands.

If the assignment of bands in the absorption spectrum of these polypyridyl systems is to be attempted then importance attaches to both the position and intensities

of predicted transitions, in relation to an internally consistent molecular orbital energy scheme appropriate to chromophoric centres present in the complex. Indeed in this thesis the assignment of the absorption spectrum of each complex follows a consistent deductive strategy and is fully consistent with our interpretation of the bands observed for $[\text{Ru}(\text{bipy})_3]^{2+/3+}$ and $[\text{Ru}(\text{bipy})_2\text{Cl}_2]^{0/+}$. That is, we have accumulated electrochemical data for the complexes above, and for a series of closely related systems, then utilised this information to predict the transition energy required for each anticipated optical excitation.

Several voltammetric studies on $[\text{Ru}(\text{bipy})_3]^{2+}$, $[\text{Ru}(\text{bipy})_2\text{Cl}_2]$, $[\text{Ir}(\text{bipy})_3]^{3+}$ and $[\text{Ir}(\text{bipy})_2\text{Cl}_2]^+$ have been reported;⁴⁰⁻⁴³ our results are consistent with this reported data and are listed in table 1. Bard and co-workers⁴⁴ have also examined the oxidative electrochemical behaviour of $[\text{Ru}(\text{bipy})_3]^{2+}$ and $[\text{Os}(\text{bipy})_3]^{2+}$ in liquid sulphur dioxide providing further useful information at relatively inaccessible highly positive potentials. These workers observed two one-electron oxidative waves for $[\text{Os}(\text{bipy})_3]^{2+}$ assigning these to the Os(II/III) and Os(III/IV) couples. The gap between these redox couples is measured to be 1.61 volts which we note compares closely with the measured difference between the $[\text{Ru}(\text{bipy})_2\text{Cl}_2]^{0/+}$ and $[\text{Ru}(\text{bipy})_2\text{Cl}_2]^{+/2+}$ redox processes. Bard⁴⁴ has also shown that in contrast the second oxidation observed for $[\text{Ru}(\text{bipy})_3]^{2+}$ (i.e. beyond the Ru(II/III) couple) should

be classified as ligand-centred, presenting Raman, n.m.r. and absorption spectra as evidence. We may however estimate a value for the hypothetical Ru(III/IV) couple (i.e. $[\text{Ru(III)(bipy)}_3]^{3+}/[\text{Ru(IV)(bipy)}_3]^{4+}$) for $[\text{Ru(bipy)}_3]^{3+}$ using the data available for $[\text{Os(bipy)}_3]^{2+}$ and $[\text{Ru(bipy)}_2\text{Cl}_2]$. In both the latter cases the M(II/III) - M(III/IV) separation is directly observable and found to be approximately 1.6-1.65 volts.

Previous work in our laboratories has shown that the potential required to reversibly reduce an individual bipyridyl ligand in $[\text{M(bipy)}_3]^{n+}$ (i.e. E° for $[\text{M(bipy)}_3]^{n+}/[\text{M(bipy}^\circ)_2(\text{bipy}^-)]^{(n-1)+}$) is directly related to the charge on the central metal M, with a value of 0.32 volts per unit charge being measured. Strictly this observation pertains to the redox activity localised in $\pi(7)\text{bipy}^\circ$ (see later). Then by analogy to the filled $\pi(6)$ level we may estimate a value for the hypothetical oxidation of bipyridyl on a ruthenium(II) centre.

Table 1: Pertinent Electrochemical Data^a for the
Complexes $[\text{Ru}(\text{bipy})_3]^{2+/3+}$ and $[\text{Ru}(\text{bipy})_2\text{Cl}_2]^{0/+}$

	<u>$[\text{Ru}(\text{bipy})_3]^{2+}$</u>	<u>$[\text{Ru}(\text{bipy})_2\text{Cl}_2]^{0+}$</u>
$E^{\circ} \text{Ru(II/III)}$	+0.96	+0.01
$E^{\circ} \text{Ru(III/IV)}$	+2.7 ^b	+1.66
$E^{\circ} \text{bipy}^{0/-} \text{Ru(II)}$	-1.66	-1.95
$E^{\circ} \text{bipy}^{0/-} \text{Ru(III)}$	-1.34 ^c	-1.63 ^c
$E^{\circ} \text{bipy}^{0/+} \text{Ru(II)}$	+2.39 ^c	+2.09 ^{c,d}
$E^{\circ} \text{bipy}^{0/+} \text{Ru(III)}$	+2.71	+2.41 ^d

Note: a) All potentials above are specified vs a Ag/Ag^+ reference electrode in 0.1M $\text{TBABF}_4/\text{CH}_3\text{CN}$.
(Numerical values without annotation are directly measured).

- b) Value estimated from the measured $E[\text{M(II/III)} - \text{M(III/IV)}]$ gap for $[\text{Os}(\text{bipy})_3]^{2+}$ and $[\text{Ru}(\text{bipy})_2\text{Cl}_2]$.
- c) Estimated from the 0.32V shift per unit charge observed on the bipyridine $\pi(7)$ level for $[\text{M}(\text{bipy})_3]^{n+}$ and this behaviour is extrapolated to the $\pi(6)$ level.
- d) Extrapolation of the 0.3V shift noted on the $\pi(7)$ level on replacement of one bipyridine ligand by two chloride ligands to the $\pi(6)$ level.

Using these data it is possible to estimate values for the optical transitions proposed for these complexes.

$d^6\text{Ru(II)}$ Complexes

In these systems the energy required for a $\pi(6) \rightarrow \pi(7)$ intraligand transition may be predicted by measuring the gap between the estimated $\text{bipy}^{0/+}$ couple on ruthenium(II), which allows us to map $\pi(6)$, and the directly measured $\text{bipy}^{0/-}$ couple, which maps $\pi(7)$. The correlation is extremely good (32.7kK electrochemically vs 34.8kK optically). The lowest energy metal-to-ligand charge-transfer transition ($\text{Ru(II)}d\pi \rightarrow \text{bipy}\pi(7)$) is then represented by the gap between the Ru(II/III) couple and the $\text{bipy}^{0/-}$ couple on ruthenium(II). An examination of the ultra-violet spectrum of each system then allows us to measure the $\pi(7) \rightarrow \pi(8)$ gap on bipyridine since the band at approximately $40\,000\text{ cm}^{-1}$ in these complexes is recognised to be due to a $\pi(6) \rightarrow \pi(8)$ bipy^0 transition.⁴⁵ This observation then allows us to predict a value for the higher order $\text{Ru(II)}d\pi \rightarrow \text{bipy}\pi(8)$ MLCT transition.

$d^5\text{Ru(III)}$ Systems

In these systems a value for the $\pi(6) \rightarrow \pi(7)$ bipy^0 transition may again be predicted utilising the data pertinent to the Ru(III) centre. However, our previous assumption that the $\pi(6)$ level on bipyridine is lowered to the same extent as the $\pi(7)$ level does not permit us to rationalise the observed shift of the internal ligand

$\pi(6) \rightarrow \pi(7)$ transition to longer wavelength on oxidation. This suggests we have overestimated the effect on the $\pi(6)$ level on moving from Ru(III) to Ru(II) however these values are used in our further calculations since we have no suitable model on which we may map the bipyridine $\pi(6)$ level on ruthenium(II).

A prediction of the lowest energy MLCT transition ($\text{Ru(III)}d\pi^5 \rightarrow \text{bipy}^0(7)$) may be made by examination of the gap between the Ru(III/IV) couple and the predicted value for bipyridyl reduction on a ruthenium centre. For Ru(III)-bipyridyl complexes, a ligand-to-metal charge-transfer may also occur with the value for a $\text{bipy } \pi(6) \rightarrow \text{Ru(III)}d\pi$ transition being represented by the gap between the $\text{bipy}^{0/+}$ couple, measured on ruthenium(III), and the observed Ru(II/III) couple.

By using the methods described above we may predict values for the transitions anticipated for $[\text{Ru}(\text{bipy})_3]^{2+/3+}$ and $[\text{Ru}(\text{bipy})_2\text{Cl}_2]^{0/+}$ which are shown in table 2. On examination of the absorption spectrum of each species, shown in figures 3 and 4, we may now assign the observed bands as shown in table 3.

It is useful to construct a schematic molecular orbital scheme to relate these predictions and assignments as shown in figure 5.

Table 2: Predicted Values for the Anticipated

Transitions in $[\text{Ru}(\text{bipy})_3]^{2+/3+}$ and
 $[\text{Ru}(\text{bipy})_2\text{Cl}_2]^{0/+}$ from Electrochemical Data

<u>Complex</u>	<u>Transition</u>			
	$\frac{\pi(6) \rightarrow \pi(7)}{\text{bipy}^0}$	$\frac{\text{Ru(III)d}\pi}{\rightarrow \text{bipy}^0 \pi(7)}$	$\frac{\text{Ru(II)d}\pi}{\rightarrow \text{bipy}^0 \pi(7)}$	$\frac{\text{bipy}^0 \pi(6)}{\rightarrow \text{Ru(III)d}\pi}$
$[\text{Ru}(\text{bipy})_3]^{2+}$	4.05 <u>32.7</u>	-	2.62 <u>21.1</u>	-
$[\text{Ru}(\text{bipy})_3]^{3+}$	4.05 <u>32.7</u>	4.05+ <u>32.7</u>	-	1.75 <u>14.1</u>
$[\text{Ru}(\text{bipy})_2\text{Cl}_2]^0$	4.04 <u>32.6</u>	-	1.96 <u>15.8</u>	-
$[\text{Ru}(\text{bipy})_2\text{Cl}_2]^+$	4.04 <u>32.6</u>	3.29 <u>26.5</u>	-	2.40 <u>18.4</u>

Note: (a) Tabulated figures are expressed in units of electron volts and those in italics in units of 10^{-3}cm^{-1} ($1 \text{eV} \approx 8065 \text{cm}^{-1}$)

Figure 3: Absorption Spectra of $[\text{Ru}(\text{bipy})_3]^{2+/3+}$ in Dichloromethane at Room Temperature

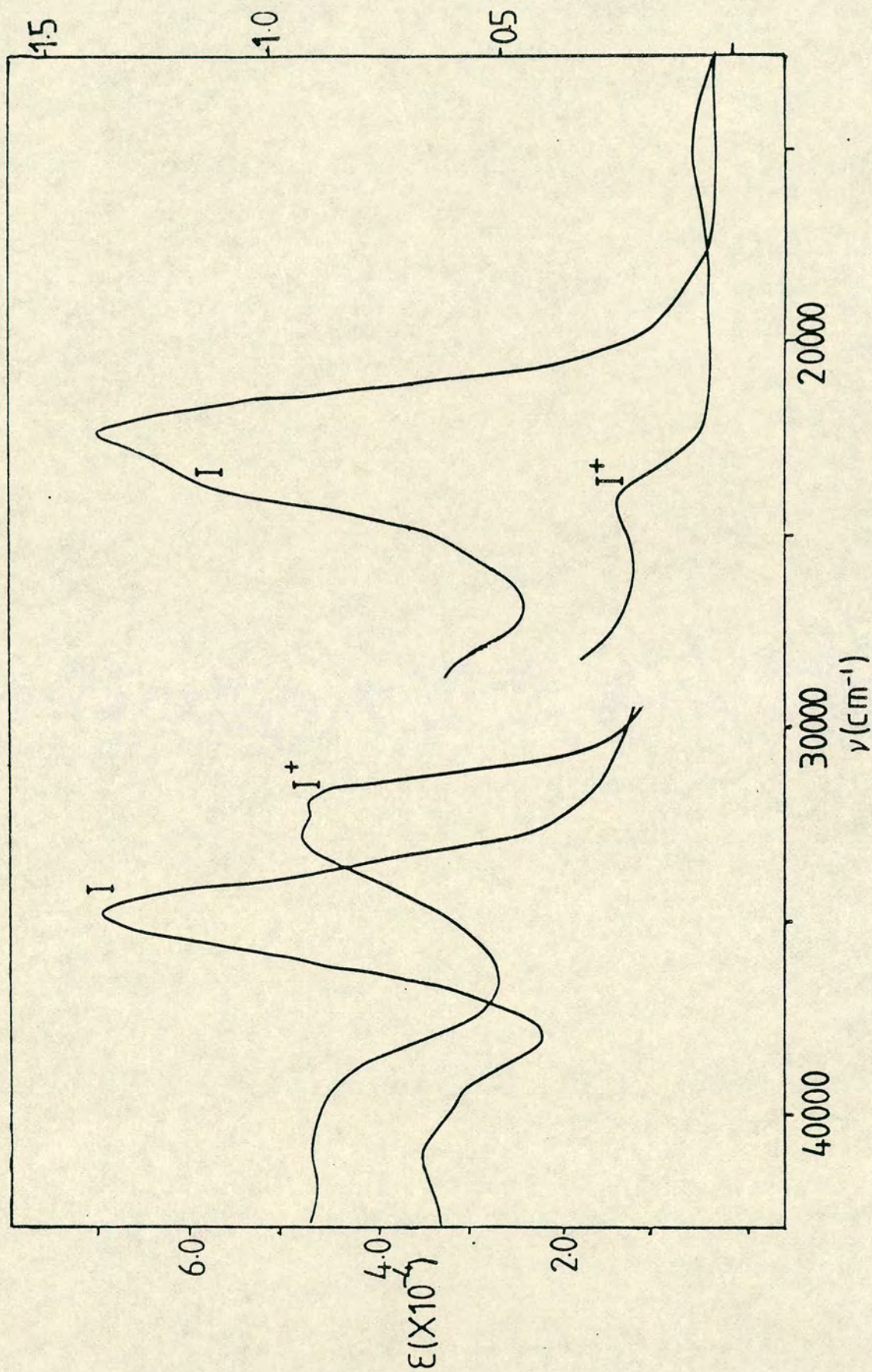


Figure 4: Absorption Spectra of $[\text{Ru}(\text{bipy})_2\text{Cl}_2]^{+0}$ in Dichloromethane at Room Temperature

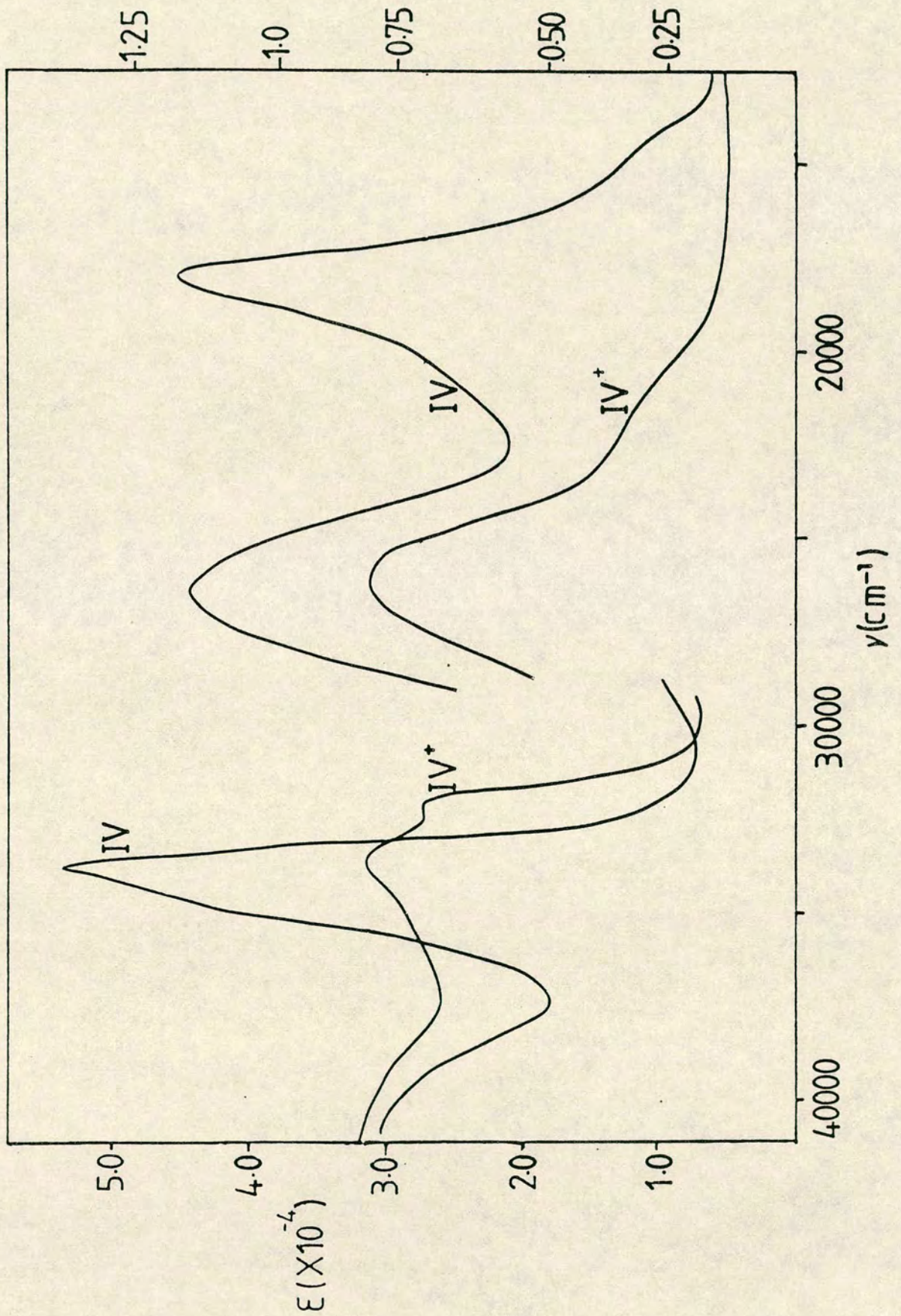


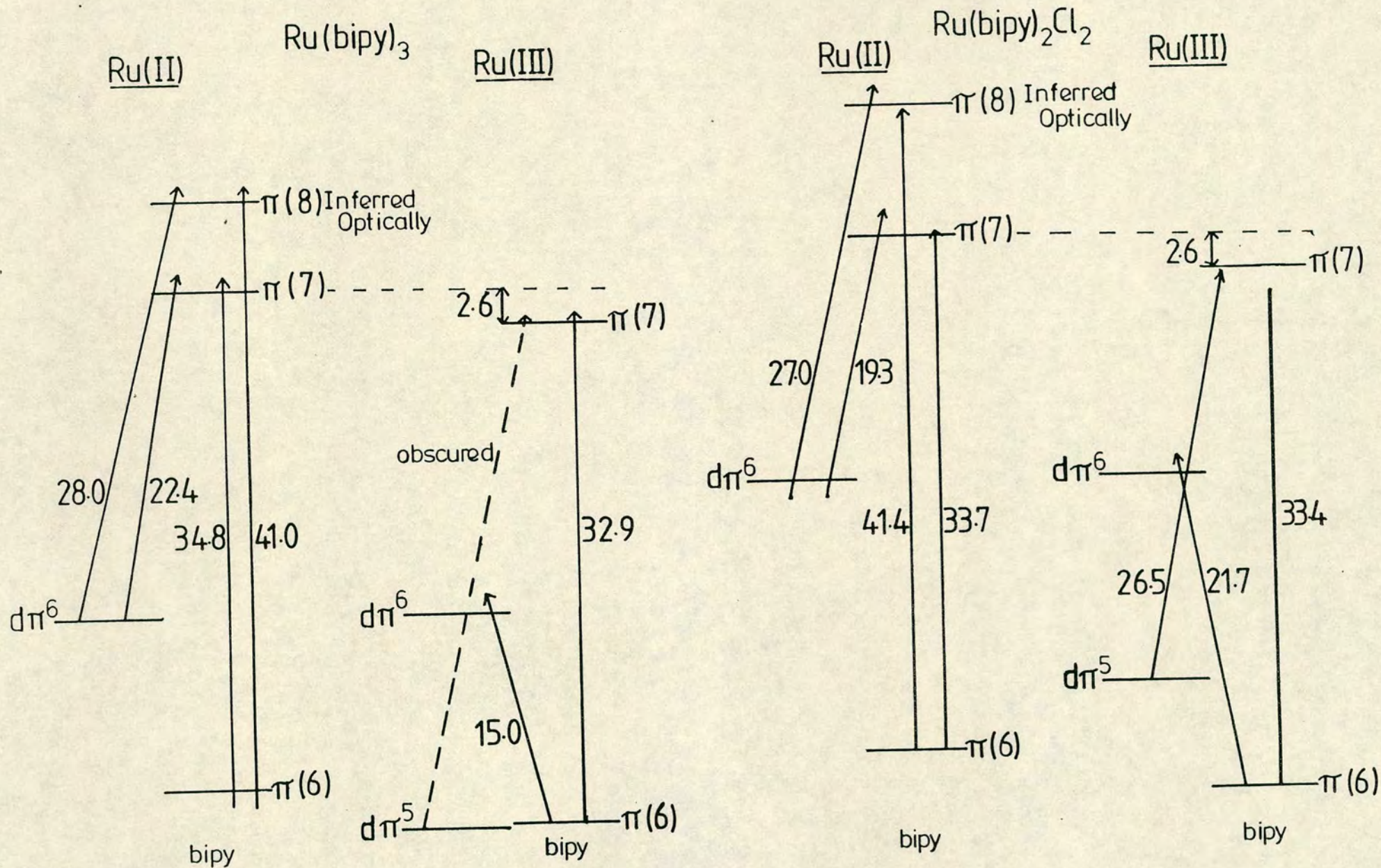
Table 3: Assignment of the Observed Bands in

Complex	$\pi(5) \rightarrow \pi(7)$	$\pi(6) \rightarrow \pi(7)$	Transition		$\text{bipy}\pi(5)$	$\text{bipy}\pi(6)$	$\frac{[\text{Ru}(\text{bipy})_3]^{2+/3+} \text{ and } [\text{Ru}(\text{bipy})_2\text{Cl}_2]^{0/+}}{\times 10^{-3} \text{ cm}^{-1} (\times 10^{-4})}$
	$\pi(6) \rightarrow \pi(8)$	bipy^{O}	$\text{Ru d}\pi$ $\rightarrow \text{bipy}\pi(8)$	$\text{Ru d}\pi$ $\rightarrow \text{bipy}\pi(7)$	$\rightarrow \text{Ru d}\pi$	$\rightarrow \text{Ru d}\pi$	
$[\text{Ru}(\text{bipy})_3]^{2+}$	39.5 sh 41.0 (3.50)	34.8 (7.06)	28.0 (0.63)	22.4 (1.37)	-	-	
$[\text{Ru}(\text{bipy})_3]^{3+}$	40.3 (4.55)	32.9 (4.73) 31.8 (4.61)	a	a	23.8 (0.28) ^b	15.0 (0.08)	
$[\text{Ru}(\text{bipy})_2\text{Cl}_2]^{\text{O}}$	41.4 (3.02)	33.7 (5.36)	27.0 (1.18)	19.3 (1.20)	-	-	
$[\text{Ru}(\text{bipy})_2\text{Cl}_2]^+$	41.2 (2.98)	33.3 (3.12) 32.1 (2.68)	a	26.5 (0.78) ^c	a, b	21.7 (0.28)	

Note: a - Band obscured

b - This band is assigned to a ligand-to-metal charge-transfer from a lower level since we have assumed the $\pi(7) - \pi(8)$ and $\pi(5) - \pi(6)$ gaps are comparable.

c - $\text{Cl}^- \rightarrow \text{Ru}(\text{III})$ charge-transfer occurs at $28\,000 \text{ cm}^{-1}$ in RuCl_6^{3-} .

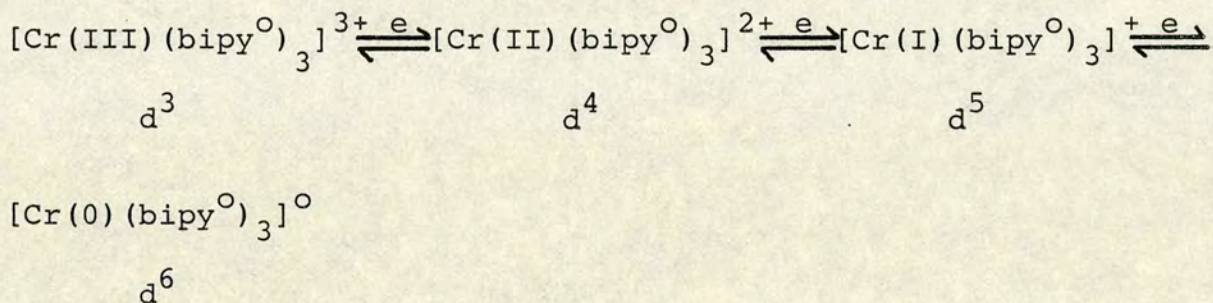


Note

All the energy levels marked — are inferred electrochemically.
All arrows shown above refer to optical maxima. (Numbers listed are optically measured transitions)

As described in the following chapters, we have utilised the electrochemical data collected for many polypyridyl species in order to model the frontier orbitals of each system. This has allowed us to estimate the energy required to enable both intra-ligand and charge-transfer transitions to occur and thus assign the bands in each absorption spectrum.

The bipyridyl ligand has the pronounced ability to stabilise low oxidation state metal centres due, it is presumed, to the possibility of $d\pi \rightarrow \pi^*$ back-bonding. For example tris-bipyridyl transition metal complexes may undergo successive reductions of the metal centre as shown below for $[\text{Cr}(\text{bipy})_3]^{3+}$.

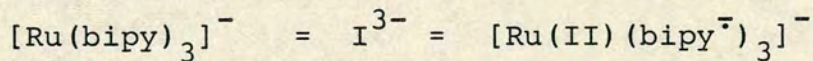
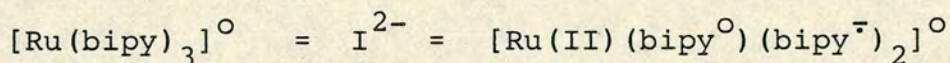
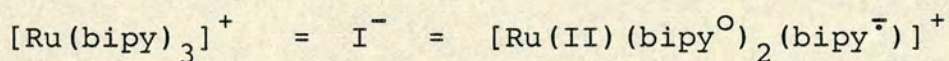
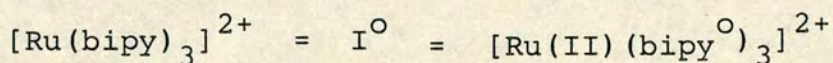


This system is studied in detail in Chapter 3 with the absorption spectrum of each species shown above being assigned. However, in this species the central metal may efficiently back-bond to bipyridine. This is due to the ligand having a low-lying acceptor orbital which implies bipy itself may undergo reduction. Indeed we have shown that $[\text{Cr}(\text{bipy})_3]^{3+}$ undergoes a fourth reduction which is

bipyridyl based, by spectroscopic characterisation of $[\text{Cr}(\text{bipy})_3]^-$.

For $[\text{Ru}(\text{bipy})_3]^{2+}$, electrochemical studies have revealed the presence of three one-electron reductions.^{40,41} For several years, it was assumed, wrongly, that each electron added to the system was entering a molecular orbital spanning all three bipyridine ligands. Recently several studies have focussed on the reduced species of $[\text{Ru}(\text{bipy})_3]^{2+}$ in an attempt to model the excited state complex. Electron spin resonance,⁴⁶ absorption spectral⁴⁷ and resonance Raman⁴⁸ studies of the reduced species $[\text{Ru}(\text{bipy})_3]^{+/0/-}$ have all produced strong evidence that each electron added to I is in fact localised on a separate bipyridine ligand. That is, the reduced species should be formulated as in table 4.

Table 4: Formulation of $[\text{Ru}(\text{bipy})_3]^{2+/+/0/-}$

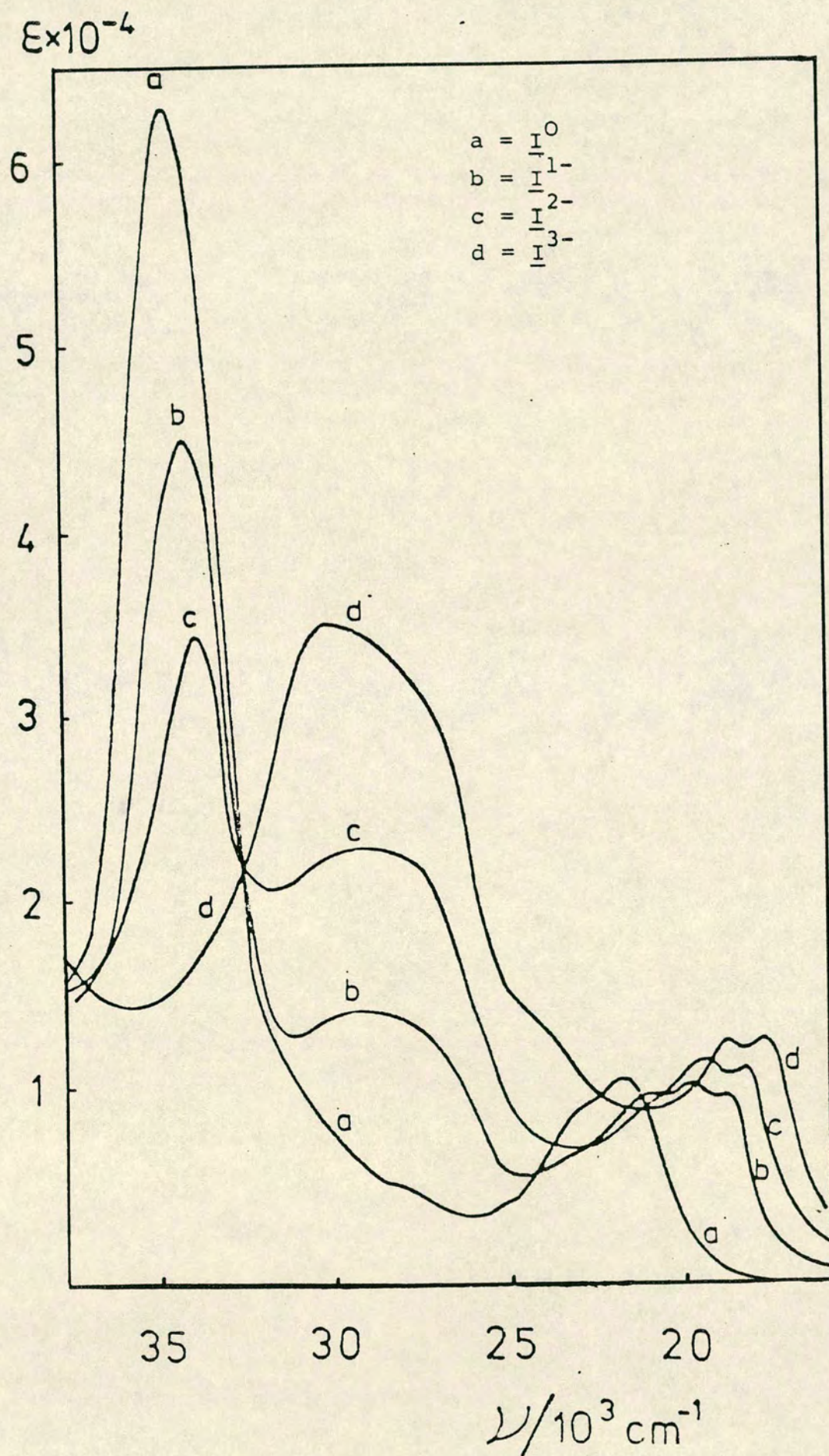


The progression in absorption spectra as a function of oxidation state with which this thesis is primarily concerned, revealed that for $[\text{Ru}(\text{bipy})_3]^{2+}$ the electronic

absorption spectrum could be interpreted in terms of three separate bipyridine ligand moieties. In the conventional oxidation state, $[\text{Ru}(\text{bipy})_3]^{2+}$, we have shown the absorption bands may be assigned to intraligand and charge-transfer transitions of $\text{Ru}(\text{II})(\text{bipy}^0)$ chromophores. For the one-electron reduced product, best obtained by controlled potential electrolysis, the absorption spectrum reveals a new set of bands which strongly resemble those in Li^+bipy^- ⁴⁹ together with the familiar $\text{Ru}^{II}/\text{bipy}^0$ bands at decreased intensity. This indicates the discrete reduction of one bipyridyl ligand has in fact taken place. If the electron has entered an orbital which is delocalised over all three ligands then in the reduced complex we would not anticipate observing any absorption bands which are characteristic of the isolated $\text{Ru}-(\text{bipy}^0)$ chromophore. However if we examine the ultra-violet region of the absorption spectrum of $[\text{Ru}(\text{bipy})_3]^+$ a band is observed at $35\,000\text{ cm}^{-1}$ which has been assigned to a $\pi\pi^*\text{bipy}^0$ transition.⁴⁷ As shown in figure 6, this band is approximately two-thirds the intensity of the band in $[\text{Ru}(\text{bipy})_3]^{2+}$ which is consistent with the loss of one $\text{Ru}-(\text{bipy}^0)$ chromophore.

The separate electrogeneration of the second and third reduced products allows the absorption spectrum of each species to be measured, as shown in figure 6. Thus, an examination of tris-bipyridine ruthenium(II) in these four differing redox states shows that there is a progressive loss of the $\text{Ru}-\text{bipy}^0$ chromophore accompanied by a linear growth of the $\text{Ru}-\text{bipy}^-$ moiety. These spectra, together

Figure 6: Absorption spectra of $[\text{Ru}(\text{bipy})_3]^{2+/1+/0/1-}; \text{I}^{0/1-/2-/3-}$ in dimethyl sulphoxide at room temperature.



with complementary electron spin resonance⁴⁶ and resonance Raman⁴⁸ studies on these species, give compelling evidence that a localised model is applicable in these reduced systems. That is they contain discrete bipy^0 and bipy^- ligands.

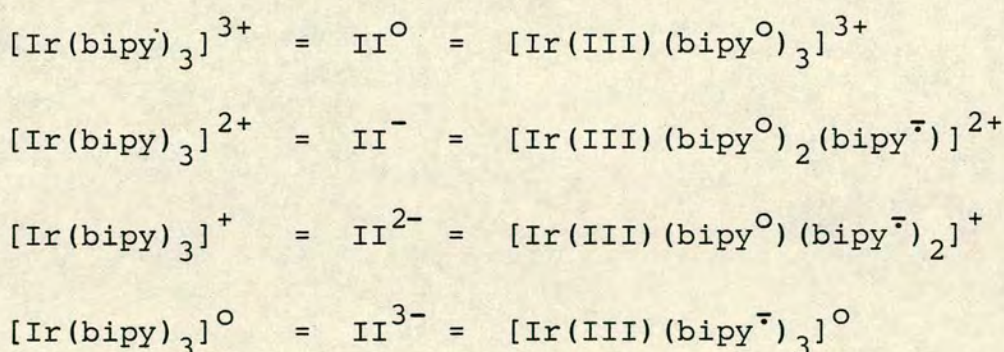
Electrode potential correlations of numerous tris-bipyridyl transition metal complexes have shown that the ligand-orbital energies are strongly determined by central ion valency. Accordingly the ligands in neighbouring isoelectronic $[\text{Rh}(\text{bipy})_3]^{3+}$ should then be easier to reduce, but Rh(III/I) reduction intervenes and this complex undergoes the irreversible loss of a bipyridyl ligand.⁵⁰

$[\text{Ir}(\text{bipy})_3]^{3+}$ on the other hand undergoes reversible reductions which are relatively facile in comparison to $[\text{Ru}(\text{bipy})_3]^{2+}$. It is approximately 0.4V easier to reduce $[\text{Ir}(\text{bipy})_3]^{3+}$ than $[\text{Ru}(\text{bipy})_3]^{2+}$. Indeed six reversible one-electron reductions have been observed for $[\text{Ir}(\text{bipy})_3]^{3+}$, in two groups of three closely-spaced waves. The first set of waves corresponds to the reduction of each bipyridyl ligand to bipy^- , whilst the second series is due to the addition of a second electron to each ligand to give coordinated bipy^{2-} .⁵¹ For $[\text{Ir}(\text{bipy})_3]^{3+}$, no oxidation of the metal centre is observed at moderate potentials which implies the $d\pi$ -manifold is stabilised to a greater extent by the central metal charge in $[\text{Ir}(\text{bipy})_3]^{3+}$, like $[\text{Ru}(\text{bipy})_3]^{3+}$, than $[\text{Ru}(\text{bipy})_3]^{2+}$. The $d\pi$ level in fact falls to a similar level to the ligand HOMO which means, on examination of the absorption spectrum of $[\text{Ir}(\text{bipy})_3]^{3+}$, that $\pi-\pi^*$ bands

rather than MLCT bands dominate the visible and near ultra-violet region. The MLCT band is in fact shifted to a significantly higher energy and we have been able to determine that it is concealed by the much more intense intraligand band at $33\,000\text{ cm}^{-1}$, (see chapter 3). A related prediction is that, at extreme positive potentials, ligand oxidation rather than metal oxidation would ensure.

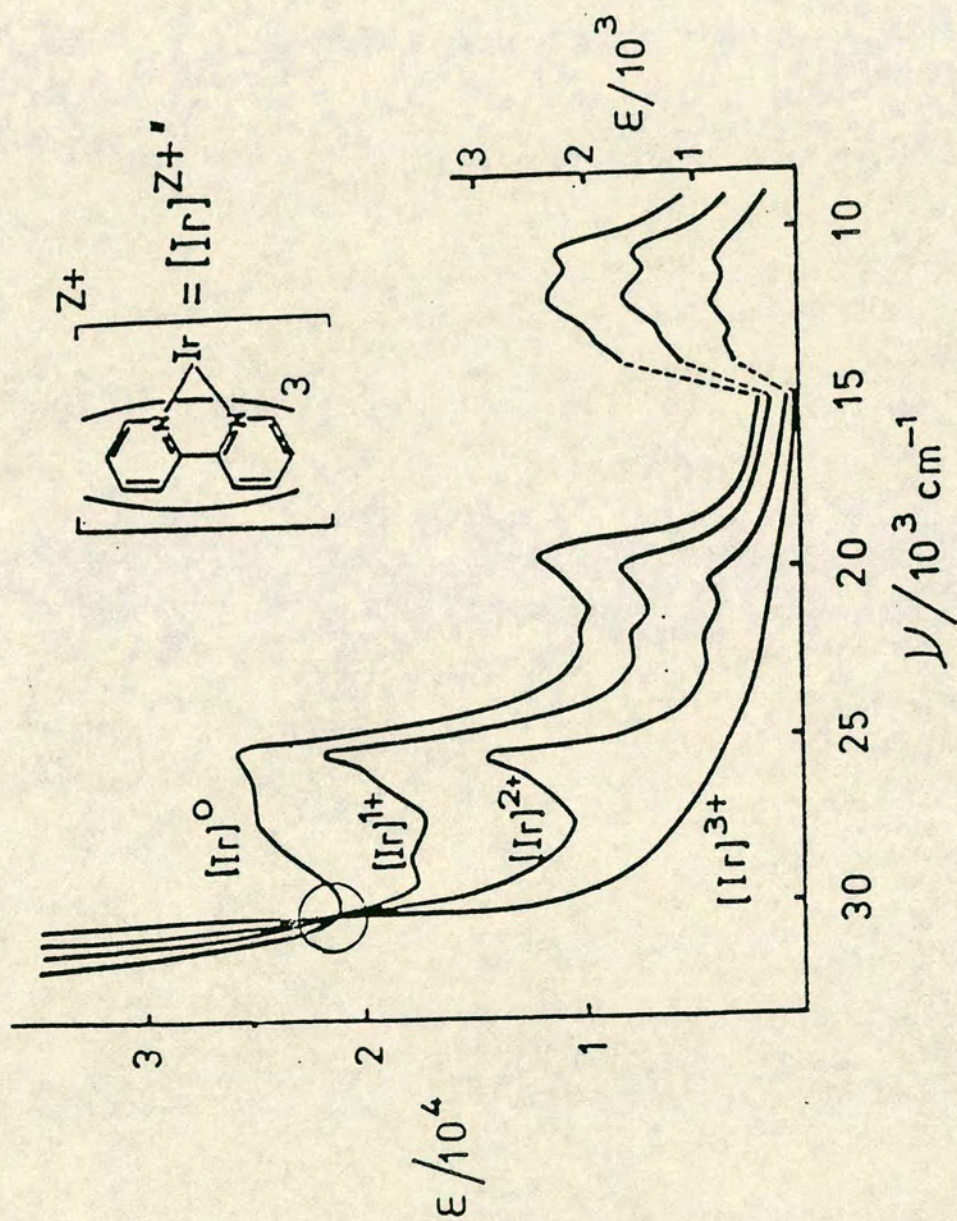
The absorption spectra of the first three reduced forms of $[\text{Ir}(\text{bipy})_3]^{3+}$ have also been measured.⁴⁹ In the redox series $[\text{Ir}(\text{bipy})_3]^{3+/2+/+/\circ}$ the progressive loss of bands assigned to intraligand $\pi\pi^*\text{bipy}^{\circ}$ transitions is noted together with the corresponding linear growth of the set of bands which correspond to the $\text{bipy}^{\bar{\cdot}}$ chromophore as shown in figure 7. Each electron added to $[\text{Ir}(\text{bipy})_3]^{3+}$ is evidently localised on a separate bipyridyl ligand implying the reduced species should be formulated as in table 5.

Table 5: Formulation of $[\text{Ir}(\text{bipy})_3]^{3+/2+/+/\circ}$



It should be noted that $[\text{Ru}(\text{bipy})_3]^{+}$ and $[\text{Ir}(\text{bipy})_3]^{2+}$ are closely related with a common electronic configuration

Figure 7: Absorption Spectra of $[\text{Ir}(\text{bipy})_3]^{3+/2+/+/0}$ in Acetonitrile at Room Temperature



$\text{Mdp}^6/(\text{bipy}^0)_2(\text{bipy}^-)$, however the corresponding excited state species I^* and II^* differ fundamentally. As described above I^* is formed due to metal-to-ligand charge-transfer excitation, however in $^*[\text{Ir}(\text{bipy})_3]^{3+}$ an intra-ligand $\pi \rightarrow \pi^*$ transition is involved as confirmed by photoemission spectroscopy.¹²

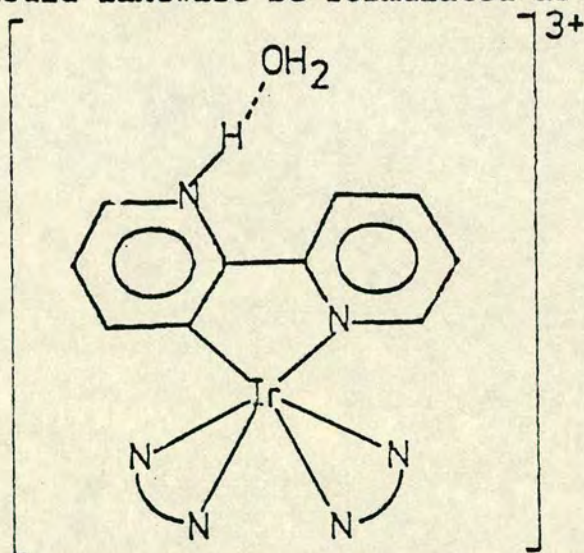
However, since it is apparent that the potential required to reduce a bipyridyl ligand is dependent upon the central metal charge, in some respects $[\text{Ir}(\text{bipy})_3]^{2+}$ (that is $[\text{Ir}(\text{III})(\text{bipy}^0)_2(\text{bipy}^-)]^{2+}$) provides a better model for the ligand array in I^* than $[\text{Ru}(\text{bipy})_3]^+$.

In this investigation we have studied $[\text{Ir}(\text{bipy})_3]^{3+}$ and several closely-related substituted bis(bipyridyl) iridium(III) species $[\text{Ir}(\text{bipy})_2\text{L}_2]^{n+}$, where L can be an anionic or neutral ligand. On reducing these species, by controlled potential electrolysis, we have shown these systems should be classified in terms of the localised model. However, some remarkable dissociation and substitution reactions involving these species in solution have also been discovered.

A complex, discovered in 1977 by Watts et al.⁵², which is closely related to $[\text{Ir}(\text{bipy})_3]^{3+}$ has recently been the centre of much interest. This complex, which is a commonly encountered major by-product in the earliest synthetic route to $[\text{Ir}(\text{bipy})_3]^{3+}$ ⁵³, has the stoichiometry equivalent to $[\text{Ir}(\text{bipy})_3.\text{OH}]^{2+}$ or $[\text{Ir}(\text{bipy})_3.\text{H}_2\text{O}]^{3+}$ dependent upon the prevailing pH. This reversible deprotonation is not observed for $[\text{Ir}(\text{bipy})_3]^{3+}$.

An examination of the voltammetric behaviour of this complex reveals two sets of two (only) closely-spaced one-electron reductions (c.f. $[\text{Ir}(\text{bipy})_3]^{3+}$ where two sets of three closely-spaced reductions are observed). This observation implies that one of the bipyridyl ligands is rendered inert towards reduction.

Several contrasting suggestions have been made concerning the formulation of this complex (see chapter 4), however we undertook comprehensive ^1H and ^{13}C n.m.r. studies of the solution structure of this species which established a remarkable internal rearrangement had taken place with the formation of an Ir-C bond. A recently published X-ray structure of this complex⁵⁴ illustrated that the crystalline complex should likewise be formulated as below.



The original penetrating suggestion for this unprecedented "roll-over" was made on the basis of very ambiguous data for the related protonated complex.

As described previously, the photolysis of water into its elements by sunlight is potentially one of the most attractive routes to solar energy conversion and

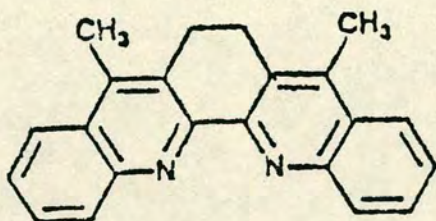
storage.^{16,34-38,56} Its practical utilisation is still far in the future although this process has been considerably developed^{17,18,56,67} in the last few years.

To date the most commonly discussed photosensitiser for water-splitting experiments has been $[\text{Ru}(\text{bipy})_3]^{2+}$ because of its favourable photochemical, photophysical and electrochemical properties.¹⁶⁻¹⁸ This complex, however, has two important drawbacks. Firstly, $[\text{Ru}(\text{bipy})_3]^{2+}$ can only collect a small fraction of the solar energy available. Secondly, when, for example, methylviologen is used as a quencher a large fraction (~75%) of the photoreaction products undergo a back electron-transfer, which means most of the converted energy is dissipated as unrecoverable heat.^{17,58}

The search for new photosensitisers has been most active,⁶⁰⁻⁸⁸ but the requirements each complex must meet are so multifarious and stringent that it is no easy matter to discover a system which is more useful than $[\text{Ru}(\text{bipy})_3]^{2+}$ itself. Naturally many diverse pigments are under consideration, several reports having appeared suggesting that porphyrins may be of some use in this context.⁶⁰⁻⁶² Indeed Borgarello *et al.*⁶² have shown that in the presence of a Pt and RuO_2 catalyst which is codeposited on TiO_2 the complex zinc-tetramethylpyridineporphyrin $[\text{ZnTMpyP}]^{4+}$ may cause the evolution of both hydrogen and oxygen from water when irradiated with visible light. The excited state of this porphyrin system has a long-lifetime of 655 μs at room temperature in water.⁶¹ Other groups have shown that

phthalocyanines, such as magnesium phthalocyanine,⁶³ or completely inorganic photosensitisers, such as $[\text{TBA}]_2^- [\text{Mo}_6\text{Cl}_{14}]$,⁶⁴ when excited by irradiation with visible light may be quenched by, for example, methylviologen therefore allowing the conversion of light into chemical energy. Magnesium phthalocyanine has been shown to have a lifetime of 280 μs in water at room temperature⁶³ whilst $[\text{TBA}][\text{Mo}_6\text{Cl}_{14}]$ has a lifetime of 210 μs in the solid phase at 80K.⁶⁴

However a range of polypyridyl complexes have been prepared in order to investigate any possible advantages of these systems as photosensitisers over $[\text{Ru}(\text{bipy})_3]^{2+}$ ⁶⁵⁻⁸⁸ It is well known that for these bipyridyl and substituted bipyridyl complexes the excited state lifetime depends sensitively on the ligand nature.^{64,65} A range of these species has been prepared which appears to have superior properties than $[\text{Ru}(\text{bipy})_3]^{2+}$ as a photosensitiser in some respects (but regrettably not others). For example, the complex $[\text{Ru}(\text{bipy})_2(\text{DMCH})]^{2+}$ where DMCH is the 2,2'-biquinolyl derivative shown below is able to absorb a larger fraction



DMCH = 3,3'-dimethylene-4,4'-dimethyl-
2,2'-biquinolyl

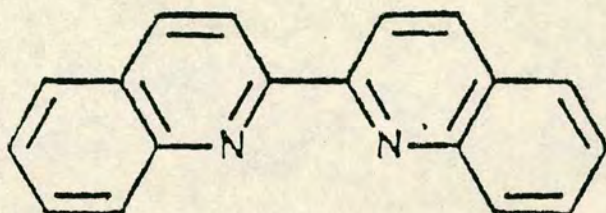
of solar energy⁶⁸ than $[\text{Ru}(\text{bipy})_3]^{2+}$. The extended aromaticity in a ligand such as DMCH means that these ligands may be "superior electron traps", that is they are liable to be more readily reduced. Examination of the emission spectra of $[\text{Ru}(\text{bipy})_2(\text{DMCH})]^{2+}$, $[\text{Ru}(\text{bipy})(\text{DMCH})_2]^{2+}$ and $[\text{Ru}(\text{DMCH})_3]^{2+}$ shows that the threshold energy to form the lowest excited state of each species is significantly lower than in $[\text{Ru}(\text{bipy})_3]^{2+}$. This is a distinct advantage since in principle the excited state of these DMCH complexes could be obtained using lower-energy sensitisers.

Fortunately, the corresponding lower energy content of the excited state DMCH complexes, compared to $^*[\text{Ru}(\text{bipy})_3]^{2+}$, should not compromise the use of these species in the water-splitting cycle. The "molar-free-thermodynamic energy" required to split water is 1.23eV, a magnificent redundancy in excess of this is simply dissipated anyway. It has been pointed out⁶⁶ that $[\text{Ru}(\text{bipy})_2(\text{DMCH})]^{2+}$ is particularly suitable as a sensitiser since, whereas this modification of $[\text{Ru}(\text{bipy})_3]^{2+}$ does not undermine either the reductive or the oxidative steps of the water-splitting cycle, the overall efficiency of energy conversion should be improved as a larger fraction of the solar system can be collected for photoexcitation.

Many of the modified bipyridine ligands which have been used in preparing these complexes are very bulky. In these systems, therefore, incorporation of two or three of these ligands then may lead to considerable steric interactions. We could anticipate either metal-ligand bond strain

or mutual ligand-ligand conformational adjustments.

A close examination of the visible absorption spectrum of such complexes, for example the series of complexes $[\text{Ru}(\text{bipy})_n(\text{biq})_{3-n}]^{2+}$ (where $n = 0$ to 3), show the presence of several anomalies.



2,2'-biquinoline

As discussed in chapter 5, mixed-ligand species such as $[\text{Ru}(\text{L})_n(\text{L}')_{3-n}]^{2+}$ (where L and L' are distinct diimine type ligands and n is 1 or 2) should show separate identifiable $\text{Ru}(\text{d}\pi) \rightarrow \text{L}(\pi^*)$ and $\text{Ru}(\text{d}\pi) \rightarrow \text{L}'(\pi^*)$ charge-transfer bands, respectively similar to those in the parent complexes $[\text{Ru}(\text{L})_3]^{2+}$ and $[\text{Ru}(\text{L}')_3]^{2+}$. In practice such behaviour is not always observed. This might call into question the general applicability of the localised model for the reduced complexes. We have, therefore, carried out a detailed analysis of these systems both in their familiar oxidation state and their reduced forms.

Another area of interest for polypyridyl transition metal complexes is their potential use in the general field of organometallic catalysis. As we discuss in chapter 2, the complex $[\text{Ru}(\text{bipy})_2\text{CO}.\text{Cl}]^+$ has been shown to catalyse

the water-gas shift reaction.

Our studies on this complex and a series of analogous systems $[\text{Ru}(\text{bipy})_2\text{CO.X}]^{n+}$ ($\text{X} = \text{MeCN}, \text{py}, \text{CO}$) have shown that the localised model is again applicable on reducing each complex. Furthermore, some remarkable substitution reactions have also been discovered involving these species when they are oxidised or reduced. These systems may be decarbonylated or alternatively may exchange the sixth ligand X depending on the particular complex and the prevailing conditions. As discussed in chapter 2 this is related to the unique trans-directing influence of the discrete bipy^- ligand. We conclude that the charge-trapped ligand model is pertinent to the general reactivity of such complexes as well as the redox and photochemical phenomena for which the model emerged.

References

1. D.M. Klassen and G.A. Crosby; J.Chem.Phys., 48, 1853 (1968).
2. F.E. Lytle and D.M. Hercules; J.Am.Chem.Soc., 99, 253 (1969).
3. R.W. Harrigan and G.A. Crosby; J.Chem.Phys., 59, 3468 (1973).
4. G.D. Hayer and G.A. Crosby; J.Am.Chem.Soc., 97, 7031 (1975).
5. G.A. Crosby; Acc.Chem.Res., 8, 231 (1975).
6. M. Gleria, F. Minto, G. Beggiato and P. Bertolus; J.Chem.Soc.,Chem.Comm., 285 (1978).
7. P.E. Hoggard and G.B. Porter; J.Am.Chem.Soc., 100, 1457 (1978).
8. K. Itoh and K. Honda; Chem.Lett., 99 (1979).
9. K.W. Hipps; Inorg.Chem., 19, 1390 (1980).
10. B. Darham, J.L. Walsh, C.L. Carter and T.J. Meyer; Inorg.Chem., 19, 860 (1980).
11. T.J. Kemp; Prog.React.Kinet., 10, 301 (1980).
12. M.K. DeArmond and C.L. Carlin; Coord.Chem.Rev., 36, 325 (1981).
13. J. van Houten and R.J. Watts; Inorg.Chem., 17, 3381 (1981).
14. K. Kalyanasundaram; Coord.Chem.Rev., 46, 159 (1982).
15. T.J. Meyer; Isr.J.Chem., 15, 200 (1977).
16. V. Balzani, F. Bolletta, M.T. Gandolfi and M. Maestri; Top.Curr.Chem., 75, 1 (1978).

17. N. Sutin and C. Creutz; Pure Appl.Chem., 52, 2717 (1980).
18. D.G. Whitten; Acc.Chem.Res., 13, 83 (1980).
19. M. Graetzel; Acc.Chem.Res., 14, 376 (1981).
20. M. Graetzel; 'Energy Resources by Photochemistry and Catalysis', Academic Press, New York (1983).
21. J. Rabani, 'Photochemical Conversion and Storage of Solar Energy', Weizmann, Science Press, Jerusalem (1982).
22. G.A. Crosby and W.H. Elfring; J.Phys.Chem., 80, 2206 (1976).
23. N. Sutin and C. Creutz; Adv.Chem.Ser., 168, 1 (1978).
24. W.H. Elfring and G.A. Crosby; J.Am.Chem.Soc., 103, 2683 (1981).
25. R.F. Dallinger and W.H. Woodruff; J.Am.Chem.Soc., 101, 4391 (1978).
26. M. Forster and R.E. Hester; Chem.Phys.Lett., 81, 42 (1981).
27. U. Lachisch, P.P. Infelta and M. Graetzel; Chem.Phys.Lett., 62, 317 (1979).
28. P.G. Bradley, N. Kress, B.A. Homberger, R.F. Dallinger and W.H. Woodruff; J.Am.Chem.Soc., 103, 7441 (1981).
29. P.S. Braterman, A. Harriman, G.A. Heath and L.J. Yellowlees; J.Chem.Soc., Dalton Trans., 1801 (1983).
30. C. Creutz and N. Sutin; J.Am.Chem.Soc., 98, 6384 (1976).
31. C. Creutz and N. Sutin; Inorg.Chem., 15, 496 (1976).

32. C.R. Bock, T.J. Meyer and D.G. Whitten; J.Am.Chem. Soc., 96, 4710 (1974).
33. B. Durham, W.J. Dressick and T.J. Meyer; J.Chem.Soc., Chem.Comm., 381 (1979).
34. U. Lachish, M. Ottolenghi and J. Rabuni; J.Am.Chem. Soc., 99, 8062 (1977).
35. P.A. Lay and W.H.F. Sasse; Inorg.Chem., 24, 4707 (1985).
36. K. Kalyanasundaram and M. Graetzel; Agnew.Chem.Int. Ed.Engl., 18, 701 (1979).
37. D.P. Rillema, W.J. Dressick and T.J. Meyer; J.Chem. Soc.,Chem.Comm., 247 (1980).
38. M. Kirch, J.-M. Lehn and J.P. Sauvage; Helv.Chim. Acta, 62, 1345 (1979).
39. A.B.P. Lever, 'Inorganic Electronic Spectroscopy,' Elsevier Publishing Company, Amsterdam (1968).
40. T. Saji and S. Aogagui; J.Electroanal.Chem., 58, 401 (1975).
41. N.E. Tokel-Takvoryan, R.E. Hemingway and A.J. Bard; J.Am.Chem.Soc., 95, 6582 (1973).
42. B.P. Sullivan, D.J. Salmon, T.J. Meyer and J. Peedin; Inorg.Chem., 18, 3369 (1979).
43. J.L. Kahl, K.W. Hanck and M.K. DeArmond; J.Phys.Chem., 82, 540 (1978).
44. J.G. Gaudiello, P.R. Sharp and A.J. Bard; J.Am.Chem. Soc., 104, 6373 (1982); J.G. Gaudiello, P.G. Bradley, K.A. Norton, W.H. Woodruff and A.J. Bard; Inorg.Chem., 23, 3 (1984).

45. L.J. Yellowlees; Ph.D. Thesis, University of Edinburgh, (1982).
46. (a) A.G. Motten, K.W. Hanck and M.K. DeArmond;
Chem.Phys.Lett., 79, 541 (1981);
(b) D.E. Morris, K.W. Hanck and M.K. DeArmond;
J.Am.Chem.Soc., 105, 3032 (1983).
47. P.S. Braterman, G.A. Heath and L.J. Yellowlees;
J.Chem.Soc.,Chem.Comm., 287 (1981).
48. S.M. Angel, M.K. DeArmond, R.J. Donohue, K.W. Hanck
and D.W. Wertz; J.Am.Chem.Soc., 106, 3688 (1984).
49. E. König and S. Kremer; Chem.Phys.Lett., 5, 87 (1970).
50. G. Kew, K. DeArmond and K.W. Hanck; J.Phys.Chem.,
78, 727 (1974).
51. V.T. Coombe, G.A. Heath, A.J. Mackenzie and
L.J. Yellowlees; Inorg.Chem., 23, 3423 (1984).
52. R.J. Watts, J.S. Harrington and J. Van Houten;
J.Am.Chem.Soc., 99, 2179 (1977).
53. C. Flynn and J. Demas; J.Am.Chem.Soc., 96, 1959
(1974).
54. G. Nord, A.C. Hazell, R.G. Hazell and O. Farver;
Inorg.Chem., 22, 3429 (1983).
55. W.A. Wickramasinghe, P.H. Bird and N. Serpone;
J.Chem.Soc.,Chem.Comm., 1284 (1981).
56. J.S. Connolly, 'Photochemical Conversion and Storage
of Solar Energy', Academic Press, New York (1981).
57. J. Kiwi, E. Borgarello, E. Pellizzetti, M. Visca
and M. Graetzel; Agnew Chem.Int.Ed.Engl., 19, 646
(1980).

58. E. Borgarello, J. Kiwi, E. Pellizzetti, M. Visca and M. Graetzel; Nature, 289, 158 (1981).
59. M. Maestri and D. Sandrini; Nouv.J.Chim., 5, 639 (1981).
60. D.P. Rillema, J.K. Nagle, L.F. Barringer and T.J. Meyer; J.Am.Chem.Soc., 103, 56 (1981).
61. A. Harriman, G. Porter and M. Richoux; J.Chem.Soc., Faraday Trans.II, 77, 833 (1981).
62. E. Borgarello, K. Kalyanasandaram, Y. Okuno and M. Graetzel; Helv.Chim.Acta, 64, 1937 (1981).
63. A. Harrison, G. Porter and M.C. Richoux; J.Chem.Soc., Faraday Trans.II, 77, 1175 (1981).
64. A.W. Maverick and H.B. Gray; J.Am.Chem.Soc., 103, 1298 (1981).
65. S. Anderson, K.R. Seddon, R.D. Wright and A.T. Cocks; Chem.Phys.Lett., 71, 220 (1980).
66. C.-T. Lin, W. Brettcher, M. Chou, C. Creutz and N. Sutin; J.Am.Chem.Soc., 98, 6536 (1976).
67. N. Serpone, M.A. Jamieson, M.S. Henry, M.Z. Hoffman, F. Bolletta and M. Maestri; J.Am.Chem.Soc., 101, 2907 (1979).
68. A. Juris, V. Balzani, P. Belser and A. Von Zelewsky; Helv.Chim.Acta, 64, 2175 (1981).
69. S.F. Agnew, H.L. Stone and G.A. Crosby; Chem.Phys.Lett., 85, 57 (1982).
70. A. Basu, M.A. Weiner, T.C. Streaks and H.D. Gafney; Inorg.Chem., 21, 1085 (1982).
71. D.P. Seyers and M.K. DeArmond; J.Phys.Chem., 86, 3768 (1982).

72. P. Belser, A. Von Zelewsky, A. Juris, F. Barigelletti, A. Tucci and V. Balzani; Chem.Phys.Lett., 89, 101 (1982).
73. D.M. Klassen; Chem.Phys.Lett., 93, 383 (1982).
74. R.J. Crutchley, M. Kress and A.B.P. Lever; J.Am. Chem.Soc., 105, 1170 (1983).
75. D.M. Manuta and A.J. Lees; Inorg.Chem., 22, 572 (1983).
76. P.J. Steel, F. Lahousse, D. Lermer and C. Marzin; Inorg.Chem., 22, 1488 (1983).
77. P. Belser, A. Von Zelewsky, A. Juris, F. Barigelletti, and V. Balzani; Gazzetta Chimica Italiana, 113, 731 (1983).
78. F. Barigelletti, A. Juris, V. Balzani, P. Belser and A. Von Zelewsky; Inorg.Chem., 22, 3335 (1983).
79. D.P. Rillema, G. Allen, T.J. Meyer and D. Conrad; Inorg.Chem., 22, 1617 (1983).
80. N. Kitamura, Y. Kawashini, S. Tazaki; Chem.Phys.Lett., 97, 103 (1983).
81. G.H. Allen, R.P. White, D.P. Rillema and T.J. Meyer; J.Am.Chem.Soc., 106, 2613 (1984).
82. W.R. Cherry and L.J. Henderson jr.; Inorg.Chem., 23, 983 (1984).
83. D.E. Morris, Y. Ohsawa, D.P. Segers, M.K. DeArmond and K.W. Hanck; Inorg.Chem., 23, 3010 (1984).
84. M.N. Ackerman and L.V. Interrante; Inorg.Chem., 23, 3904 (1984).
85. A. Juris, F. Barigelletti, V. Balzani, P. Belser and A. Von Zelewsky; Inorg.Chem., 24, 202 (1985).

86. A. Juris, P. Belser, F. Barigelletti, A. Von Zelewsky and V. Balzani; Inorg.Chem., 25, 1738 (1986).
87. N. Sabbatini, S. Dellonte, A. Bonazzi, M. Ciano and V. Balzani; Inorg.Chem., 25, 1738 (1986).
88. K.J. Brewer, W.R. Murphy, jr., S.R. Shurlin and J.D. Peterson; Inorg.Chem., 25, 882 (1986).

Chapter 2

Electrochemical and Absorption Spectral Studies (45 000 - 12 500 cm^{-1}) of cis-Bis-2,2'-bipyridyl Carbonyl Complexes of Ruthenium(II)

In chapter 1 we reported on the interest which has been shown in the complex $[\text{Ru}(\text{bipy})_3]^{2+}$, I, due to its unusual photoredox properties and the thermodynamic capability of its excited state species to photodissociate water. Much of this interest was aroused by a report that the visible light irradiation of a monolayer sample of a surfactant derivative of $[\text{Ru}(\text{bipy})_3]^{2+}$, immersed in water, led to the evolution of hydrogen. However, later studies²⁻⁵ proved that highly purified samples of this material were inactive, and it was suggested that some form of catalytically active impurity, an unidentified ruthenium complex, was present in the original sample.⁶

It was later reported⁷ that the complex cis- $[\text{Ru}(\text{bipy})_2\text{CO.Cl}]^+$, III, a by-product in the synthesis of cis- $[\text{Ru}(\text{bipy})_2\text{Cl}_2]$, IV, catalysed the photochemical water-gas shift reaction. More recently Tanaka⁸ and co-workers have shown that the same complex also catalyses the water-gas shift reaction in the absence of light.

The optical and redox properties of cis- $[\text{Ru}(\text{bipy})_2\text{CO.Cl}]^+$, II, and related complexes are then of great interest, therefore we studied the voltammetric behaviour of a range of substituted carbonyl-bis-bipyridine ruthenium(II) complexes.

The absorption spectra of these species, both in their "familiar oxidation state" and in their electro-reduced and oxidised forms are also examined.

However, since many of the electrogenerated species we wish to study are extremely air sensitive they must be generated in situ, in the beam of a spectrophotometer, in order that their absorption spectra may be examined. We can achieve this by utilising a transparent working electrode, in our case a platinum gauze which is sandwiched between two quartz plates in a modified 0.5mm cell. This type of system is known as an optically transparent thin layer electrode, O.T.T.L.E.,¹⁰ and it is mounted in a gas-tight block as shown in figure 1.

The complexes examined here are of the general form $[\text{Ru}(\text{bipy})_2\text{CO.X}]^{n+}$ and range from species where X is the strong π -acceptor ligand, carbonyl, to the pronounced π -donor ligand, chloride. Pertinent electrochemical data obtained in these studies are collected in table 1.

From table 1 it is apparent that the electrode potentials characteristic of each species are markedly dependent on the nature of the sixth ligand. A comparison of $[\text{Ru}(\text{bipy})_2\text{CO.Cl}]^+$, III, with $[\text{Ru}(\text{bipy})_3]^{2+}$ and $\text{Ru}(\text{bipy})_2\text{Cl}_2$ allows us to interpret our electrochemical data.

It is known that the oxidation of the complexes $[\text{Ru}(\text{bipy})_3]^{2+}$ and $[\text{Ru}(\text{bipy})_2\text{Cl}_2]$ is metal-based,¹²

$\text{Ru(II)}/\text{Ru(III)}$, with the dichloro-complex being oxidised more readily. This is due to the negative charge and π -donor properties of the chloride ligands which replace the third bipyridine ligand and stabilise Ru(III) relative to

Key to Figure 1

- A - Counter Electrode
- B - Reference Electrode
- C - Working Electrode connection protected from bulk solution by PTFE sleeve
- D - PTFE cell cap
- E - Test solution, deoxygenated with Ar or N₂
- F - 0.5mm Infrasil quartz cell containing platinum grid working electrode
- G - Platinum grid working electrode
- H - PTFE cell block
- I - Variable temperature nitrogen inlet ports to allow cooling of cell and test solution
- J - Dry nitrogen inlet ports (to prevent fogging of inner quartz windows)
- K - Infrasil quartz cell block windows

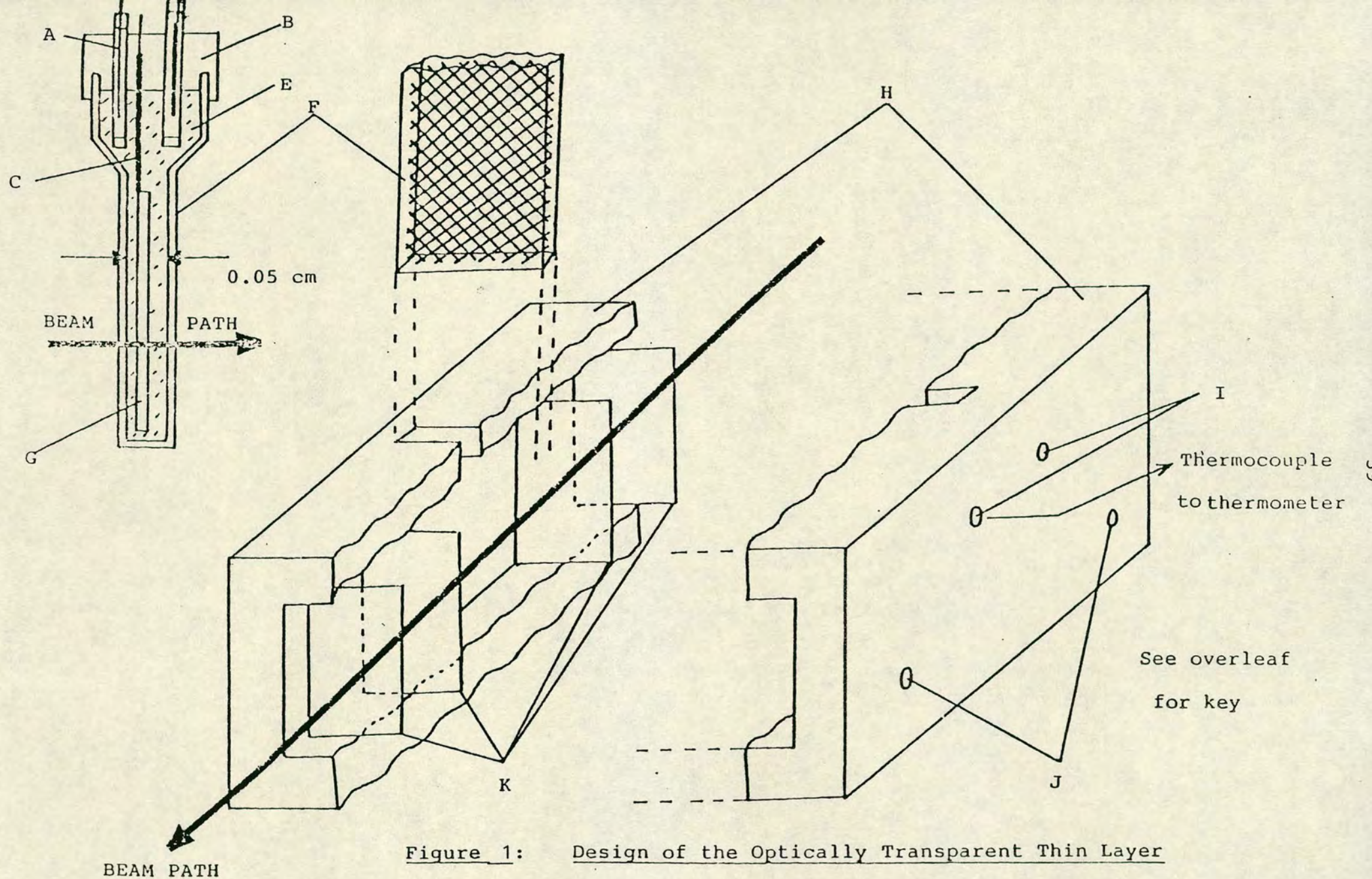


Figure 1: Design of the Optically Transparent Thin Layer
Electrode

Ru(II). The d^5 Ru(III) centre is a good π -acceptor owing to the vacancy in the $d\pi$ sub-shell and its high core charge. Incorporation of a π -acceptor carbonyl ligand allows back-donation of electronic charge from the metal centre to take place, more from Ru(II) than Ru(III). The Ru(II) $d\pi^6$ orbital manifold in $[\text{Ru}(\text{bipy})_2\text{CO}.\text{Cl}]^+$ is therefore stabilised with respect to $[\text{Ru}(\text{bipy})_2\text{Cl}_2]$. This is reflected in the observed RuII/III potentials where we find, as expected, it is 1.2 volts more difficult to oxidise $[\text{Ru}(\text{bipy})_2\text{CO}.\text{Cl}]^+$ than $[\text{Ru}(\text{bipy})_2\text{Cl}_2]$.

Before examining the reductive behaviour of these complexes, it should be noted that, for tris-bipyridyl metal complexes it has been shown that the potential required to reduce each bipyridyl ligand is dependent upon the central metal charge.¹³ Those studies illustrated that for each unit of positive charge on the central metal it was approximately 0.4 volts easier to reduce the bipyridine ligand. However, in the series of complexes now under study the first reduction potential depends upon the extent of π -back-bonding from the ligands present to the metal centre. This is illustrated by a comparison of $[\text{Ru}(\text{bipy})_3]^{2+}$ with $[\text{Ru}(\text{bipy})_2(\text{CO})_2]^{2+}$ and $[\text{Ru}(\text{bipy})_2\text{Cl}_2]$.

Viewed in this way, replacement of one π -acceptor bipyridine ligand, in $\text{Ru}(\text{bipy})_3^{2+}$, by two π -donating chloride ligands leads to a decrease in the effective central metal charge and a corresponding increase in the difficulty of reduction of the first bipyridine ligand by approximately

Table 1: Electrochemical Results for Ruthenium
Bipyridyl Systems^a

<u>Complex</u>	<u>E(ox)^b</u>	<u>E(red 1.)</u>	<u>E(red 2)</u>
¹¹ [Ru(bipy) ₂ Cl ₂]	+0.01	-1.95	-2.06
⁶ [Ru(bipy) ₂ CO.H] ⁺	+0.86 ^c	-1.71	-1.90
¹² [Ru(bipy) ₃] ²⁺	+0.96	-1.66	-1.83
⁶ [Ru(bipy) ₂ CO.Cl] ⁺	+1.20	-1.61	-1.82
⁶ [Ru(bipy) ₂ CO.py] ²⁺	+1.80	-1.46	-1.64
⁶ [Ru(bipy) ₂ CO.MeCN] ²⁺	+1.91	-1.43	-1.62
⁶ [Ru(bipy) ₂ (CO) ₂] ²⁺	+2.4 ^d	-1.23	-1.43

a - All data presented above have been collected in this study. Previous reports of each systems voltammetric behaviour are cited separately.

b - All potentials measured at 20°C in both acetonitrile and dichloromethane, scan rate 100mV/s, Ag/Ag⁺ reference electrode.

c - Irreversible oxidation.

d - Estimated value obtained by extrapolation of the oxidation potential for [Ru(bipy)₂Cl₂] and [Ru(bipy)₂CO.Cl]⁺ to [Ru(bipy)₂(CO)₂]²⁺.

0.4 volts. Contrastingly, by replacing one bipyridine ligand, in $\text{Ru}(\text{bipy})_3^{2+}$ by two stronger π -acceptor carbonyl ligands, $\text{Ru}(\text{bipy})_2(\text{CO})_2^{2+}$ becomes 0.4 volts easier to reduce.

By using the electrochemical data in table 1 we may construct a schematic frontier molecular orbital diagram relating the species described above since we know that the oxidation of each species is metal-based and each reduction is bipyridine based. This diagram is shown in figure 2.

For a $\text{Ru}(\text{II})$ bipyridine species we expect the absorption spectrum to contain bands due to:

- i) metal to ligand charge transfer transitions, that is $(\text{Ru}(\text{II})d\pi \rightarrow \pi^*(\text{bipy}))$;
- ii) intraligand $\pi\pi^*$ transitions of bipy;
- iii) transitions corresponding to i) and ii) for the accompanying ligand X; depending on the nature of X these transitions may not be visible.

Transition i) is illustrated in figure 3.

It is evident that the metal to ligand charge-transfer (MLCT) band which dominates the visible region of the electronic spectrum in $[\text{Ru}(\text{bipy})_3]^{2+}$ and $[\text{Ru}(\text{bipy})_2\text{Cl}_2]$ should be moved to higher energies in $[\text{Ru}(\text{bipy})_2\text{CO.Cl}]^+$ and $[\text{Ru}(\text{bipy})_2(\text{CO})_2]^{2+}$. Indeed, this is observed with the MLCT band in $[\text{Ru}(\text{bipy})_2\text{CO.Cl}]^+$ being blue-shifted towards the ultra-violet region where it is observed as a shoulder at $24\,100\text{ cm}^{-1}$.

A strong correlation emerges for the gap between the oxidation and the first reduction of each complex and the

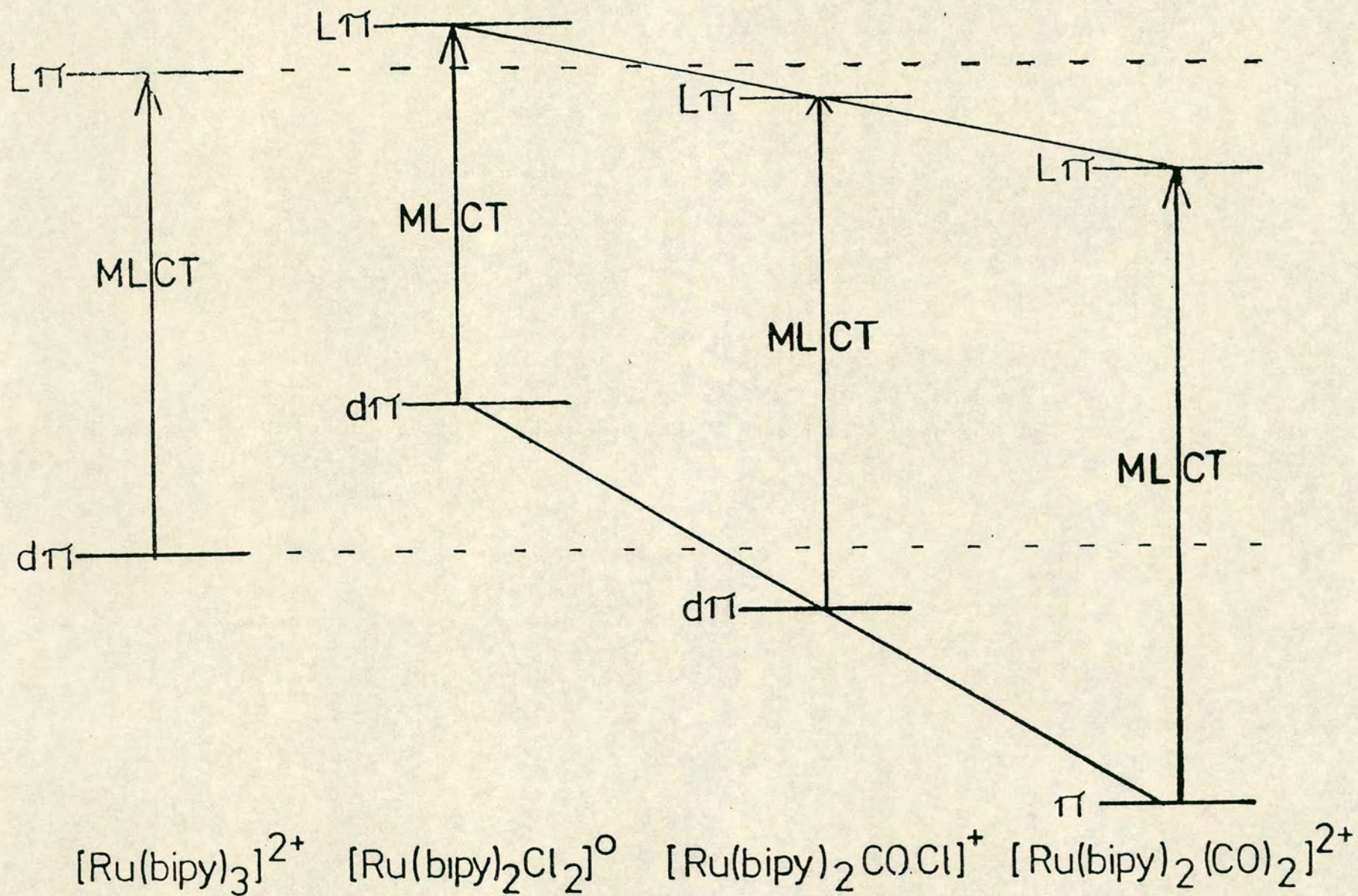
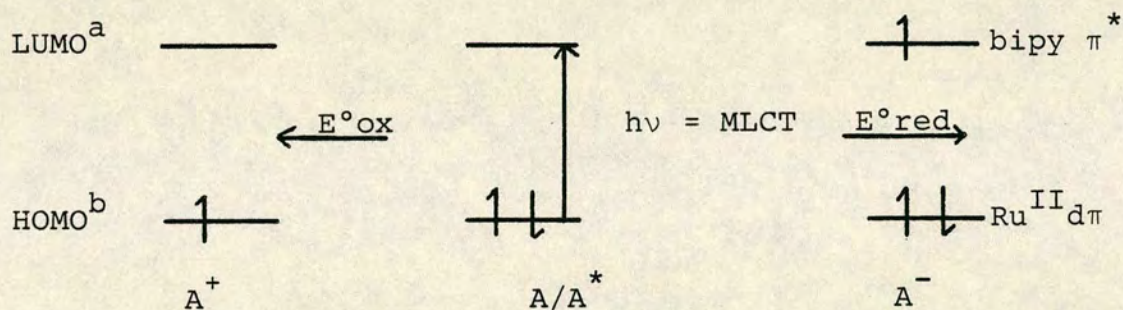


Figure 2: Schematic Energy Level Scheme for a Series of Complexes $[\text{Ru}(\text{bipy})_2(\text{X})(\text{Y})]^{n+}$

position of the metal-to-ligand charge-transfer band. As we have shown in chapter 1, the optical transition in $[\text{Ru}(\text{bipy})_3]^{2+}$ involves the transfer of an electron from the metal core to an acceptor orbital localised on one bipyridyl ligand. This transition is therefore assigned as $d\pi^6 \pi^*0 \rightarrow d\pi^5 \pi^*1$ as shown in figure 3.

Figure 3: Spectral/Electrochemical Correlation of the Frontier Orbitals in Ruthenium(II)-Bipyridine Complexes



a - LUMO = Lowest Unoccupied Molecular Orbital

b - HOMO = Highest Occupied Molecular Orbital.

As shown in table 2 the complexes under study follow this model well.

Table 2: Correlation of Electrochemical and Spectroscopic Data for Ruthenium(II)-bipyridine Complexes

<u>Complex</u>	<u>(E^{ox}-E^{red}/eV)</u>	<u>MLCT/eV</u>
Ru(bipy) ₂ Cl ₂	1.96	2.2
Ru(bipy) ₃ ²⁺	2.62	2.7
Ru(bipy) ₂ CO.Cl ⁺	2.81	3.0
Ru(bipy) ₂ CO.MeCN ²⁺	3.34	3.3
Ru(bipy) ₂ CO.py ²⁺	3.26	3.2
Ru(bipy) ₂ CO.H ⁺	2.57	2.7

It should be noted however that there is an intrinsic difference between the spectroscopic and electrochemical phenomena. The optical event may be described as a vertical transition which involves an electronic promotion to obtain the excited state species, with this vibrationally excited species retaining its ground state geometry. The electrode-potential data however always refer to thermally equilibrated molecules in the geometry appropriate to their respective oxidation states and therefore have thermodynamic significance.

The ultra-violet spectra of the complexes $[\text{Ru}(\text{bipy})_2\text{CO.X}]^{n+}$ ($\text{X}=\text{Cl}, \text{py}, \text{CO}, \text{MeCN}$) as a class exhibit three bands which we would readily assign to intra-ligand $\pi\pi^*$ bipyridyl transitions. Interestingly the lowest energy component of these bands, at approximately $32\,000\text{ cm}^{-1}$, which is not observed in $[\text{Ru}(\text{bipy})_3]^{2+}$ or $[\text{Ru}(\text{bipy})_2\text{Cl}_2]$, exhibits a striking resemblance to a band observed in many Ru(III)(bipy)_n complexes.¹³⁻¹⁵ It has been proposed independently that the electron-withdrawing capability of the carbonyl ligand, in these systems, causes a reduction in electron density at the bipyridyl ligands which is comparable to that experienced in ruthenium(III) complexes.⁶

The behaviour of the catalytically-active complex $[\text{Ru}(\text{bipy})_2\text{CO.Cl}]^+$ and the related systems is then of great interest. We have examined these systems obtaining their absorption spectra in both their reduced and oxidised forms. The bands observed in each spectrum have been assigned in relation to self-consistent energy level schemes.

cis-Carbonylchlorobis(bipyridine)ruthenium(II), (III)

A cyclic voltammogram of $[\text{Ru}(\text{bipy})_2\text{CO.Cl}](\text{BPh}_4)$ recorded at room temperature, in dichloromethane at a platinum microelectrode, is shown in figure 4. One reversible one-electron oxidation and two reversible one-electron reductions are observed. This complex was also studied in acetonitrile and dimethylsulphoxide with the potentials of the reductive processes found to be invariant. Equally the position of the oxidative wave $\text{III}^+/\text{III}^0$ did not vary when studies were carried out in acetonitrile and dichloromethane however, the limited anodic range of dimethylsulphoxide meant that the $\text{III}^+/\text{III}^0$ couple could not be measured in this solvent. These experiments show that there is no important interaction between the complex and the solvent, in its rest state or its reduced or oxidised forms.

Although the reductions of this complex are closely spaced (210mV separation) each reduced species can be selectively generated in bulk by controlled potential electrosynthesis at a large electrode in a conventional electrochemical cell.

A bulk electrogeneration of the one-electron oxidation product gives the species $[\text{Ru}(\text{bipy})_2\text{CO.Cl}]^{2+}$, which is stable if stored under argon. Generation of III^+ at a platinum O.T.T.L.E., at +1.50V vs Ag/Ag^+ , is shown in figure 5.

During the course of this oxidation clear isosbestic points are observed, four in number, which imply a simple one-to-one conversion of III to III^+ has taken place.

Figure 4: Cyclic Voltammogram of $[\text{Ru}(\text{bipy})_2\text{CO.Cl}]^+$
in Dichloromethane at Room Temperature

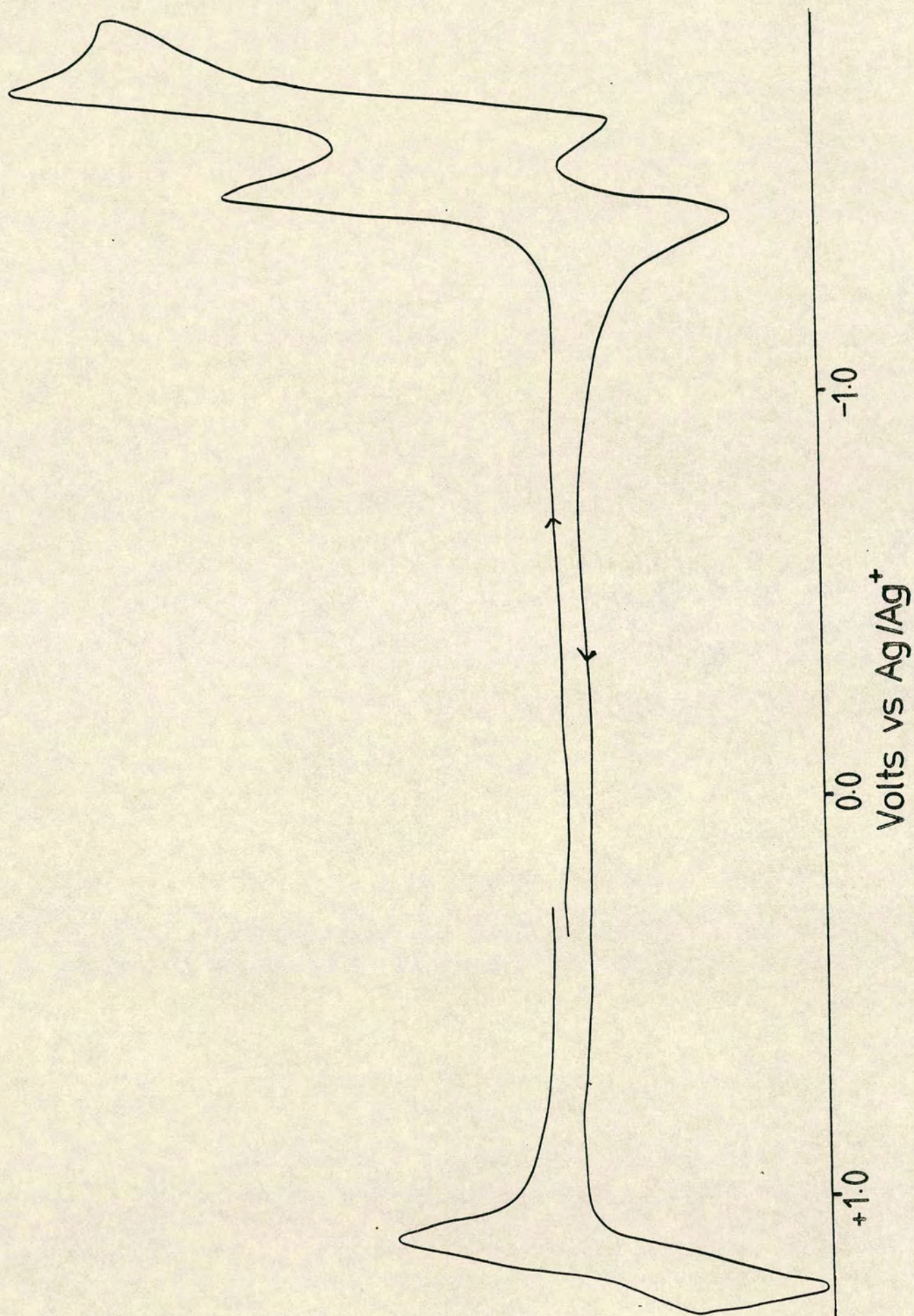
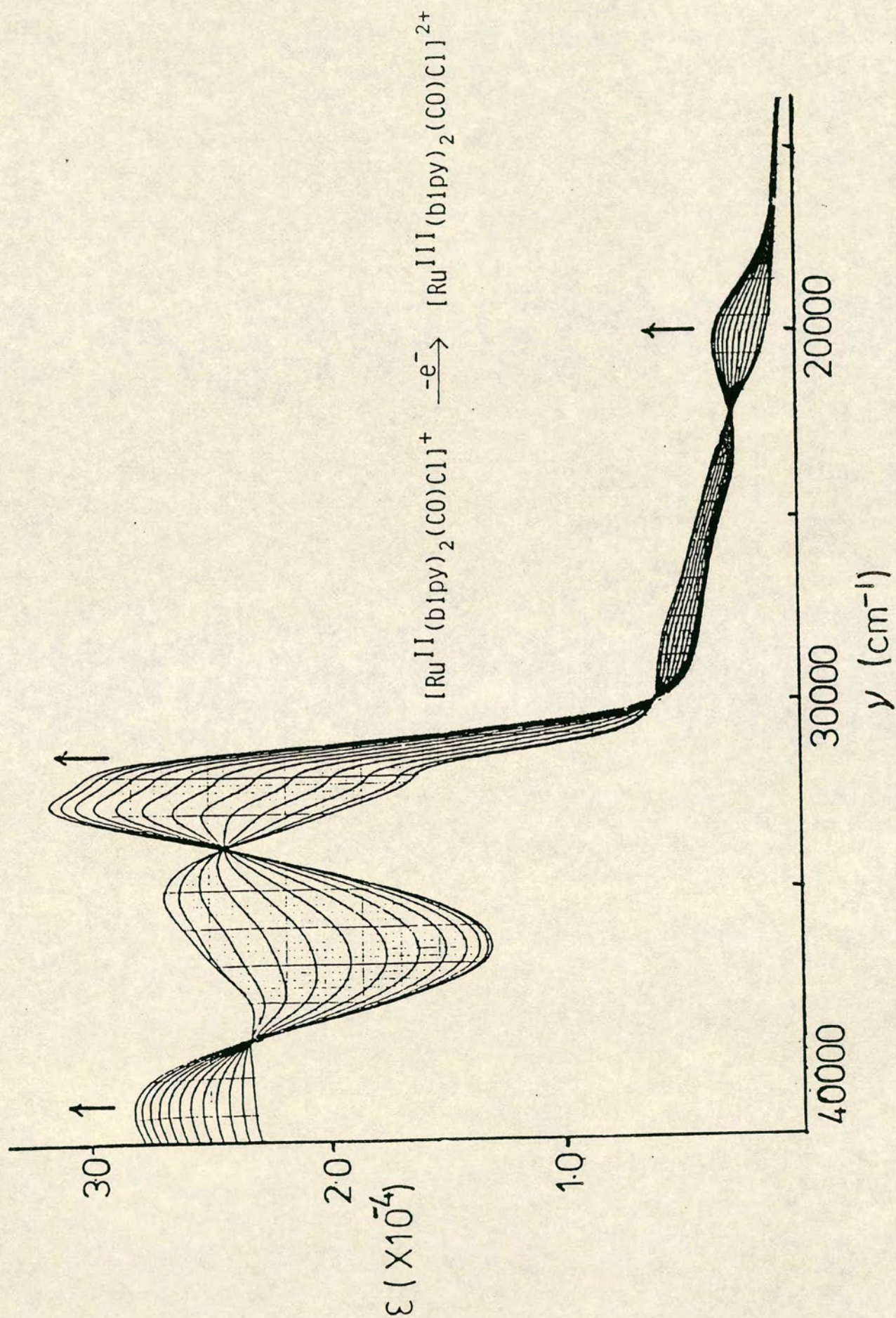


Figure 5: Absorption Spectra of $[\text{Ru}(\text{bipy})_2\text{CO}.\text{Cl}]^{+2+}$ in Dichloromethane at Room Temperature



The complete conversion to the oxidised species is indicated by the achievement of a steady-state spectrum and the decay of the electrosynthesis current. As in all experiments of this type, the results were only accepted if the original spectrum could then be regained in its original intensity by reversal of the applied potential to zero volts.

Some bands are observed to collapse while new bands grow during the course of electrolysis. If this oxidation is indeed metal-based then we would expect to observe bands due to:

- i) intraligand transitions in the bipyridine ligand ($\pi \rightarrow \pi^*$ bipy⁰). Experience suggests that these should be shifted to lower energies upon oxidation due to the increase in the central metal charge (compare $[\text{Ru}(\text{bipy})_3]^{2+}$, where the lowest intraligand band is observed at $34\,800\text{ cm}^{-1}$, with $[\text{Ir}(\text{bipy})_3]^{3+}$ where the band is found at $32\,200\text{ cm}^{-1}$);
- ii) ligand-to-metal charge-transfer transitions from both chloride and bipyridine to the Ru(III) core, that is $((\text{Cl}^-)\pi \rightarrow \text{Ru(III)}d\pi)$ and $(\text{bipy})\pi \rightarrow \text{Ru(III)}d\pi$;
- iii) to metal-to-ligand charge-transfer transitions from the ruthenium(III) centre to bipyridine, that is $\text{Ru(III)}d\pi \rightarrow (\text{bipy})\pi^*$.

Assignment of the bands in the absorption spectrum of III^+ is aided by comparison with the spectra of $[\text{Ru}(\text{bipy})_3]^{3+}$ and $[\text{Ru}(\text{bipy})_2\text{Cl}_2]^+$ which were discussed in chapter 1 with the observed bands listed in table 3.

The strong π -acceptor characteristics of the carbonyl

Table 3: Assignment of the Absorption Bands in
 $[\text{Ru}(\text{bipy})_3]^{3+}$ and $[\text{Ru}(\text{bipy})_2\text{Cl}_2]^+$ $\times 10^{-3}/\text{cm}^{-1}$
 $(\epsilon \times 10^{-4})$

<u>Complex</u>	<u>Transition</u>				
	$\pi(6) \rightarrow \pi(8)$ $\underline{\text{bipy}^0}$	$\pi(6) \rightarrow \pi(7)$ $\underline{\text{bipy}^0}$	$\text{Ru(III)}\text{d}\pi$ $\underline{\rightarrow \text{bipy}(7)}$	$\pi(5)\text{bipy}$ $\underline{\rightarrow \text{Ru(III)}\text{d}\pi}$	$\pi(6)\text{bipy}$ $\underline{\rightarrow \text{Ru(III)}\text{d}\pi}$
$[\text{Ru}(\text{bipy})_3]^{3+}$	40.3(4.55)	32.9(4.73) 31.8(4.61)	a	23.8(0.28)b	15.0(0.08)
$[\text{Ru}(\text{bipy})_2\text{Cl}_2]^+$	41.2(2.88)	33.3(3.12)	26.5(0.78)c	a,b	21.7(0.28)
		32.1(2.68)			

a - Band obscured

b - Assuming the $\pi(5)-\pi(6)$ and $\pi(7)-\pi(8)$ gaps are of similar energy

c - $\text{Cl}^- \pi \rightarrow \text{Ru(III)d}\pi$ is observed at $28\,000\text{ cm}^{-1}$ in $[\text{RuCl}_6]^{3-}$ (16)



ligand in $[\text{Ru}(\text{bipy})_2\text{CO.Cl}]^+$, III, which significantly lowered the energy of the $d\pi$ level in III relative to $[\text{Ru}(\text{bipy})_3]^{2+}$ and $[\text{Ru}(\text{bipy})_2\text{Cl}_2]^+$ are important when interpreting the absorption spectrum of III^+ . If we consider $[\text{Ru}(\text{bipy})_3]^{3+}$, I^+ , and $[\text{Ru}(\text{bipy})_2\text{CO.Cl}]^{2+}$, III^+ , the ligand orbitals are found to be at similar energies hence the ML(bipy)CT transition should be moved to higher frequencies in $[\text{Ru}(\text{bipy})_2\text{CO.Cl}]^{2+}$ with the lowest energy L(bipy)MCT transition therefore being observed at a lower frequency than for $[\text{Ru}(\text{bipy})_3]^{3+}$.

The absorption spectrum of III^+ fulfils these expectations therefore we could realistically interpret this species in terms of the chromophores present as $[\text{Ru}(\text{III})(\text{bipy})^0_2\text{CO.Cl}]^{2+}$ with the bands assigned as in table 4.

Construction of a self-consistent energy-level diagram, which relates III and III^+ , allows us to test these assignments. In figure 8 we have taken the Ru(II) complex and mapped the energy levels of the oxidised species in relation to it. Since it is known that the reduction of a M(III)-bipy system is approximately 0.32V ($2\ 600\ \text{cm}^{-1}$) easier than the corresponding M(II) system (from the difference in the first reduction potentials of $[\text{Ru}(\text{bipy})_3]^{2+}$ and $[\text{Ir}(\text{bipy})_3]^{3+}$) we can position the $\pi(7)$ level. Then by noting the estimated potential of the Ru(III/IV) couple and the lowest energy $\pi\pi^*$ bipy⁰ transition in $[\text{Ru}(\text{bipy})_2\text{CO.Cl}]^{2+}$, III^+ , the ruthenium(III) $d\pi$ orbital and the highest filled π -level of bipyridine may be located.

Table 4: Absorption Bands in $[\text{Ru}(\text{bipy})_2\text{CO.Cl}]^{+/2+} (\text{III}^{\text{O}/+}) \nu \times 10^{-3}/\text{cm}^{-1} (\epsilon \times 10^{-4})$

Complex	Transition						
	$\frac{\pi(6) \rightarrow \pi(8)}{\text{bipy}^{\text{O}}}$	$\frac{\pi(6) \rightarrow \pi(7)}{\text{bipy}^{\text{O}}}$	$\frac{\text{Ru}d\pi}{\rightarrow \text{bipy}\pi(8)}$	$\frac{\text{Ru}d\pi}{\rightarrow \text{bipy}\pi(7)}$	$\frac{\text{Cl}^-\pi \rightarrow}{\text{Ru(III)}d\pi}$	$\frac{\text{bipy}\pi(5)}{\rightarrow \text{Ru(III)}d\pi}$	$\frac{\text{bipy}\pi(6)}{\rightarrow \text{Ru(III)}d\pi}$
$[\text{Ru}(\text{bipy})_2\text{CO.Cl}]^+$	31.0(2.29)	35.1(2.63) 32.0(1.58)	29.0(0.46) ^b	24.1(0.22) ^b	-	-	-
$[\text{Ru}(\text{bipy})_2\text{CO.Cl}]^{2+}$	40.8(2.76)	32.8(3.08) 32.0(2.95)	a	a	26.8(0.23) ^c	20.5(0.21) ^d	11.4(0.05)

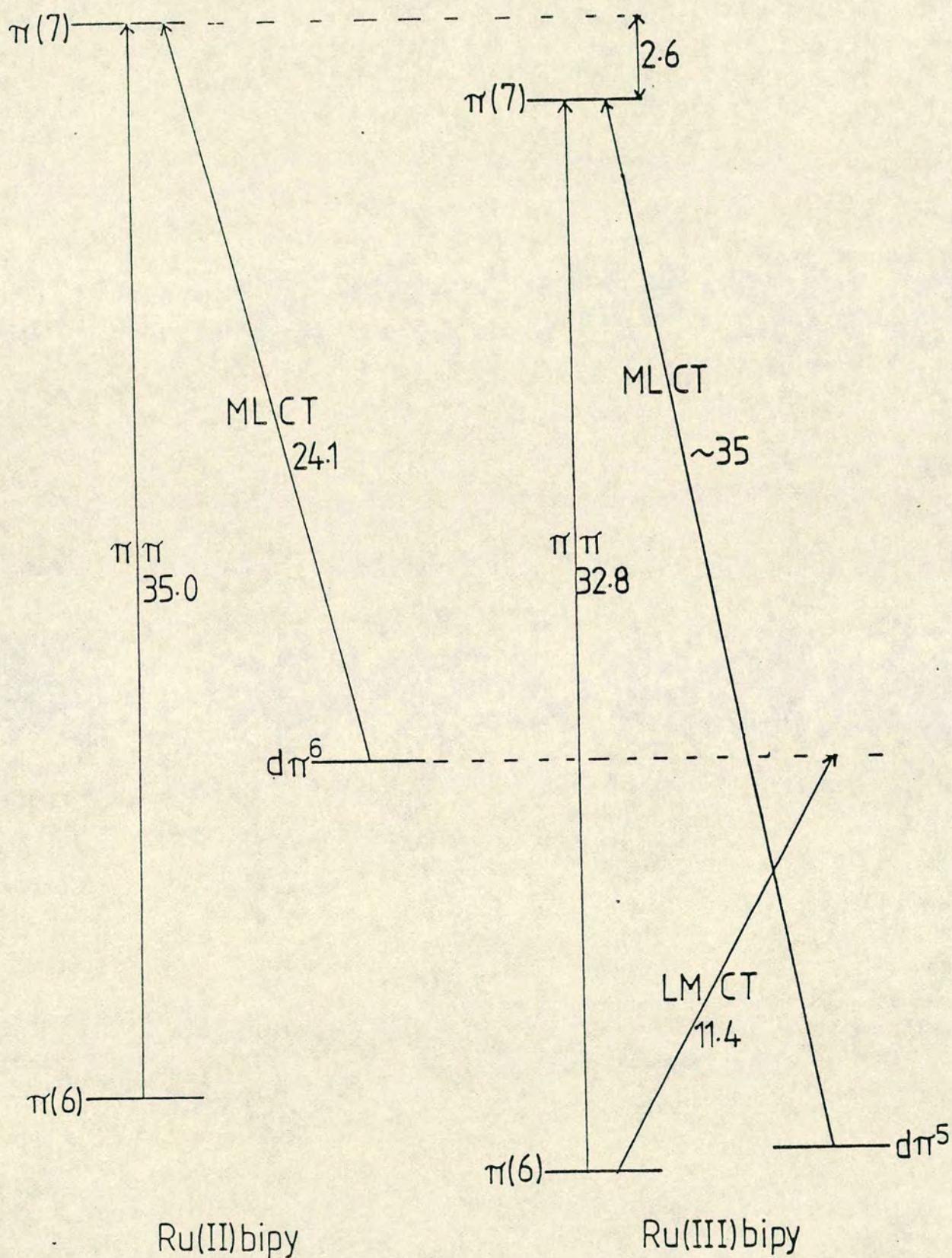
a - Band obscured

b - Band observed as a shoulder

c - $\text{Cl}^- \rightarrow \text{Ru(III)}$ is observed at $28\,000\text{ cm}^{-1}$ in $[\text{Ru Cl}_6]^{3-}$

d - Assuming the $\pi(5)-\pi(6)$ and $\pi(7)-\pi(8)$ gaps are of similar energy (16)

Figure 6: Schematic Energy Level Scheme for $[\text{Ru}(\text{bipy})_2\text{CO.Cl}]^{+/2+}$



Note

- The Ru(III)/(IV) couple is estimated to be 1.6 volts ($\equiv 12\,900\text{ cm}^{-1}$) beyond the Ru(II/III) wave.
- The figures listed above are directly measured optical transitions.

The bands observed in these species may all be satisfactorily assigned with the absorption at $11\,400\text{ cm}^{-1}$ being in agreement with our predicted value for the $\text{bipy}\pi(6) \rightarrow \text{Ru(III)}d\pi$ transition of $11\,300\text{ cm}^{-1}$.

We have therefore characterised $[\text{Ru}(\text{bipy})_2\text{CO.Cl}]^{2+}$ as a ruthenium(III) carbonyl complex. Although several such systems are known¹⁷ it is relatively unusual to find complexes containing the $\text{Ru(III)}-\text{CO}$ moiety in company with two π -acceptor ligands,^{18,19} such as bipyridine, which prefer to stabilise low oxidation state metal centres.

The two one-electron reduced species III^- and III^{2-} were separately generated at a platinum O.T.T.L.E., at -1.70V and -1.90V vs Ag/Ag^+ respectively, at -40°C , in dichloromethane. If the localised theory of bipyridine reductions is applicable to this complex then the stepwise growth of bands characteristic of a $\text{Ru(II)}-\text{bipy}^\cdot$ chromophore accompanied by the loss of bands characteristic of the neutral bipyridine ligand should be observed.

The absorption spectra of the species $\text{III}^{0/-/2-}$ are shown in figure 7. Examination of the visible and near ultra-violet spectrum of III^- and III^{2-} reveals the emergence of three bands. A comparison with the published spectrum of $\text{Li}^+\text{bipy}^\cdot$ ²⁰ (figure 8) shows the principal bands in $\text{III}^{-/2-}$ to be characteristic of the bipyridyl anion (see chapter 1). It would be expected that on reduction of this complex a progressive loss of the metal-to-ligand charge-transfer bands would be observed, however the $\pi \rightarrow \pi^*$ bipy^\cdot band which grows at approximately $27\,000\text{ cm}^{-1}$ is much more

Figure 7: Absorption Spectra of $[\text{Ru}(\text{bipy})_2\text{CO}_2\text{Cl}]^{+/-}$ in Dichloromethane at -40°C

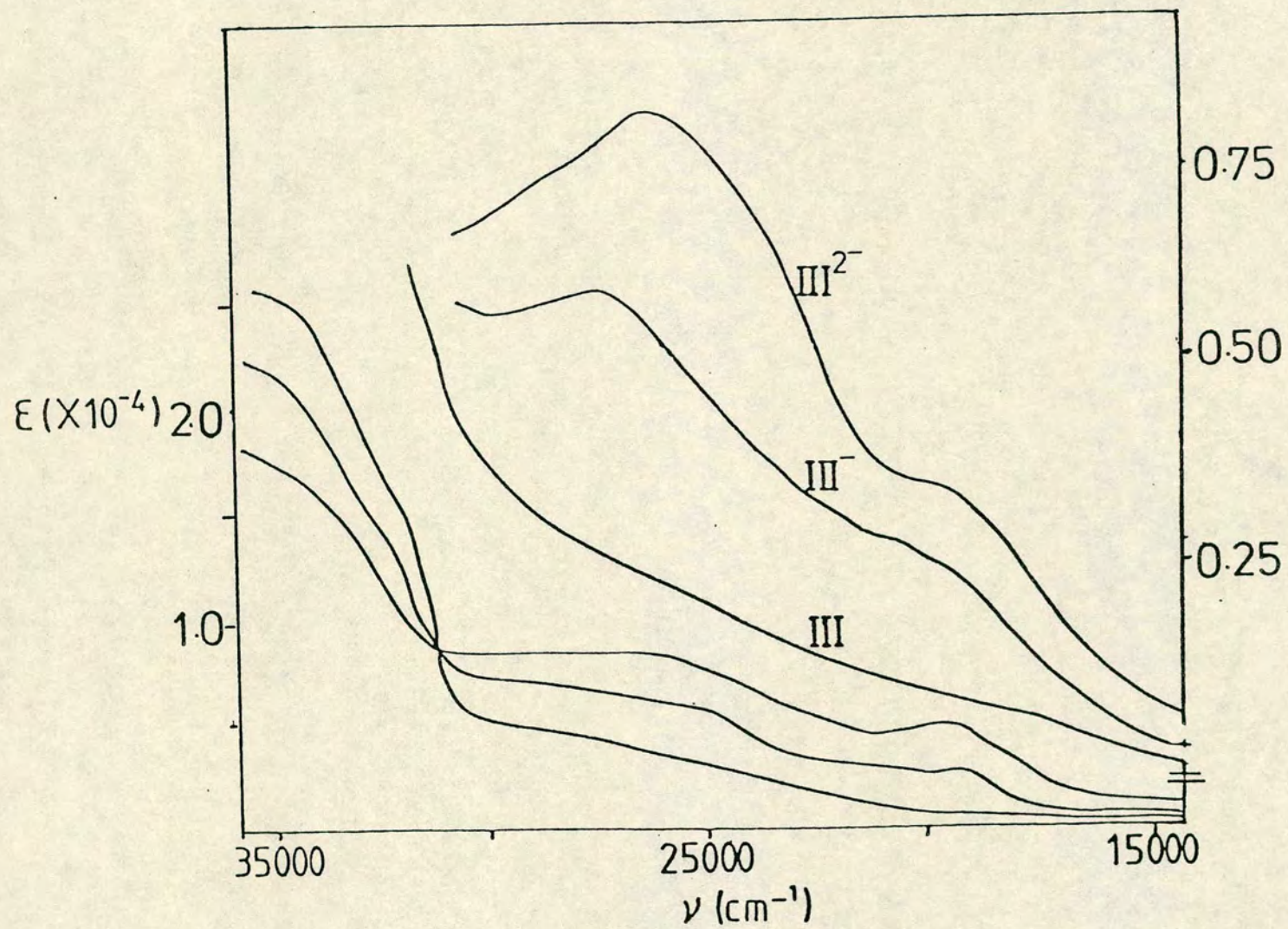


Figure 8: Absorption Spectrum of Li^+bipy^- in Tetrahydrofuran at Room Temperature

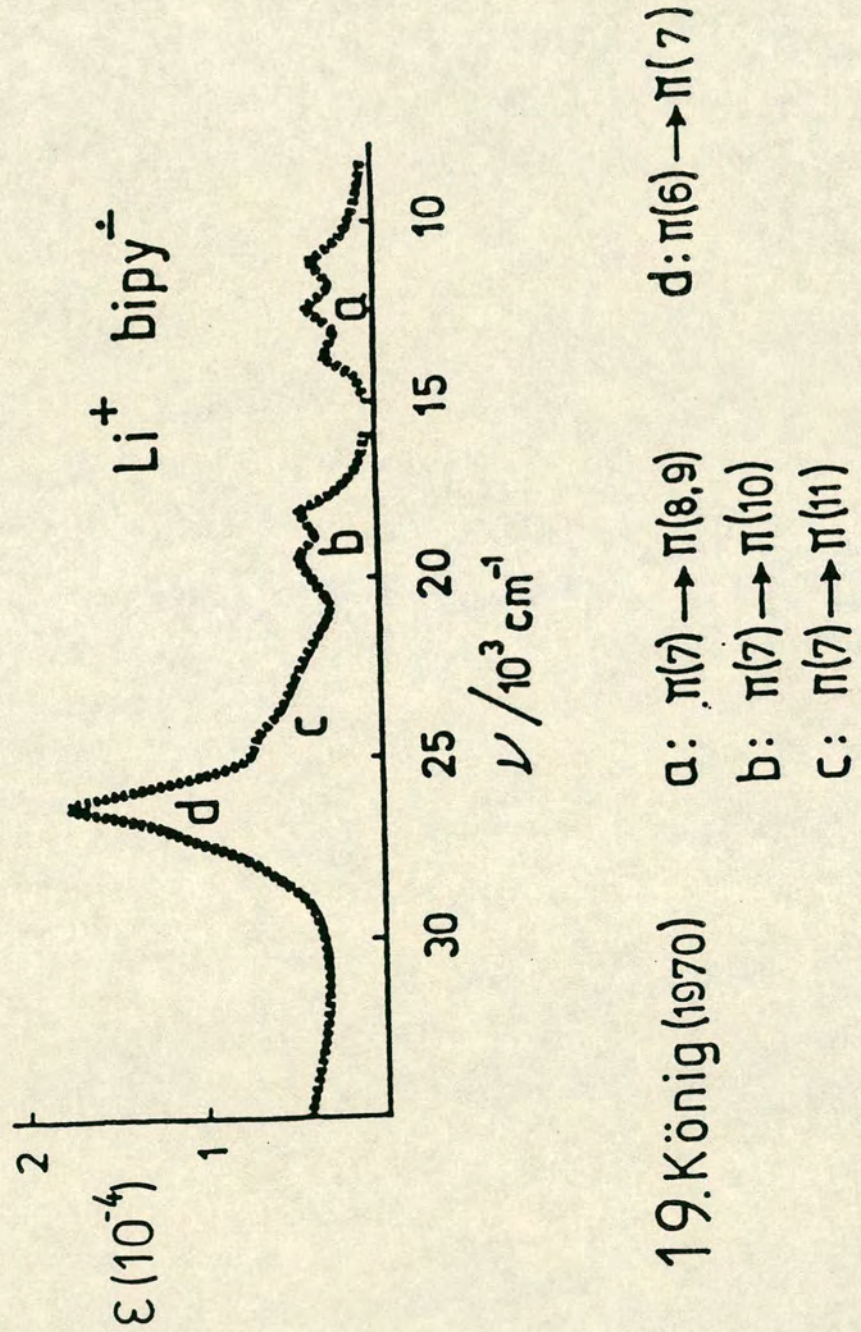


Table 5: $\frac{\text{Absorption Bands in } [\text{Ru}(\text{bipy})_2\text{CO.Cl}]^{+/-}}{\nu \times 10^{-3} / \text{cm}^{-1} \text{ (ex } 10^{-4})}$

Complex	Transition			
	$\frac{\pi(6) \rightarrow \pi(7)}{\text{bipy}^{\text{O}}}$	$\frac{\text{Ru(II)} d\pi}{\rightarrow \pi(8) \text{bipy}}$	$\frac{\text{Ru(II)} d\pi}{\rightarrow \pi(7) \text{bipy}^{\text{O}}}$	$\frac{\pi \rightarrow \pi^*}{\text{bipy}^{\cdot-}}$
$[\text{Ru}(\text{bipy})_2\text{CO.Cl}]^{+}$	35.1 (2.63) ^b 32.0 (1.58) sh	28.5 (0.46) sh	24.1 (0.22) sh	-
$[\text{Ru}(\text{bipy})_2\text{CO.Cl}]^{\text{O}}$	35.0 (2.13) ^b 31.8 (1.13) sh	a	a	27.2 (0.63) 20.5 (0.25) 19.4 (0.21)
$[\text{Ru}(\text{bipy})_2\text{CO.Cl}]^{-}$	-	-	-	26.6 (0.85) 20.0 (0.34)

a - Band obscured

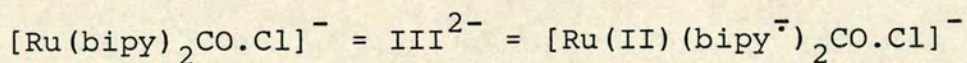
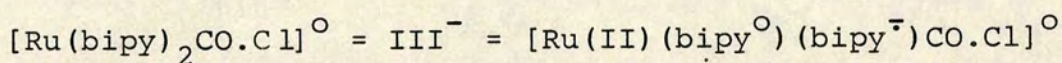
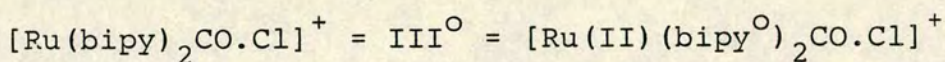
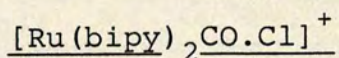
b - Contribution from BPh_4^{-} subtracted

intense than the charge-transfer transition. The loss of these bands is therefore concealed.

In the ultra-violet, upon reduction there is a stepwise loss of the bands at 32 000 and 35 000 cm^{-1} , which we assign to intraligand transitions in the bipyridine ligand. The bands in $\text{III}^{0/-/2-}$ are assigned in table 5.

Therefore it appears that this system is most realistically understood in terms of the localised model and the reduced species can be formulated as in table 6.

Table 6: Formulation of the Reduced Complexes of



These studies on the cathodic behaviour of III, which is a monocation, were carried out on the tetraphenylboron, BPh_4 , salt. The cyclic voltammogram of the perchlorate salt of III showed no apparent difference in behaviour on this timescale. However, the attempted electrogeneration of the mono-reduced species in bulk, from the perchlorate salt, unexpectedly led to the irreversible conversion to a

new product. (The electrogeneration of $[\text{Ru}(\text{bipy})_2\text{CO}.\text{Cl}]^{\circ}$ from $[\text{Ru}(\text{bipy})_2\text{CO}.\text{Cl}](\text{BPh}_4)$ was however straightforward.) In both dichloromethane and acetonitrile electrogeneration caused the yellow starting complex to be converted rapidly to a deep purple species. This was unambiguously identified as $[\text{Ru}(\text{bipy})_2\text{Cl}_2]$ by its infra-red and absorption spectra and its voltammetric behaviour. Reduction of the tetraphenylboron salt of III, giving the stable species $[\text{Ru}(\text{bipy})_2\text{CO}.\text{Cl}]^{\circ}$, followed by the addition of tetrabutylammonium chloride again led to the production of $[\text{Ru}(\text{bipy})_2\text{Cl}_2]$. Significantly, repeating the generation of III^- , from the BPh_4 salt, then adding chloride-free tetrabutylammonium perchlorate caused rapid decarbonylation of the complex under study and formation of $[\text{Ru}(\text{bipy})_2\text{Cl}_2]$. No evidence for any reaction between free chloride and the complex in its rest state was obtained over a period of several months although Kelly and co-workers⁶ have shown that $[\text{Ru}(\text{bipy})_2\text{CO}.\text{Cl}]^+$ may undergo photolytic decarbonylation to give $(\text{Ru}(\text{bipy})_2(\text{solvent})\text{Cl})^+$. The bipyridyl anion is effectively acting as a labilising agent towards decarbonylation of $[\text{Ru}(\text{bipy})_2\text{CO}.\text{Cl}]^{\circ}$ by chloride.

By controlling the amount of perchlorate added to III^- and monitoring the absorption spectrum of the product it was possible to obtain confirmatory evidence that the chloride which was replacing the carbonyl was indeed acquired from the perchlorate anion. As shown in figure 9 the addition of a half-molar equivalent of perchlorate to III^- gives an absorption spectrum which is consistent with equimolar quantities of $[\text{Ru}(\text{bipy})_2\text{CO}.\text{Cl}]^+$ and

$[\text{Ru}(\text{bipy})_2\text{Cl}_2]$ being present, when we return to rest potential. Indeed figure 9 also shows that addition of a molar equivalent of perchlorate to III^- led to the full conversion to $[\text{Ru}(\text{bipy})_2\text{Cl}_2]$. If we had merely catalysed chloride transfer from $[\text{Ru}(\text{bipy})_2\text{CO.Cl}]^+$ then the limiting yield of $[\text{Ru}(\text{bipy})_2\text{Cl}_2]$ would have been 50%. Electro-generation of III^- at a platinum O.T.T.L.E. allowed the changes in the absorption spectrum to be monitored. The absence of isosbestic points linking III and IV confirms the conversion takes place through some intermediate species, presumably III^- .

Tetrabutylammonium perchlorate is commonly used as a supporting electrolyte and is not observed to undergo reduction within the limits of the solvents we are employing. It therefore appears that the perchlorate anion must be reduced by the ruthenium complex.

A few reports have appeared suggesting certain penta- and hexa-aquoruthenium(II) complexes have reduced perchlorate anions in aqueous media, with the liberation of chloride.²¹⁻²³ In this case the neutral complex, III^- , is potentially a strong reducing agent towards the perchlorate salt.

Although we have no evidence to describe the mechanism of this decarboxylation reaction some important points should be noted.

If we assume III^- does enable the liberation of chloride from ClO_4^- then the initial product of the attack of Cl^- on $[\text{Ru}(\text{bipy})_2\text{CO.Cl}]^0$ is $[\text{Ru}(\text{bipy})_2\text{Cl}_2]^-$, IV^- . This oxidation state is unstable at the prevailing electrode potential

Figure 9: Absorption Spectra Recorded During the Conversion of $[\text{Ru}(\text{bipy})_2\text{CO}\cdot\text{Cl}]^+$ to $[\text{Ru}(\text{bipy})_2\text{Cl}_2]$

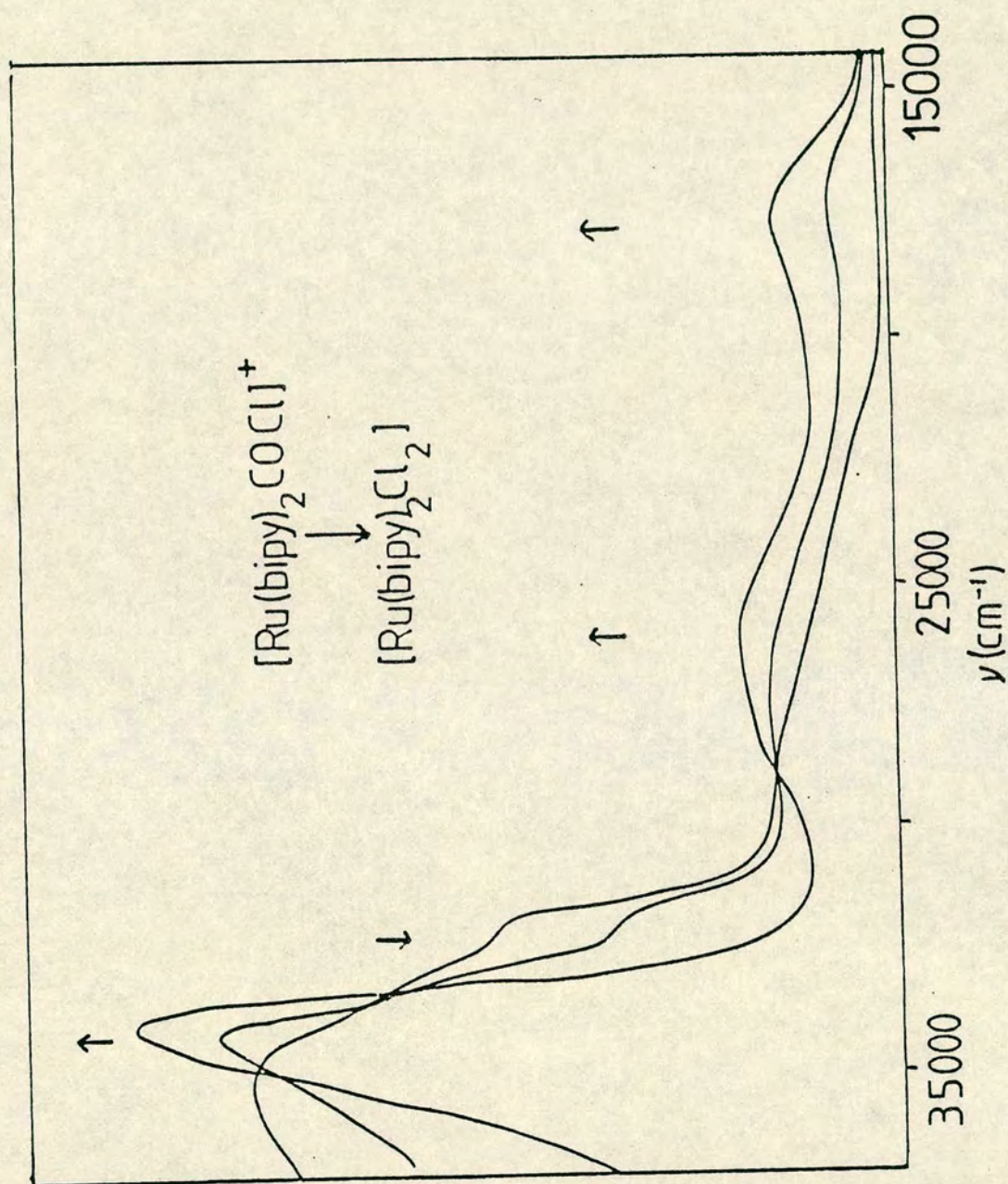
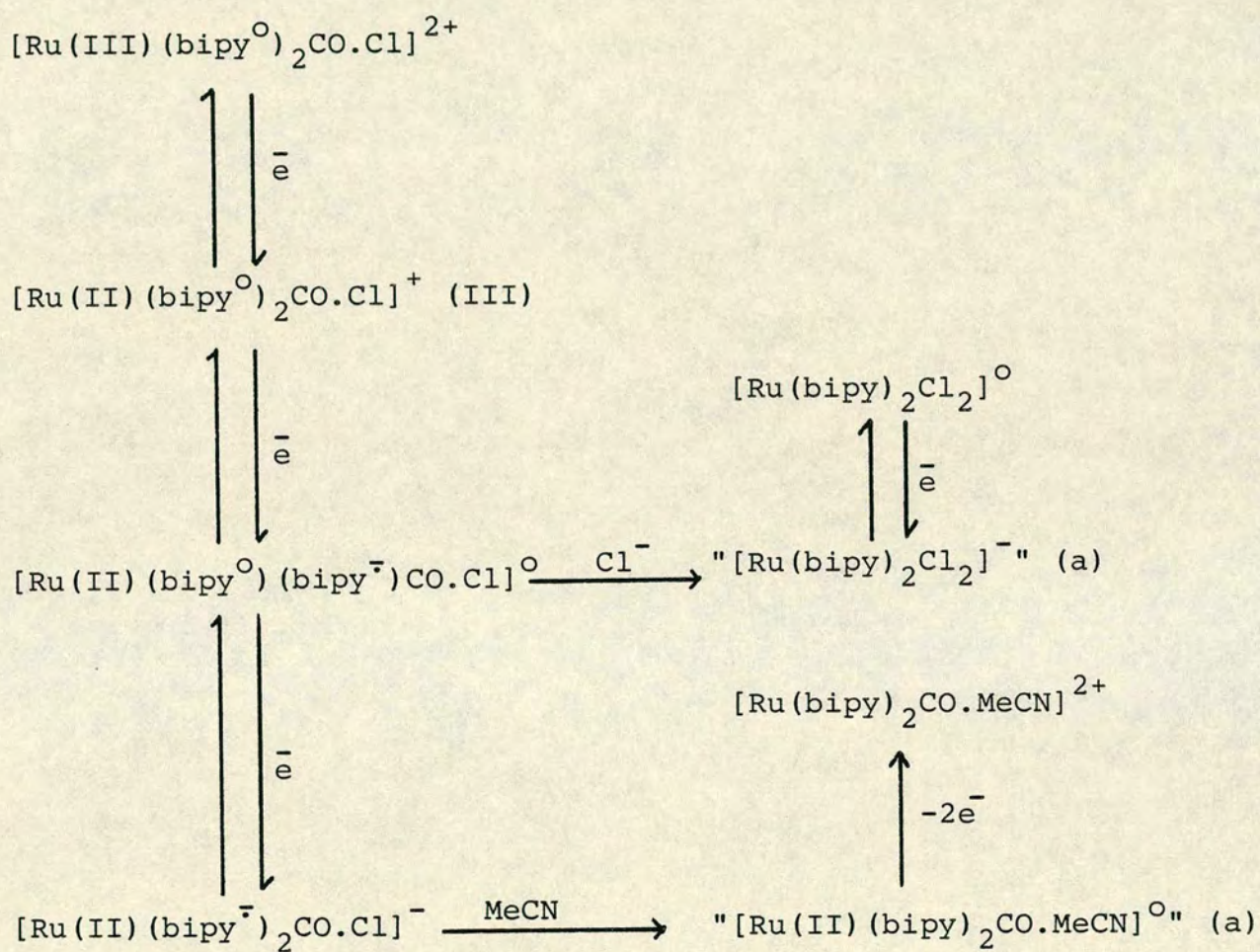


Figure 10: The behaviour of $\text{cis-}[\text{Ru}(\text{bipy})_2\text{CO.Cl}]^+$ in its reduced and oxidised states



a - Transient species

(IV being reduced at a potential 0.4V more negative than III) and would therefore be a more powerful reducing agent than III^- . The complex IV^- should then be capable of reducing perchlorate to free more chloride to then attack III^- ultimately allowing the full conversion to $[\text{Ru}(\text{bipy})_2\text{Cl}_2]$ to take place. Indeed it may be shown that $[\text{Ru}(\text{bipy})_2\text{Cl}_2]^-$ independently reduces ClO_4^- to chloride.

These observations may be contrasted with the results of Meyer *et al.*²⁴ which were reported during the course of this study. These workers studied III, as the hexafluorophosphate salt, in acetonitrile. On electrogenerating at a potential beyond the second reduction of III, at room temperature, they obtained electrochemical evidence for the expulsion of chloride leading to the partial conversion to $[\text{Ru}(\text{bipy})_2\text{CO.MeCN}]^{2+}$.

We can summarise the behaviour of III in figure 10.

cis-Acetonitrilecarbonylbis(bipyridine)ruthenium(II), V

The complex $\text{cis-}[\text{Ru}(\text{bipy})_2\text{CO.MeCN}]^{2+}$, V, exhibits an absorption spectrum broadly similar to $[\text{Ru}(\text{bipy})_2\text{CO.Cl}]^+$ with the presence of the carbonyl ligand again appearing to split the lowest energy $\pi \rightarrow \pi^*$ bipyridine transition into two components. A blue-shift of the ML(bipy)CT band, relative to $[\text{Ru}(\text{bipy})_3]^{2+}$, is again noted due to the increased stabilisation of the $\text{Ru(II)}d\pi$ level in V.

Replacement of the π -donating chloride ligand in III by acetonitrile causes a shift in the observed electrode potentials. Electrochemical studies on V carried out in

acetonitrile, reveal one one-electron oxidation at a more positive potential than III, as well as two more easily achieved (less negative) one-electron reductions. In this case acetonitrile was chosen as the electrochemical solvent due to its relatively large anodic range and, more particularly, in order to suppress any reductively induced loss of the MeCN ligand.

We attempted to generate the one-electron oxidation product at a platinum O.T.T.L.E., at +2.0V vs Ag/Ag⁺. However the spectral changes which occurred were not accompanied by any isosbestic points, indicating that a simple one-to-one conversion of V to V⁺ had not taken place. Moreover returning the applied potential to 0 Volts did not lead to the recovery of the original spectrum of V; rather an absorption spectrum consistent with the complex [Ru(bipy)₂(MeCN)₂]²⁺, VI, was observed.^{25,26} This new species, VI, could now be re-oxidised at +1.30V in the O.T.T.L.E. to produce the same spectrum as the original product which is clearly [Ru(bipy)₂(MeCN)₂]³⁺, VI⁺, as shown in figure 11.

As anticipated the loss of the carbonyl ligand means that the absorption spectrum of [Ru(bipy)₂(MeCN)₂]³⁺ is much simplified. The absorption bands in the complexes V, VI and VI⁺ are assigned in table 7.

We have therefore observed an anodically-catalysed ligand substitution reaction of V.

The one-electron reduction product [Ru(bipy)₂CO.MeCN]⁺, V⁻, was generated from V at a platinum O.T.T.L.E. at -1.53V

Figure 11: Absorption Spectra of $[\text{Ru}(\text{bipy})_2\text{CO.MeCN}]^{2+}$ and $[\text{Ru}(\text{bipy})_2(\text{MeCN})_2]^{2+/3+}$ in Acetonitrile at Room Temperature

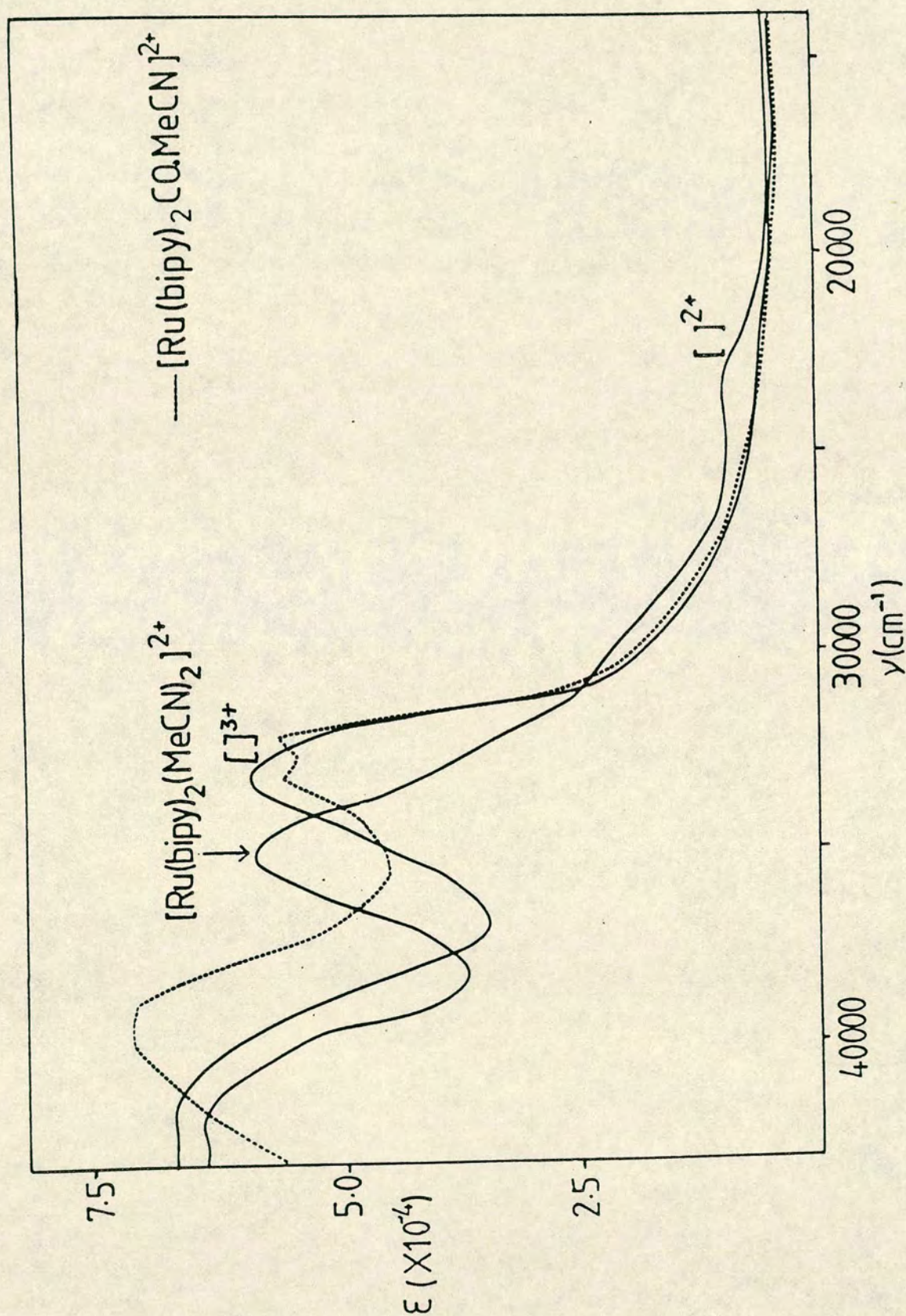


Table 7:

Absorption bands in $[\text{Ru}(\text{bipy})_2\text{CO.MeCN}]^{2+}$ and $[\text{Ru}(\text{bipy})_2(\text{MeCN})_2]^{2+/3+}$ $\times 10^{-3}/\text{cm}^{-1}$ ($\times 10^{-4}$)

<u>Complex</u>	<u>Transition</u>			
	<u>Intraligand</u>		<u>ML(bipy) CT</u>	
	$\pi(6) \rightarrow \pi(8)$ <u>bipy</u>	$\pi(6) \rightarrow \pi(7)$ <u>bipy</u>	$\text{Ru(II)} d\pi$ $\rightarrow \pi(7) \text{bipy}$	$\text{Ru(III)} d\pi$ $\rightarrow \pi(7) \text{bipy}$
$[\text{Ru}(\text{bipy})_2\text{CO.MeCN}]^{2+}$	39.2(7.04)	33.0(5.72) 31.9(5.88)	27.0(0.58)	-
$[\text{Ru}(\text{bipy})_2(\text{MeCN})_2]^{2+}$	42.0(6.31)	35.5(5.98)	23.6(0.79)	-
$[\text{Ru}(\text{bipy})_2(\text{MeCN})_2]^{3+}$	41.5(6.64)	33.2(6.03)	-	obsured

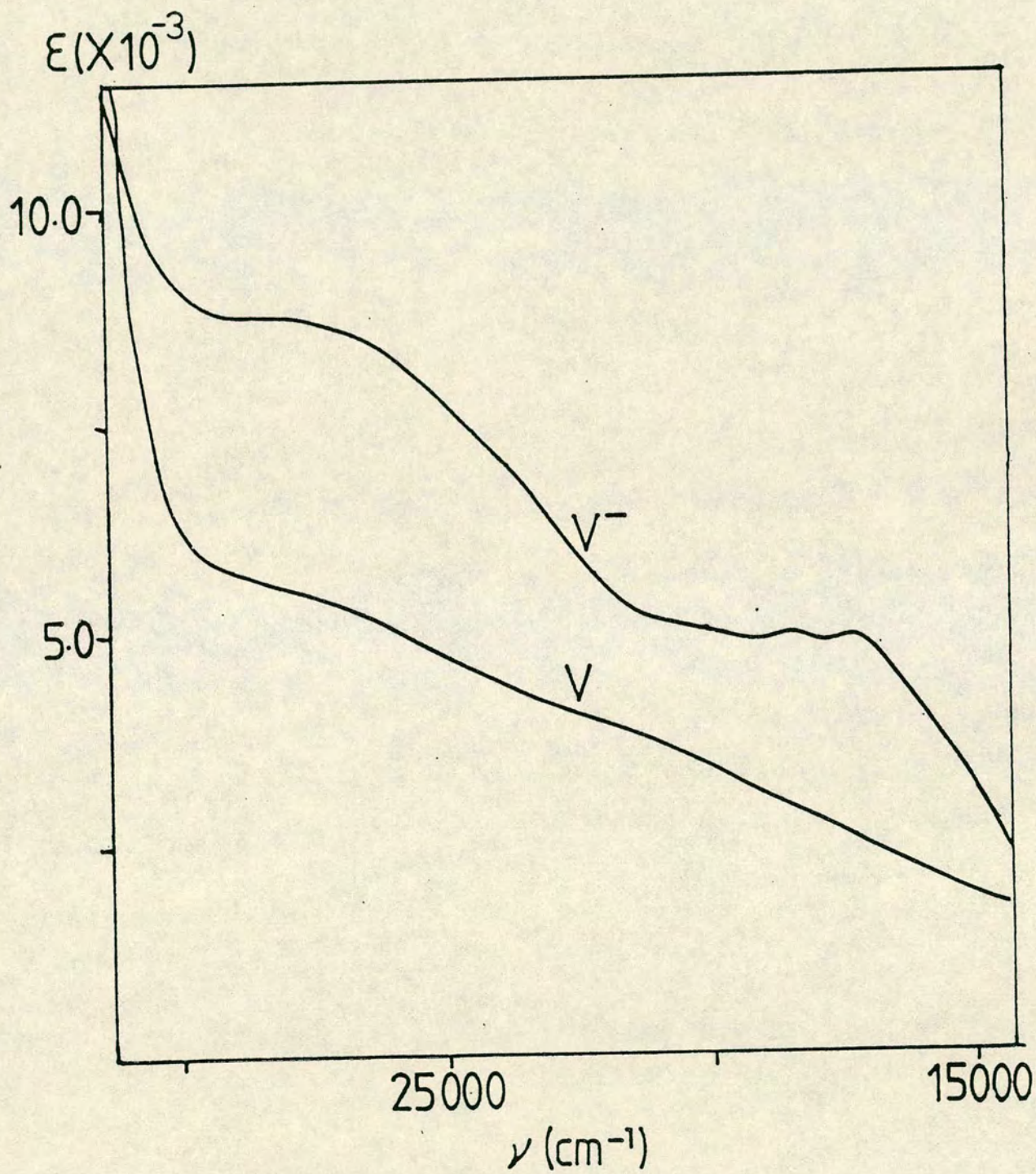
vs Ag/Ag^+ , in acetonitrile at -35°C . The growth of the set of bands corresponding to the bipy^\cdot chromophore was observed whilst those transitions assigned to the metal bipyridyl ligand began to collapse. The limiting spectrum obtained for $[\text{Ru}(\text{bipy})_2\text{CO.MeCN}]^+$ is illustrated in figure 12 with the assignment of bands shown in table 8.

Table 8: Assignment of the Absorption Bands in
 $[\text{Ru}(\text{bipy})_2\text{CO.MeCN}]^{2+}/^+ \quad \nu \times 10^{-3}/\text{cm}^{-1} \quad (\epsilon \times 10^{-4})$

<u>Complex</u>	<u>Transition</u>		
	<u>$\pi(6) \rightarrow \pi(7) \text{bipy}^{\text{O}}$</u>	<u>$\text{Ru(II)} d\pi \rightarrow \pi(7) \text{bipy}^{\text{O}}$</u>	<u>$\pi \rightarrow \pi^* \text{bipy}^\cdot$</u>
V	33.0 (5.72) 31.9 (5.88)	27.0 (0.58)	-
V ⁻	-	-	26.8 (0.85) 18.5 (0.52) 17.4 (0.52)

As reported for $\text{III}/\text{III}^\cdot$, the expected loss of the $\text{ML}(\text{bipy})\text{CT}$ band is swamped by the growth of the absorption representing the bipy^\cdot chromophore. Attempts to electrogenerate and stabilise the second reduction product

Figure 12: Visible Absorption Spectra of
 $[\text{Ru}(\text{bipy})_2\text{CO}.\text{MeCN}]^{2+/+}$ in Acetonitrile at -35°C



of V met with failure with decomposition of the neutral complex taking place. No further work was pursued on this decomposition product.

The studies detailed above were carried out on the tetraphenylboron salt of $[\text{Ru}(\text{bipy})_2\text{CO}.\text{MeCN}]^{2+}$. Due to the remarkable participation of ClO_4^- previously observed upon reduction of $[\text{Ru}(\text{bipy})_2\text{CO}.\text{Cl}](\text{ClO}_4)$, we decided to examine the cathodic behaviour of the perchlorate salt of V. With this anion present, attempts to generate the one-electron reduction product V^- , both in a conventional electrochemical cell and at a platinum O.T.T.L.E., led to the formation of $\text{cis}[\text{Ru}(\text{bipy})_2\text{CO}.\text{Cl}]^+$. This product was identified by examination of its electrochemical behaviour and its absorbance spectrum. The successive spectra recorded during this electrolysis are shown in figure 13. As for the decarbonylation caused by the attack of chloride on $\text{III}^{\text{bipy}^-}$ again appears to act as a labilising ligand.

Indeed if we now attempt to reduce this initial product then a smooth conversion to $[\text{Ru}(\text{bipy})_2\text{Cl}_2]$ is again observed.

It would appear that the reducing agent V^- is able to catalyse the release of chloride from perchlorate. Then the bulk of the reduced complex, V^- , is susceptible to attack by the chloride (in its resting oxidation state V is stable in the presence of Cl^- over a period of several days) with the displacement of MeCN instead of the carbonyl ligand on this occasion.

This initial product of this reaction $[\text{Ru}(\text{bipy})_2\text{CO}.\text{Cl}]^0$

Figure 13: Absorption Spectra Recorded During the Reductive Electrolysis of $[\text{Ru}(\text{bipy})_2\text{CO.MeCN}]^{2+}$ in the Presence of Perchlorate Salts

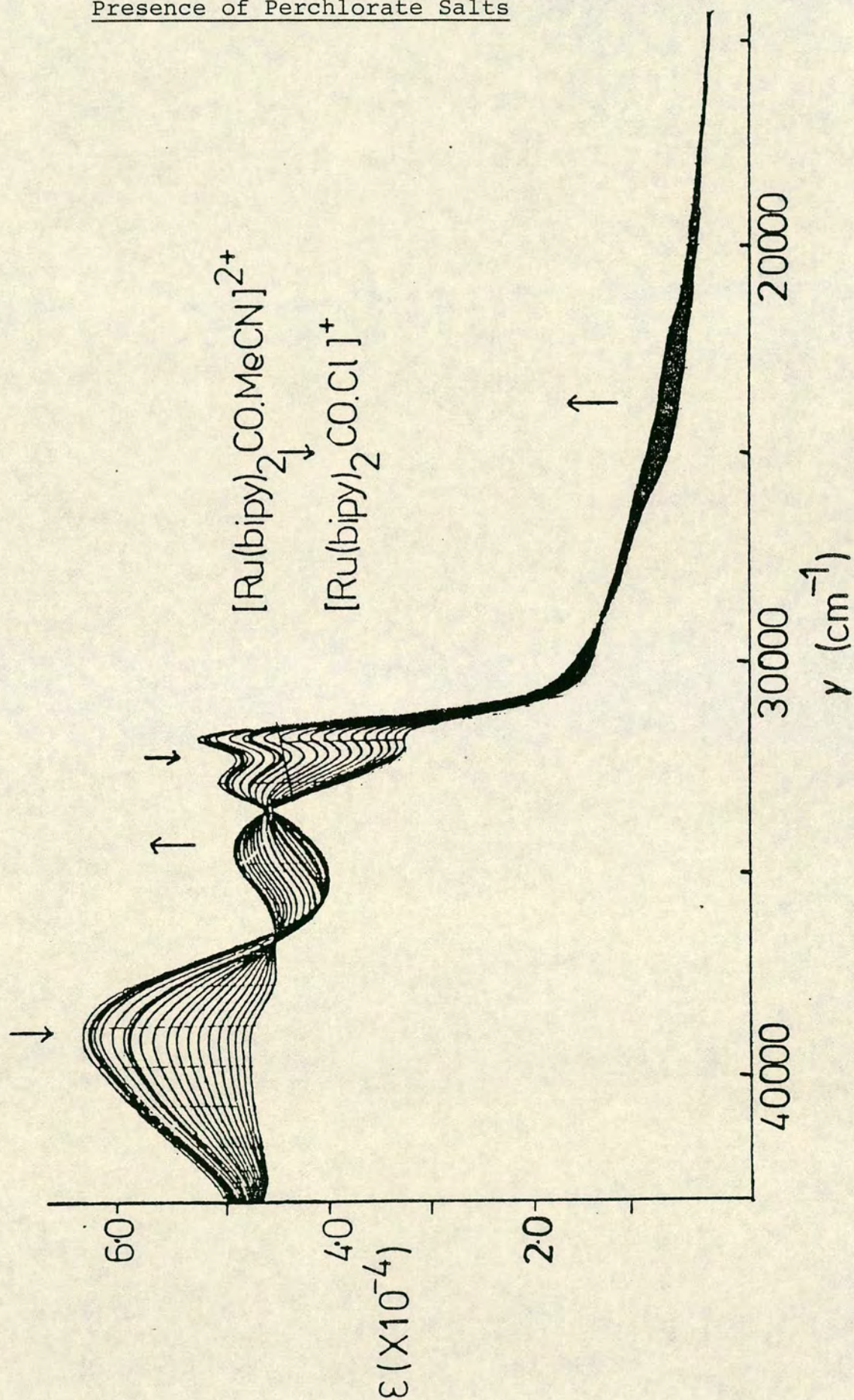
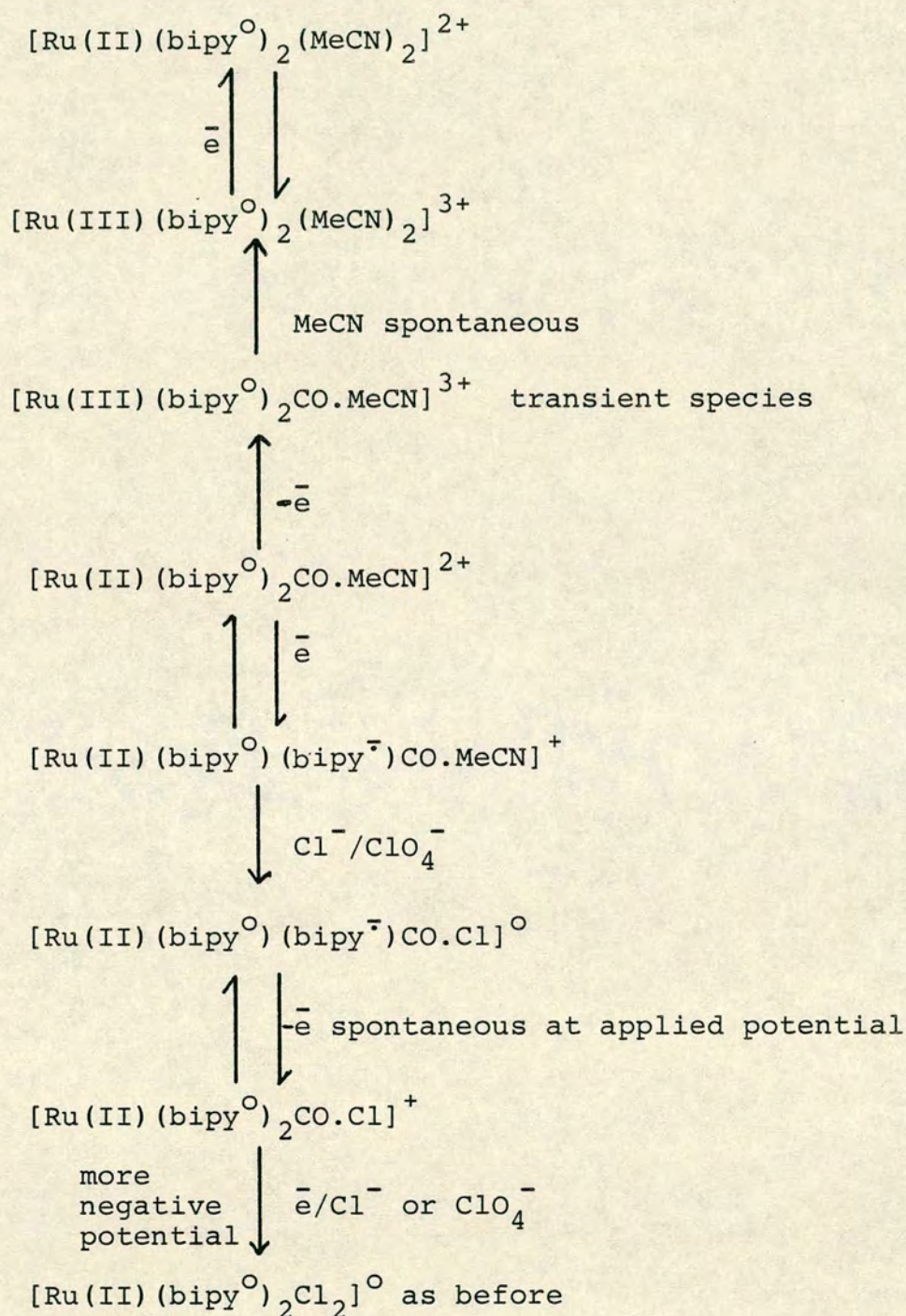


Figure 14: Substitution Reactions of $[\text{Ru}(\text{bipy})_2\text{CO.MeCN}]^{2+}$



would be unstable at the potential applied (III is reduced at a potential 180mV more negative than V) and therefore should be a stronger reducing agent than V^- . As we have already suggested, this species III could then instigate reduction of the perchlorate anion releasing chloride, whilst it is itself oxidised to $[\text{Ru}(\text{bipy})_2\text{CO.Cl}]^+$.

The complex $[\text{Ru}(\text{bipy})_2\text{CO.MeCN}]^{2+}$ has therefore been shown to undergo another electrode-catalysed ligand substitution on this occasion at the cathode.

In summary we can represent the substitution reactions of cis $[\text{Ru}(\text{bipy})_2\text{CO.MeCN}]^{2+}$ as in figure 14.

cis-Carbonylpyridinebis(bipyridine)ruthenium(II), VII

The complex $[\text{Ru}(\text{bipy})_2\text{CO.py}]^{2+}$ exhibits an absorption spectrum with the familiar splitting of the lowest energy $\pi\pi^*$ bipyridine transition characteristic of the $\text{Ru}(\text{CO})/\text{bipy}^0$ chromophore. The higher energy intraligand band is broadened due to the overlap of a $\pi\pi^*$ pyridine transition.^{12,13,27} Again the MLCT transitions this time to pyridine as well as bipyridine, are moved to higher energies than in $[\text{Ru}(\text{bipy})_3]^{2+}$ and $[\text{Ru}(\text{bipy})_2(\text{py})_2]^{2+}$ due to the increased stabilisation of the $d\pi$ level caused by carbonyl. The absorption bands in VII are assigned in table 9.

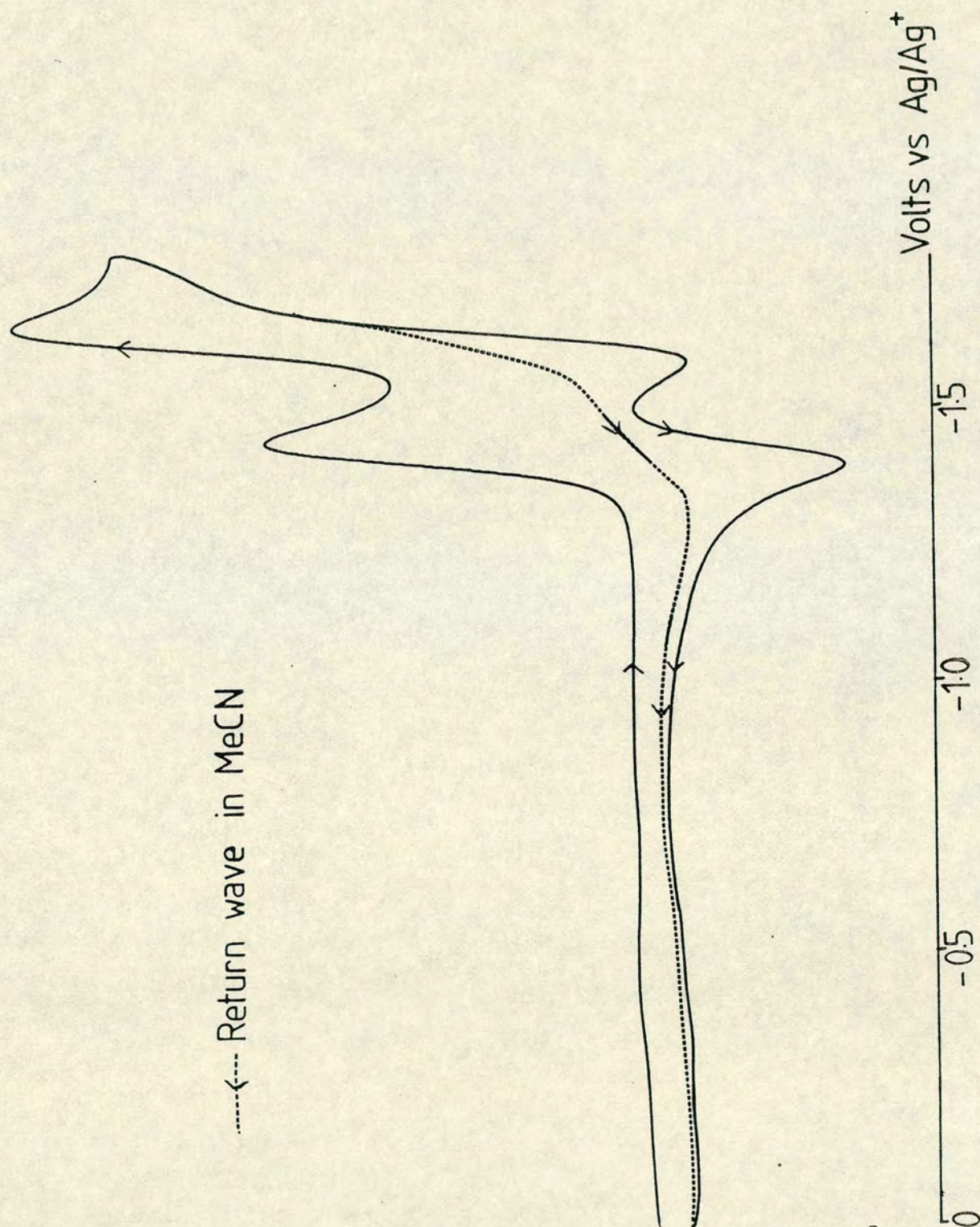
Table 9: Absorption bands in $[\text{Ru}(\text{bipy})_2\text{CO.py}]^{2+}$
 $\nu \times 10^{-3}/\text{cm}^{-1}$ ($\epsilon \times 10^{-4}$)

<u>Band</u>	<u>Assignment</u>
38.8(2.72)	$\pi\pi^* \text{ bipy}^{\circ} + \pi\pi^* \text{ py}$
33.3(2.29), 32.3(2.29)	$\pi\pi^* \text{ bipy}^{\circ}$
obscured	$\text{ML(py)CT}; d\pi \rightarrow \pi^* \text{ py}$
26.3(0.26)	$\text{ML(bipy)CT}; d\pi \rightarrow \pi^* \text{ bipy}$

An electrochemical study of VII in acetonitrile reveals a single one-electron oxidation and two quasi-reversible one-electron reductions. However if VII is studied in pyridine, two reversible one-electron reductions are found as shown in figure 15.

An attempt was made to generate the one-electron oxidation product at a platinum O.T.T.L.E. at +1.95V vs Ag/Ag^+ . No isosbestic points were observed in the accompanying spectral change implying that smooth conversion to $[\text{Ru}(\text{bipy})_2\text{CO.py}]^{3+}$ was not taking place. Returning the applied potential to 0 volts did not lead to the recovery of the original spectrum; rather a spectrum consistent with the formation of $[\text{Ru}(\text{bipy})_2\text{py.MeCN}]^{2+}$, VIII, was obtained.²⁵ Re-oxidation of VIII, at +1.30V

Figure 15: Cyclic Voltammogram of $[\text{Ru}(\text{bipy})_2\text{CO.py}]^{2+}$
in Acetonitrile and Pyridine



vs Ag/Ag^+ , allowed us to regain the spectrum of the original product which we therefore interpret as being $[\text{Ru}(\text{bipy})_2\text{py}.\text{MeCN}]^{3+}$, VIII^+ , as shown in figure 16. The absorption spectra of VIII and VIII^+ are assigned in table 10.

The replacement of carbonyl by the more weakly π -accepting pyridine ligand causes the lowest energy $\pi\pi^*$ bipy transition to be blue-shifted to $35\,000\text{ cm}^{-1}$, (c.f. $[\text{Ru}(\text{bipy})_3]^{2+}$ and $[\text{Ru}(\text{bipy})_2(\text{py})_2]^{2+}$ where the lowest $\pi\pi^*$ bipy band is found at $35\,000\text{ cm}^{-1}$). A shoulder observed at approximately $31\,000\text{ cm}^{-1}$, however, is due to the π -acceptor pyridine ligand which has a similar, though weaker, effect on the ruthenium centre as a carbonyl ligand. In table 10 we have assigned MLCT bands from the Ru(II) centre to both bipyridine and pyridine. Since it is known that it is approximately 600mV ($\sim 5000\text{ cm}^{-1}$) more difficult to reduce free pyridine than free bipyridine,²⁸ the π^* level is therefore sited at higher energy in pyridine. This observation allowed us to assign the bands involving pyridine in VIII.

On allowing the complex $[\text{Ru}(\text{bipy})_2\text{py}.\text{MeCN}]^{2+}$ to stand in acetonitrile over a period of approximately six hours a further change in the absorption spectrum was noted. The ML(bipy)CT transition moves to a slightly higher frequency accompanied by the loss of the ML(py)CT bands. As previously reported,¹² this behaviour is consistent with the formation of $[\text{Ru}(\text{bipy})_2(\text{MeCN})_2]^{2+}$. Such a solvolysis reaction is not surprising given the prevailing vast excess of acetonitrile over pyridine.

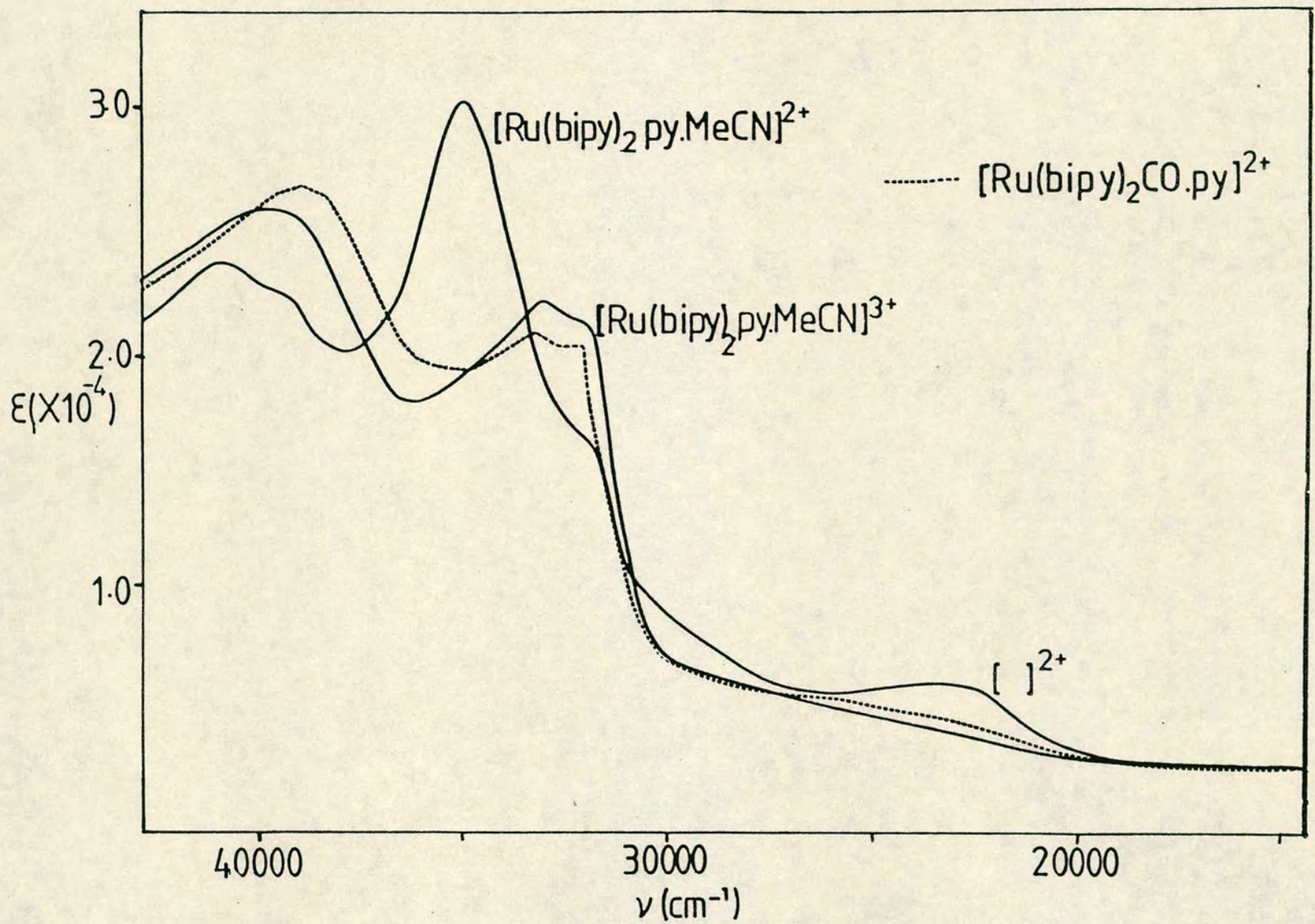


Figure 16: Absorption Spectra of $[\text{Ru}(\text{bipy})_2\text{CO.py}]^{2+}$ and $[\text{Ru}(\text{bipy})_2\text{py.MeCN}]^{2+/3+}$ in Acetonitrile

Table 10: Assignment of the absorption bands in

<u>Complex</u>	<u>Transition</u>			
	<u>Intraligand</u>	<u>Charge-Transfer</u>		
	$\pi\pi^*$ <u>bipy+py</u>	$\pi\pi^*$ <u>bipy</u>	<u>ML(py)CT</u>	<u>ML(bipy)CT</u>
[Ru(bipy) ₂ py.MeCN] ²⁺	41.1 (2.42)	35.0 (3.08)	29.0 sh	23.0 (0.60)
	39.3 (2.37)	32.0 (1.80) sh		
[Ru(bipy) ₂ py.MeCN] ³⁺	39.1 (2.63)	33.0 (2.37)	a	a
		31.8 (2.35)		

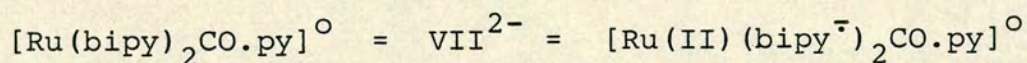
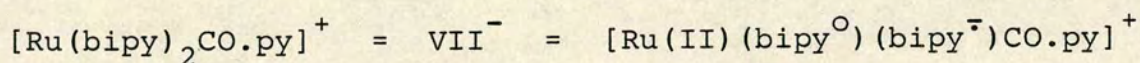
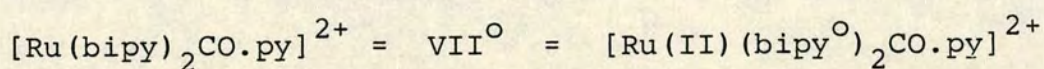
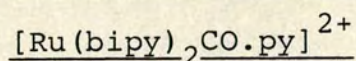
a - Obscured

[Ru(bipy)₂py.MeCN]^{2+/3+} $\nu \times 10^{-3} / \text{cm}^{-1}$ ($\epsilon \times 10^{-4}$)

The two reduced species VII^- and VII^{2-} were separately generated at a platinum O.T.T.L.E. at -1.54V and -1.72V vs Ag/Ag^+ respectively, in pyridine. A family of bands corresponding to the bipy^- chromophore is seen to emerge in accordance with the spectrum of Li^+bipy^- ²⁰ as shown in figure 17. Table 11 shows the assignments of these bands.

The limited spectral window of this solvent means that we cannot observe the progressive loss of the bands due to the neutral bipyridine ligands. However, by analogy with our previous results we can formulate the reduction products VII^- and VII^{2-} in terms of the localised model as in table 12.

Table 12: Formulation of the Reduced Complexes of



Attempted generation of $[\text{Ru}(\text{bipy})_2(\text{MeCN})\text{py}]^+$, VIII^- , in acetonitrile led only to the decomposition of the complex therefore no further work was attempted in this solvent.

Figure 17: Absorption Spectra of $[\text{Ru}(\text{bipy})_2\text{CO.py}]^{2+}/+/o$
in Pyridine at Room Temperature

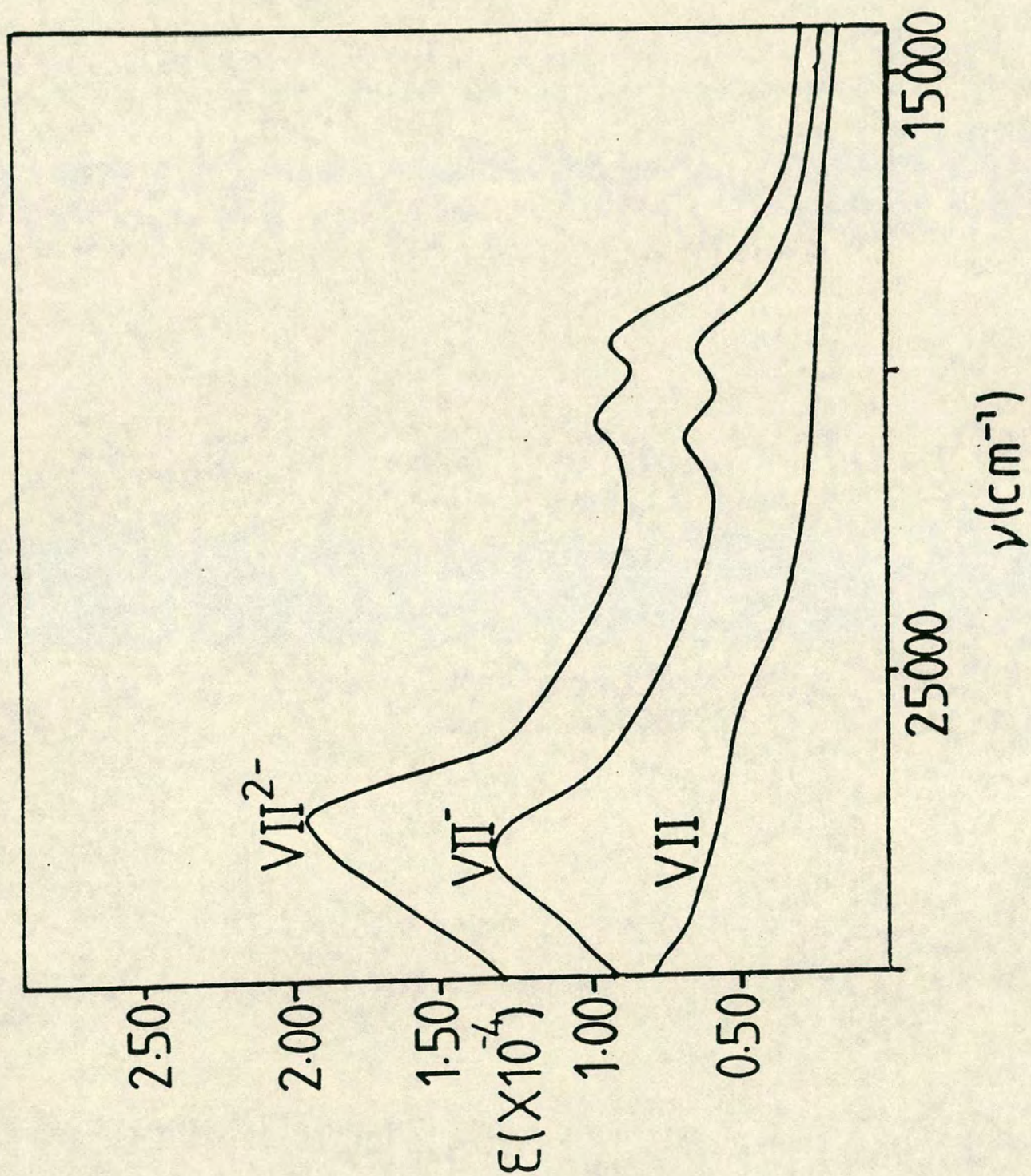


Table 11: Absorption Bands in $[\text{Ru}(\text{bipy})_2\text{CO.py}]^{+10}$
 $\nu \times 10^{-3} / \text{cm}^{-1}$ ($\epsilon \times 10^{-4}$)

<u>Complex</u>	<u>Transitions</u>	
	<u>$\pi \rightarrow \pi^* \text{bipy}^-$</u>	<u>$\pi \rightarrow \pi^* \text{bipy}^-$</u>
VII^-	27.8 (1.28)	21.3 (0.68)
		<u>19.6 (0.64)</u>
VII^{2-}	27.2 (1.96)	20.8 (1.01)
		<u>19.5 (0.96)</u>
$\text{Li}^+ \text{bipy}^-$	25.9 (2.95)	18.8 (0.62)
		17.8 (0.65)

cis-Biscarbonylbis(bipyridine)ruthenium(II), IX.

As we have discussed, the presence of a strongly π -accepting carbonyl ligand causes a reduction in the metal electron density experienced by the bipyridine ligands to a level comparable with that in ruthenium(III) complexes in the series of complexes $[\text{Ru(II)(bipy)}_2\text{CO.Z}]^{n+}$. This explanation was used to rationalise the appearance of a lower energy component of the intraligand $\pi\pi^*$ bipyridyl transition. By studying the complex where the sixth ligand, Z, is also carbonyl it is possible to gain more evidence for the postulate above.

In $\text{cis-}[\text{Ru(bipy)}_2(\text{CO})_2]^{2+}$, IX, the intensity of the lower frequency component of the bipyridyl transition is enhanced relative to the other systems we have studied while the band normally observed in Ru(II)bipy complexes at $35\,000\text{ cm}^{-1}$ has disappeared. Also the extra stabilisation of the $d\pi$ level in IX has further blue-shifted the ML(bipy)CT band into the ultra-violet region to such a high frequency that it may not be observed as it lies under the lowest intraligand transition.

An anodic scan of IX, in acetonitrile shows no oxidation to be observed within our solvent limit. By consideration of the series of complexes $[\text{Ru(bipy)}_2\text{Cl}_2]$, $[\text{Ru(bipy)}_2\text{CO.Cl}]^+$ and $[\text{Ru(bipy)}_2(\text{CO})_2]^{2+}$ we can, however, predict a value for the RuII/III couple in IX. It has already been noted that the replacement of one chloride ligand in $[\text{Ru(bipy)}_2\text{Cl}_2]$ by carbonyl lowers the energy of the $\text{Ru(II)}d\pi$ level by 1.2 volts

and that such ligation changes have a generally systematic effect on E° values.

Therefore replacement of the second chloride ligand by carbonyl should have a similar effect in the metal core, suggesting that the RuII/III couple for this species is +2.4V vs Ag/Ag⁺, which is indeed beyond the anodic limit of this solvent. It was not possible therefore to study the electrogenerated Ru(III) complex.

Examination of the cathodic behaviour of IX, as the hexafluorophosphate salt, revealed two one-electron quasi-reversible reductions which are, as anticipated, easier to achieve than those of Ru(bipy)₂CO.Cl⁺. The mono-reduced complex, IX⁻, was stabilised in dichloromethane at -40°C, at a platinum O.T.T.L.E. at -1.30V vs Ag/Ag⁺ in the presence of excess bipyridyl ligand as shown in figure 18.

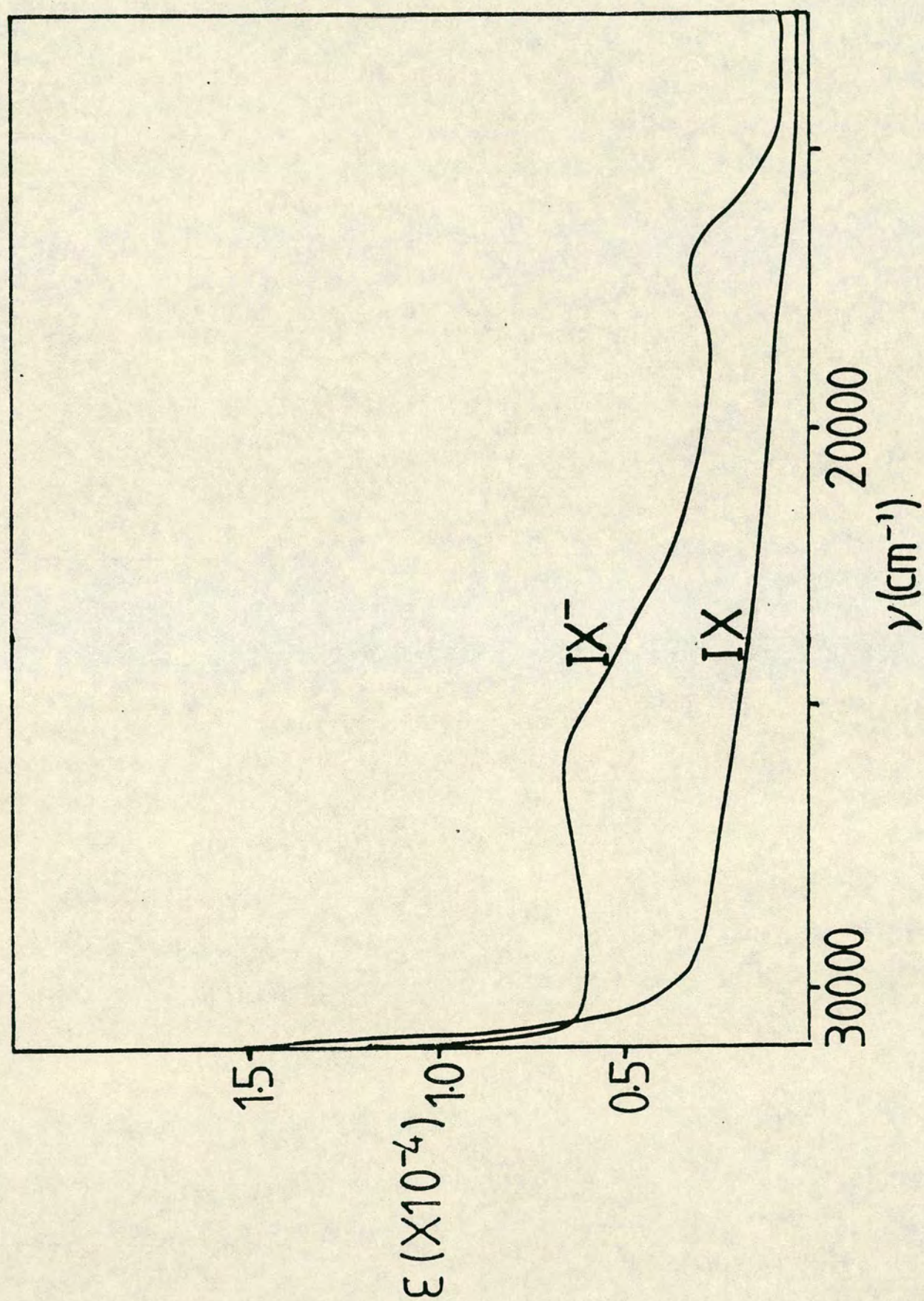
All attempts to stabilise the second reduction product led only to the decomposition of the complex.

The absorption spectrum of IX⁻ shows the growth of a set of bands which correspond to the bipy⁻ chromophore as detailed in Table 13.

Table 13: Absorption Bands in [Ru(bipy)₂(CO)₂]⁺
 $\nu \times 10^{-3}/\text{cm}^{-1}$ ($\epsilon \times 10^{-4}$)

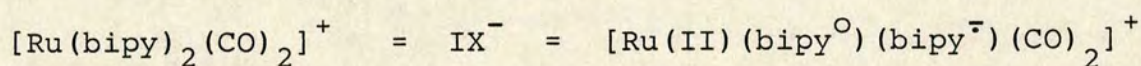
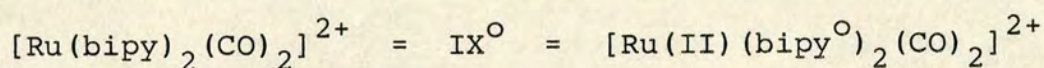
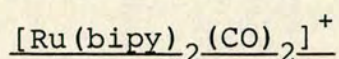
<u>Complex</u>	<u>Transition</u>	
	<u>$\pi \rightarrow \pi^*$ bipy⁻</u>	<u>$\pi \rightarrow \pi^*$ bipy⁻</u>
IX ⁻	26.0 (0.70)	17.0 (0.30)
Li ⁺ bipy ⁻²⁰	25.9 (2.95)	18.8 (0.62)
		17.8 (0.65)

Figure 18: Absorption Spectra of $[\text{Ru}(\text{bipy})_2(\text{CO})_2]^{2+/+}$
in Dichloromethane at -40°C



The excess bipyridyl ligand present, which absorbs at $34\,000\text{ cm}^{-1}$, masks the loss of bands assigned to bipy^{O} in IX and IX⁻. However, by comparison with the previous studies we can classify the species $[\text{Ru}(\text{bipy})_2(\text{CO})_2]^+$ in terms of the localised model as shown in table 14.

Table 14: Formulation of the Reduced Complex



cis-Carbonylhydridobis(bipyridine)ruthenium(II), X

The complex $\text{cis-}[\text{Ru}(\text{bipy})_2\text{CO.H}]^+$, X, is worthy of further study since $\text{Ru}(\text{bipy})_2$ -hydride complexes have been suggested as intermediates in the water-gas shift reaction promoted by $[\text{Ru}(\text{bipy})_2\text{CO.Cl}]^+$ ^{7,8}. Moreover, we are able to characterise the influence of the H^- ligand in comparison with the others in this context. As for the other carbonyl complexes in this series the lowest-energy $\pi\pi^*$ bipyridine transition is again split into two components however, the metal-to-ligand charge-transfer band is shifted to lower energy than in $[\text{Ru}(\text{bipy})_2\text{CO.Z}]^{n+}$ (where $\text{Z}=\text{Cl}$, MeCN, py and CO). This shift is directly attributable to the strong

σ -donor properties of the hydride in relation to other substituents and allows us to observe the metal-to-ligand charge-transfer to the next empty bipyridine level ($\pi(8)$), which has been concealed in the other complexes studied (see figures 19 and 20 and table 15).

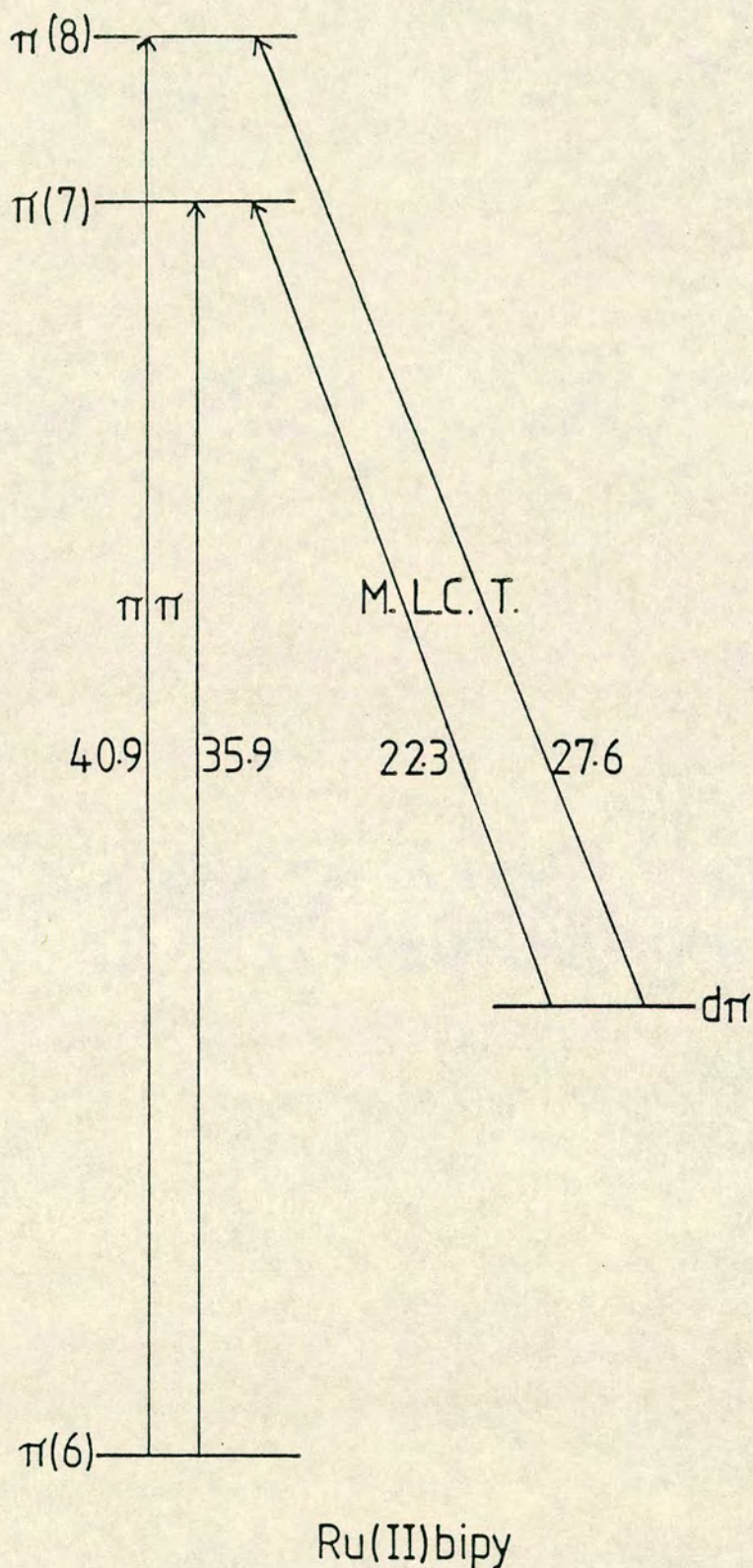
Table 15: Assignment of the Absorption Bands in
 $[\text{Ru}(\text{bipy})_2\text{CO.H}]^+$, X. $\nu \times 10^{-3}/\text{cm}^{-1}$ ($\epsilon \times 10^{-4}$)

<u>Complex</u>	<u>Transition</u>			
	<u>$\pi(6) \rightarrow \pi(8)$</u>	<u>$\pi(6) \rightarrow \pi(7)$</u>	<u>$\text{Ru(II)} d\pi$</u>	<u>$\text{Ru(II)} d\pi$</u>
	<u>bipy^{O}</u>	<u>bipy^{O}</u>	<u>$\rightarrow \pi(8) \text{bipy}^{\text{O}}$</u>	<u>$\rightarrow \pi(7) \text{bipy}^{\text{O}}$</u>
IX	40.9 (2.26)	35.9 (3.02)	27.6 (0.50)	22.3 (0.31)
		31.2 sh		

A cyclic voltammetric study of X, as the hexafluorophosphate salt, in dichloromethane reveals two one-electron reductions and one irreversible oxidation as shown in figure 21.

On scanning beyond the irreversible oxidative wave, in dichloromethane a second reversible oxidation is observed at a potential corresponding to that of the $[\text{Ru}(\text{bipy})_2\text{CO.Cl}]^{+/2+}$ couple, implying this complex forms in situ. Similarly if the complex is studied in acetonitrile a second wave is now observed at the potential corresponding to the oxidation

Figure 19: Schematic Energy Level Scheme for $[\text{Ru}(\text{bipy})_2\text{CO.H}]^+$



Note: The figures listed above are optically measured transitions in units of 10^{-3} cm^{-1} .

Figure 20: Absorption Spectrum of $[\text{Ru}(\text{bipy})_2\text{CO.H}]^+$ in Dichloromethane at Room Temperature

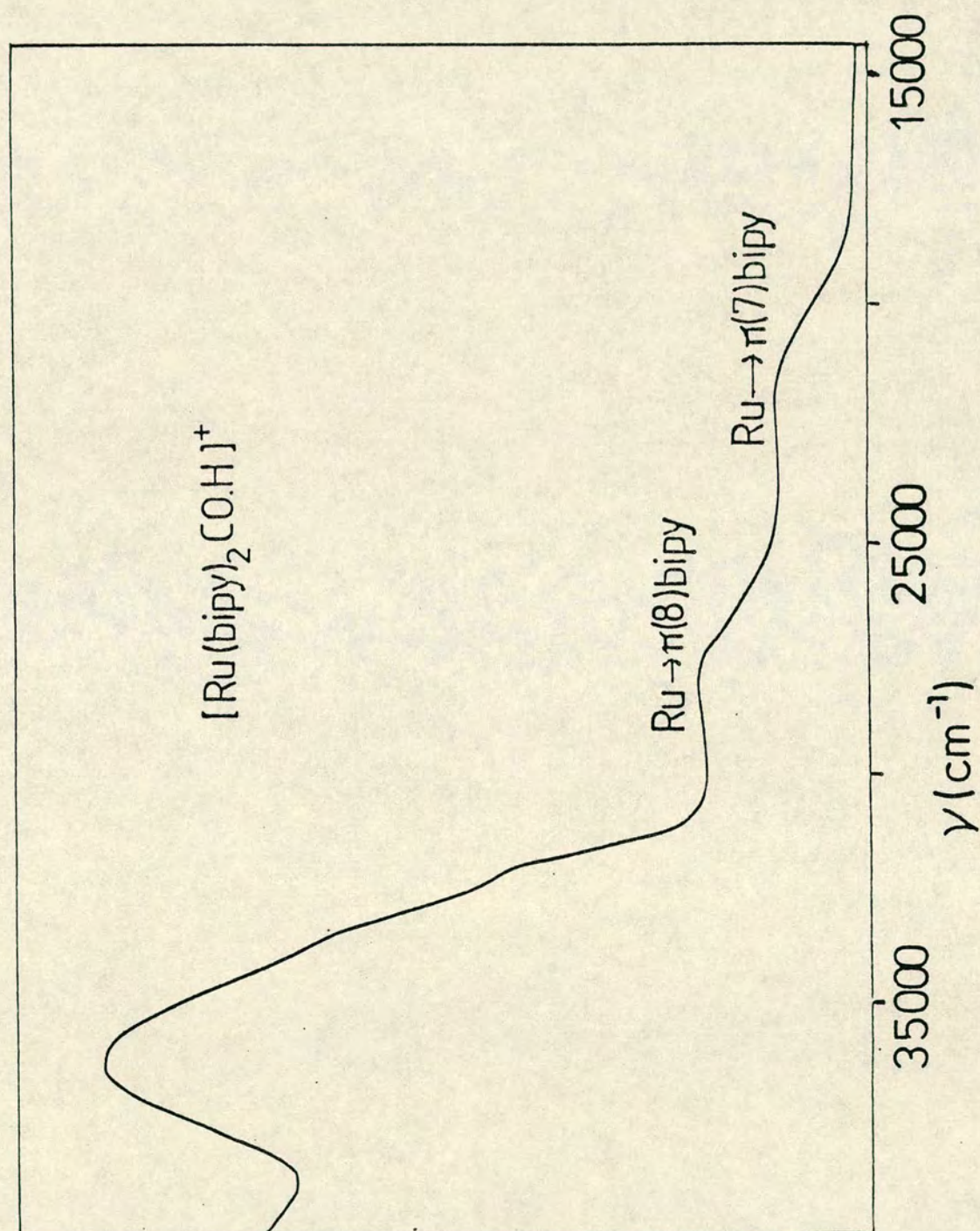
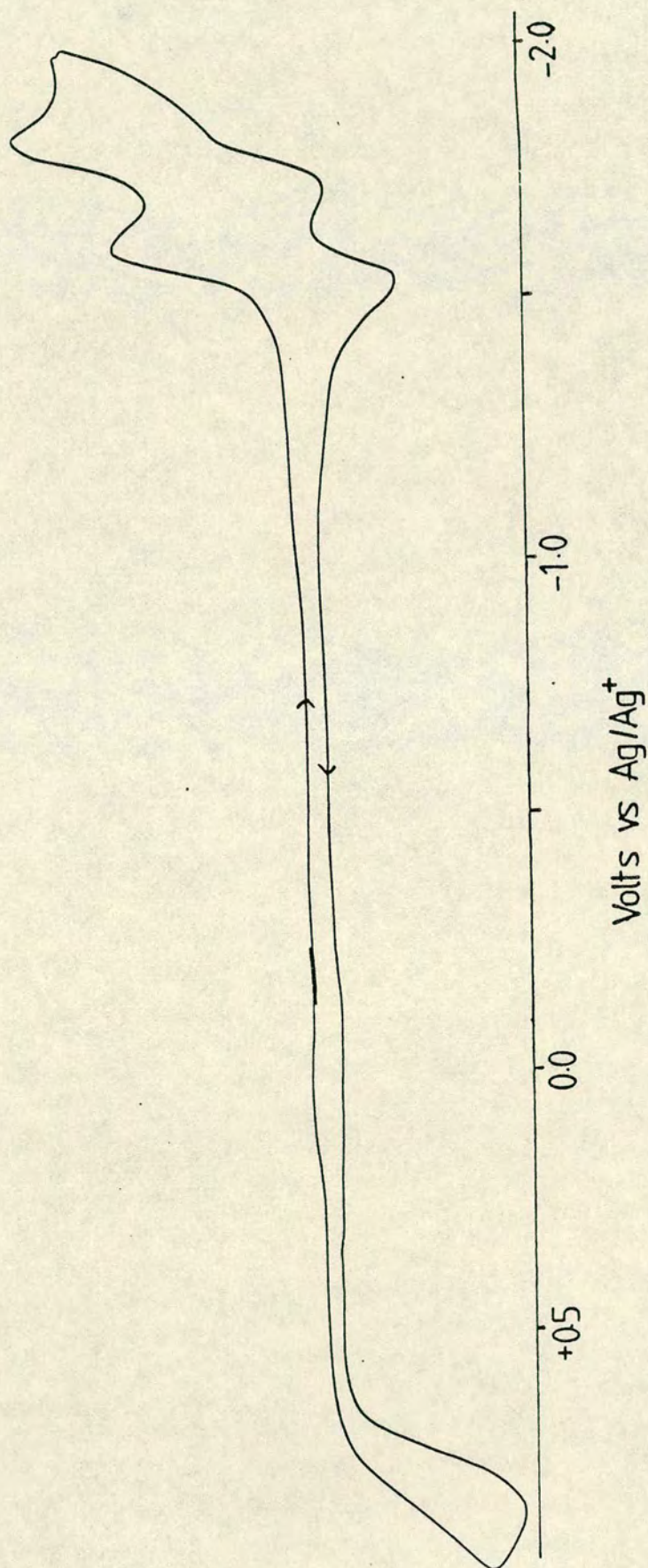


Figure 21: Cyclic Voltammogram of $[\text{Ru}(\text{bipy})_2\text{CO}_2\text{H}]^+$
in Dichloromethane at Room Temperature



of $[\text{Ru}(\text{bipy})_2\text{CO.MeCN}]^{2+}$.

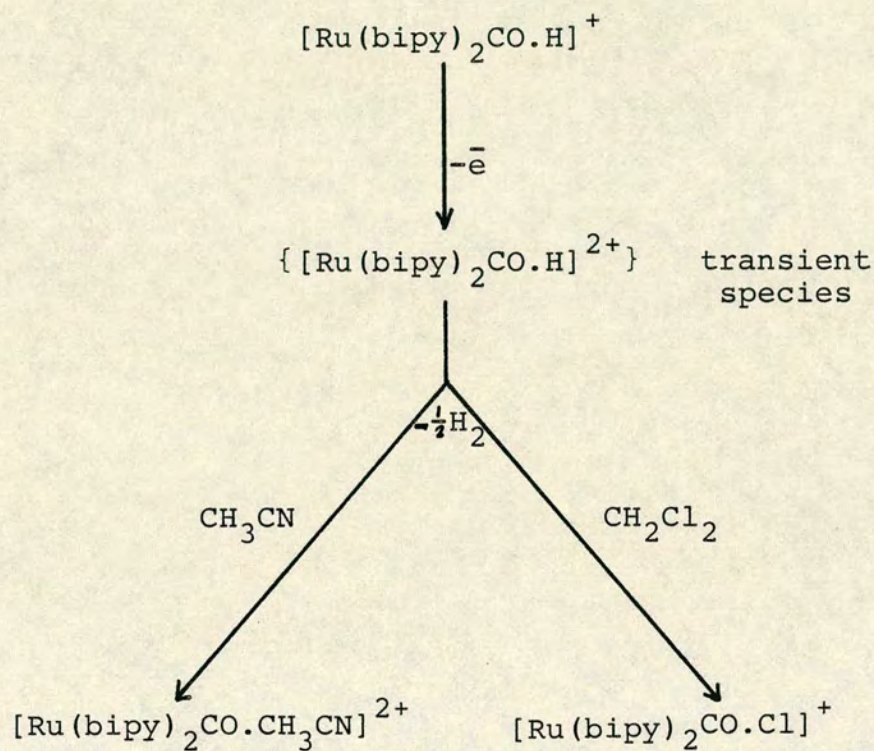
It would appear therefore that the one-electron oxidation product immediately loses $\frac{1}{2}\text{H}_2$ thereby spontaneously returning to ruthenium(II) and in the process binds a sixth ligand derived from the solvent. Electrogeneration at +1.0V vs Ag/Ag^+ , in a conventional electrochemical cell or at a platinum O.T.T.L.E. allowed the products to be examined electrochemically and their absorption spectra to be measured. These experiments, performed in both dichloromethane and acetonitrile, confirmed the formation of the products proposed above as illustrated in figure 22.

Acetonitrile is widely recognised as a co-ordinating solvent therefore its incorporation is no surprise in this case. On the other hand, dichloromethane is generally an inert non-coordinating solvent, although a few reports of chloride abstraction from this medium have appeared.³⁰⁻³² The purified electrochemical solvent was repeatedly checked and shown to contain no free chloride.

Reduction of X, on the cyclic voltammetric timescale, appeared to show two one-electron reversible reductions. However attempts to stabilise the mono-reduced species, X^- , all failed, even at low temperatures and in the presence of excess bipyridyl ligand.

In summary, our studies have shown that these complexes have a well-defined redox chemistry. Many of the reduced species can be stabilised, and they can all be rationalised in terms of the localised model. It is apparent, however,

Figure 22: Substitution Reactions of $\text{cis-}[\text{Ru}(\text{bipy})_2\text{CO.H}]^{2+}$



that these systems also tend to undergo remarkable and clear-cut ligand substitution reactions induced by both cathodic and anodic processes.

Experimental

$\text{Ru}(\text{bipy})_3\text{Cl}_2 \cdot \text{H}_2\text{O}$ was purchased from G.F. Smith & Co. The fluoroborate salt was obtained by metathesis with aqueous NaBF_4 and was recrystallised twice from water. $\text{Ru}(\text{bipy})_2\text{Cl}_2$ was prepared following the method of Sullivan, Salmon and Meyer.³³ $[\text{Ru}(\text{bipy})_2\text{CO} \cdot \text{Cl}](\text{ClO}_4)$, $[\text{Ru}(\text{bipy})_2\text{CO} \cdot \text{MeCN}](\text{ClO}_4)_2$, $[\text{Ru}(\text{bipy})_2\text{CO} \cdot \text{py}](\text{PF}_6)_2$, $[\text{Ru}(\text{bipy})_2(\text{CO})_2](\text{PF}_6)_2$ and $[\text{Ru}(\text{bipy})_2\text{CO} \cdot \text{H}](\text{PF}_6)$ were kindly supplied by Dr. J.M. Kelly of the University of Dublin, *and Dr. J.C. Vos of N.I.H.E. (Dublin)*. The tetraphenylboron salts of $[\text{Ru}(\text{bipy})_2\text{CO} \cdot \text{Cl}]^+$ and $[\text{Ru}(\text{bipy})_2\text{CO} \cdot \text{MeCN}]^{2+}$ were obtained by metathesis with methanolic NaBPh_4 and were recrystallised from methanol.

Acetonitrile was purified using the seven stage process reported by Walter and Ramaley.³⁴ Dichloromethane was stored over potassium hydroxide pellets for one week then distilled from P_2O_5 .³⁵ Pyridine was freshly distilled from KOH .³⁶ Dimethylsulphoxide was used as supplied. The supporting electrolyte, tetrabutylammonium tetrafluoroborate was prepared by the method of Heath *et al.*,³⁷ with tetraethylammonium hydroxide replaced by tetrabutylammonium hydroxide. The electrolyte concentration was 0.1M in acetonitrile, pyridine and dimethylsulphoxide and 0.5M in dichloromethane.

A conventional cell, utilising a three-electrode configuration consisting of a platinum microelectrode, a Ag/Ag^+ reference electrode separated from the bulk solution by a glass frit³⁸ and a platinum counter electrode, was used to perform the voltammetric experiments. Replacement of the platinum microelectrode by a larger platinum electrode (surface area 15 cm^2) and isolation of the secondary electrode from the bulk solution by the use of a glass frit allowed electrogeneration experiments to be performed. The solutions were rendered oxygen-free by purging with argon. Cyclic voltammograms and electrogeneration experiments were carried out using a Princeton Applied Research Model 170 instrument. Cyclic voltammetric scans were recorded at rates varying from 20mV/s to 500mV/s with routine measurements made at 100mV/s .

Spectroelectrochemical studies were made at a platinum O.T.T.L.E. in a cell block (see figure 1) mounted in the beam of a spectrophotometer (Unicam SP800 and Perkin-Elmer Lambda 9). Reference and auxiliary electrodes were as described above with both separated from the bulk solution to prevent contamination. Nitrogen was used to purge the solution and spectrophotometer compartment prior to electrogeneration. Constant potentials were supplied by a Metrohm E506 potentiostat. At lower temperatures the apparent extinction coefficients of all the absorption bands became higher and this is ascribed to be due almost entirely to solvent contraction. Since standard solutions of all the complexes studied were prepared at 20°C appropriate corrections have been made.

References

1. G. Sprintschnik, H.W. Sprintschnik, P.P. Kirsch and D.G. Whitten; J.Am.Chem.Soc., 98, 2337 (1976).
2. G. Sprintschnik, H.W. Sprintschnik, P.P. Kirsch and D.G. Whitten; J.Am.Chem.Soc., 99, 4947 (1977).
3. S.J. Valenty and G.L. Gaines; J.Am.Chem.Soc., 99, 1285 (1977).
4. A. Harriman; J.Chem.Soc.,Chem.Comm., 777 (1977).
5. L.J. Yellowlees, R.G. Dickinson, C.S. Halliday, J.S. Bonham and L.E. Lyons; Aust.J.Chem., 31, 431 (1978).
6. J.M. Kelly, C.M. O'Connell and J.G. Vos; J.Chem.Soc., Dalton Trans., 253 (1986).
7. D. Choudhury and D.J. Cole-Hamilton; J.Chem.Soc., Dalton Trans., 1885 (1982).
8. K. Tanaka, M. Moromito and T. Tanaka; Chem.Lett., 901 (1983).
9. J.M. Clear, J.M. Kelly, C.M. O'Connell, J.G. Vos, C.J. Cardin and S.R. Costa; J.Chem.Soc.,Chem.Comm., 750 (1980).
10. R.W. Murray, W.R. Heineman and G.W. O'Dom; Anal. Chem., 39, 1666 (1967).
11. N.E. Tokel-Takvoryan, R.E. Hemingway and A.J. Bard; J.Am.Chem.Soc., 95, 6582 (1973),
12. B.P. Sullivan, D.J. Salmon, T.J. Meyer and J. Peedin; Inorg.Chem., 18, 3369 (1979).
13. L.J. Yellowlees; Ph.D. Thesis, University of Edinburgh (1982).

14. G.M. Bryant, J.E. Ferguson and H.K.J. Powell;
Aust.J.Chem., 24, 257 (1971).
15. T.R. Weaver, T.J. Meyer, S.A. Adeyemi, G.M. Ekborg,
W.E. Hatfield, E.C. Johnson, R.W. Murray and
D. Umtereker; J.Am.Chem.Soc., 97, 3039 (1975).
16. A.B.P. Lever; 'Inorganic Electronic Spectroscopy',
Elsevier, Netherlands (1984) p.227.
17. E.A. Seddon and K.R. Seddon; 'The Chemistry of
Ruthenium', Elsevier (1984) and references therein.
18. L. Vaska; Chem.Ind., (London) 1402 (1961).
19. T.A. Stephenson and G. Wilkinson; J.Inorg.Nucl.Chem.,
28, 945 (1966).
20. E. König and S. Kremer; Chem.Phys.Lett., 5, 87 (1970).
21. E.E. Mercer and R.R. Buckley; Inorg.Chem., 4, 1692
(1965).
22. T.W. Kallen and J.E. Earley; Inorg.Chem., 10, 1152
(1971).
23. J.A. Rard; Chemical Reviews, 85, 31 (1985).
24. B.P. Sullivan, D. Conrad and T.J. Meyer; Inorg.Chem.,
24, 3640 (1985).
25. G.M. Brown, R.W. Callachan and T.J. Meyer; Inorg.
Chem., 14, 1915 (1975).
26. B. Durham, J.L. Walsh, C.L. Carter and T.J. Meyer;
Inorg.Chem., 19, 860 (1980).
27. C.M. Carlin and M.K. DeArmond; Chem.Phys.Lett., 89,
297 (1982).
28. K.B. Wiberg and T.P. Lewis; J.Am.Chem.Soc., 92,
7154 (1970).

29. J.M. Kelly and J.G. Vos; J.Chem.Soc.,Dalton Trans., 1045 (1986).
30. O.J. Scherer and H. Jungmann; J.Organomet.Chem., 208, 153 (1981).
31. G. Bellachiona, G. Cardaci and G. Recchenbach; J.Organomet.Chem., 221, 291 (1981).
32. R.N. Bagchi, A.M. Bond, C.L. Heggie, T.L. Henderson, E. Mocellin and R.A. Seckel; Inorg.Chem., 22, 3007 (1983).
33. B.P. Sullivan, D.J. Salmon and T.J. Meyer; Inorg.Chem., 17, 3334 (1978).
34. M. Walter and L. Ramaley; Anal.Chem., 45, 165 (1973).
35. D.D. Perrin, W.L.F. Armareger and D.R. Perrin; 'Purification of Laboratory Chemicals', Pergamon Press (1980).
36. R. Lindauer and L.M. Mukherjee; Pure Appl.Chem., 27, 267 (1971).
37. G.A. Heath, G.T. Hefter, T.W. Bogle, C.D. Desjardines and D.W.A. Sharp; J.Fluor.Chem.II, 399 (1978).
38. D.T. Sawyer and J.L. Roberts; 'Experimental Electrochemistry for Chemists', Wiley-Interscience, New York (1974).

Chapter 3

Further Spectro-electrochemical Studies on Reduction of Contrasting Iridium(III) and Chromium(III) Bipyridyl Complexes

In this chapter we consolidate our interpretation of $d\pi^6 [\text{Ir}(\text{bipy})_3]^{3+/2+/+/\circ}$ firstly by addressing lower symmetry Ir(III) systems whose behaviour should none-the-less closely resemble $[\text{Ir}(\text{bipy})_3]^{3+}$ if the charge-trapping by individual ligands faithfully describe the tris complex. Secondly, we take the opportunity to compare and contrast $[\text{Cr}(\text{bipy})_3]^{3+}$ where we anticipate extremely different properties over the first three reductions converging however at the $d\pi^6$ (Cr^0) level to a ligand-reducible system isoelectronic with $[\text{Ir}(\text{bipy}^0)_3]^{3+}$.

Incidentally these diverse complexes [Ir(III) and Cr(III)] show a common problem of intrinsically difficult synthesis due to the sluggishness of ligand substitution reactions at the metal centres concerned $\text{Cr(III)}d^3$ and $\text{Ir(III)}d^6$. In the former case this is overcome by the elegant proven strategy of accomplishing the substitution at the Cr(II) labile level and in the latter case after much difficulty by developing routes via mixed-ligand complexes $[\text{Ir}(\text{bipy})_2(\text{X})(\text{Y})]^{n+}$ where X and Y are intrinsically exceptionally labile ligands.

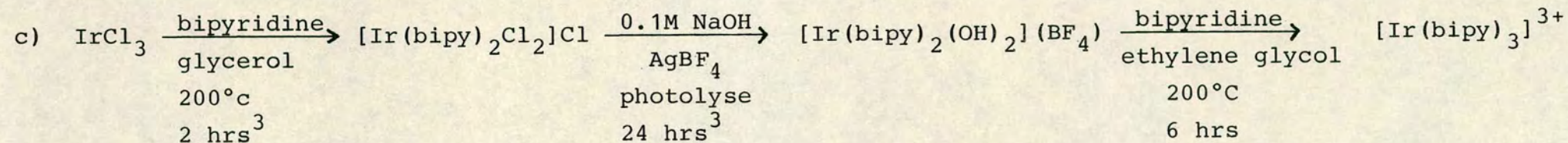
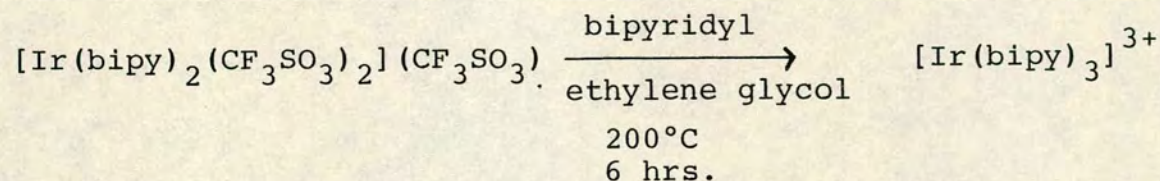
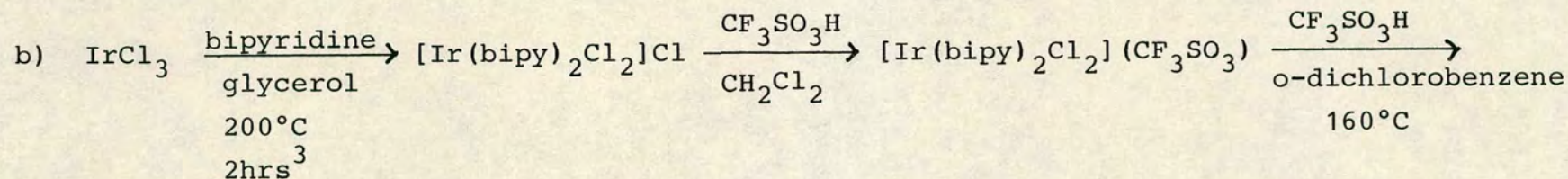
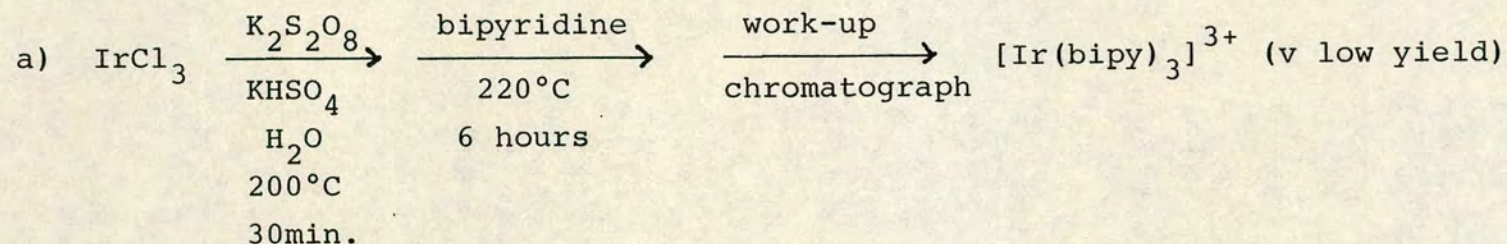
Although of considerable interest the complex

$[\text{Ir}(\text{bipy})_3]^{3+}$ has historically proved extremely difficult to prepare with the only genuine synthetic route¹ yielding an irretrievable carbon metallated biproduct as the major component. This complex is considered in detail in chapter 4.

However, a new preparation of $[\text{Ir}(\text{bipy})_3]^{3+}$ has recently been devised by Sullivan and Meyer² which has allowed this complex to be obtained in high yield as shown in scheme 1. In our laboratories we have also devised a reliable two-step preparation via the complex $[\text{Ir}(\text{bipy})_2(\text{OH})_2]^+$ (see experimental section).

In the course of this study we have carried through the Meyer preparation to $[\text{Ir}(\text{bipy})_3]^{3+}$ and examined the hitherto vaguely characterised complexes successfully manipulating them redox-wise as described later. We have also discovered that the four accessible oxidation states of chromium in the system $[\text{Cr}(\text{bipy})_3]^n$ show a richly informative spectral progression which yields to our strategy for correlating E^0 data with MLCT, LMCT and $\pi\pi^*$ transitions.

The absorption and emission spectra of $[\text{Ir}(\text{bipy})_2\text{Cl}_2]\text{Cl}$, XI, which is the initial complex prepared in this synthesis, have been reported previously.³ An electrochemical study on the nitrate salt of this complex has also been reported,⁴ however our investigations have revealed marked differences in the voltammetric behaviour of $[\text{Ir}(\text{bipy})_2\text{Cl}_2]^+$ depending upon the anions present.



Note: a) Reference 1. Major product is a C-metallated derivative (see chapter 4).
 b) Reference 2.
 c) Present work. See experimental section.

Kahl, Hanck and DeArmond⁴ report that $[\text{Ir}(\text{bipy})_2\text{Cl}_2]$ (NO_3) undergoes two quasi-reversible one-electron reductions on the cyclic voltammetric timescale. However controlled potential electrosynthesis, at a potential beyond the first reduction, leads to decomposition of the complex; the presence of free chloride in solution is then noted.

Our study on the chloride salt of XI showed similar electrochemical behaviour. The A.C. polarogram of $[\text{Ir}(\text{bipy})_2\text{Cl}_2]\text{Cl}$, shown in figure 1, reveals several cathodic waves indicating some decomposition occurring subsequent to the first reduction. Consistent with this, attempted electrosynthesis of the one-electron reduction product, $[\text{Ir}(\text{bipy})_2\text{Cl}_2]^0$, fails with the liberation of bipyridine from the complex detected. Our attempts to suppress this dissociation by carrying out this electrolysis in the presence of excess bipyridine ligand were unsuccessful, with degradation of the complex again observed.

However, when this dichloro-complex cation is isolated as its trifluoromethanesulphonate (CF_3SO_3^-) salt and purified, examination of its electrochemical behaviour, in $\text{CH}_2\text{Cl}_2/\text{TBABF}_4$ reveals two reversible one-electron reductions (see figure 2 and table 2); both of these reduced species could be electrogenerated in bulk at -30°C in dichloromethane or acetonitrile.

In order to examine further this anion-sensitive dissociation reaction, we generated $[\text{Ir}(\text{bipy})_2\text{Cl}_2]^0$, at -30°C , and added a series of anions; we then examined the electrochemical behaviour of the resultant solutions.

Figure 1: A.C. Polarogram of $[\text{Ir}(\text{bipy})_2\text{Cl}_2]\text{Cl}$
in Acetonitrile at -30°C

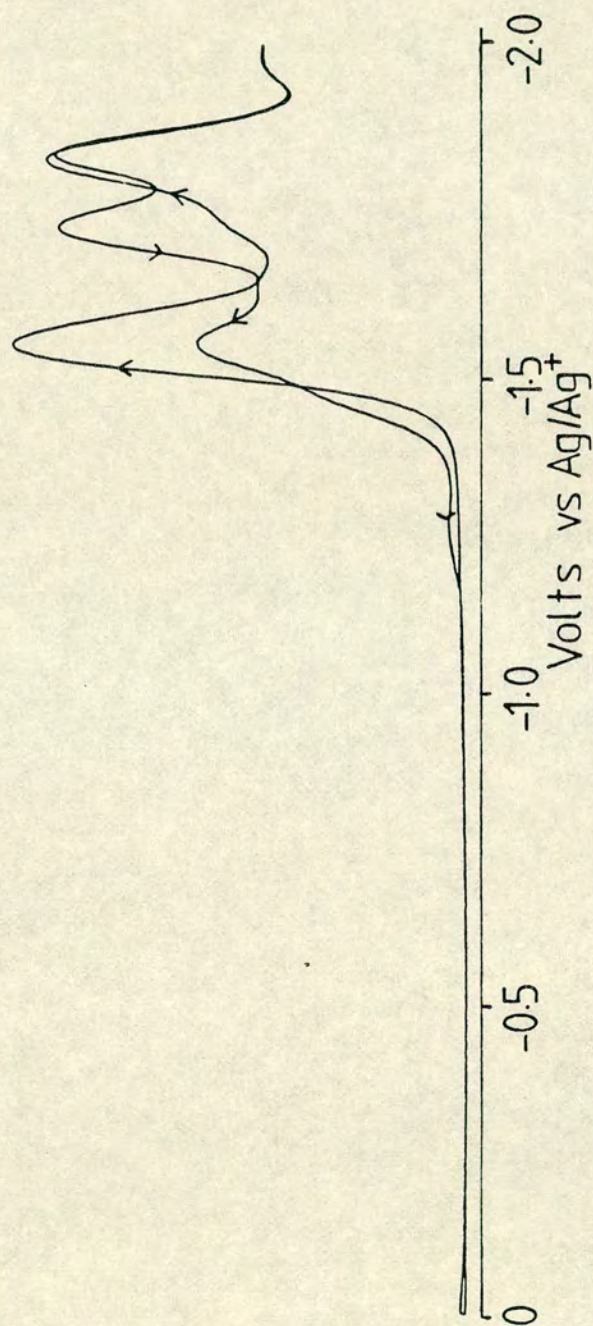
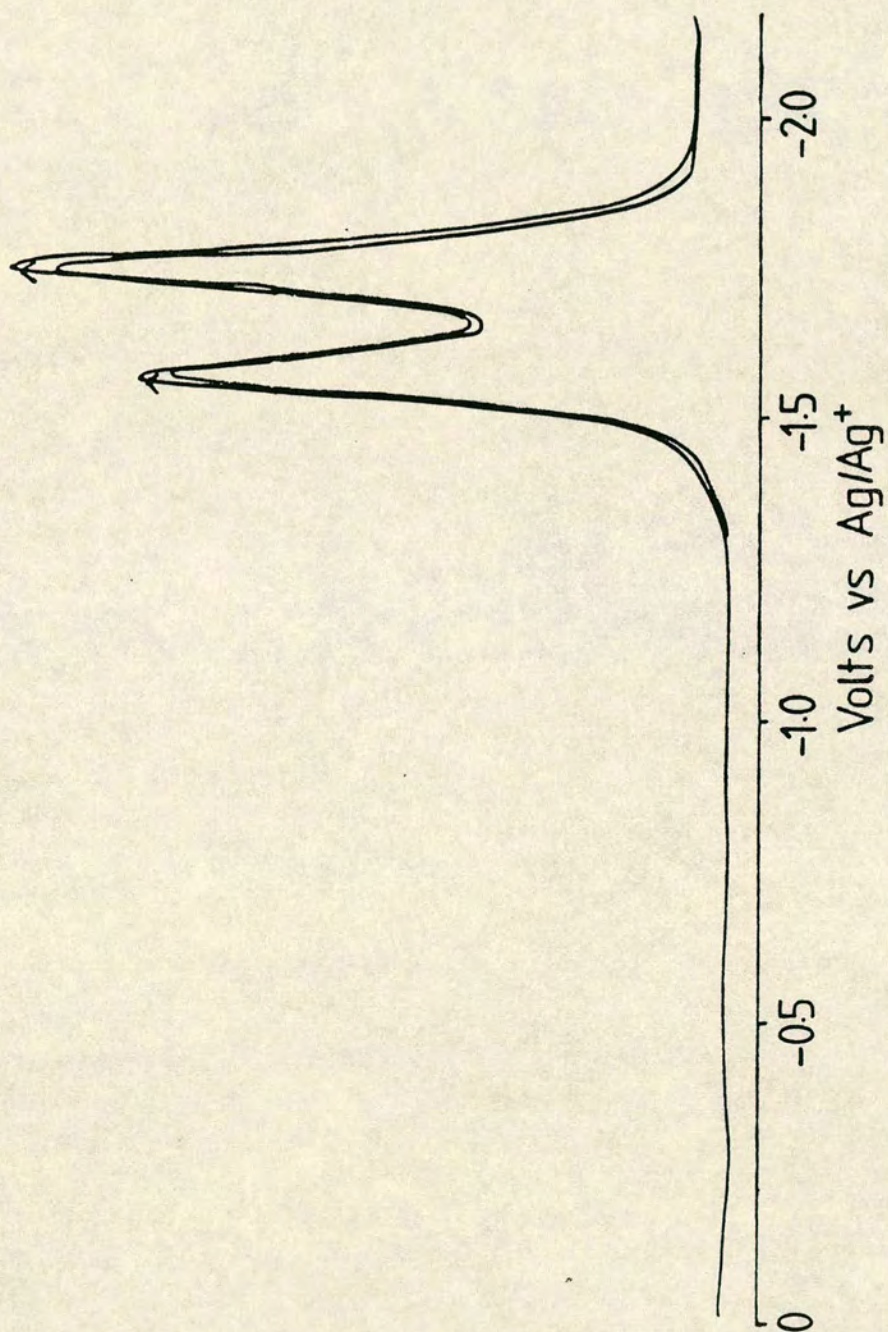


Figure 2: A.C. Polarogram of $[\text{Ir}(\text{bipy})_2\text{Cl}_2](\text{CF}_3\text{SO}_3)$
in Acetonitrile at -30°C



On addition of tetrabutylammonium iodide $[\text{TBA}^+\text{I}^-]$ to $[\text{Ir}(\text{bipy})_2\text{Cl}_2]^0$ no change in the voltammetric behaviour of this system is noted with the initial complex $[\text{Ir}(\text{bipy})_2\text{Cl}_2]^+$ being regenerated in its original concentration. Similar behaviour is noted on addition of tetrabutylammonium bromide to XI^- .

However if tetrabutylammonium chloride (TBA^+Cl^-) is added to a similarly prepared solution of $[\text{Ir}(\text{bipy})_2\text{Cl}_2]^0$ then decomposition of the complex is again noted.

We explain this behaviour by considering the solution structure of the complex $[\text{Ir}(\text{bipy})_2\text{Cl}_2]\text{Cl}$ which may exist as a tightly-bound ion-pair in CH_2Cl_2 . Then on ligand-localised reduction of XI, accompanied by the presumed labilisation of the complex, the chloride anion in the solvation shell would be in a favoured position to engage in ligand-substitution reactions displacing bipy^0 or bipy^- . This suggestion is consistent with the observations noted with the larger bromide and iodide anions present, where greater ionic radii will be reflected in weaker ionic pairing.

In the studies now described on the absorption spectra of $[\text{Ir}(\text{bipy})_2\text{Cl}_2]^{+0/-}$ we have therefore utilised the trifluoromethanesulphonate salt.

The reduction products $[\text{Ir}(\text{bipy})_2\text{Cl}_2]^0$ and $[\text{Ir}(\text{bipy})_2\text{Cl}_2]^-$ were separately electrogenerated, at -1.60 and -1.80V respectively, at -30°C , in a platinum O.T.T.L.E. cell; the absorption spectra obtained are shown in figure 3 with the bands observed assigned in table 1.

Figure 3: Absorption Spectra of $[\text{Ir}(\text{bipy})_2\text{Cl}_2]^{+/-}$ in Acetonitrile at -30°C

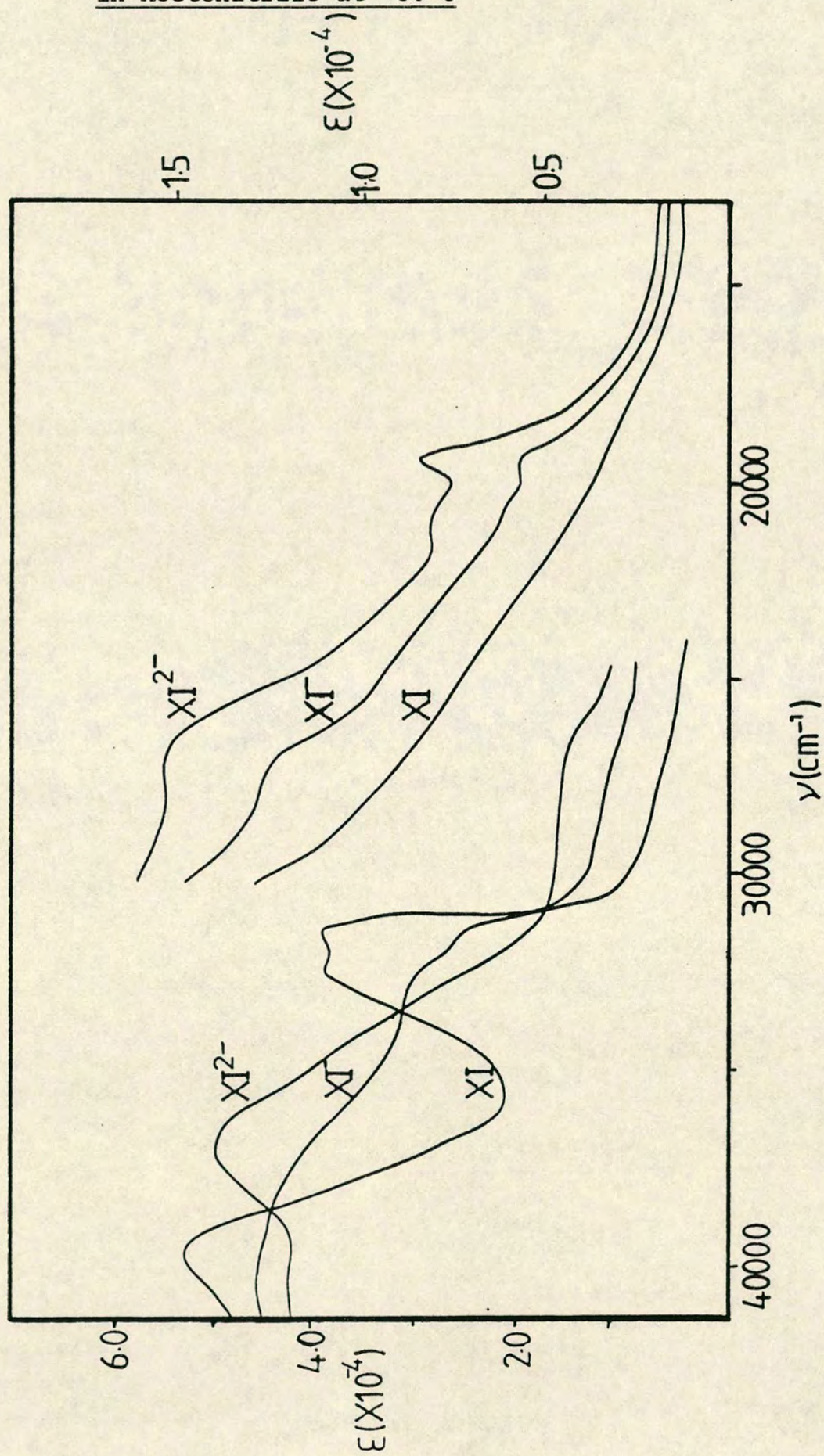
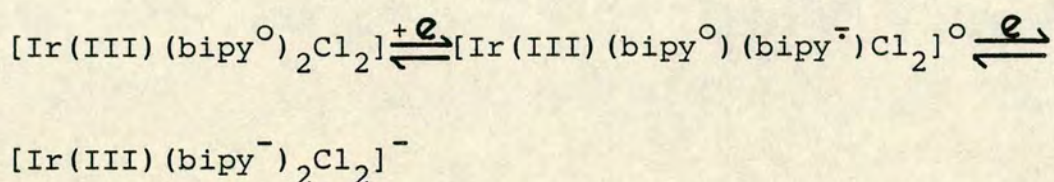


Table 1: Assignment of the Absorption Bands in $[\text{Ir}(\text{bipy})_2\text{Cl}_2]^{+/0/-}$ $\nu \times 10^{-3}/\text{cm}^{-1}$ ($\epsilon \times 10^{-4}$)

<u>Complex</u>	<u>Transition</u>			
	$\frac{\pi(6) \rightarrow \pi(8)}{\text{bipy}^{\text{O}}}$	$\frac{\pi \rightarrow \pi^*}{\text{bipy}^{\bar{-}}}$	$\frac{\pi(6) \rightarrow \pi(7)}{\text{bipy}^{\text{O}}}$	$\frac{\pi \rightarrow \pi^*}{\text{bipy}^{\bar{-}}}$
$[\text{Ir}(\text{bipy})_2\text{Cl}_2]^+$	39.9 (5.31)	-	32.9 (3.80) 31.8 (3.82)	-
$[\text{Ir}(\text{bipy})_2\text{Cl}_2]^0$	40.6 sh	37.3 sh	33.1 (3.00) 32.0 (2.51)	27.6 (1.28) 20.7 (0.68) 19.6 (0.65)
$[\text{Ir}(\text{bipy})_2\text{Cl}_2]^-$	-	37.0 (4.99)	-	27.0 (1.60) 20.6 (0.85) 19.4 (0.87)
$\text{Na}^+\text{bipy}^{\bar{-}9}$		36.3 (0.82)		25.9 (2.95) 18.8 (0.62) 17.8 (0.65)

On successive reductions a steady loss of the bands characteristic of the neutral bipyridine ligands is noted accompanied by the stepwise growth of the $\text{bipy}^{\cdot-}$ chromophore. It is apparent therefore that these reduced species should be formulated in terms of the localised model as shown below.



In scheme 1 the synthetic precursor to $[\text{Ir}(\text{bipy})_3]^{3+}$ is the complex $[\text{Ir}(\text{bipy})_2(\text{CF}_3\text{SO}_3)_2](\text{CF}_3\text{SO}_3)$, XII. Considerable doubt was however expressed over the formulation of this system; the complex may be a dication with one chelated trifluoromethanesulphonate ligand and two CF_3SO_3^- anions or a monocation with two CF_3SO_3^- ligands and one anion.

An examination of the electrochemical behaviour of this system allows us to predict which formulation of this complex is correct.

We have previously shown that the potential required to reduce a bipyridyl ligand is dependent upon:

a) the central metal charge for $[\text{M}(\text{bipy})_3]^{n+}$ systems.

For example $E_{\text{red}}(\text{I})[\text{Ru}(\text{bipy})_3]^{2+} = -1.66\text{V}$ and

$E_{\text{red}}(\text{I})[\text{Ir}(\text{bipy})_3]^{3+} = -1.26\text{V}$ vs Ag/Ag^+ ;

b) the charge on any ligand replacing bipyridine in

$[M(\text{bipy})_3]^{n+}$. For example $\text{Ered}(1)[\text{Ru}(\text{bipy})_3]^{2+} = -1.66\text{V}$ and $\text{Ered}(1)[\text{Ru}(\text{bipy})_2\text{Cl}_2]^0 = -1.95\text{V}$ vs Ag/Ag^+ . (c.f. $\text{Ered}(1)[\text{Ru}(\text{bipy})_2(\text{py})_2]^{2+} = -1.66\text{V}$).

If we compare the potentials measured for the first two reductions of $[\text{Ir}(\text{bipy})_2(\text{CF}_3\text{SO}_3)_2](\text{CF}_3\text{SO}_3)$ with $[\text{Ir}(\text{bipy})_2\text{Cl}_2](\text{CF}_3\text{SO}_3)$ and $[\text{Ir}(\text{bipy})_3](\text{PF}_6)_3$ as shown in table 2, it may be noted that the chloride and trifluoromethanesulphonate ligands have similar cumulative inductive effects on the bipyridyl ligands. This strongly suggests the chelated formulation $[\text{Ir}(\text{bipy})_2(\text{CF}_3\text{SO}_3)]^{2+}$ can be set aside.

Table 2: Reduction Potentials for a Series of Iridium Complexes^a

<u>Complex</u>	<u>Ered(1)</u>	<u>Ered(2)</u>
$[\text{Ir}(\text{bipy})_3]^{3+}$	-1.26	-1.39
^b $[\text{Ir}(\text{bipy})_2(\text{bipy}')]^{2+}$	-1.40	-1.58
$[\text{Ir}(\text{bipy})_2\text{Cl}_2](\text{CF}_3\text{SO}_3)$	-1.54	-1.73
$[\text{Ir}(\text{bipy})_2(\text{CF}_3\text{SO}_3)_2](\text{CF}_3\text{SO}_3)$	-1.55	-1.75

a - All potentials are measured vs Ag/Ag^+ in 0.5M $\text{TBABF}_4/\text{CH}_2\text{Cl}_2$, 0.1M $\text{TBABF}_4/\text{CH}_3\text{CN}$ or 0.1M $\text{TBABF}_4/(\text{CH}_3)_2\text{SO}$.

b - The unique bipyridyl ligand carries an effective one negative charge (see chapter 4).

An examination of the ^{19}F n.m.r. spectrum of $[\text{Ir}(\text{bipy})_2(\text{CF}_3\text{SO}_3)_2](\text{CF}_3\text{SO}_3)$ in d^6 -dimethylsulphoxide reveals two different CF_3 -groups represented by two singlets (in an approximately 2:1 ratio) which is also consistent with the monocation formulation; see table 3.

Table 3: ^{19}F n.m.r. data for $[\text{Ir}(\text{bipy})_2(\text{CF}_3\text{SO}_3)_2](\text{CF}_3\text{SO}_3)$

<u>Complex</u>	<u>Resonance</u>	<u>Relative Ratio</u>
$[\text{Ir}(\text{bipy})_2(\text{CF}_3\text{SO}_3)_2](\text{CF}_3\text{SO}_3)$	-78.28	2
	-78.63	1
$\text{TBA}^+\text{CF}_3\text{SO}_3^-$	-78.65	

As shown in figure 4, $[\text{Ir}(\text{bipy})_2(\text{CF}_3\text{SO}_3)_2](\text{CF}_3\text{SO}_3)$ undergoes two quasi-reversible reductions when studied at -40°C in dichloromethane. If, however, a six-fold excess of tetrabutylammonium trifluoromethanesulphonate ($\text{TBA}^+\text{CF}_3\text{SO}_3^-$) is added to the electrolytic solution then two reversible one-electron reductions may be observed. This interesting observation confirms that $[\text{Ir}(\text{bipy}^0)(\text{bipy}^\cdot)(\text{CF}_3\text{SO}_3)_2]^\circ$ is more labile than the unreduced compound, and prone to expelling CF_3SO_3^- .

Since $\text{TBA}^+\text{CF}_3\text{SO}_3^-$ is transparent in the ultra-violet/visible region of the absorption spectrum, each of these reduced species may be electrogenerated at a platinum

Figure 4: A.C. Polarogram of $[\text{Ir}(\text{bipy})_2(\text{CF}_3\text{SO}_3)_2(\text{CF}_3\text{SO}_3)]$ at -30°C , also in the Presence of Excess $\text{TBA}^+\text{CF}_3\text{SO}_3^-$

\rightarrow Forward scan
 \leftarrow Reverse scan
 Reverse scan in the presence of excess $\text{TBA}^+\text{CF}_3\text{SO}_3^-$

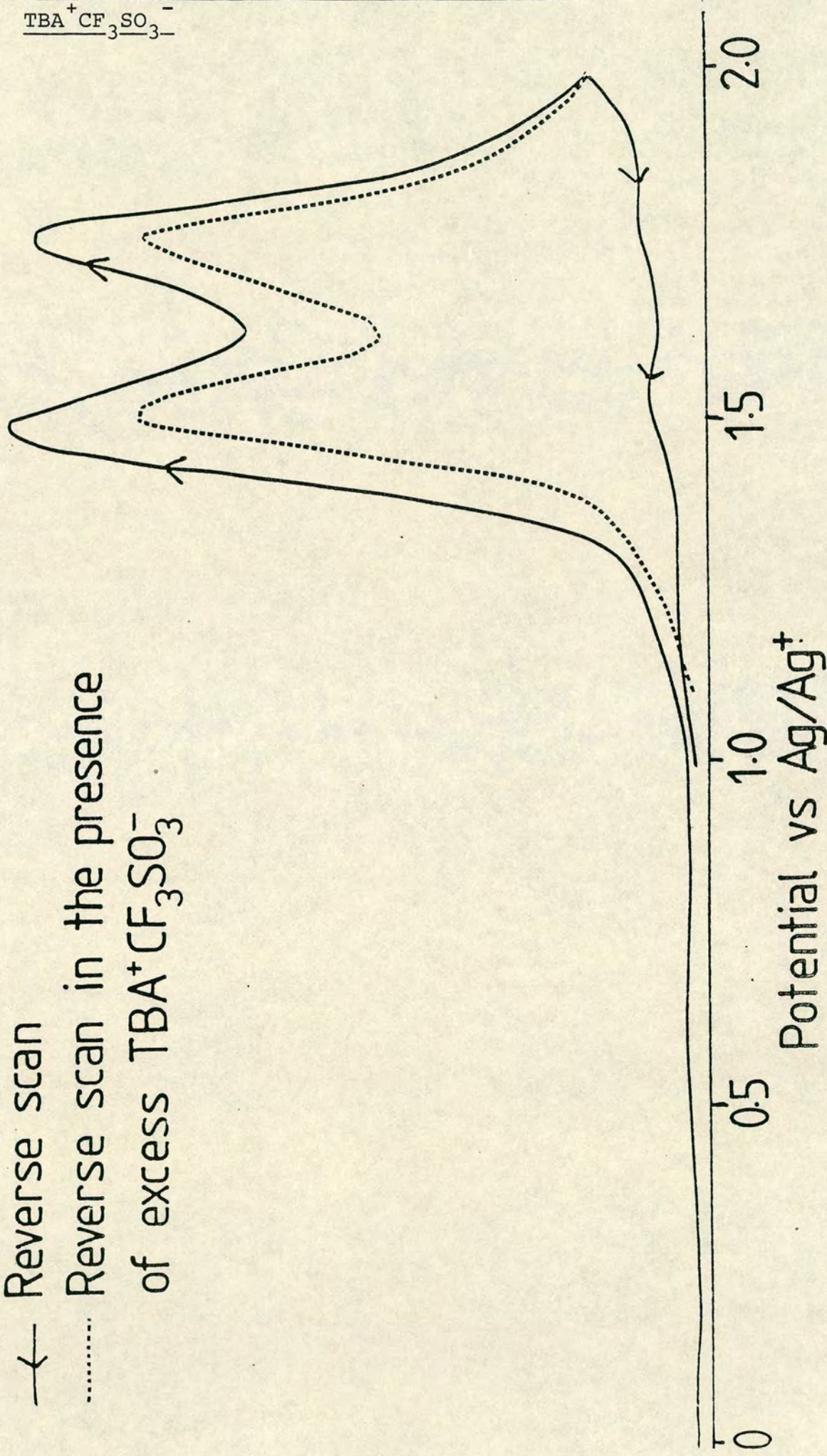


Figure 5: Absorption Spectra of $[\text{Ir}(\text{bipy})_2(\text{CF}_3\text{SO}_3)_2]^{+/-}$ in Dichloromethane at -30°C in the Presence of Excess $\text{TBA}^+\text{CF}_3\text{SO}_3^-$

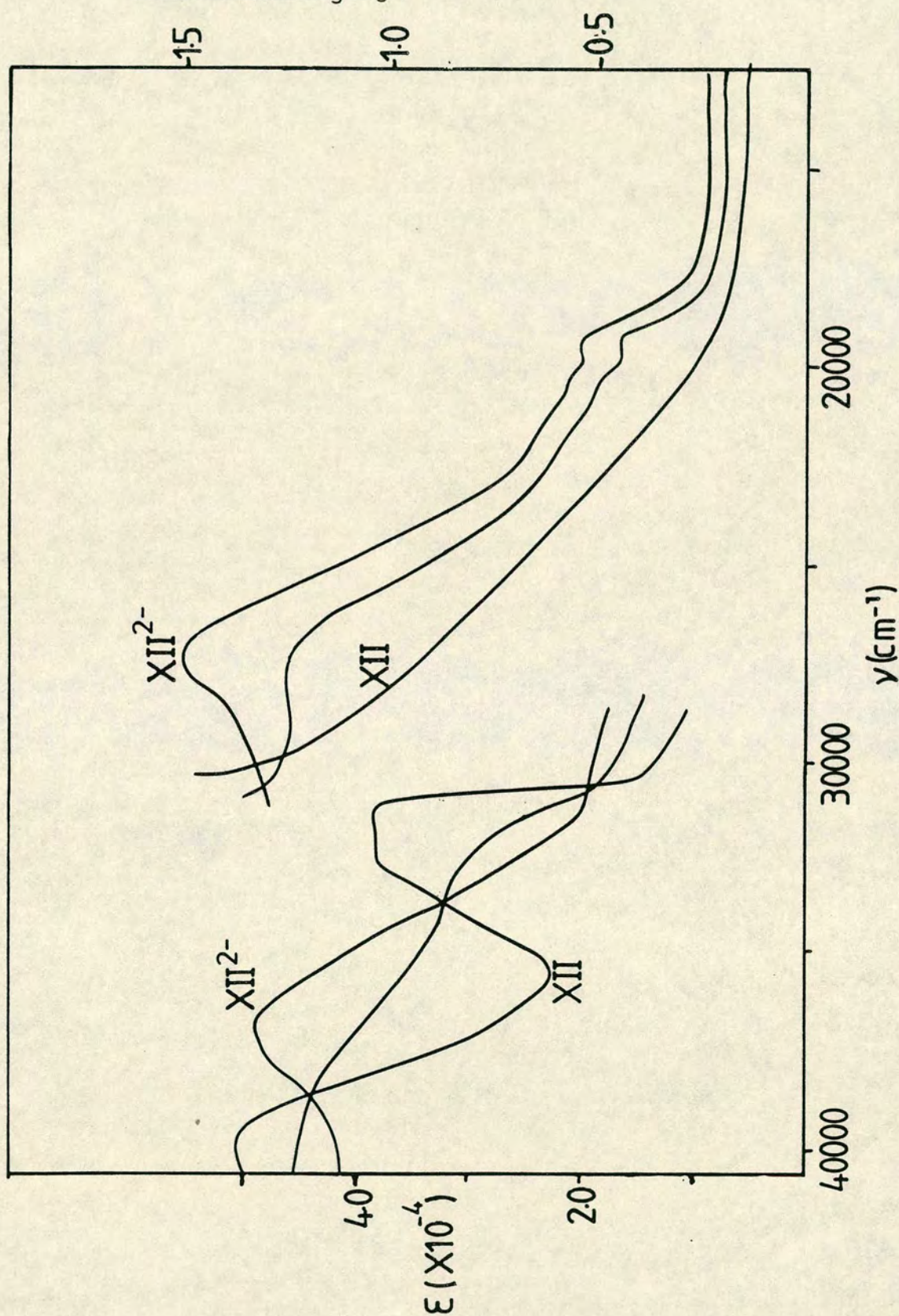


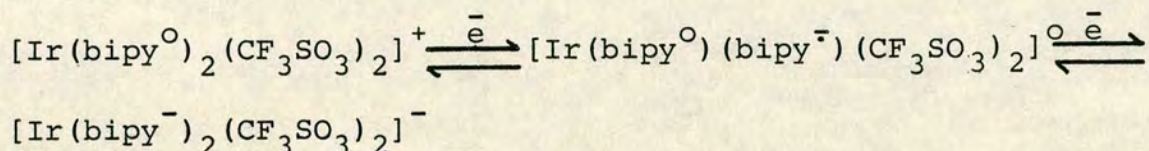
Table 4: Assignment of the Absorption Bands Observed in $[\text{Ir}(\text{bipy})_2(\text{CF}_3\text{SO}_3)_2]^{+/-}$
 $\nu \times 10^{-3}/\text{cm}^{-1}$ ($\epsilon \times 10^{-4}$)

<u>Complex</u>	<u>Transition</u>				
	$\frac{\pi(6) \rightarrow \pi(8)}{\text{bipy}^{\text{O}}}$	$\frac{\pi \rightarrow \pi^*}{\text{bipy}^-}$	$\frac{\pi(6) \rightarrow \pi(7)}{\text{bipy}^{\text{O}}}$	$\frac{\pi \rightarrow \pi^*}{\text{bipy}^-}$	$\frac{\pi \rightarrow \pi^*}{\text{bipy}^-}$
$[\text{Ir}(\text{bipy})_2(\text{CF}_3\text{SO}_3)_2]^+$	39.9 (5.06)	-	32.2 (3.97) 31.0 (3.98)	-	-
$[\text{Ir}(\text{bipy})_2(\text{CF}_3\text{SO}_3)_2]^{\text{O}}$	a	a	32.0 sh	27.0 (1.25)	20.4 (0.47) 19.2 (0.45)
$[\text{Ir}(\text{bipy})_2(\text{CF}_3\text{SO}_3)_2]^-$	-	36.9 (4.89)	-	27.1 (1.50)	20.3 (0.57) 19.3 (0.54)
$\text{Na}^+ \text{bipy}^-$ 5		36.3 (0.82)		25.9 (2.95)	18.8 (0.62) 17.8 (0.65)

a - Band obscured

O.T.T.L.E., in the presence of $\text{TBA}^+\text{CF}_3\text{SO}_3^-$, allowing their electronic spectra to be measured. The absorption spectrum of each species is shown in figure 6, with the observed bands assigned in table 4.

We may therefore classify these reduced species in terms of the ligand localised model.



The complex $[\text{Ir}(\text{bipy})_3]^{3+}$ has been shown to undergo six one-electron reversible reductions⁴ which have been assigned in terms of the ligand localised model, see chapter 1.

In this study we now present the ultra-violet spectra of the first three one-electron reduction products of $[\text{Ir}(\text{bipy})_3]^{3+}$ as shown in figure 6. We may now fully assign the ultra-violet/visible spectrum of each species in table 5.

An examination of a cyclic voltammogram of $[\text{Cr}(\text{III})(\text{bipy})_3]^{3+}$, see figure 7, reveals the presence of six one-electron reductions (superficially analogous to $[\text{Ir}(\text{bipy})_3]^{3+}$ with two sets of three regularly spaced waves) however the reductive processes involved in this case are markedly different.

$[\text{Cr}(\text{bipy})_3]^{3+}$, XIII, is a yellow $d\pi^3$ complex which has been the subject of some interest in relation to solar energy conversions;^{6,7} its lowest excited state involves

Figure 6: Absorption Spectra of $[\text{Ir}(\text{bipy})_3]^{3+/2+/+/0}$
in Dichloromethane at Room Temperature

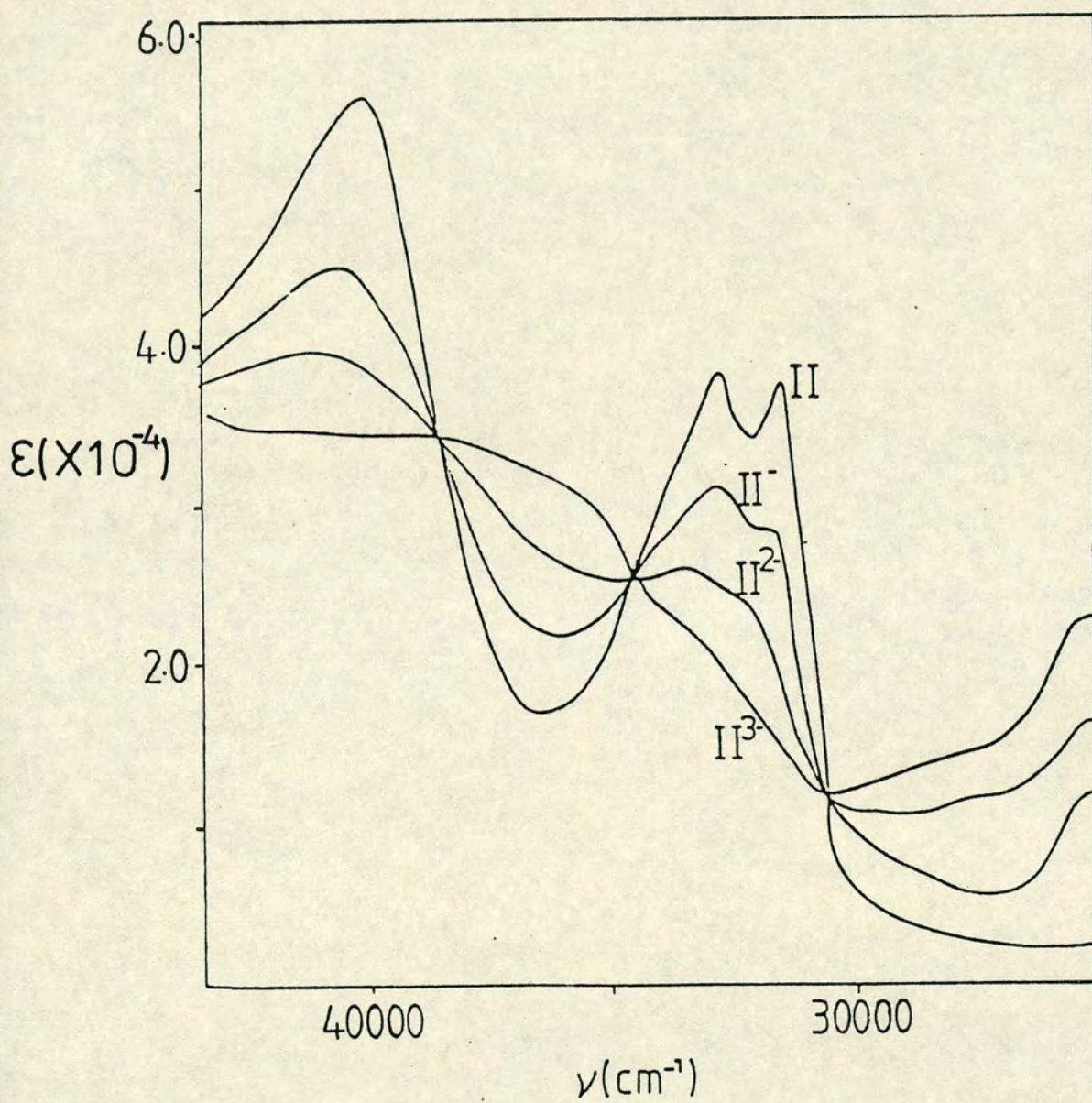
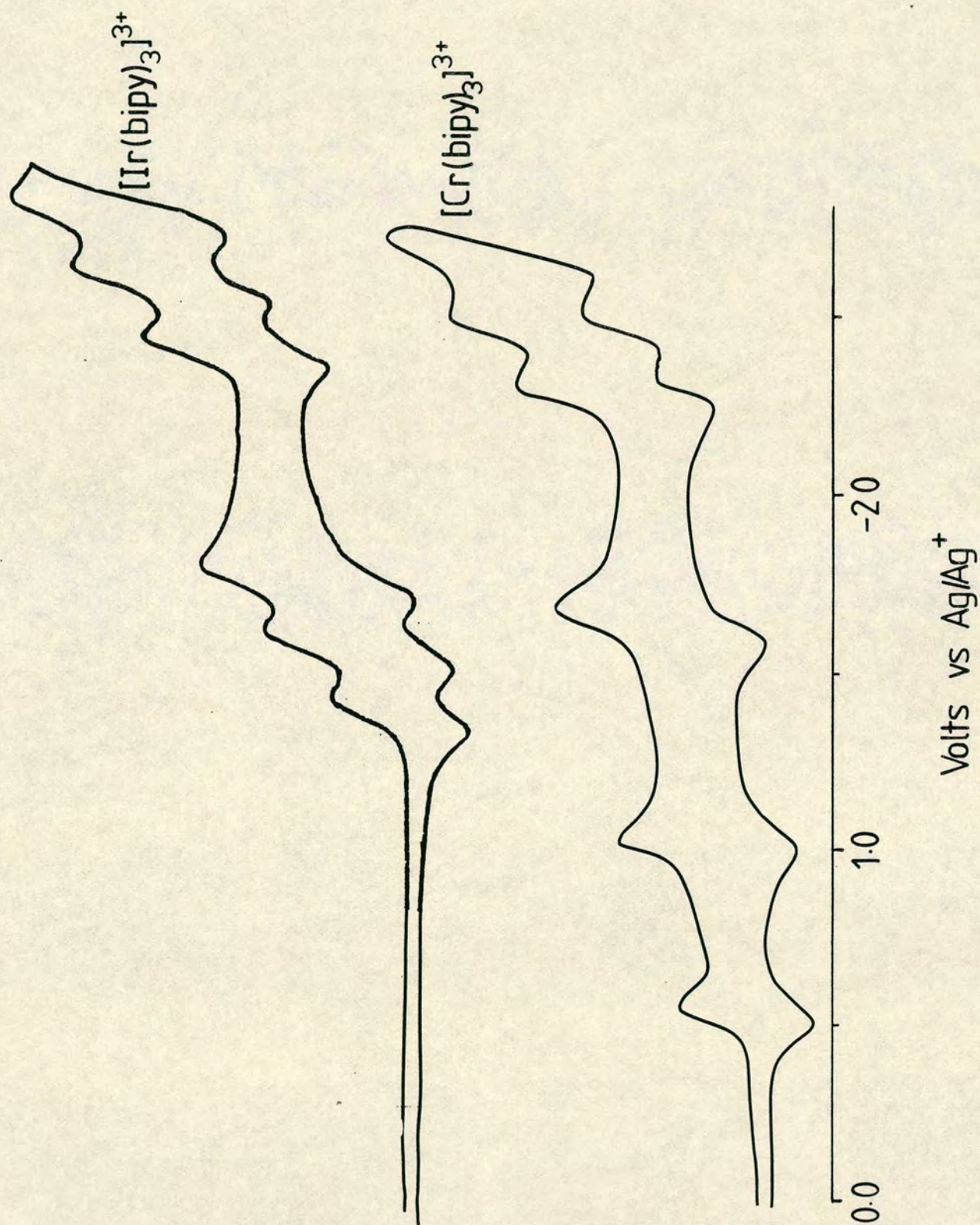


Table 5: Assignment of the Absorption Bands in $[\text{Ir}(\text{bipy})_3]^{3+/2+/+/0}$
 $\nu \times 10^{-3}/\text{cm}^{-1}$ ($\epsilon \times 10^{-4}$)

<u>Complex</u>	<u>Transition</u>				
	$\frac{\pi(6) \rightarrow \pi(8)}{\text{bipy}^0}$	$\frac{\pi \rightarrow \pi^*}{\text{bipy}^-}$	$\frac{\pi(6) \rightarrow \pi(7)}{\text{bipy}^0}$	$\frac{\pi \rightarrow \pi^*}{\text{bipy}^-}$	$\frac{\pi \rightarrow \pi^*}{\text{bipy}^-}$
$[\text{Ir}(\text{bipy})_3]^{3+}$	40.0 (5.61)	-	31.5 (4.47) 32.7 (4.50)	-	-
$[\text{Ir}(\text{bipy})_3]^{2+}$	40.4 (4.50)	a	31.7 (2.96) 32.8 (3.12)	25.6 (1.04)	22.2 (0.46) 20.4 (0.44)
$[\text{Ir}(\text{bipy})_3]^+$	40.6 (3.91)	a	31.7 (2.37) 32.9 (2.57)	25.4 (1.72)	22.0 (0.79) 20.0 (0.83)
$[\text{Ir}(\text{bipy})_3]^0$	-	35.6 (3.06)	-	25.4 (2.29)	21.9 (1.04) 19.6 (0.65)
$^5\text{Na}^+\text{bipy}^-$	-	36.3 (0.82)	-	25.9 (2.95)	18.8 (0.62) 17.8 (0.65)

a - Band obscured

Figure 7: Cyclic Voltammograms of $[\text{Ir}(\text{bipy})_3]^{3+}$ and $[\text{Cr}(\text{bipy})_3]^{3+}$ in Acetonitrile



a metal-centred ligand-field transition.⁶ This state is both long-lived in deaerated aqueous solutions (lifetime of 63 μ s at room temperature⁸) and highly reactive towards redox quenchers.^{9,10}

The electrode potentials measured for the six reductions of XIII are listed in table 6 and are in agreement with previous results.¹¹⁻¹⁴

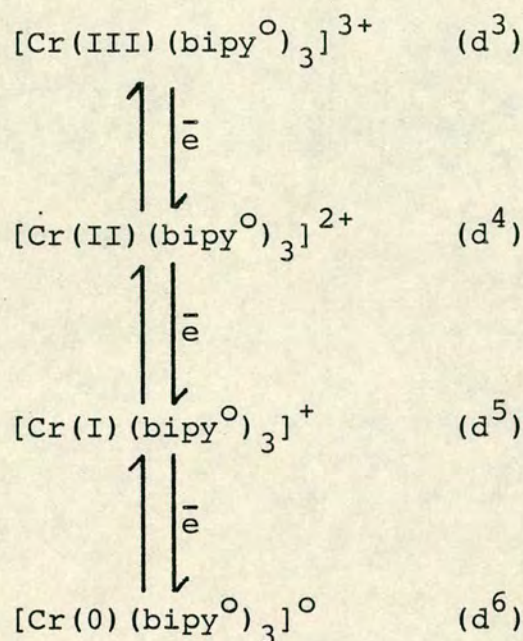
As we have previously discussed, the potential required to reduce a bipyridyl ligand in $[M(\text{bipy})_3]^{n+}$ is directly related to the central metal charge¹. In this case the first reductive wave (-0.53V) is not at the potential predicted for a bipyridyl-based reduction on a metal +3 centre (c.f. $[\text{Ir}(\text{bipy})_3]^{3+}$ $E_{\text{red}}(1) = -1.26\text{V}$). The separation of the first three reductive waves for $[\text{Cr}(\text{bipy})_3]^{3+}$ (500mVs apart) is also not typical of that observed for bipyridyl-based reductions (normally 200mV separation).

These observations require the first three cathodic processes to be classified as metal-based reductions,¹¹ in agreement with previously reported magnetic studies¹⁵ carried out on polycrystalline samples of $[\text{Cr}(\text{bipy})_3]^{3+/2+/+/0}$ which have shown the presence of 3, 2, 1 and 0 unpaired electrons respectively.

Table 6: Electrode Potentials for $[\text{Cr}(\text{bipy})_3]^{3+}$, XIII

<u>Couple</u>	$E_{\frac{1}{2}}/\text{V}^{\text{a}}$
$[\text{Cr}(\text{bipy})_3]^{3+/2+}$	-0.53
$[\text{Cr}(\text{bipy})_3]^{2+/-}$	-1.03
$[\text{Cr}(\text{bipy})_3]^{+/\text{o}}$	-1.61
$[\text{Cr}(\text{bipy})_3]^{0/-}$	-2.24
$[\text{Cr}(\text{bipy})_3]^{-/2-}$	-2.51
$[\text{Cr}(\text{bipy})_3]^{2-/3-}$	-2.74

a - All potentials are listed vs a Ag/Ag^+ reference electrode in 0.1M $\text{TBABF}_4/\text{CH}_3\text{CN}$



In the present work the complexes XIII^- , XIII^{2-} and XIII^{3-} were separately electrogenerated, in acetonitrile solution, at room temperature, at a platinum O.T.T.L.E. The resulting absorption spectra are shown in figures 8 and 9.

The complexes XIII^{2-} and XIII^{3-} could only be stabilised in the presence of excess bipyridyl thus masking the ultra-violet spectrum of each species; the $\pi(6) \rightarrow \pi(7)$ intraligand transition of uncoordinated bipyridyl occurs at $34\,800\text{ cm}^{-1}$.

The absorption spectra shown in figures 8 and 9 are in close agreement with earlier published reports^{11,12,14} however our assignments of the observed bands are quite different.

As we have demonstrated in chapters 1 and 2, there is a necessary relationship between the electrochemical

Figure 8: Ultra-violet Absorption Spectra of
 $[\text{Cr}(\text{bipy})_3]^{3+/2+}$ in Acetonitrile at Room
Temperature

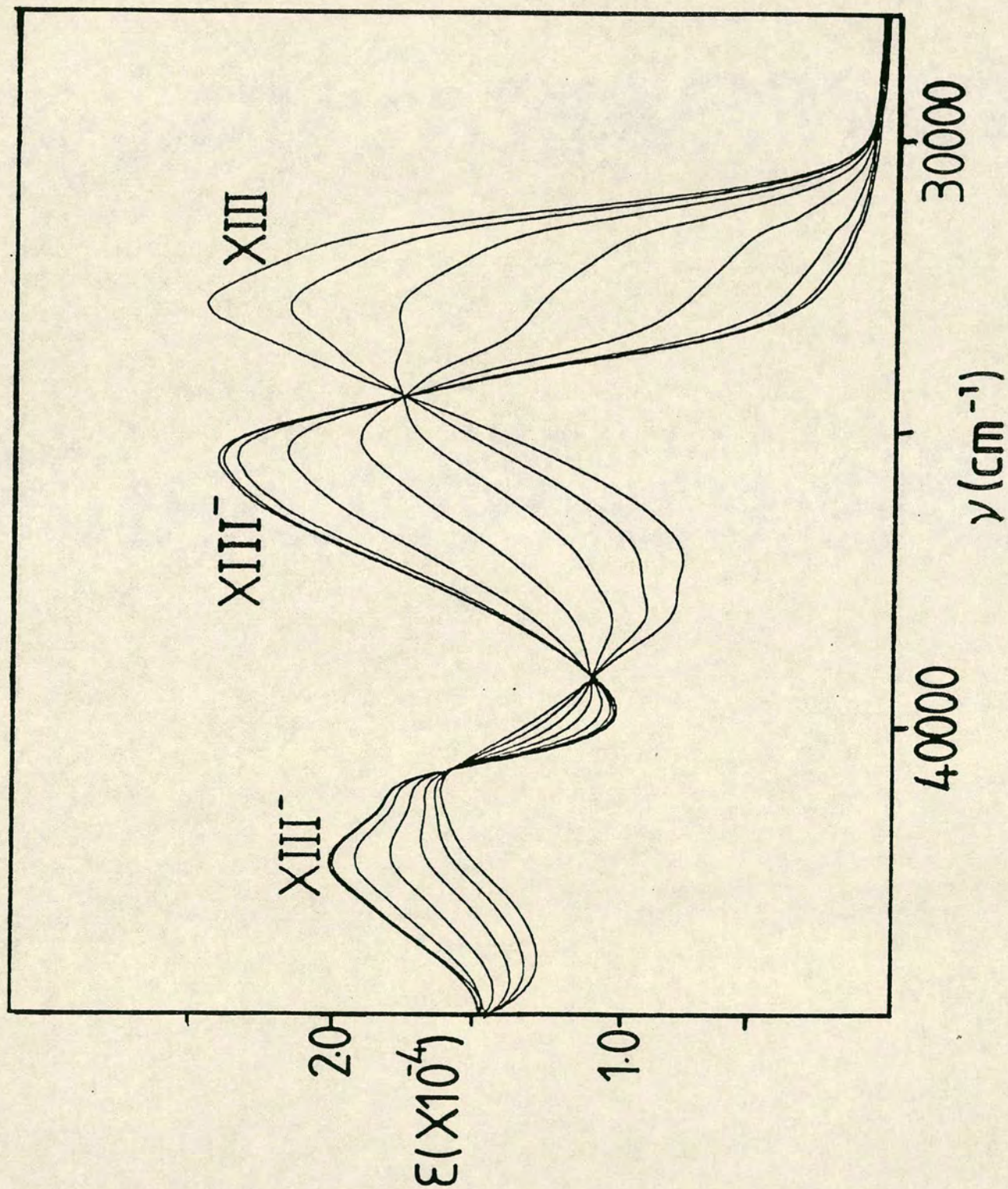
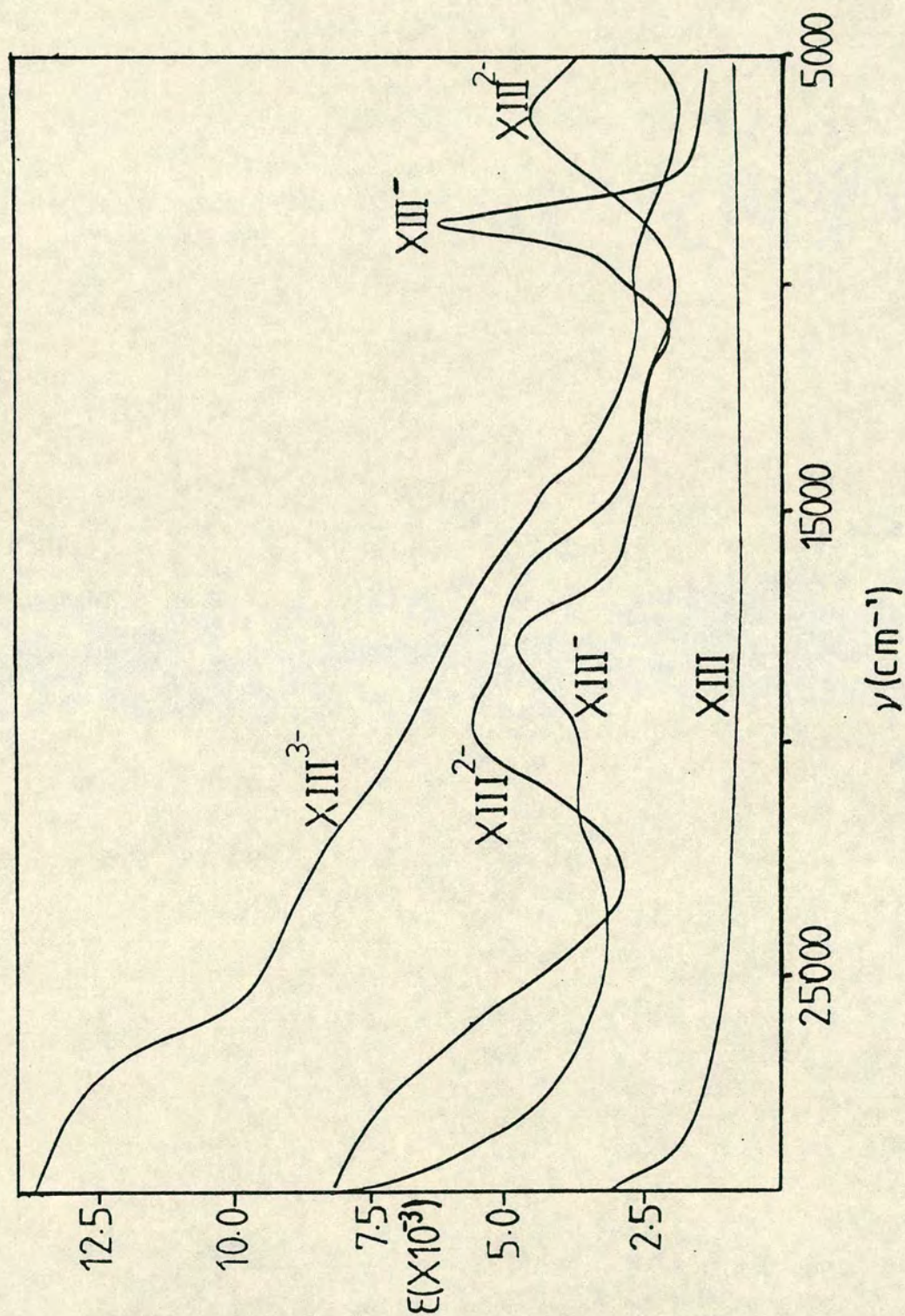


Figure 9 : Near Infra-red/Visible Absorption Spectra of
 $[\text{Cr}(\text{bipy})_3]^{3+/2+/+0}$ in Acetonitrile at -30°C
in the Presence of Excess Bipyridine



data and the absorption spectra encountered for many transition metal bipyridyl complexes. This principle is again applicable to the reduced chromium species.

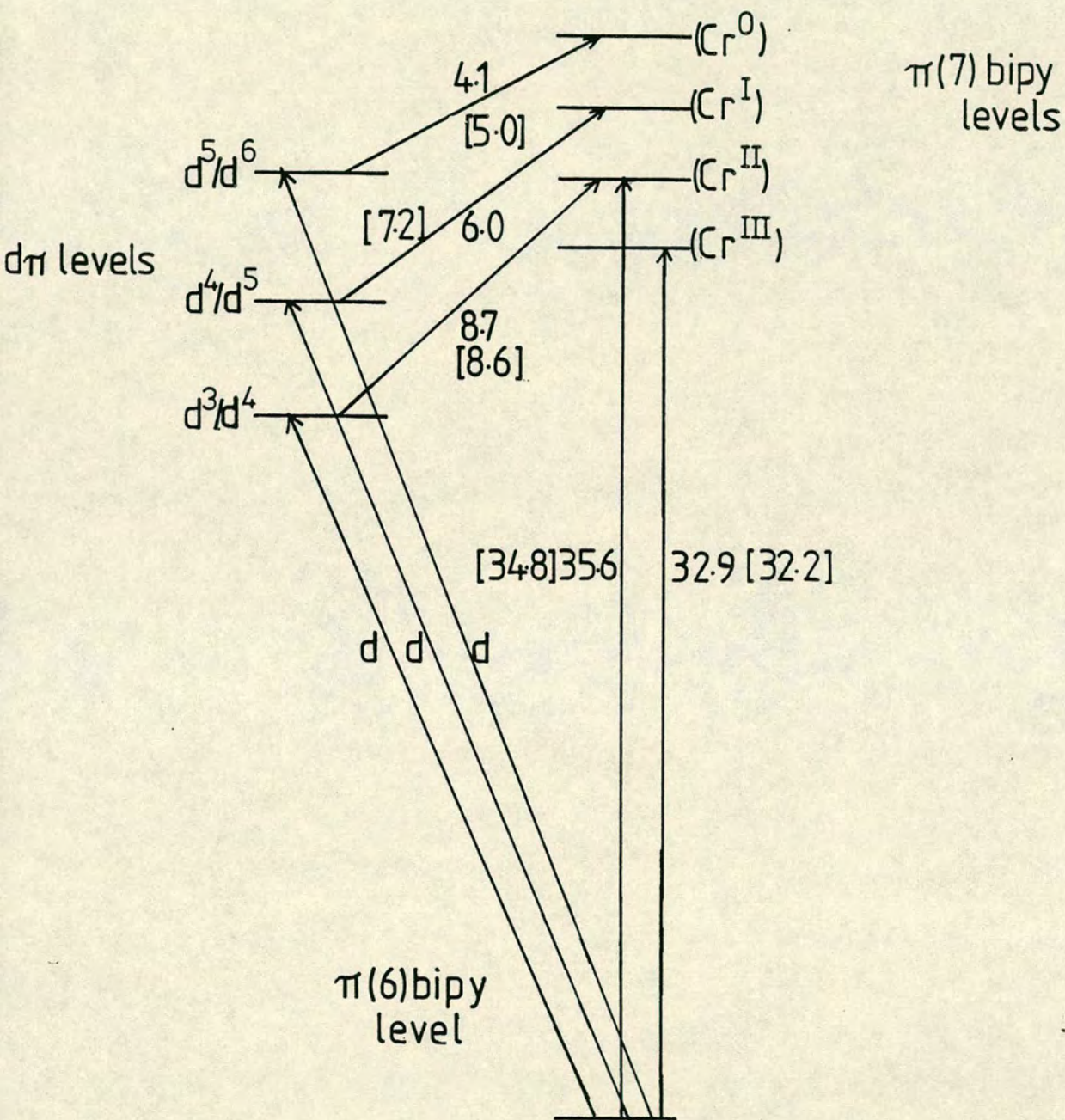
If we first consider the absorption spectrum of $[\text{Cr}(\text{bipy})_3]^{3+}$, XIII, it is noted that the near infra-red and visible regions show no indication of any charge-transfer bands (either $\text{M} \rightarrow \text{L}$ or $\text{L} \rightarrow \text{M}$). Though not discernable in figure 10, several low intensity ($\epsilon \sim 500$) bands have been assigned to spin-allowed d-d transitions.^{14,15} The ultra-violet spectrum of XIII is dominated by two bands which have been assigned to $\pi(6) \rightarrow \pi(7)$ and $\pi(6) \rightarrow \pi(8)$ bipyridine transitions. On one-electron reduction of this system the familiar shift of these bands to higher energy is noted (c.f. $[\text{Ru}(\text{bipy})_3]^{2+/3+}$).

Using the electrochemical data available for $[\text{Cr}(\text{bipy})_3]^{3+}$ and the earlier contrasting tris-bipyridyl transition metal complexes and the optical data available for $[\text{Cr}(\text{bipy})_3]^{3+/2+/+/0}$, we may construct a schematic energy level scheme relating $\text{XIII}^{0/-/2-/3-}$ as shown in figure 10.

From figure 10 it may be noted that the lowest energy ligand-to-metal charge-transfer transitions are anticipated to lie at energies over $26\,000\text{ cm}^{-1}$. It is also noted that the lowest energy $\pi \rightarrow \pi^*$ bipyridyl transition lies at approximately $32\,000\text{ cm}^{-1}$ in XIII and at approximately $35\,000\text{ cm}^{-1}$ in XIII^- .

It is therefore reasonable to assume that the bands lying at energies below $25\,000\text{ cm}^{-1}$ must in each species be attributable to metal-to-ligand charge-transfer.

Figure 10: Schematic Energy Level Scheme for $[\text{Cr}(\text{bipy})_3]^{3+/2+/+/0}$



Figures in brackets are the electrochemical predictions for certain transitions.

Notes. See overleaf

Notes to figure 10

- a - The $d\pi$ levels on $[\text{Cr}(\text{bipy})_3]^{3+/2+/+/\circ}$ and the $\pi(7)$ level on $[\text{Cr}(\text{bipy})_3]^\circ$ are fixed by direct electrochemical measurement.
- b - The $\pi(7)$ bipyridine levels on $[\text{Cr}(\text{bipy})_3]^{3+/2+/+}$ are mapped from the $\text{Cr}(0)$ -bipy $\pi(7)$ level by invoking the 0.32 electronvolts shift per unit charge rule.
- c - The $\pi(6)$ bipyridine level on $[\text{Cr}(\text{bipy})_3]^{3+}$ is assumed equal to the same level on $[\text{Ru}(\text{III})(\text{bipy})_3]^{3+}$ and is thus directly electrochemically determined by the $[\text{Ru}(\text{bipy})_3]^{3+/4+}$ couple. This is found to excellently match the optically measured $\pi(6) \rightarrow \pi(7)$ gap on $[\text{Cr}(\text{bipy})_3]^{3+}$. Indeed the optically measured $\pi(6) \rightarrow \pi(7)$ gap on $[\text{Cr}(\text{bipy})_3]^{2+}$ suggests the $\pi(6)$ level is invariant for $[\text{Cr}(\text{bipy})_3]^{2+/3+}$.
- d - The lowest lying LMCT band is predicted to lie at an energy in excess of $26\,000\text{ cm}^{-1}$ in each species; i.e. $3.24\text{eV} = 26\,000\text{ cm}^{-1}$ in $[\text{Cr}(\text{III})(\text{bipy}^\circ)_3]^{3+}$ and at higher energy in each successive reduced complex.
- e - The numbers listed in figure 10 are the observed optical transitions in units of 10^3 cm^{-1} . The figures in parentheses are the predicted energies of each transition from electrochemical data.

transitions, presumably overlying weaker ligand-field transitions. As shown in figure 10 we may predict a value for the lowest energy metal-to-ligand charge-transfer transition ($\text{Crd}\pi \rightarrow \pi(7)\text{bipy}$) for each reduced species using our voltammetric data.

If we examine the ultra-violet spectra of XIII and XIII^- , see figure 8, then since we have assigned the observed bands to $\pi(6) \rightarrow \pi(7)$ and $\pi(6) \rightarrow \pi(8)$ transitions in the bipyridyl ligand we may deduce a value for the $\pi(7) \rightarrow \pi(8)$ energy gap. It is then possible to predict a value for the higher energy metal-to-ligand charge-transfer transition ($\text{Crd}\pi \rightarrow \pi(8)\text{bipy}$) for XIII and XIII^- with the bands assigned in table 7.

From figure 9, it may be noted that further absorptions are observed for $\text{XIII}^{-/2-/3-}$ at higher energies than the ($\text{Crd}\pi \rightarrow \pi(8)\text{bipy}$) transition yet at lower energies than would be expected for the lowest lying ligand-to-metal and intraligand transitions. We therefore tentatively suggest these absorptions may be attributable to transitions from the $\text{Crd}\pi$ level to higher energy bipyridine levels ($\pi(9)$, $\pi(10)$). In principle charge-transfer transitions may also occur from lower lying chromium levels to the unoccupied bipyridine orbitals ($\pi(7)$ etc).

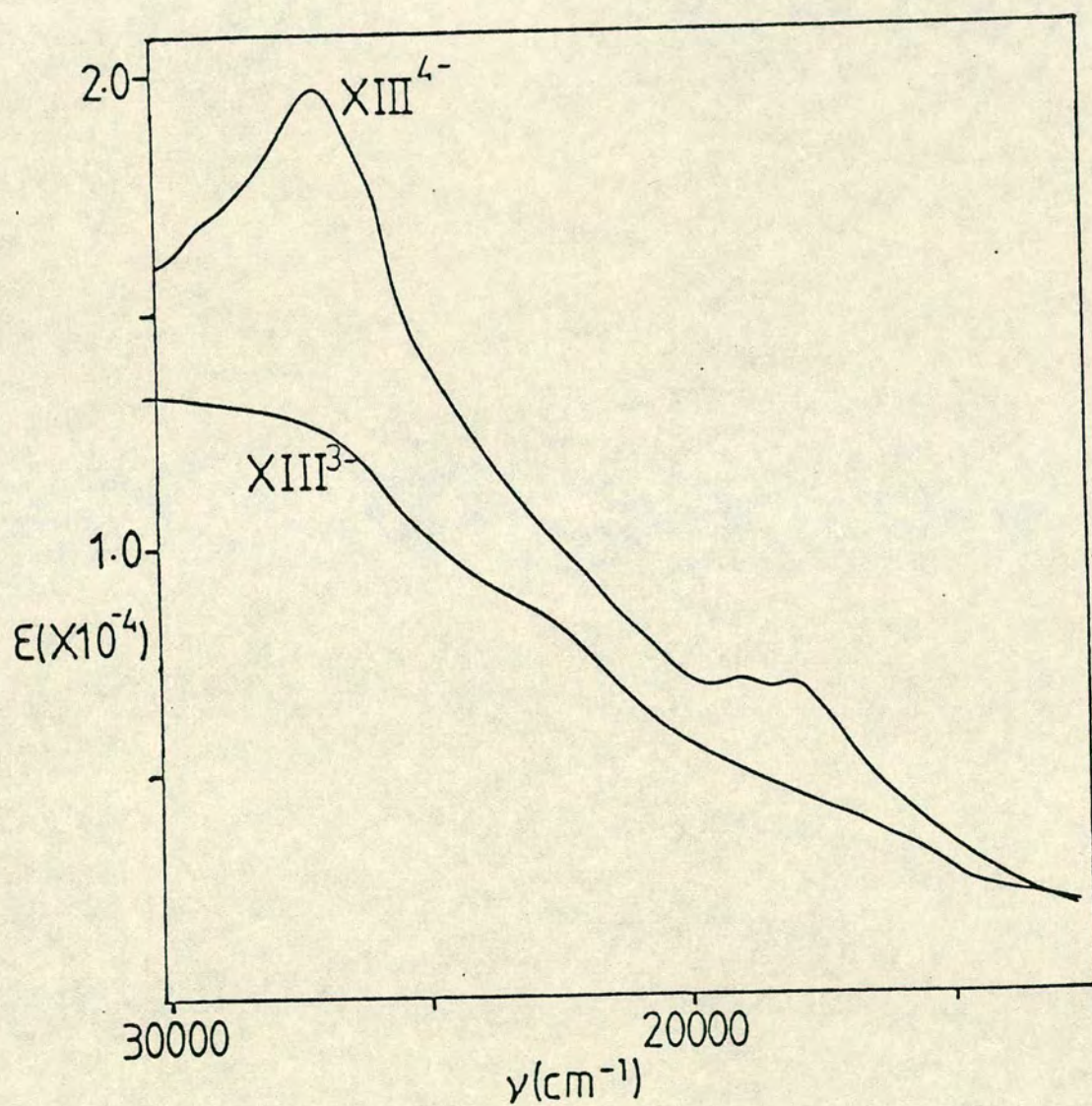
The four-electron reduced monoanionic species, $[\text{Cr}(\text{bipy})_3]^-$, may only be reversibly electrogenerated at -30°C in dry tetrahydrofuran. The absorption spectrum obtained on generation of XIII^{4-} at a platinum O.T.T.L.E. is shown in figure 11 and is consistent with the emergence

Table 7: Assignment of the Absorption Bands in $[\text{Cr}(\text{bipy})_3]^{3+/2+/+/0} \nu \times 10^{-3}/\text{cm}^{-1}$ ($\epsilon \times 10^{-4}$)

Complex	Transition				
	$\pi(6) \rightarrow \pi(8)$ <u>bipy⁰</u>	$\pi(6) \rightarrow \pi(7)$ <u>bipy⁰</u>	$\text{Cr}d\pi \rightarrow$ <u>$\rightarrow \text{bipy}^c$</u>	$\text{Cr}d\pi \rightarrow$ <u>$\pi(8)\text{bipy}$</u>	$\text{Cr}d\pi \rightarrow$ <u>$\pi(7)\text{bipy}$</u>
$[\text{Cr}(\text{bipy})_3]^{3+}$	40.9 (1.59)	31.8 sh 32.9 (2.48)	-	a	a
$[\text{Cr}(\text{bipy})_3]^{2+}$	42.2 (2.01)	35.6 (2.41)	21.8 (0.36)	17.8 (0.48)	8.7 (0.62)
$[\text{Cr}(\text{bipy})_3]^+$	b	b	18.6 (0.57) 25.7 (0.68)	13.1 (0.39) 15.9 (0.49)	6.0 (0.44)
$[\text{Cr}(\text{bipy})_3]^0$	b	b	15.0 sh 22.0 sh 27.2 (1.28)	10.0 (0.28)	4.1 (0.41) ^d

Note: a - Obscured by coordinated bipyridyl; b - Obscured by excess bipyridyl
c - See text. Tentatively assigned to $\text{Cr}d\pi$ to higher energy bipyridine levels.
d - Superimposed upon background solvent absorptions.

Figure 11: Absorption Spectra of $[\text{Cr}(\text{bipy})_3]^{0/-}$ in Tetrahydrofuran at -30°C in the Presence of Excess Bipyridine

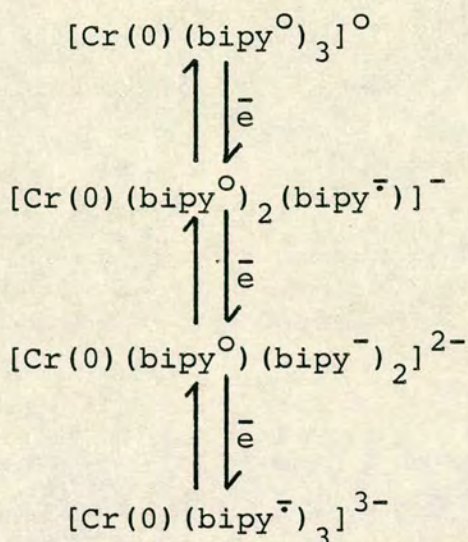


of the $\text{bipy}^{\cdot-}$ chromophore; bands observed are assigned in table 8.

Table 8: Absorption Bands in $[\text{Cr}(\text{bipy})_3]^-$
 $\nu \times 10^{-3}/\text{cm}^{-1}$ ($\epsilon \times 10^{-4}$)

<u>Complex</u>	<u>Transition</u>	
	$\frac{\pi \rightarrow \pi^*}{\text{bipy}^{\cdot-}}$	$\frac{\pi \rightarrow \pi^*}{\text{bipy}^{\cdot-}}$
$[\text{Cr}(\text{bipy})_3]^-$	27.1 (1.99)	19.7 (0.77)
		18.9 (0.76)
$\text{Na}^+ \text{bipy}^{\cdot- 5}$	25.9 (2.95)	18.8 (0.62)
		17.8 (0.65)

All attempts to electrogenerate XIII^{5-} and XIII^{6-} only led to decomposition of the complex. However the pattern of the second set of reductions suggests these species should be formulated in terms of the localised model as shown below.



If the localised model is indeed applicable in this case then, as for $[\text{Cr}(\text{bipy})_3]^0$, $[\text{Cr}(\text{bipy})_3]^-$ also contains the $\text{Cr}^0(\text{bipy}^0)$ chromophore. The visible spectrum of XIII^{4-} will then contain absorption bands due to low-energy chromium(0) $d\pi$ to $\text{bipy}^0\pi^*$ MLCT transitions which would rationalise the excess intensities of the $\pi \rightarrow \pi^*$ bipy^- bands compared with those observed for $[\text{Ir}(\text{III})(\text{bipy}^0)_2(\text{bipy}^-)]^{2+}$.

It is apparent therefore that although the electrochemical behaviour of isovalent $[\text{Ir}(\text{bipy})_3]^{3+}$ and $[\text{Cr}(\text{bipy})_3]^{3+}$ seems at first glance very similar (two sets of three regularly spaced waves) the reductive processes involved are markedly different. In $[\text{Ir}(\text{bipy})_3]^{3+}$ all six reductions are ligand-based whereas in $[\text{Cr}(\text{bipy})_3]^{3+}$ the first three processes involve reduction of the metal centre.

Experimental

$[\text{Ir}(\text{bipy})_2\text{Cl}_2]\text{Cl}$ was prepared by the method of Watts, Harrington and Van Houten.³ The complexes $[\text{Ir}(\text{bipy})_2\text{Cl}_2](\text{CF}_3\text{SO}_3)$, $[\text{Ir}(\text{bipy})_2(\text{CF}_3\text{SO}_3)_2](\text{CF}_3\text{SO}_3)$ and $[\text{Ir}(\text{bipy})_3](\text{PF}_6)_3$ were prepared by the method of Sullivan and Meyer.² $[\text{Cr}(\text{bipy})_3](\text{BF}_4)_3$ was prepared by the method of Hein and Herzog.¹⁸

In the course of this study we devised an alternative route to $[\text{Ir}(\text{bipy})_3](\text{PF}_6)_3$. The complex $[\text{Ir}(\text{bipy})_2(\text{OH})_2](\text{BF}_4)$ was prepared from $[\text{Ir}(\text{bipy})_2\text{Cl}_2]\text{Cl}$ by the method of Watts, Harrington and Van Houten.³ $[\text{Ir}(\text{bipy})_2(\text{OH})_2](\text{BF}_4)$ (0.200 g) was dissolved in ethylene glycol (10 ml) with a twentyfold excess of bipyridyl (1.00 g) and heated at reflux, under an atmosphere of nitrogen, for six hours. $[\text{Ir}(\text{bipy})_3]^{3+}$ was then precipitated as its hexafluorophosphate salt in a moderate yield of 0.034 g (10%).

All electrochemical and spectroelectrochemical techniques and solvent purifications used were as described in chapter 2.

References

1. C. Flynn and J. Demas; J.Am.Chem.Soc., 96, 1959 (1974).
2. B.P. Sullivan and T.J. Meyer; J.Chem.Soc.,Chem. Commun., 403 (1984).
3. R.J. Watts, J.S. Harrington and J. Van Houten; J.Am.Chem.Soc., 99, 2179 (1977).
4. J.L. Kahl, K.W. Hanck and M.K. DeArmond; J.Phys. Chem., 82, 540 (1978).
5. C. Mahon and W.L. Reynolds; Inorg.Chem., 6, 1927 (1967).
6. N. Serpone, M.A. Jamieson, M.S. Henry, M.Z. Hoffman, F. Bolletta and M. Maestri; J.Am.Chem.Soc., 101, 2907 (1979).
7. V. Balzani, F. Bolletta, M.T. Gandolfi and M. Maestri; Top.Curr.Chem., 75, 1 (1978).
8. M. Maestri, F. Bolletta, L. Moggi, V. Balzani, M.S. Henry and M.Z. Hoffman; J.Am.Chem.Soc., 100, 2694 (1978).
9. A. Juris, M.F. Manfrin, M. Maestri and N. Serpone; Inorg.Chem., 17, 2258 (1978).
10. R. Ballardini, G. Varani, M.T. Indelli, F. Scandola and V. Balzani; J.Am.Chem.Soc., 100, 7219 (1978).
11. L.J. Yellowlees; Ph.D. Thesis, University of Edinburgh (1982).
12. T. Sage and S. Aoyogui; J.Electroanal.Chem., 60, 1 (1975).

13. M.C. Hughes, J.M. Rao and D.J. Macerco; Inorg. Chem. Acta, 35, L321 (1979).
14. T. Saji and S. Aoyagui; J. Electroanal. Chem., 63, 405 (1975).
15. E. Konig and S. Herzog; J. Inorg. Nucl. Chem., 32, 585 (1970).
16. J.G. Gaudellio, P.R. Sharp and A.J. Bard; J. Am. Chem. Soc., 104, 6373 (1982).
17. J.G. Gaudellio, P.G. Bradley, K.A. Norton, W.H. Woodruff and A.J. Bard; Inorg. Chem., 23, 3 (1984).
18. F. Hein and S. Herzog; Z. Anorg. Allg. Chem., 267, 337 (1952).

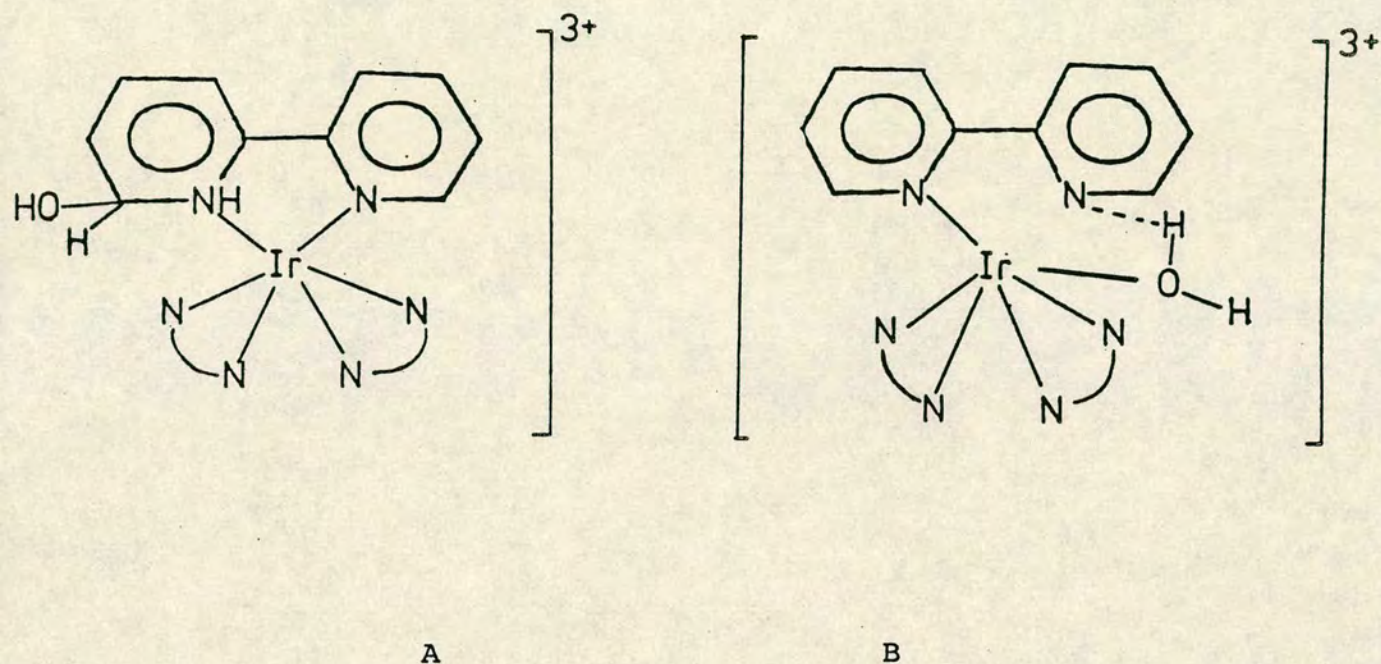
Chapter 4

C-Metallated Analogues to 2,2'-Bipyridyl Complexes.

N.m.r. and Spectroelectrochemical Studies of (2,2'-Bipyridinyl- C^3, N^1)bis(2,2'-bipyridine- N, N^1) Iridium (III) Hydrate and $[Ru(bipy)_2(phpy)]^+$.

Since the discovery in 1977 of a compound closely related, but distinct from $[Ir(bipy)_3]^{3+}$, there has been much debate concerning its structure.¹ This so-called pseudo-hydroxytris(2,2'-bipyridine) iridium(III) cation, XIV, resembles $[Ir(bipy)_3]^{3+}$ in that the monomeric system appears to have three bipyridyl ligands associated with each iridium centre. Unlike $[Ir(bipy)_3]^{3+}$, however, this complex readily undergoes reversible deprotonation (that is it exists in two distinct forms " $[Ir(bipy)_3(OH)]^{2+}$ " and " $[Ir(bipy)_3(H_2O)]^{3+}$ " which may be easily interconverted by the addition of acid or base).

These systems have been formulated in a variety of ways. The earliest rival descriptions of the acidic form of this complex are shown below.



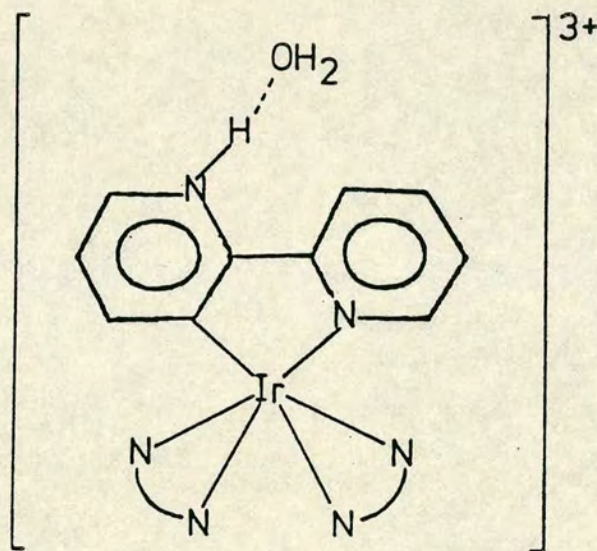
The presence of an ammonium N-H stretching band in the infrared spectrum of the acidic form of this complex at 2650 cm^{-1} , which is not present in basic solutions, was cited as evidence for these formulations.¹

Structure A contains a six-coordinate iridium(III) centre, to which two bidentate bipyridyl ligands are bound along with one "covalently-hydrated" bipyridyl ligand. The ^1H n.m.r. spectrum of XIV recorded in dimethylsulphoxide, was interpreted by Gillard and co-workers in terms of structure A.²

Structure B, however contains a six-coordinate iridium-(III) centre bound to two bidentate bipyridyl ligands, one monodentate bipyridine and one water molecule. This formulation, proposed by Spellane and Watts,³ was based

upon an examination of the ^1H n.m.r. spectrum of XIV in $\text{DCl}/\text{D}_2\text{O}$ which suggested that the water molecule is not covalently bound to bipy.

A preliminary X-ray structure analysis, published in 1981, showed three bidentate ligands apparently normally disposed about the metal. That is there is no monodentate bipyridyl ligand and also there is no evidence for a covalently hydrated bipy ligand.⁴ Weckramasinghe and co-workers proposed that this complex is related to $[\text{Ir}(\text{bipy})_3]^{3+}$ by rotation of one pyridyl ring, as in structure C.



C

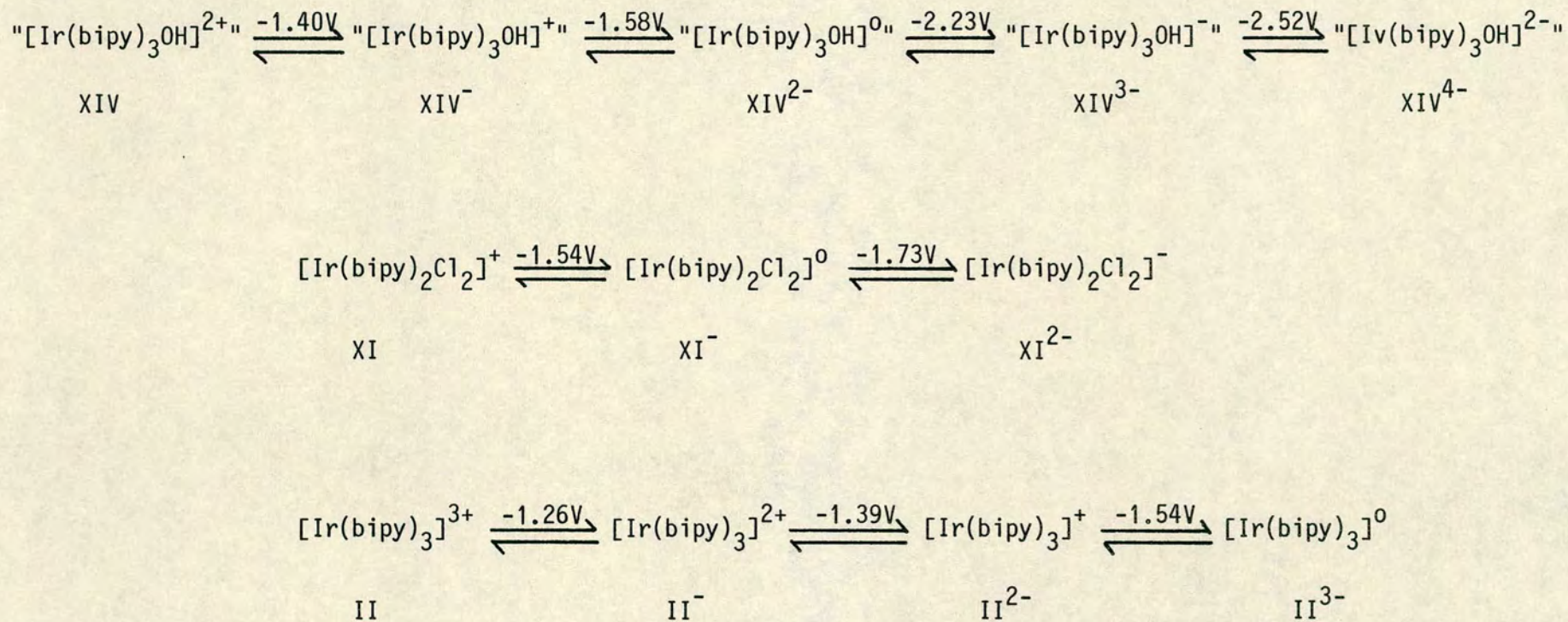
Their X-ray data, however, could not identify the interchanged C(3) carbon and nitrogen atoms with the position of the uncoordinated nitrogen being inferred, perceptively, from the position of the hydrogen-bonded water molecule. Indeed the diffraction data could not preclude the possibility that the iridium centre was bound to two α -carbon

atoms C(3) and C(3'), or neither. That is, both pyridyl rings in the unique bipyridine ligand may have undergone rotation.

This complex has been the subject of much interest in our laboratories.⁵ An examination of the voltammetric behaviour of the deprotonated form of this species, in dimethylsulphoxide and in acetonitrile, reveals two closely spaced one-electron reversible reductions followed by another two closely spaced quasi-reversible one-electron reductions at more extreme potentials as shown in figure 1.

This voltammetric behaviour coincides with previously published data⁶ and in our experience is characteristic of only two ordinary bipyridine ligands chelated to Ir(III). Furthermore, the measured electrode potentials for complex IV imply the presence of a monoanionic neighbouring ligand since the first reductive wave is observed at a potential (-1.40V) which is intermediate between that of $[\text{Ir}(\text{bipy})_3]^{3+}$ (-1.26V) and $[\text{Ir}(\text{bipy})_2\text{Cl}_2]^+$ (-1.54V). Logically this system, XIV, is then best modelled by the further reductions of $[\text{Ir}(\text{bipy})_3]^{2+}$, i.e. $[\text{Ir}(\text{III})(\text{bipy}^{\circ})_2(\text{bipy}^{\cdot-})]^{2+}$, which occur at -1.39V and -1.54V. XIV also undergoes a two-electron irreversible oxidation (at $E_p = +0.51\text{V}$) which we assign to involve the unique ligand (c.f. $[\text{Ir}(\text{bipy})_3]^{3+}$ where no oxidation is observed up to +1.6V). Thus the unique ligand is having an electrostatic effect on the two regular bipy ligands to the same degree as $\text{bipy}^{\cdot-}$, which would be consistent with the σ -bonded aryl structure of complex C. The markedly different behaviour of the complex formulated

Figure 1: Reductive Electrode Potentials for $[\text{Ir}(\text{bipy})_3]^{3+}$, $[\text{Ir}(\text{bipy})_2\text{Cl}_2]^+$ and $[\text{Ir}(\text{bipy})_3\cdot\text{H}_2\text{O}]^{3+}$



as $[\text{Ir}(\text{bipy})_2(\text{phen}')(\text{OH})]^{2+}$ (where phen represents bidentate and phen' monodentate o-phenanthroline) should be noted.⁷ This species has been shown to undergo three reductions at moderate potentials.

In our laboratories⁵ the electronic spectra of XIV, XIV^- and XIV^{2-} have all been obtained by the separate electrogeneration of each species at a platinum O.T.T.L.E. (see Chapter 2). As shown in figure 2 the species XIV and XIV^- (but not XIV^{2-}) show the well-known⁸ $\pi(6) \rightarrow \pi(7)$ transition of coordinated bipy around $33\,000\text{ cm}^{-1}$. The intensity of this band in XIV is reduced relative to $[\text{Ir}(\text{bipy})_3]^{3+}$ due to there being one less conventionally-bound bipyridine ligand. The band observed in $\text{XIV}^{0/-/2-}$ are assigned in table 1.

On successive generation of XIV^- and XIV^{2-} , the linear growth of bands characteristic of the bipy^- chromophore is again observed.⁹ It should also be noted that the species XIV^- (but not XIV or XIV^{2-}) shows a band at approximately 5000 cm^{-1} ($\epsilon = 220\text{ mol dm}^{-3}\text{ cm}^{-1}$) which is characteristic of ligand-ligand ($\text{bipy}^- \rightarrow \text{bipy}^0$) intervalence charge-transfer. This phenomenon is discussed in Appendix 1.

The absence of an intervalence charge-transfer band in XIV^{2-} gives further evidence that bipy^0 and the uniquely bound ligand (bipy') are not interchangeable. An examination of these absorption spectra suggests that the reduced species of these complexes should be formulated in terms of the localised model.

Figure 2: Absorption Spectra of $[\text{Ir}(\text{bipy})_2(\text{bipy}')]^{2+ / + / 0}$ in Dichloromethane at Room Temperature

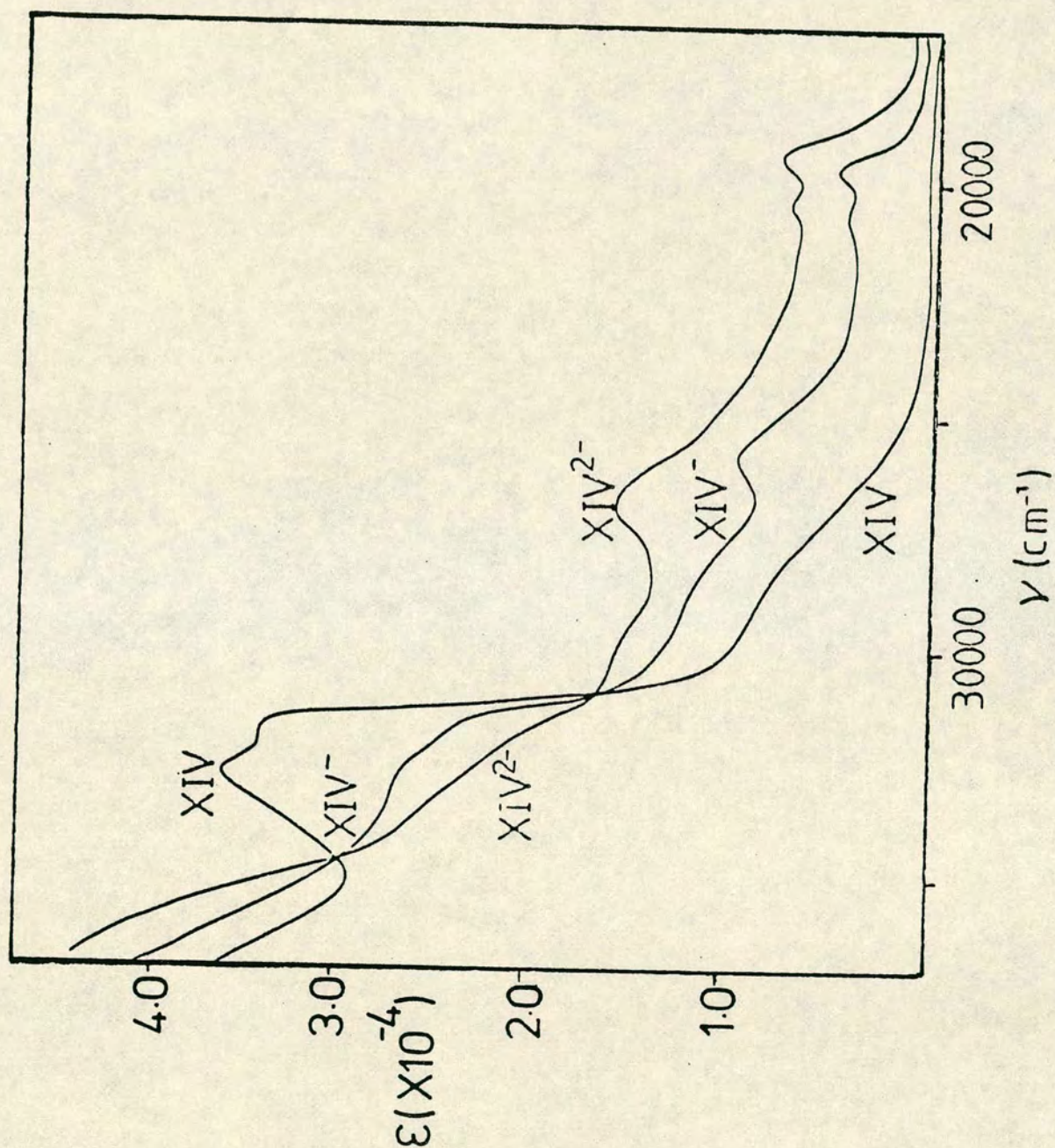
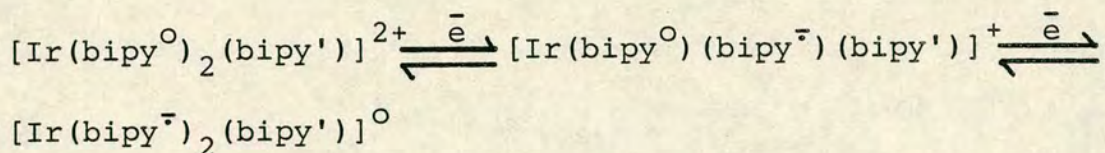


Table 1: Assignment of the absorption bands in
 $[\text{Ir}(\text{bipy})_2\text{OH}(\text{bipy}')]^{2+ / + / 0}$

<u>Complex</u>	<u>Transition</u> ($\nu_{\text{max}}/10^3 \text{cm}^{-1} (\epsilon \times 10^{-4})$)		
	$\frac{\pi(6) \rightarrow \pi(7)}{\text{bipy}^{\text{O}}}$	$\frac{\pi \rightarrow \pi^*}{\text{bipy}^{\cdot -}}$	$\frac{\pi \rightarrow \pi^*}{\text{bipy}^{\cdot -}}$
XIV	32.5 (3.65) 31.6 (3.52)	-	-
XIV ⁻	32.9 (2.78)	25.2 (0.96)	20.5 (0.40) 19.6 (0.45)
XIV ²⁻	-	26.6 (1.52)	20.1 (0.72) 19.3 (0.75)



The voltammetric and spectroelectrochemical studies carried out in our laboratories imply that the crystallographic structure proposed by Wickramasinghe *et al.*⁴ is indeed the most likely for this complex in solution as well.

In order to confirm this proposal we undertook a series of detailed nuclear magnetic resonance (n.m.r.) experiments. Previously published ¹H and ¹³C n.m.r. spectra have confirmed the low molecular symmetry of the complex but they have not been satisfactorily assigned, even for salient features relating to the modified ligand.^{11,12}

We have collected the 200- and 300-MHz ¹H n.m.r. spectra of the deprotonated form of this complex (studied as its BF₄⁻ salt) in MeOH-d⁴, Me₂CO-d⁶ and Me₂SO-d⁶ as shown in figures 3 to 5. These spectra are complicated but the maximum number of 23 separately detectable aromatic resonances are observed. This observation immediately excludes structure A where covalent hydration was proposed. In particular the systematic comparison of these spectra allows the identification of the doublet-of-doublet signals for each of the three protons in the uniquely attached ring (a).

Figure 3: ^1H n.m.r. Spectrum of $[\text{Ir}(\text{bipy})_2(\text{bipy}')]^{2+}$
in $\text{d}^4\text{-MeOH}$

$\text{d}^4\text{-MeOH}$

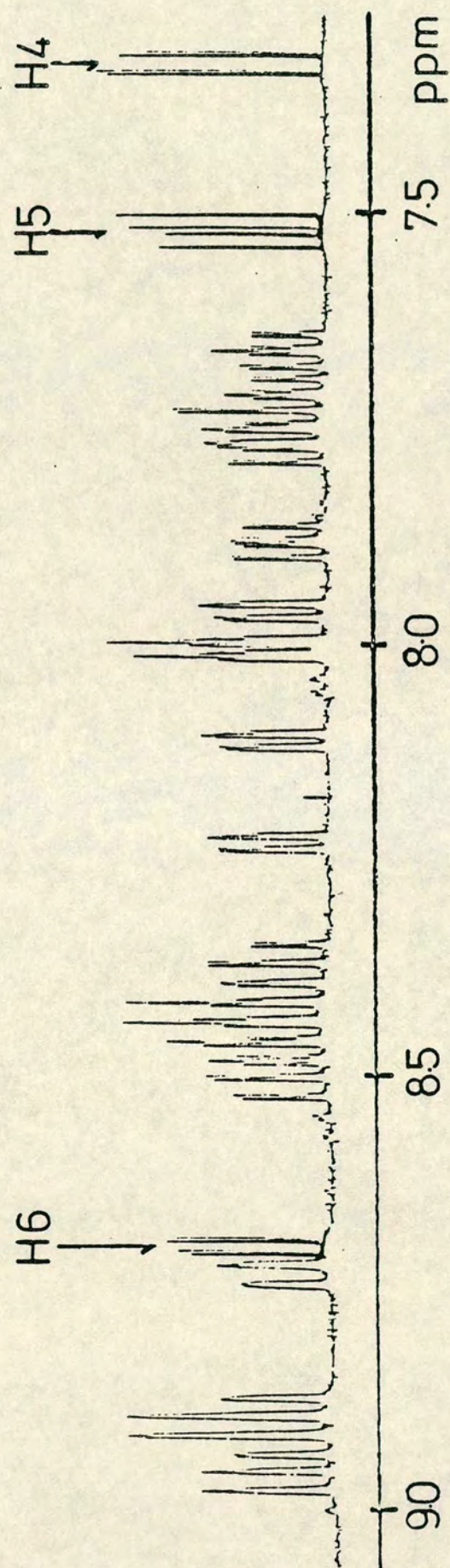


Figure 4: ^1H n.m.r. Spectrum of $[\text{Ir}(\text{bipy})_2(\text{bipy}')]^{2+}$ in $\text{d}^6\text{-(Me)}_2\text{SO}$

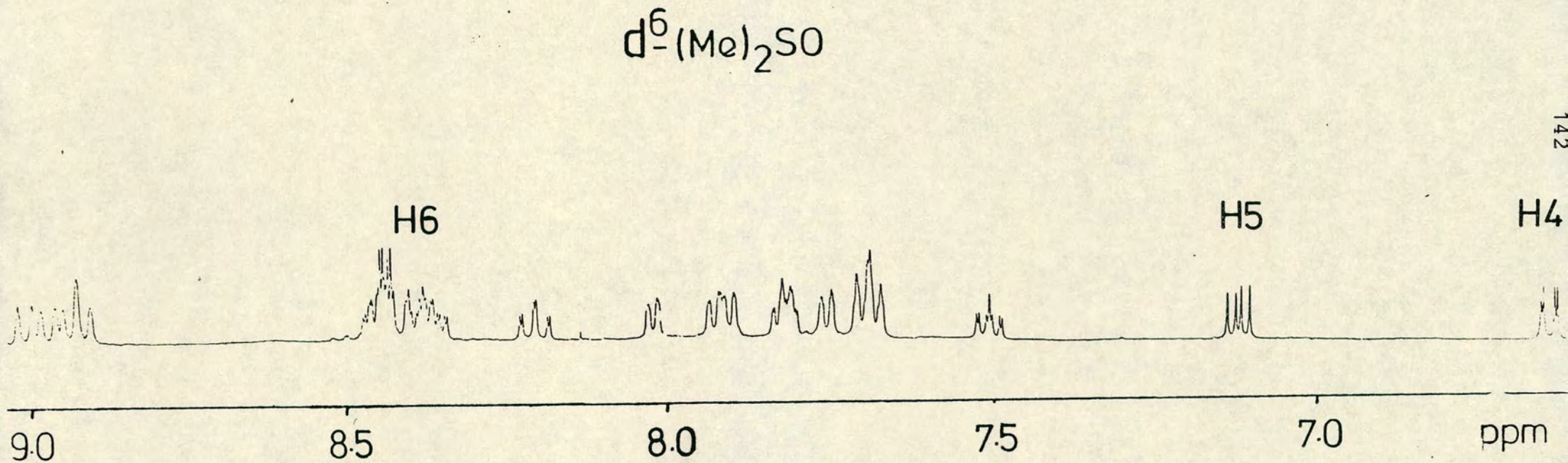
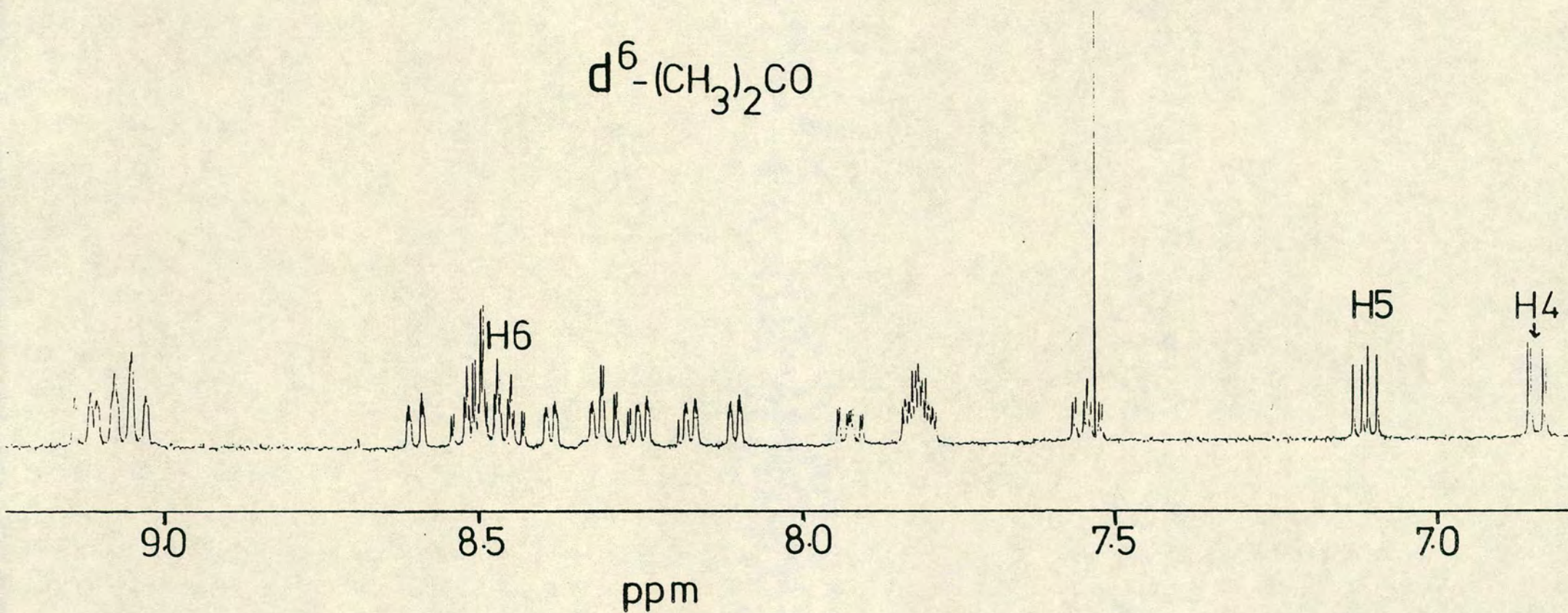
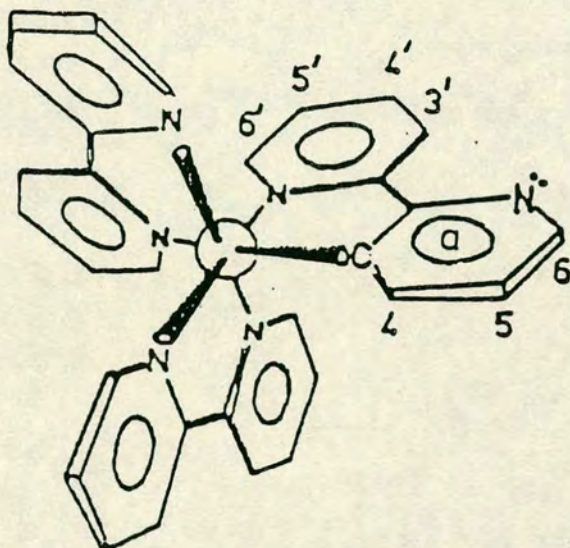


Figure 5: ^1H n.m.r. Spectrum of $[\text{Ir}(\text{bipy})_2(\text{bipy}')]^{2+}$ in $\text{d}^6-(\text{Me})_2\text{CO}$





In $\text{Me}_2\text{SO}-d^6$ for example the resonances at $\delta 6.60$ and 7.09 are coupled to each other and to the resonance at $\delta 8.44$. These three resonances are not coupled to any other resonance and each of the three integrates to one proton in approximately twenty-three. The particular solvent sensitivity of these resonances suggests these protons must be attached to the unique carbon-bound ligand. This solvent sensitivity is presumably due to dipolar interactions with the neighbouring uncoordinated nitrogen atom.

The mutual couplings of these resonances has been confirmed by using double-resonance techniques as shown in tables 2 and 3.

Further examination of these ^1H n.m.r. spectra reveals four more solvent sensitive multiplets. These resonances, centred at $\delta 7.66$, 8.23 , 8.37 and 8.73 in $\text{MeOH}-d^4$, have been shown to be coupled to each other. The proton at $\delta 7.66$ resonates in an open portion of the spectrum without overlap of other resonances which further implies it is most likely associated with the pyridyl group adjacent to the C-

Table 2: ^1H n.m.r. Assignment for the C-Metallated
Ring^a

<u>Solvent</u>	<u>H₄</u>	<u>H₅</u>	<u>H₆</u>
$\text{Me}_2\text{SO-d}^6$	6.60	7.09	8.44
$\text{Me}_2\text{CO-d}^6$	6.85	7.10	8.47
MeOH	7.33	7.52	8.70

a - All δ values recorded at 360.13MHz.

Table 3: Coupling Constants between Protons in the
C-Metallated Ring

<u>Solvent</u>	$\underline{J}_{4,5}^a$	$\underline{J}_{5,6}$	$\underline{J}_{4,6}$
Me ₂ SO-d ⁶	7.7	4.7	1.6
Me ₂ CO-d ⁶	7.7	4.7	1.6
MeOH-d ⁴	7.8	5.3	1.3

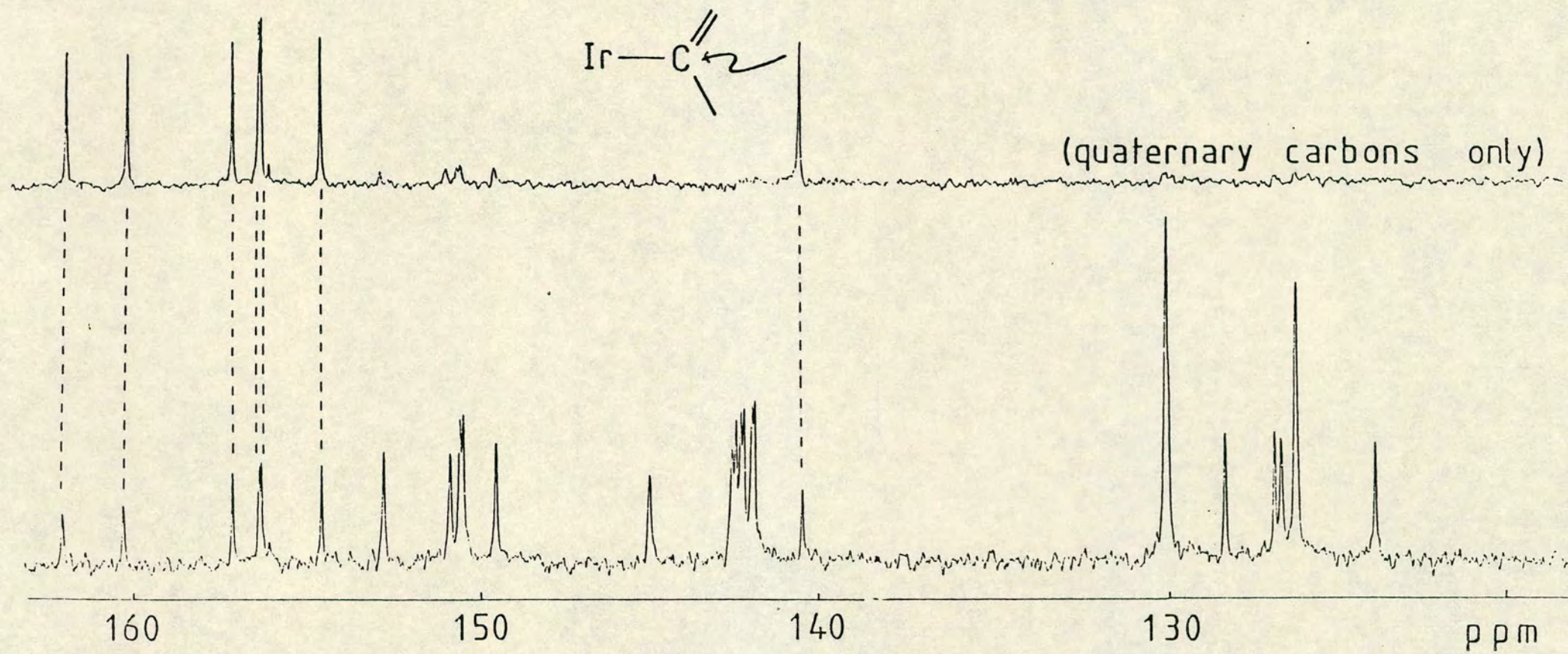
a - All coupling constants expressed in Hz.

metallated ring.

Spellane, Watts and Curtis¹⁴ have recently examined the ^1H n.m.r. spectrum of the protonated form of this complex. In a similar manner these workers have assigned the resonances due to the unique bipyridine ligand, in close agreement with this work. They have further assigned the other resonances by use of two-dimensional homonuclear techniques. The three resonances in the unique pyridine ring were again noted to be particularly solvent-sensitive. Addition of a lanthanide shift reagent, $\text{Pr}(\text{fod})_3$, to a $\text{CH}_3\text{CN}-d^3$ solution of the protonated complex resulted in a significant increase in the width of the aromatic region of the spectrum with the protons assigned to the C-metallated ring again being most sensitive. The effect of $\text{Pr}(\text{fod})_3$ gives further evidence for a site of Lewis basicity in this complex which is consistent with their being an uncoordinated nitrogen atom in this system.

The 90-MHz ^{13}C n.m.r. spectrum of this species, measured in $\text{Me}_2\text{SO}-d^6$, shown in figure 6, reveals the presence of thirty nonequivalent carbon atoms. If the spectrum is remeasured in a spectroscopic mode which is specific for non-H-bearing carbon atoms, then seven single resonances are observed. Six of these resonances, in the range 154-162 p.p.m. with respect to Me_4Si , correspond to the ring-ring bridging positions (c.f. 155.7 p.p.m. in $[\text{Ir}(\text{bipy})_3]^{3+}$) while the seventh, standing apart at 140 p.p.m. is clearly due to the unique, presumably iridium-bound carbon atom. This unique signal has moved by about 15 p.p.m. from the

Figure 6: ^{13}C n.m.r. Spectrum of $[\text{Ir}(\text{bipy})_2(\text{bipy}')]\text{d}^6-(\text{Me})_2\text{SO}$



normal C₃ position due presumably to the decreased shielding of the carbon nucleus when it is attached to iridium(III).

Recently the ¹³C n.m.r. spectrum of the protonated form of this complex has been published.¹⁴ Watts et al. have also identified 23 distinct resonances in this species. Using single-frequency off-resonance decoupling these workers have shown that all but seven of these signals show strong proton (one-bond) coupling. Thus they also assign the six bridging 2 and 2'-carbon atoms to the resonances at the low-field end of the spectrum (δ154.1→162.6 p.p.m.) and the seventh resonance which is shifted to a lower frequency (139.5 p.p.m.) to the presumably iridium-bound carbon.

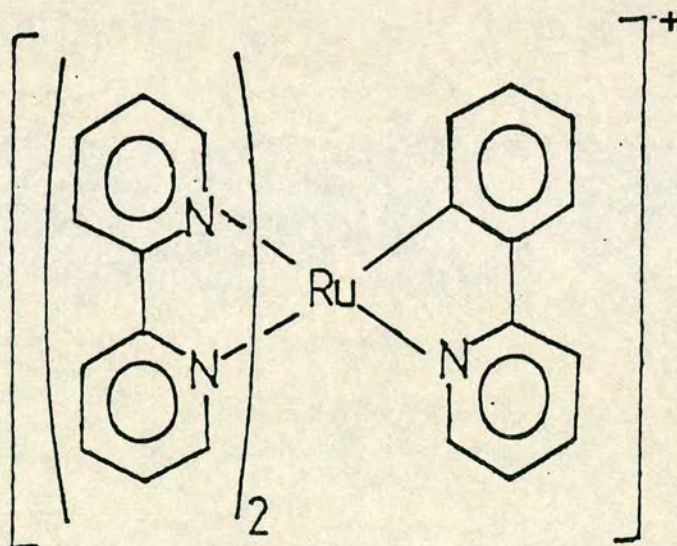
Collectively the electrochemical, spectroelectrochemical and n.m.r. data demonstrate clearly that this species contains a deprotonated N,C-bound ligand which in non-aqueous solution is indeed physically and electronically unique and remains distinct from the accompanying normal bipyridine ligands.

Indeed since this work was undertaken superior X-ray structure of the protonated form of this complex has been published clearly showing the presence of one N,C-bound bipyridyl ligand.

In the last few years several cyclometallated complexes have been prepared¹⁶⁻²⁰ which involve ligands that contain a phenyl group adjacent to a good ligating functionality such as pyridine. More recently the first examples of such carbon-metallated complexes of ruthenium(II) have been prepared.²¹⁻²⁴ These species should allow us to expand

our understanding of inorganic excited-state processes since the replacement of a nitrogen donor by an effectively carbanion donor drastically alters the electron density around the metal atom thus leading to substantial variations in both the ground- and excited-state redox properties. Consequently excited states involving such a ligand will occur at higher energies in the cyclometallated complex which may then result in substantial changes to the photophysical and photochemical properties of that species.

The complex we have studied is the recently prepared^{23,24} bis(2,2'-bipyridine)(2-phenylpyridine-C,N) ruthenium hexafluorophosphate, $[\text{Ru}(\text{bipy})_2(\text{phpy})](\text{PF}_6)$, XV.



XV

Two groups of workers have independently prepared this complex and analysed its ^1H n.m.r. spectrum using two-dimensional homonuclear experiments²³ and extensive decoupling techniques.²⁴ This has allowed all twenty-four proton resonances to be assigned.

A cyclic voltammogram of $[\text{Ru}(\text{bipy})_2(\text{phpy})]^+$ in dichloromethane is shown in figure 7. One reversible one-electron oxidation and two reversible one-electron reductions are observed. The measured potentials of these waves are shown in table 4.

The voltammetric data presented for $[\text{Ru}(\text{bipy})_2(\text{phpy})]^+$ is in good agreement with that of Reveco *et al.*²³ but differs from that of Constable²⁴ in the potential required to reduce the complex, both these published investigations having been carried out in acetonitrile.

The substantial decrease in the oxidation potential of $[\text{Ru}(\text{bipy})_2(\text{phpy})]^+$ relative to $[\text{Ru}(\text{bipy})_3]^{2+}$ is undoubtedly due to the replacement of a π -acceptor diimine nitrogen atom by the strong σ -donor carbanion. Since the oxidation is metal-centred, with an electron being removed from a metal t_2 orbital, this shift is due to the destabilisation of the t_2 orbital by the strong σ -donor carbanion. The oxidation potential of $[\text{Ru}(\text{bipy})_2\text{py.Cl}]^+$ is observed from table 4 to be 0.47V which then places phenylpyridine above chloride/pyridine in its ability to transfer negative charge to the metal centre.

An examination of the cathodic behaviour of $[\text{Ru}(\text{bipy})_2(\text{phpy})]^+$ reveals two reversible one-electron reductions which we assign to bipyridyl-based reductions after examining the behaviour of free phenylpyridine.

A voltammetric study in acetonitrile shows phenylpyridine to undergo an irreversible oxidation at +1.73V vs Ag/Ag^+ but no reduction within the solvent window as shown in table 5.

Figure 7: Cyclic Voltammogram of $[\text{Ru}(\text{bipy})_2(\text{phpy})]^+$
in Acetonitrile at Room Temperature

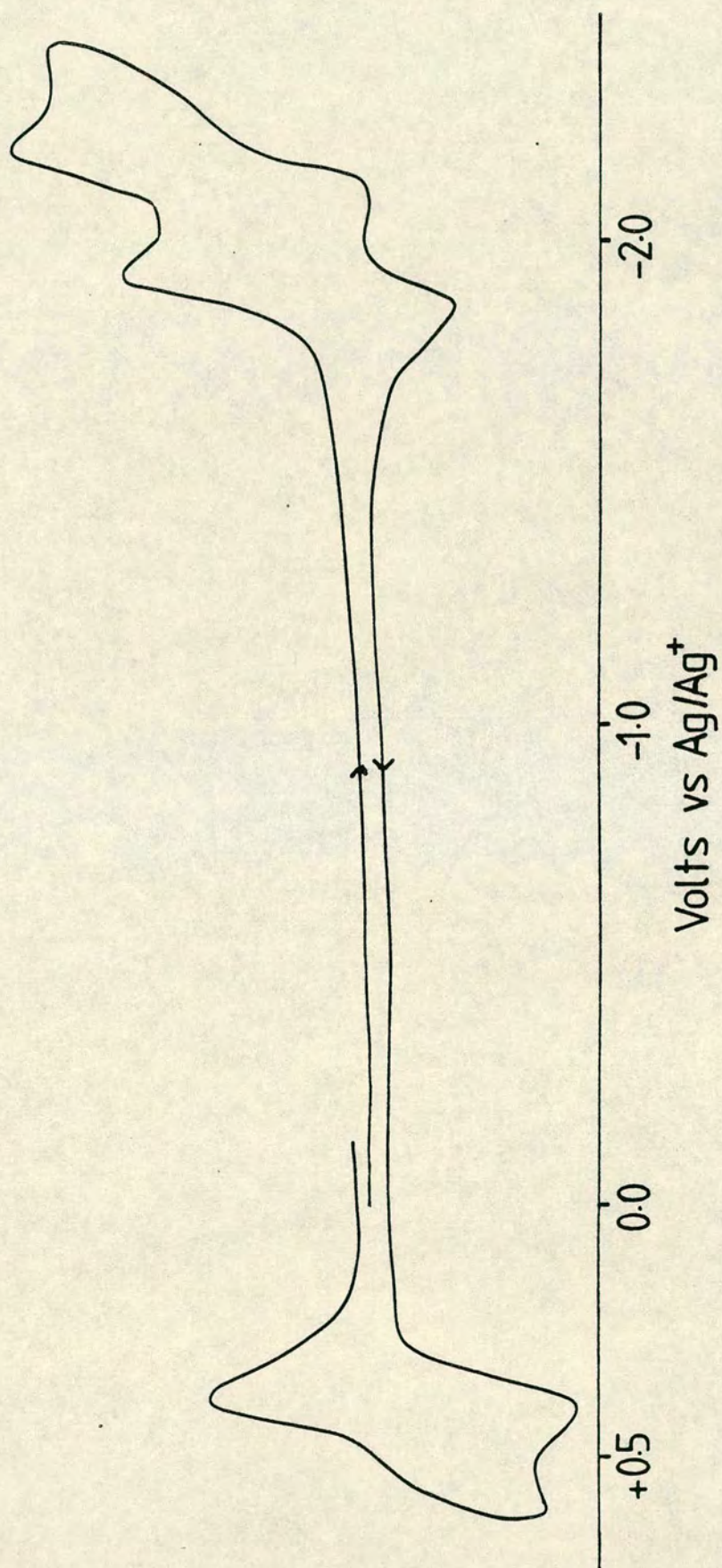


Table 4: Voltammetric Data for [Ru(bipy)₂(phpy)](PF₆) and some Related Complexes

<u>Complex</u>	<u>E(ox)^a</u>	<u>E(red1)</u>	<u>E(red2)</u>
[Ru(bipy) ₂ (phpy)] ⁺	+0.36	-1.95	-2.21
[Ru(bipy) ₃] ²⁺ (25)	+0.96	-1.66	-1.83
[Ru(bipy) ₂ (py) ₂] ²⁺ (5)	+0.97	-1.66	-1.85
[Ru(bipy) ₂ py.Cl] ⁺ (26)	+0.47	b	b
[Ru(bipy) ₂ Cl ₂] (27)	+0.01	-1.95	-2.06

a - All potentials measured in dichloromethane, at 20°C, scan rate 100mV/s, vs Ag/Ag⁺ reference electrode.

b - Unreported.

Table 5: Voltammetric Data for Phenylpyridine and Bipyridine^a

<u>Complex</u>	<u>E_{ox}</u> ^b	<u>E (red1)</u>
Phenylpyridine	+1.73	c
Bipyridine	+1.84	-2.57 ^d

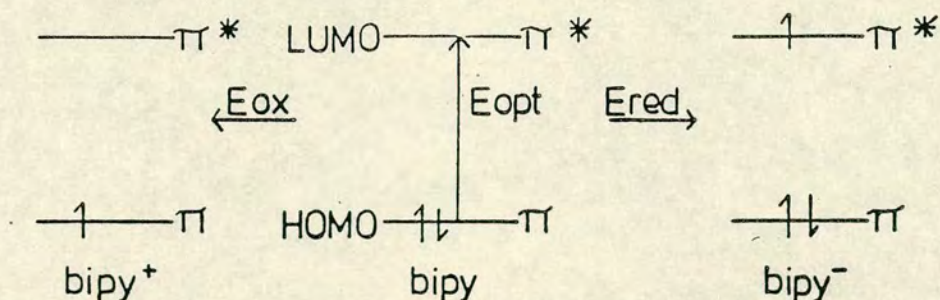
a - All experiments carried out in acetonitrile with potential measured vs Ag/Ag⁺.

b - Both oxidations totally irreversible

c - Reduction unobserved within our solvent limit.

d - Reference 6.

However by considering the absorption spectrum of phenylpyridine we may predict a value for the reduction of this ligand. An examination of the ultra-violet spectrum of bipyridine shows the lowest energy $\pi \rightarrow \pi^*$ transition to occur at $34\,800\text{ cm}^{-1}$. This optical transition involves the removal of an electron from the highest occupied molecular orbital (HOMO) of bipyridine and the promotion of this electron to the lowest unoccupied molecular orbital (LUMO). This transition should then be modelled electrochemically by consideration of the gap between the oxidation and reduction of free bipyridine as illustrated below.



$$E^{\text{ox}}(\text{bipy } o/+) - E^{\text{red}}(\text{bipy } o/-)$$

$$= +1.84 - (-2.57)$$

$$= 4.41\text{eV which is equivalent to } 35\,600\text{ cm}^{-1}$$

The observed value of $34\,800\text{ cm}^{-1}$ is in good agreement with this prediction.

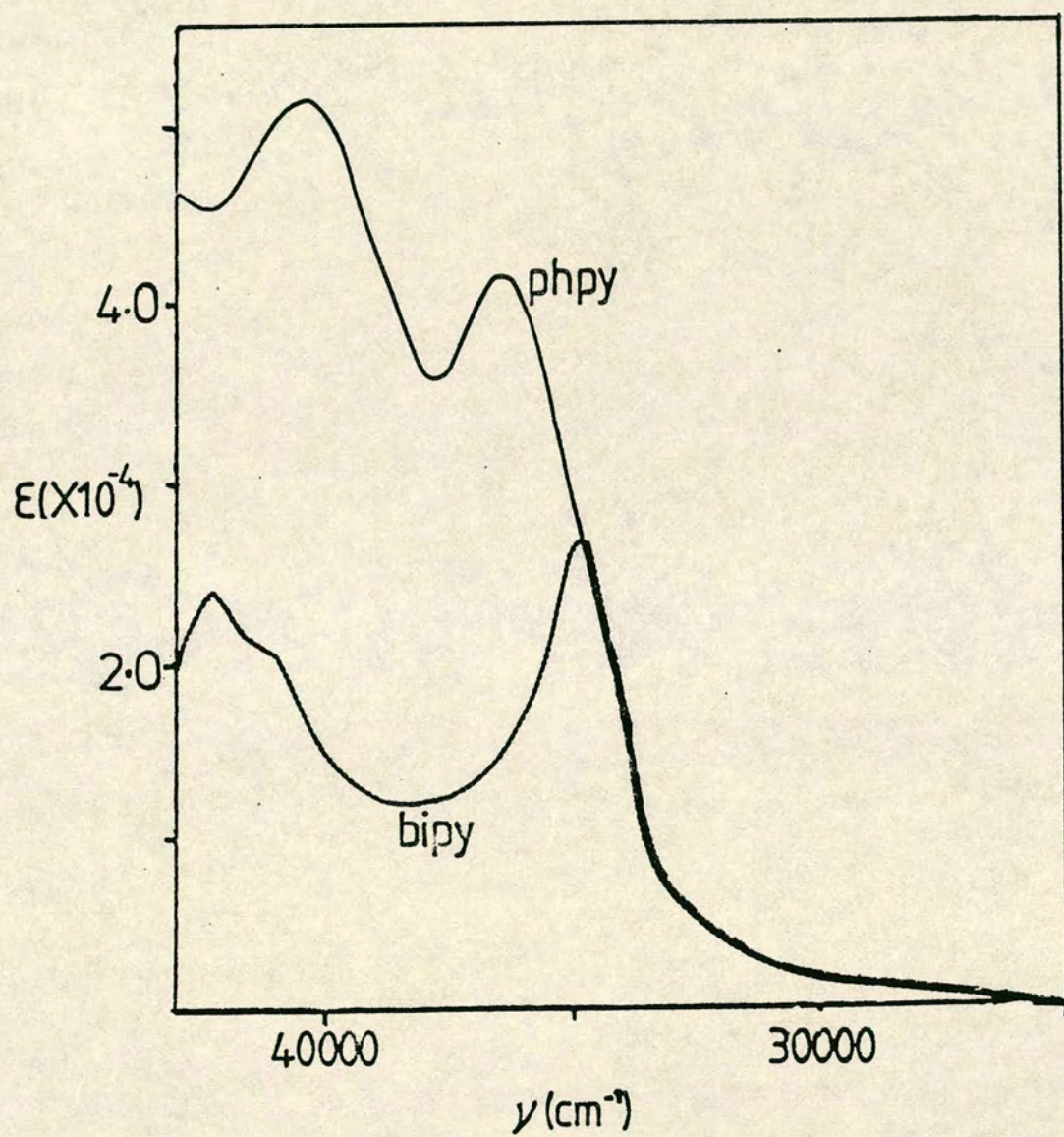
If we use this argument in reverse, for phenylpyridine, we may predict a value for the reduction of phenylpyridine. As shown in figure 8, the lowest energy $\pi \rightarrow \pi^*$ transition in phenylpyridine is observed at $36\,400\text{ cm}^{-1}$ allowing us to evaluate $E_{\text{red}}(\text{phpy } o/-)$.

$$\begin{aligned}
 E_{\text{opt}} &\equiv 36\,400\text{ cm}^{-1} \equiv 4.51\text{eV} \equiv E^{\text{ox}}(\text{phpy } o/+) - E^{\text{red}}(\text{phpy } o/-) \\
 &= 4.51 \equiv +1.73 - x \\
 &= x = -4.51 + 1.73 \\
 &= -2.78\text{V} \sim -2.8\text{V}
 \end{aligned}$$

This confirms that phenylpyridine is more difficult to reduce than bipyridine (by about 0.2eV) which implies the first two reductions of $[\text{Ru}(\text{bipy})_2(\text{phpy})]^+$ are most probably bipyridyl based.

Since the overall charge on the cyclometallated complex

Figure 8: Absorption Spectra of Bipyridine and Phenylpyridine



differs from $[\text{Ru}(\text{bipy})_3]^{2+}$ by one unit it is more appropriate to contrast the reductive behaviour of $[\text{Ru}(\text{bipy})_2(\text{phpy})]^+$ with the second and third reduction potentials of $[\text{Ru}(\text{bipy})_3]^{2+}$.

From table 4 it may be noted that the reduction potential of $[\text{Ru}(\text{bipy})_3]^+$ is -1.83V compared with the value of -1.95V for $[\text{Ru}(\text{bipy})_2(\text{phpy})]^+$. That is the presence of the cyclometallating carbanion has shifted the potential required to reduce a coordinated bipyridyl ligand to a more negative value than the presence of a bipyridyl anion. The cyclometallated ligand possesses a strong inductive effect which means the σ -bond is stronger than that in the bipyridine anion. This effectively lowers the charge on the central metal and, as we discussed in chapter 2, the charge on the central metal in these bipyridyl complexes dictates the ease of reduction of the coordinated bipyridyl ligands.⁵

It is apparent from figure 9 that the visible absorption spectrum of $[\text{Ru}(\text{bipy})_2(\text{phpy})]^+$ is considerably more complicated than that of $[\text{Ru}(\text{bipy})_3]^{2+}$.

In the manner we have described in previous chapters, we may correlate the gap between the ruthenium oxidation potential and the first bipyridine reduction potential with the observed metal-to-ligand charge-transfer band, as shown in table 6 and figure 10.

Figure 9 : Absorption Spectra of $[\text{Ru}(\text{bipy})_3]^{2+}$ and $[\text{Ru}(\text{bipy})_2(\text{phpy})]^+$ in Acetonitrile at Room Temperature

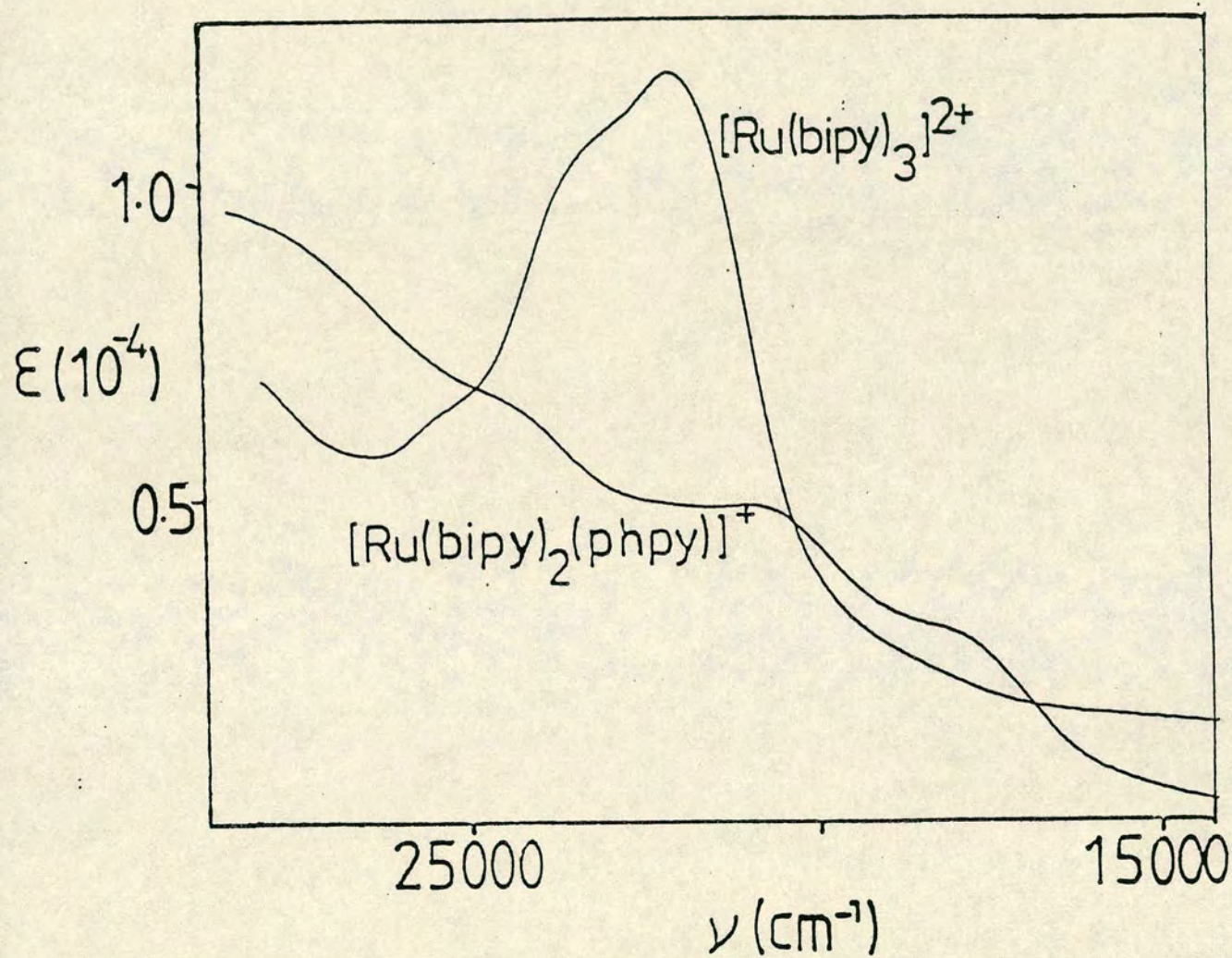


Figure 10: Comparative Energy Level Scheme for $[\text{Ru}(\text{bipy})_3]^{2+}$ and $[\text{Ru}(\text{bipy})_2(\text{phpy})]^+$

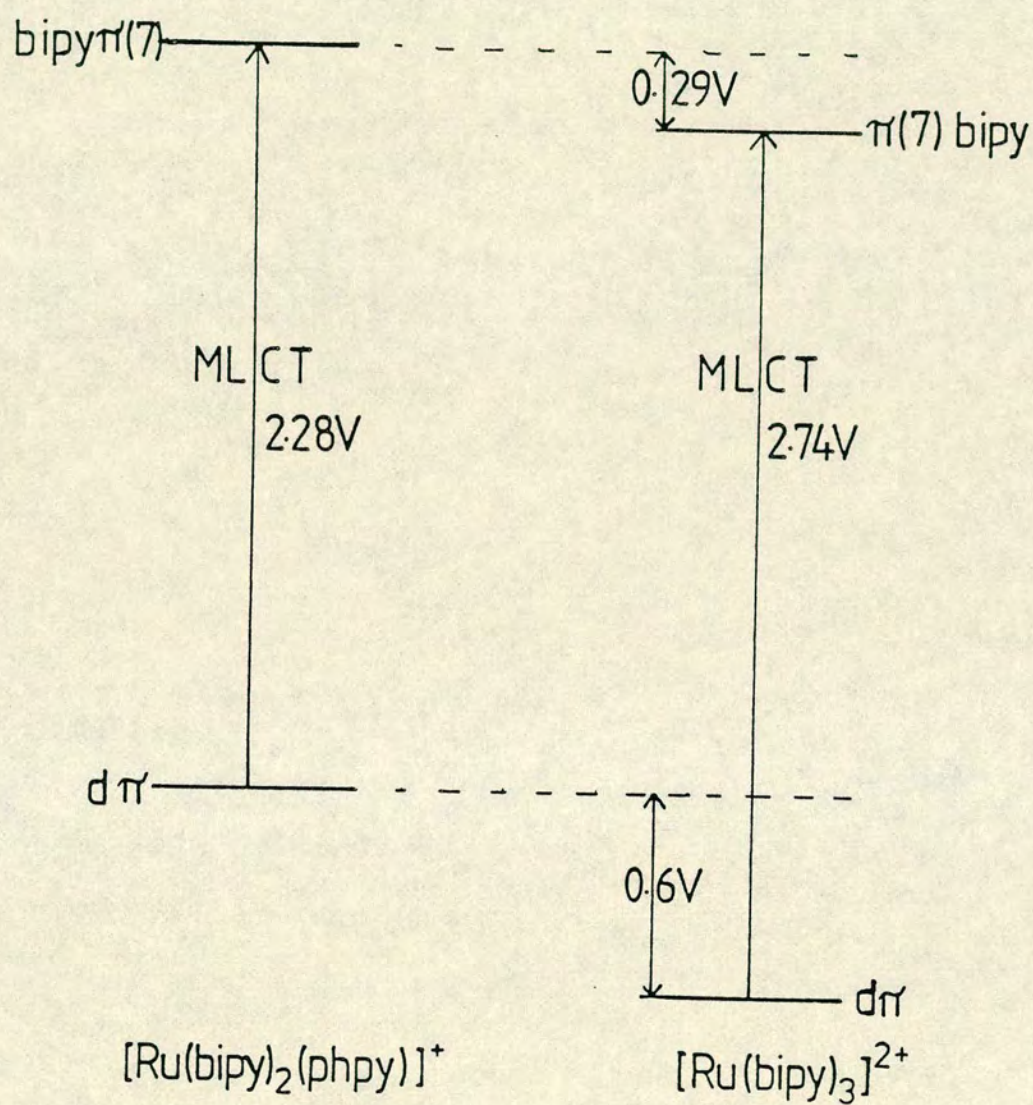


Table 6: Correlation of Electrochemical and Spectroscopic Data for $[\text{Ru}(\text{bipy})_2(\text{phpy})]^+$

<u>Complex</u>	<u>$E(\text{ox}) - E(\text{red}) / \text{eV}$</u>	<u>MLCT/eV</u>
$[\text{Ru}(\text{bipy})_2(\text{phpy})]^+$	2.31	2.28

The ML(bipy)CT transition has been moved to lower energy in $[\text{Ru}(\text{bipy})_2(\text{phpy})]^+$ with respect to $[\text{Ru}(\text{bipy})_3]^{2+}$ as shown in the schematic energy level scheme constructed in figure 10.

In the absorption spectrum of $[\text{Ru}(\text{bipy})_2(\text{phpy})]^+$ we anticipate observing bands which correspond to transitions involving:

- $\pi \rightarrow \pi^*$ intraligand transitions involving bipy^0 and phpy^-
- $\text{Ru(II)} \text{ } d\pi \rightarrow \pi^* \text{ bipy}^0$ (ML) charge-transfer
- $\text{Ru(II)} \text{ } d\pi \rightarrow \pi^* \text{ php}^-$ (ML) charge-transfer

By comparison with the absorption spectra of $[\text{Ru}(\text{bipy})_3]^{2+}$ and $[\text{Ru}(\text{bipy})_2(\text{py})_2]^{2+}$, as well as free bipyridine and free phenylpyridine, we would anticipate the bands which correspond to intraligand transitions in both bipyridine and phenylpyridine, for $[\text{Ru}(\text{bipy})_2(\text{phpy})]^+$, to be observed at energies over $30\,000 \text{ cm}^{-1}$.

This being so, then each of the bands we observe in the visible absorption spectrum of $[\text{Ru}(\text{bipy})_2(\text{phpy})]^+$ should be associated with charge-transfer transitions.

Indeed Reveco and co-workers²³ have proposed that the band at $20\,600\text{ cm}^{-1}$ should be assigned to a ML(phpy) charge-transfer. This would appear to be in agreement with our conclusion that the $\pi^*(7)$ level in phenylpyridine is found to be approximately $0.2\text{ eV} = 1600\text{ cm}^{-1}$ higher in energy than the $\pi^*(7)$ level in bipyridine.

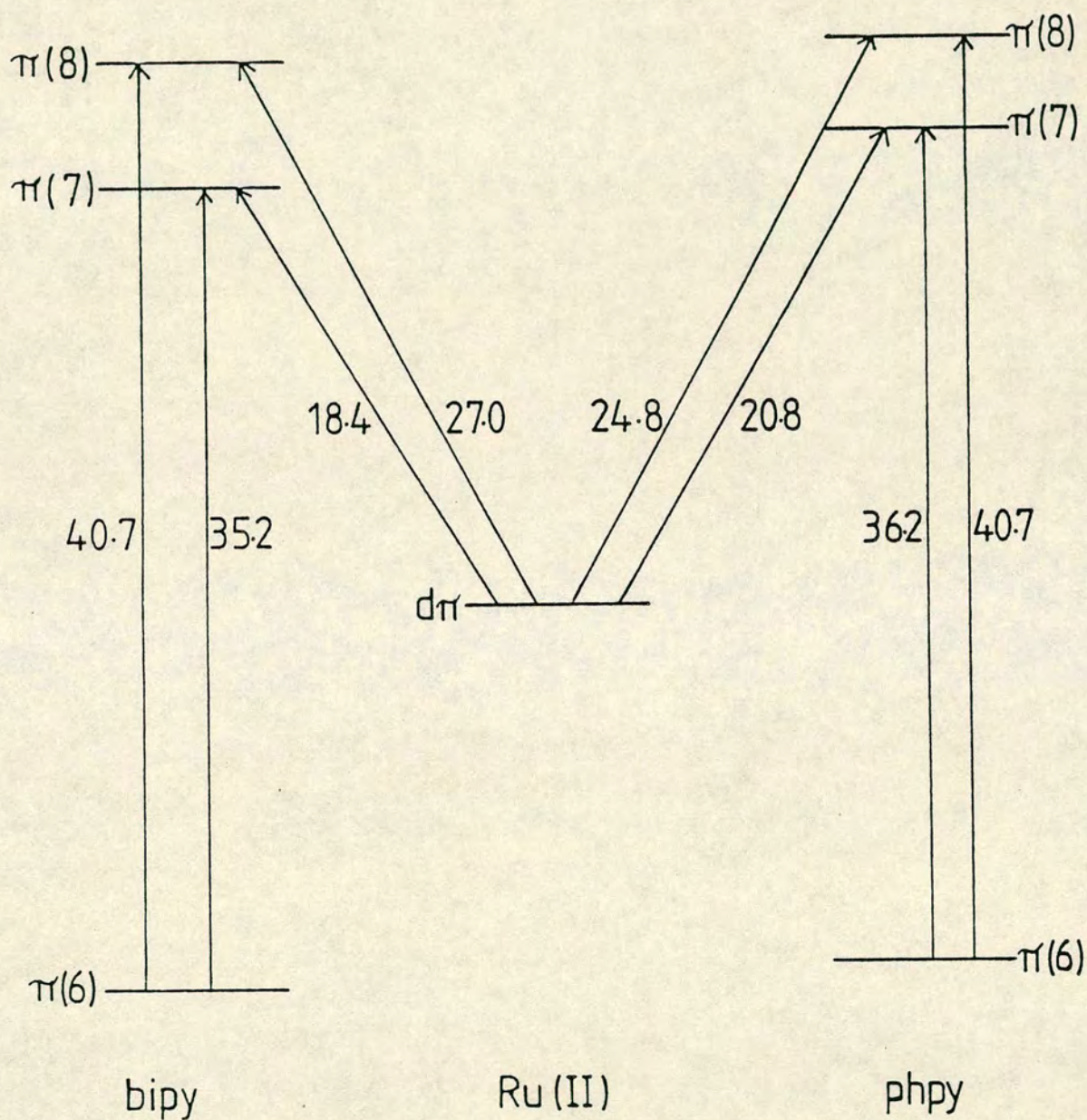
The two bands observed at higher energies ($24\,900$ and $27\,000\text{ cm}^{-1}$) may then be associated with metal-to-ligand charge-transfer from the Ru(II) centre to the $\pi^*(8)$ levels in phenylpyridine and bipyridine respectively. This view is consistent with the typical energy gap between the $\pi^*(7)$ and $\pi^*(8)$ levels. Examination of the ultra-violet spectra of the free ligands shows the gap to be approximately $7\,000\text{ cm}^{-1}$ for bipyridine and $4\,000\text{ cm}^{-1}$ for phenylpyridine. The transitions we propose are shown in figure 11.

In order to test these assignments and the associated orbital scheme we attempted to collect the absorption spectrum of this species in both its oxidised and reduced forms.

The one-electron oxidation product $[\text{Ru}(\text{bipy})_2(\text{phpy})]^{2+}$ may be prepared at a platinum O.T.T.L.E. The visible absorption spectrum of this species has been reported by Constable and Holmes,²⁴ although these workers made no attempt to assign the observed bands. They did, however, record the e.s.r. spectrum of $[\text{Ru}(\text{bipy})_2(\text{phpy})]^{2+}$ which confirmed this oxidation was indeed metal-centred.

The wide range absorption spectrum of $[\text{Ru}(\text{bipy})_2(\text{phpy})]^{2+}$ is shown in figure 12. The conversion of the rest-state complex to its oxidised form is accompanied by the

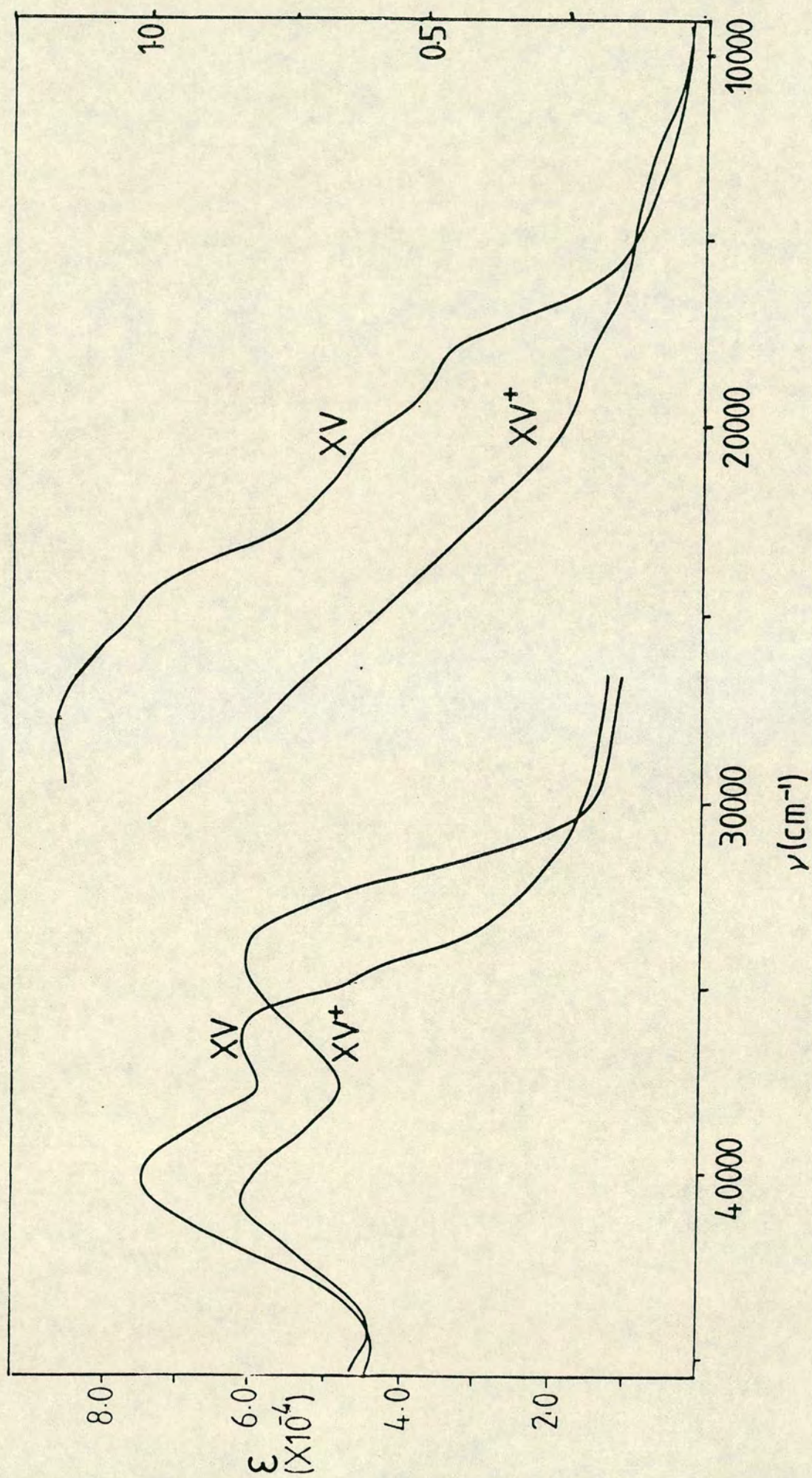
Figure 11: Schematic Energy Level Scheme for
 $[\text{Ru}(\text{bipy})_2(\text{phpy})]^+$



Note

- The broad absorption at $40\,700 \text{ cm}^{-1}$ encompasses the $\pi(6) \rightarrow \pi(8)$ transitions in both bipyridine and phenylpyridine.
- The figures listed above are optically measured transitions in units of 10^3 cm^{-1} .

Figure 12: Absorption Spectra of $[\text{Ru}(\text{bipy})_2(\text{phpy})]^{+2+}$
in Acetonitrile at Room Temperature



conservation of a series of isosbestic points, four in number, which implies a simple one-to-one conversion has taken place. On resetting the applied potential to zero volts, the spectrum of $[\text{Ru}(\text{bipy})_2(\text{phpy})]^+$ was regained in its original intensity.

The bands observed in the absorption spectra of $[\text{Ru}(\text{II})(\text{bipy})_2(\text{phpy})]^+$ and $[\text{Ru}(\text{III})(\text{bipy})_2(\text{phpy})]^{2+}$ are listed in table 7.

Table 7: Absorption Bands Observed for $[\text{Ru}(\text{bipy})_2(\text{phpy})]^{+/2+}$
 $\nu \times 10^{-3}/\text{cm}^{-1}$ ($\epsilon \times 10^{-4}$)

<u>Complex</u>	<u>$[\text{Ru}(\text{bipy})_2(\text{phpy})]^+$</u>	<u>$[\text{Ru}(\text{bipy})_2(\text{phpy})]^{2+}$</u>
	18.4 (0.48)	13.5 (0.11)
	20.8 (0.58)	18.0 (0.23)
	24.8 (1.05)	34.0 (6.02)
	27.0 (1.16)	
	35.2 (4.19) sh	41.0 (6.12)
	35.8 (6.09)	
	40.7 (7.48)	

Considering the visible spectrum of $[\text{Ru}(\text{bipy})_2(\text{phpy})]^+$ it is apparent that the bands we assign to $\text{M}(\text{Ru}(\text{II})) \rightarrow \text{L}(\text{bipy})$ and $\text{M}(\text{Ru}(\text{II})) \rightarrow \text{L}(\text{phpy})$ charge-transfers in the resting oxidation state complex have disappeared which complements

our proposal. Meanwhile, two new bands are observed at $13\,500\text{ cm}^{-1}$ and $18\,000\text{ cm}^{-1}$, the extinction coefficients of which are drastically lower than the metal-to-ligand charge-transfer bands. This observation suggests the bands in $[\text{Ru}(\text{bipy})_2(\text{phpy})]^{2+}$ are associated with ligand-to-metal charge transfers (see chapter 2).

In $[\text{Ru}(\text{bipy})_2(\text{phpy})]^{2+}$ we anticipate observing bands due to:

- a) $\pi \rightarrow \pi^*$ intraligand transitions involving bipyridine and phenylpyridine;
- b) metal-to-ligand charge-transfers from Ru(III) to bipyridine and phenylpyridine;
- c) ligand-to-metal charge-transfers from both phenylpyridine and bipyridine to ruthenium(III).

Considering the ligand-to-metal charge-transfer, we would predict the charge-transfer from the phenylpyridine ligand would occur at a lower energy since we have already observed electrochemically that the $\pi(6)$ level in free phenylpyridine is found at slightly higher energy than in bipyridine. That is the band at $13\,500\text{ cm}^{-1}$ is due to a $\text{L}(\text{phpy})\pi \rightarrow \text{Ru}(\text{III})d\pi$ transition with the band at $18\,000\text{ cm}^{-1}$ assigned to a $\text{L}(\text{bipy})\pi \rightarrow \text{Ru}(\text{III})d\pi$ charge-transfer. Absorptions from lower energy ligand orbitals to Ru(III) are swamped by more intense transitions.

From the ultra-violet absorption spectra of bipyridine and phenylpyridine it is apparent that these $\pi \rightarrow \pi^*$ intraligand transitions occur at very similar, but distinct energies. Accordingly, we assign the bands at approximately $35\,000\text{ cm}^{-1}$

in $[\text{Ru}(\text{bipy})_2(\text{phpy})]^+$ to $\pi(6) \rightarrow \pi^*(7)$ transitions. The lower energy component of this band at $35\,200\text{ cm}^{-1}$ is assigned to the bipyridyl ligand with the higher energy component therefore attributed to phenylpyridine. The broad absorption at $41\,000\text{ cm}^{-1}$ must encompass the $\pi(6) \rightarrow \pi^*(8)$ transitions in both phenylpyridine and bipyridine with the lower energy side attributed to phenylpyridine on this occasion.

However on oxidation of this complex, the lowest energy $\pi \rightarrow \pi^*$ transitions are observed to move to lower energies. This shift has previously been recognised when examining the changes in the absorption spectra of $[\text{Ru}(\text{bipy})_3]^{2+/3+}$, $[\text{Ru}(\text{bipy})_2\text{Cl}_2]^{0/+}$, $[\text{Ru}(\text{bipy})_2\text{CO}\cdot\text{Cl}]^{+/2+}$ and $[\text{Ru}(\text{bipy})_2(\text{MeCN})_2]^{2+/3+}$ as discussed in chapter 2.

This interpretation of the absorption spectrum of $[\text{Ru}(\text{bipy})_2(\text{phpy})]^{2+}$ confirms this oxidation is indeed metal-centred (rather than aryl-centred) and the spectrum of each species may be understood in terms of separate $\text{Ru}(\text{bipy})$ and $\text{Ru}(\text{phpy})$ chromophores.

In all, this complex also undergoes two reversible one-electron reductions and these species have been separately electrogenerated at a platinum O.T.T.L.E. with their absorption spectra being measured as shown in figure 13; the observed bands are listed in Table 8.

Figure 13: Absorption Spectra of $[\text{Ru}(\text{bipy})_2(\text{phpy})]^{+/-}$
in Acetonitrile at Room Temperature

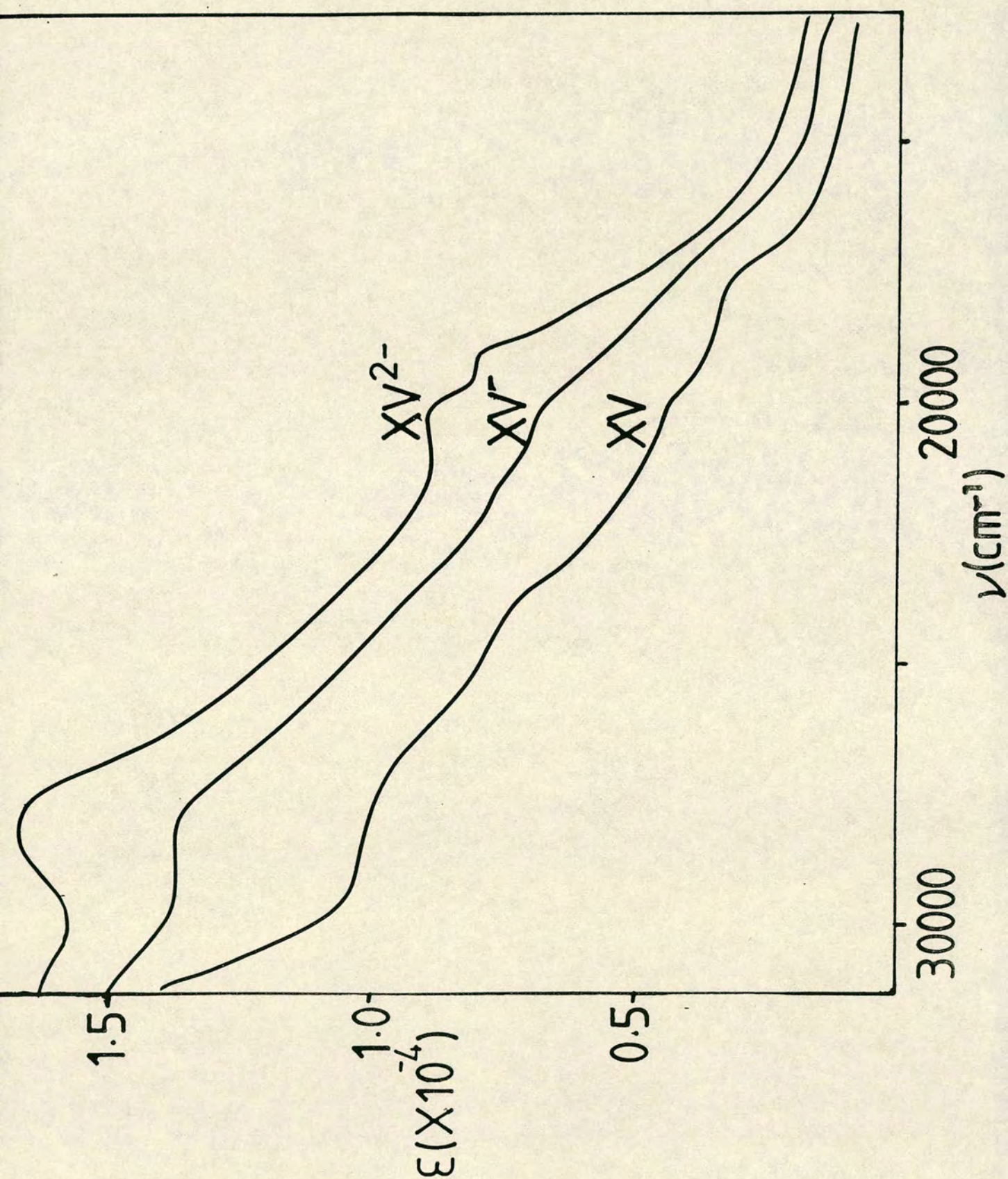
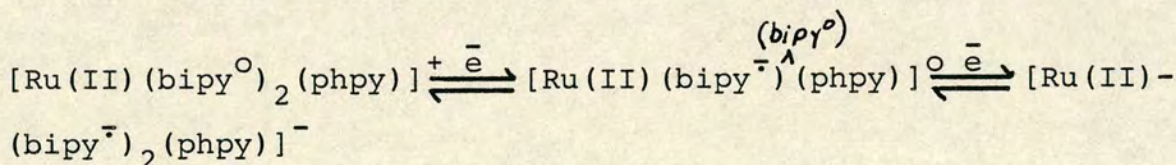


Table 8: Absorption Bands in $[\text{Ru}(\text{bipy})_2(\text{phpy})]^\circ/-$ in Acetonitrile $\nu/10^3 \text{cm}^{-1}$ ($\epsilon \times 10^{-4}$)

<u>Complex</u>	<u>Absorption Bands</u>	
$[\text{Ru}(\text{bipy})_2(\text{phpy})]^\circ$	29.0 (1.40)	20.8 (0.62)
$[\text{Ru}(\text{bipy})_2(\text{phpy})]^-$	28.5 (1.70)	20.5 (0.88)
		19.4 (0.75)

An examination of the absorption spectra of $[\text{Ru}(\text{bipy})_2(\text{phpy})]^\circ$ and $[\text{Ru}(\text{bipy})_2(\text{phpy})]^-$ shows that these reductions are indeed bipyridyl-based. A progressive growth of the bands which characterise the bipy^- chromophore⁹ is again observed which means the reduced species should be formulated as shown below.



Attempts to electrogenerate the reduced forms of this complex in sufficiently low concentration to allow the ultra-violet absorption spectrum to be monitored proved fruitless.

The work described in this chapter then shows that the phenylpyridine ligand has a similar effect to the carbon-metallated bipyridine ligand on neighbouring conventionally-bound bipyridine ligands. It would appear therefore that

the diphenyl dianion would be very powerful inductively, however, no transition-metal coordination complexes containing this ligand have been prepared to date, to our knowledge.

Experimental

$[\text{Ir}(\text{bipy})_2(\mu\text{-C,N-bipy})(\text{H}_2\text{O})](\text{BF}_4)_2$ was prepared by the method of Watts et al.¹ $[\text{Ru}(\text{bipy})_2(\text{phpy})](\text{PF}_6)$ was prepared by the method of Constable and Holmes.²⁴

^1H and ^{13}C n.m.r. spectra were collected using a Bruker n.m.r. spectrometer. (360.13 MHz and 90.56 MHz respectively).

Solvent purification and electrochemical and spectroelectrochemical techniques are as described in chapter 2.

References

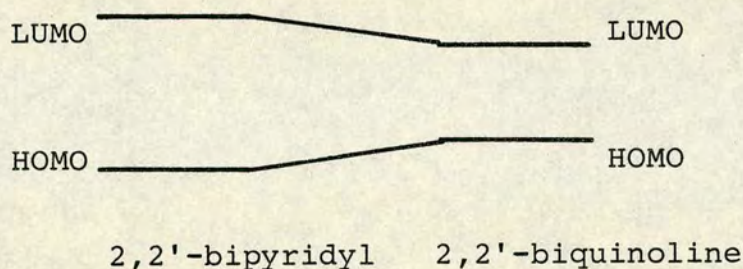
1. R.J. Watts, J.S. Harrington and J. Van Houten;
J. Am. Chem. Soc., 99, 2179 (1977),
2. R.D. Gillard, R.J. Lancashire and P.A. Williams;
J. Chem. Soc., Dalton Trans., 190 (1979).
3. P.J. Spellane and R.J. Watts; Inorg. Chem., 20, 3561
(1981).
4. W.A. Wickramasinghe, P.H. Bird and N. Serpone;
J. Chem. Soc., Chem. Commun., 1284 (1981).
5. L.J. Yellowlees; Ph.D. Thesis, University of Edinburgh
(1982).
6. J.L. Kahl, K.W. Hanck and M.K. DeArmond; J. Phys. Chem.,
82, 540 (1978).
7. J.L. Kahl, K.W. Hanck and M.K. DeArmond; J. Phys. Chem.,
83, 2611 (1979).
8. S.F. Mason; Inorg. Chim. Acta Rev., 89, 2 (1968).
9. E. König and S. Kremer; Chem. Phys. Lett., 5, 87 (1970).
10. G.A. Heath, L.J. Yellowlees and P.S. Braterman;
Chem. Phys. Lett., 92, 646 (1982).
11. N. Serpone, G. Ponterini, M.A. Jamieson, F. Belletta
and M. Maestri; Coord. Chem. Rev., 50, 209 (1983).
12. J.L. Kahl, K.W. Hanck and M.K. DeArmond; J. Inorg. Nucl.
Chem., 41, 495 (1979).
13. S. Castellano, H. Gunther, S. Ebersole; J. Phys. Chem.,
69, 4166 (1965).
14. P.J. Spellane, R.J. Watts and C.J. Curtis; Inorg. Chem.,
22, 4060 (1983).

15. G. Nord, A.C. Hazell, R.G. Hazell and O. Farver;
Inorg.Chem., 22, 3429 (1983).
16. M. Nonoyama; Bull.Chem.Soc.Jpn., 47, 767 (1974).
17. M. Nonoyama and K. Yamasaki; Inorg.Nucl.Chem.Lett.,
7, 943 (1971).
18. C.C. Yin and A.J. Deeming; J.Chem.Soc.,Dalton Trans.,
2091 (1975).
19. K. Hiraki, Y. Obayashi and Y. Oki; Bull.Chem.Soc.Jpn.,
52, 1372 (1979).
20. M.I. Bruce, B.A. Goodall and G.A. Stone; J.Organomet.
Chem., 60, 343 (1973).
21. P. Reveco, J.H. Medley, A.R. Garber, N.S. Bhacca and
J. Sellini; Inorg.Chem., 24, 1096 (1985).
22. P. Receco, R.H. Schmehl, W.R. Cherry, F.R. Fronczek
and J. Selbin; Inorg.Chem., 24, 4078 (1985).
23. R. Reveco, W.R. Cherry, J. Medley, A.R. Garber,
R.J. Gale and J. Selbin; Inorg.Chem., 25, 1842 (1986).
24. E.C. Constable and J.M. Holmes; J.Organomet.Chem.,
301, 203 (1986).
25. B.P. Sullivan, D.J. Salmon, T.J. Meyer and J. Peedin;
Inorg.Chem., 18, 3369 (1979).
26. B.P. Sullivan, D.J. Salmon and T.J. Meyer; Inorg.Chem.,
17, 3334 (1978).
27. N.E. Tokel-Takvoryan, R.E. Hemingway and A.J. Bard;
J.Am.Chem.Soc., 95, 6582 (1973).

Chapter 5

Spectroelectrochemical Characterisation of the Complexes $[\text{Ru}(\text{bipy})_n(\text{biq})_{3-n}]^{2+}$ ($n=0,1,2,3$). Examination of the Apparent Anomalous Metal-to-ligand Charge-transfer Behaviour

In discussions regarding ligand modifications to the complex $[\text{Ru}(\text{bipy})_3]^{2+}$, in order to improve its performance as a photosensitiser, it has been suggested that the ligand 2,2'-biquinoline may be of some interest,¹⁻⁶ since its first π -acceptor orbital is substantially more accessible.



The benzo-substitution with respect to 2,2'-bipyridyl causes a relatively large shift to lower energy of the $\pi-\pi^*$ bands in the absorption spectrum of the free ligand.

The complex $[\text{Ru}(\text{biq})_3]^{2+}$, prepared in 1976 by Klassen,⁷ exhibits this stabilisation of the lowest π -acceptor orbital with the lowest energy metal-to-ligand charge-transfer band being red-shifted by approximately $3\,000\text{ cm}^{-1}$ with respect to $[\text{Ru}(\text{bipy})_3]^{2+}$. More recently the series of mixed-ligand complexes $[\text{Ru}(\text{bipy})_n(\text{biq})_{3-n}]^{2+}$ ($n=1$ or 2) have also

been synthesised and some of the properties of their ground and excited state species have been studied.^{3,6}

In Ru(II)-polypyridine complexes there are three orbital types of electronically excited states namely metal-centred (MC or dd), ii) metal-to-ligand charge-transfer (MLCT or $d\pi^*$) and iii) ligand-centred (LC or $\pi\pi^*$) excited states.⁸⁻¹⁵ For differing Ru(II)-polypyridine complexes the energies of these excited states are dictated by the intrinsic spectroscopic properties of the ligands in each separate complex.

In $[\text{Ru}(\text{bipy})_3]^{2+}$ the energy ordering of the low-energy excited states is fairly well known. The lowest excited state, found at $17\,200\text{ cm}^{-1}$ above the ground state involves a $^3\text{MLCT}$ transition.¹⁶ It has been suggested that the lowest metal-centred excited state is at approximately $21\,000\text{ cm}^{-1}$ ^{10,17} with the lowest ligand-centred state lying at about $23\,100\text{ cm}^{-1}$ which is equivalent to the value observed for the phosphorescence of free bipyridine.¹⁸

In $[\text{Ru}(\text{biq})_3]^{2+}$ it has been suggested² that i) since it is considerably easier to reduce biquinoline than bipyridine the MLCT excited states should be at lower energies in $[\text{Ru}(\text{biq})_3]^{2+}$ than $[\text{Ru}(\text{bipy})_3]^{2+}$, ii) the steric hindrance among the biquinoline ligands implies longer Ru-N bond distances meaning the metal-centred excited states should also lie at lower energies in $[\text{Ru}(\text{biq})_3]^{2+}$; and iii) the lowest energy ligand-centred excited state should lie at approximately $20\,400\text{ cm}^{-1}$ equivalent to the value observed for the phosphorescence of the free ligand.

As these workers predicted,² an examination of the absorption and emission characteristics of $[\text{Ru}(\text{biq})_3]^{2+}$ shows the lowest excited species to involve a $^3\text{MLCT}$ state.

In the mixed-ligand complex $[\text{Ru}(\text{bipy})_2(\text{biq})]^{2+}$, distinct $\text{Ru(II)} \rightarrow \text{bipy}^0$ and $\text{Ru(II)} \rightarrow \text{biq}^0$ charge-transfer absorptions are present as illustrated in figure 1. However emission only occurs from the lowest excited state. A comparison of the emission spectra of $[\text{Ru}(\text{bipy})_2(\text{biq})]^{2+}$ and $[\text{Ru}(\text{biq})_3]^{2+}$ shows each system exhibits only one emission band,⁵ which has a similar energy and shape in each case. This implies emission only occurs from comparable lowest excited states of these complexes, a $\text{Ru(II)} \rightarrow \text{biq}^0$ charge-transfer state, and efficient conversion of $\text{Ru(II)} \rightarrow \text{bipy}^0$ excited states to the lowest $\text{Ru(II)} \rightarrow \text{biq}^0$ excited state must take place prior to emission.

Our interest in this series of mixed-ligand complexes arose when we considered the absorption spectra of the series of complexes $[\text{Ru}(\text{bipy})_n(\text{biq})_{3-n}]^{2+}$ ($n=1 \rightarrow 3$), shown in figure 1.

From figure 1 we may note that the visible absorption spectrum of $[\text{Ru}(\text{bipy})_3]^{2+}$ shows the presence of only one main band at $22\,100\text{ cm}^{-1}$ with an extinction coefficient of $13\,700\text{ M}^{-1}\text{cm}^{-1}$. Equally, the absorption spectrum of $[\text{Ru}(\text{biq})_3]^{2+}$ in the visible region, shows one principal band, at $19\,100\text{ cm}^{-1}$, with an extinction coefficient of $11\,000\text{ M}^{-1}\text{cm}^{-1}$.

Therefore, we would predict that on successive replacement of the bipyridine ligands in $[\text{Ru}(\text{bipy})_3]^{2+}$ by

Figure 1: Absorption Spectra of $[\text{Ru}(\text{bipy})_n(\text{biq})_{3-n}]^{2+}$
(n = 0 to 3) in Acetonitrile at Room Temperature

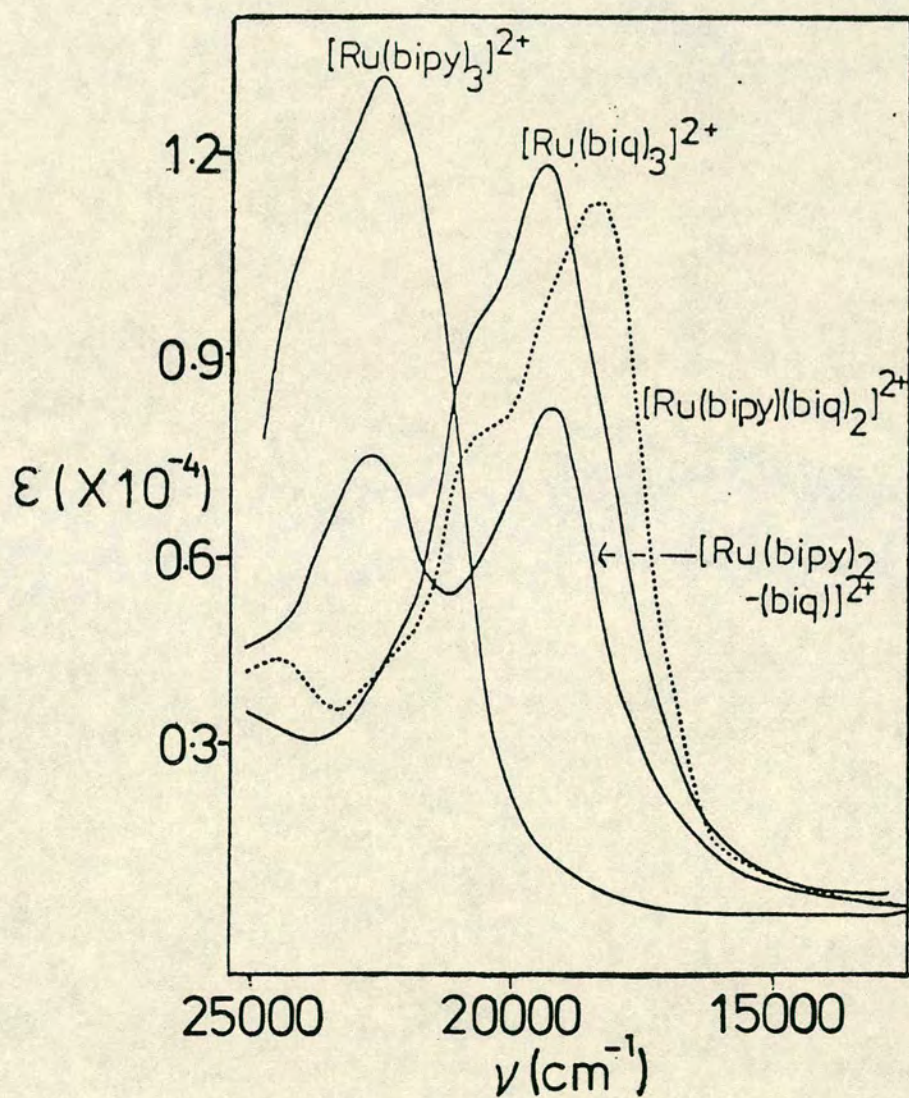
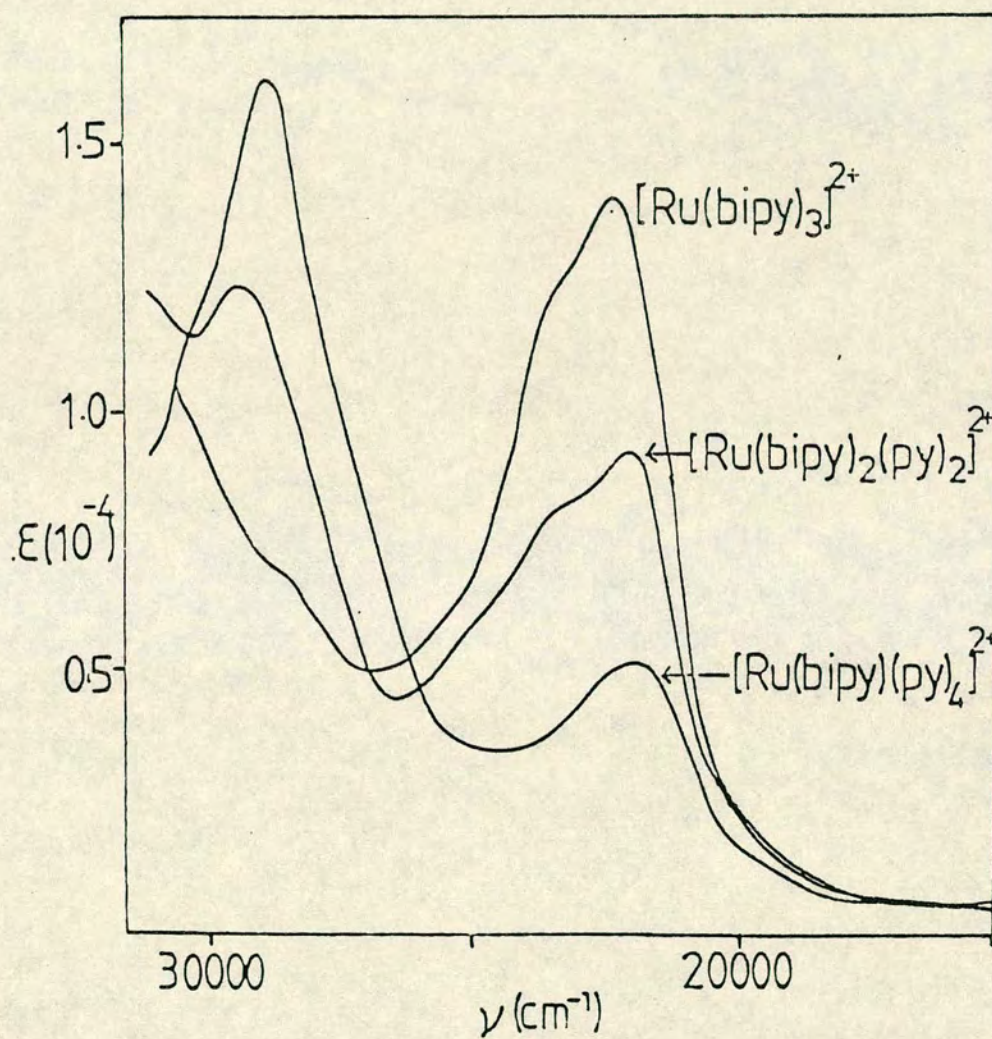


Figure 2: Absorption Spectra of $[\text{Ru}(\text{bipy})_n(\text{py})_{6-2n}]^{2+}$
($n = 0$ to 2) in Acetonitrile at Room Temperature



biquinoline a stepwise loss of the $\text{Ru(II)} \rightarrow \text{bipy}^0$ charge-transfer band intensity would be observed accompanied by a similar growth of the band characteristic of the $\text{Ru(II)} \rightarrow \text{biq}^0$ transition in a similar manner to the trend observed for the series of complexes $[\text{Ru}(\text{bipy})_n(\text{py})_{6-2n}]^{2+}$ ($n=0,1,2$) shown in figure 2.

Such behaviour is not observed in the $[\text{Ru}(\text{bipy})_n(\text{biq})_{3-n}]^{2+}$ ($n=0,1,2,3$) series with the position and intensity of the metal-to-ligand charge-transfer bands in the mixed-ligand complexes exhibiting anomalous behaviour as shown in figure 1; the bands observed are listed in table 1. In $[\text{Ru}(\text{bipy})_2(\text{biq})]^{2+}$ the $\text{Ru(II)} \rightarrow \text{bipy}^0$ band is observed as anticipated, however the $\text{Ru(II)} \rightarrow \text{biq}^0$ band, although occurring at the anticipated energy is noted to be significantly more intense than expected. It would appear that the $\text{Ru(II)} \rightarrow \text{biquinoline}$ charge-transfer in some way "steals intensity" from the $\text{Ru} \rightarrow \text{bipyridine}$ charge-transfer in this complex.

If the visible absorption spectrum of $[\text{Ru}(\text{bipy})(\text{biq})_2]^{2+}$ is now considered it would seem this "stealing of intensity" becomes more extreme with no clear evidence of the $\text{Ru(II)} \rightarrow \text{bipy}^0$ charge-transfer being observed although this band may be obscured by other absorptions at similar energies. In $[\text{Ru}(\text{bipy})(\text{biq})_2]^{2+}$ the $\text{Ru(II)} \rightarrow \text{biq}^0$ charge-transfer band is also red-shifted by approximately 840 cm^{-1} (0.1 eV) relative to both $[\text{Ru}(\text{bipy})_2(\text{biq})]^{2+}$ and $[\text{Ru}(\text{biq})_3]^{2+}$.

These observations suggest that some anomalous behaviour occurs in these mixed-ligand complexes. This perhaps draws into question the validity of the ligand localised model in

Table 1: Absorption Bands in Ruthenium bipy/py and
Ruthenium bipy/biq Complexes

<u>Complex</u>	<u>MLCT transitions $\nu/10^3\text{cm}^{-1}$ ($\epsilon \times 10^{-4}$)</u>		
	<u>$d\pi \rightarrow \pi^*$ bipy</u>	<u>$d\pi \rightarrow \pi^*$ py</u>	<u>$d\pi \rightarrow \pi^*$ biq</u>
$[\text{Ru}(\text{bipy})_3]^{2+}$	22.1 (1.37)	-	
$[\text{Ru}(\text{bipy})_2(\text{py})_2]^{2+}$	21.8 (0.87)	29.4 (1.30)	
$[\text{Ru}(\text{bipy})(\text{py})_4]^{2+}$	21.3 (0.48)	28.6 (1.61)	
$[\text{Ru}(\text{bipy})_3]^{2+}$	22.1 (1.37)		
$[\text{Ru}(\text{bipy})_2(\text{biq})]^{2+}$	22.8 (0.75)		19.0 (0.80)
$[\text{Ru}(\text{bipy})(\text{biq})_2]^{2+}$	a		18.4 (1.06)
$[\text{Ru}(\text{biq})_3]^{2+}$	-		19.1 (1.10)

a - Band unobserved

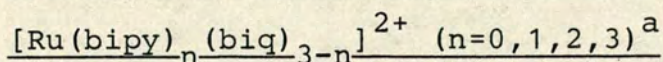
b - All spectra recorded in acetonitrile

these systems when they undergo reduction in the sense that it is the first observation not anticipated or naturally explained.

We have therefore examined the electrochemical behaviour of these systems and obtained their absorption spectra in several differing oxidation states in an attempt to further define these apparent anomalies, and to determine the applicability of the localised model in these cases.

Pertinent electrochemical data for these systems are summarised in table 2.

Table 2: Electrochemical Data for the Complexes



<u>Complex</u>	<u>E^{ox}</u>	<u>$E_{\text{red}}(1)$</u>	<u>$E_{\text{red}}(2)$</u>	<u>$E_{\text{red}}(3)$</u>
$[\text{Ru}(\text{bipy})_3]^{2+}$	+0.96	-1.66	-1.83	-2.08
$[\text{Ru}(\text{bipy})_2(\text{biq})]^{2+}$	+1.03	-1.205	-1.71	-1.97
$[\text{Ru}(\text{bipy})(\text{biq})_2]^{2+}$	+1.10	-1.12	-1.35	-1.91
$[\text{Ru}(\text{biq})_3]^{2+}$	+1.17	-1.035	-1.195	-1.55

a - All potentials are measured against a Ag/Ag^+ reference electrode in 0.1M $\text{TBABF}_4/\text{CH}_3\text{CN}$.

It should be noted from table 1 that there is a linear increase in the potential required to oxidise the ruthenium centre as successive biquinoline ligands are incorporated in place of bipyridine with this attributed to the increased stabilisation of the $d\pi$ ruthenium orbitals by the stronger π -acceptor biquinoline ligands (as illustrated in figure 3). Similarly a linear effect is noted when the first reduction of the complexes $[\text{Ru}(\text{bipy})_n(\text{biq})_{3-n}]^{2+}$ ($n=0$ to 2) is considered with this again attributable to the effect caused on the biquinoline ligand undergoing reduction by the other two diimine moieties.

As we have discussed in previous chapters we can evaluate the gap between the potentials required to oxidise the metal centre and the first ligand reduction, which models the optical metal-to-ligand charge-transfer. This comparison is of particular interest in these seemingly anomalous systems. The data for this series of biquinoline complexes is shown in table 3. There is no suggestion in the electrochemical data that the metal-to-ligand charge-transfer (to biquinoline, at least) should be affected.

It is also useful to consider the gap between the metal oxidation and the third bipyridyl-based reduction in these complexes to look for any evidence of unusual behaviour in the bipyridyl ligand in $[\text{Ru}(\text{bipy})(\text{biq})_2]^{2+}$. An examination of this data, shown in table 4 reveals that there is no evidence for any "altered energy" in the third "bipyridyl" ligand in $[\text{Ru}(\text{bipy})(\text{biq})_2]^{2+}$. That is, no explanation for

Figure 3: Comparative Energy Level Scheme for $[\text{Ru}(\text{bipy})_n(\text{biq})_{3-n}]^{2+}$ ($n = 1$ to 3)

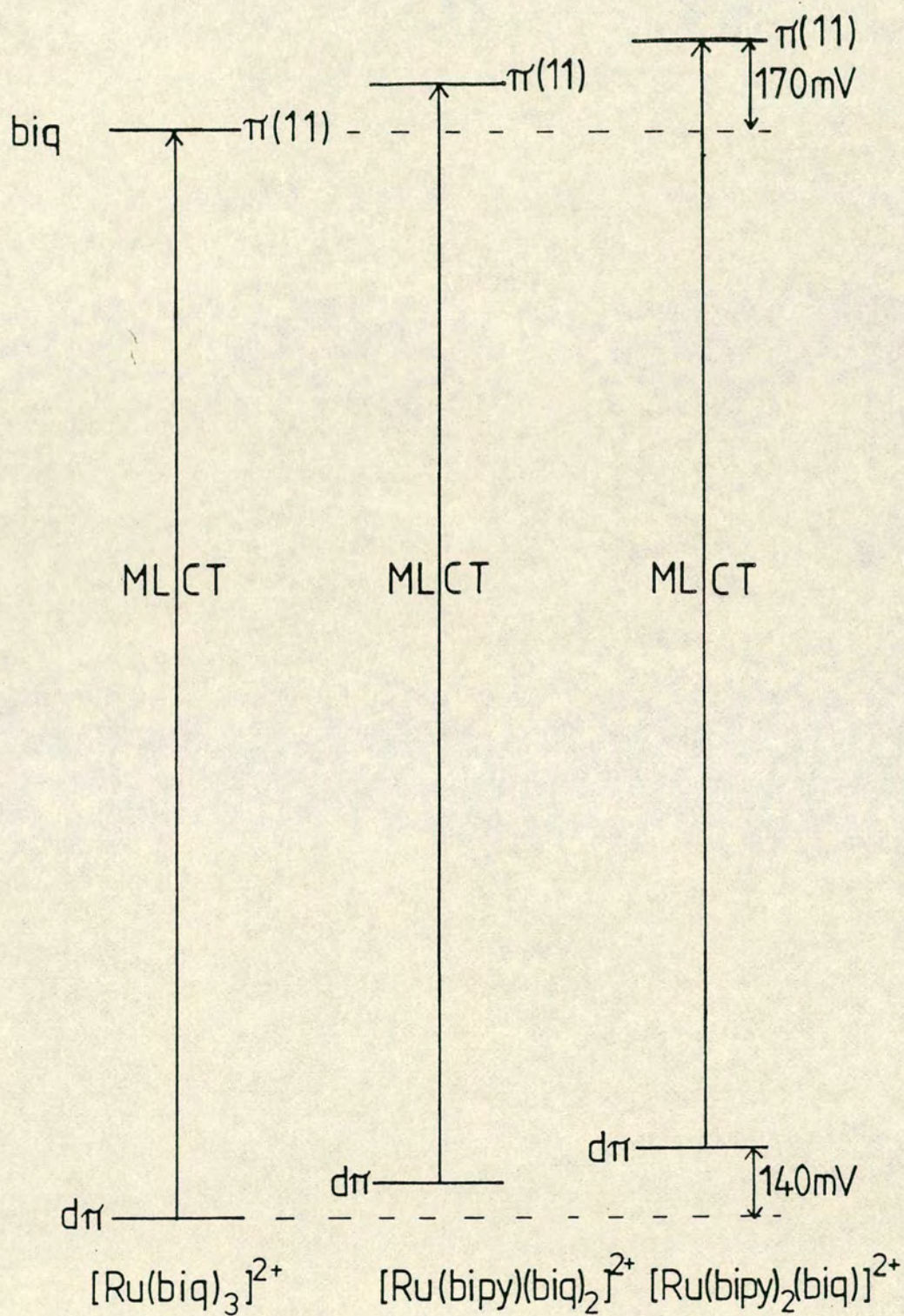


Table 3: Modelling of the Lowest Energy MLCT Transition
Using Electrochemical Data for the Complexes
 $[\text{Ru}(\text{bipy})_n(\text{biq})_{3-n}]^{2+}$ (n=0 to 3)

<u>Complex</u>	<u>E(ox)-E(red1)/eV</u>	<u>E_{opt}/eV</u>	<u>Assignment</u>
$[\text{Ru}(\text{bipy})_3]^{2+}$	2.62	2.73	Ru(II) → bipy
$[\text{Ru}(\text{bipy})_2(\text{biq})]^{2+}$	2.235	2.36	Ru(II) → biq
$[\text{Ru}(\text{bipy})(\text{biq})_2]^{2+}$	2.22	2.28	Ru(II) → biq
$[\text{Ru}(\text{biq})_3]^{2+}$	2.205	2.38	Ru(II) → biq

Table 4: Electrochemical Separation Between the Ru(II/III)
Couple and Third Reduction (Bipyridyl-based) for
the Series $[\text{Ru}(\text{bipy})_n(\text{biq})_{3-n}]^{2+}$ (n=1 to 3)

<u>Complex</u>	<u>E(ox)-E(red3)/eV</u>
$[\text{Ru}(\text{bipy})_3]^{2+}$	3.04
$[\text{Ru}(\text{bipy})_2(\text{biq})]^{2+}$	3.00
$[\text{Ru}(\text{bipy})(\text{biq})_2]^{2+}$	3.01

the anomalous behaviour of the optical metal-to-ligand (biquinoline) charge-transfer band is found in the electrochemical behaviour of this system.

Before we investigate the spectra of the reduced mixed-ligand complexes we must first examine the spectroscopic behaviour of biquinoline itself, especially upon reduction. As shown in figure 4, the absorption spectrum of 2,2'-biquinoline reveals the lowest energy ($\pi(10) \rightarrow \pi(11)$) intraligand transition occurs at approximately $4\,000\text{ cm}^{-1}$ lower energy than in bipyridine. This is qualitatively as expected for the extended conjugation and indeed fits with the directly measured electrochemical behaviour of free biquinoline with the energy of the HOMO being raised and the LUMO being lowered.

As we have discussed in previous chapters, the lowest energy $\pi \rightarrow \pi^*$ transition and the gap between the first oxidation and first reduction of the free ligand should correspond as shown in table 5.

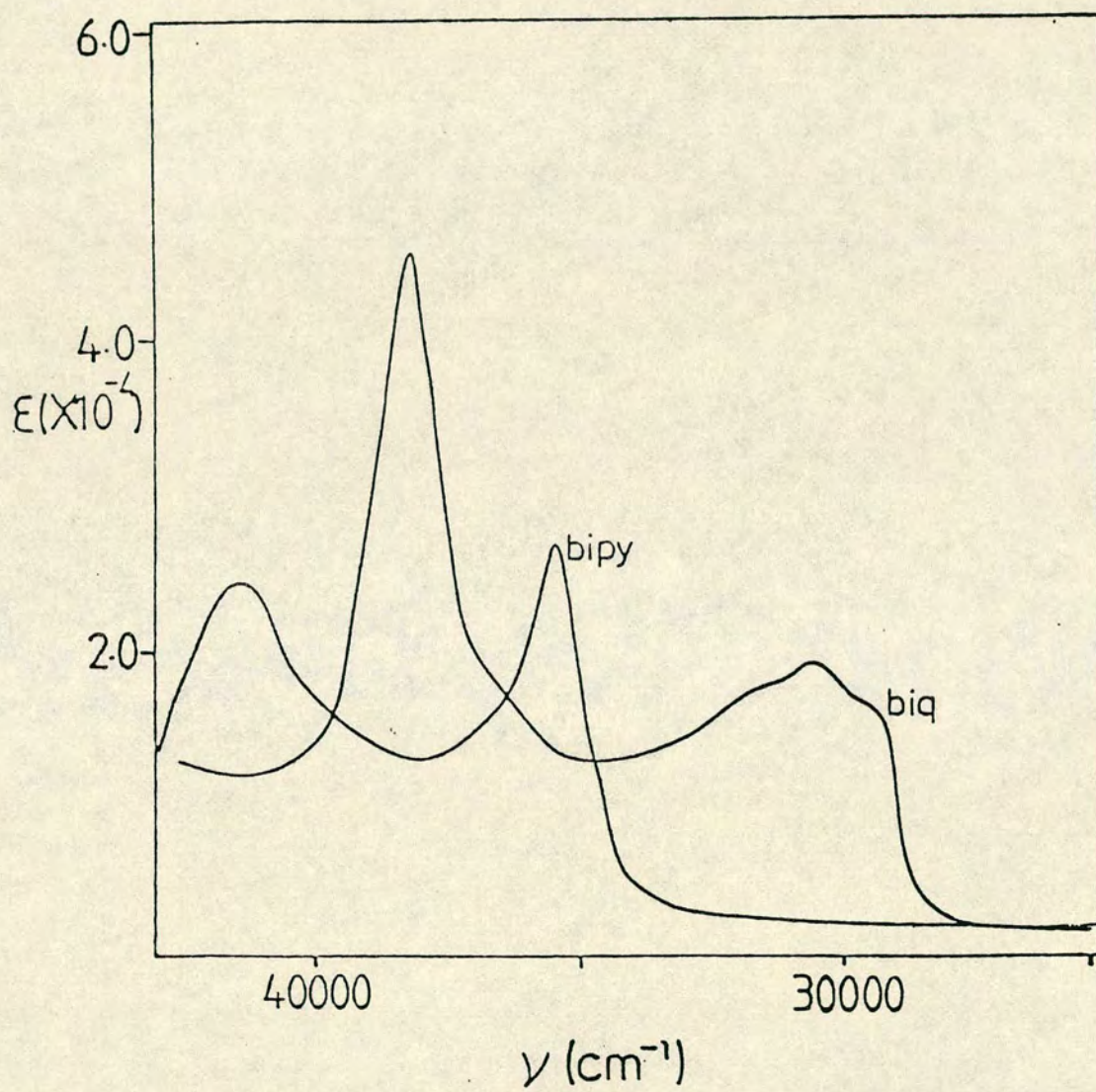
Table 5: Electrochemical Behaviour of Bipyridine and Biquinoline^a

<u>Complex</u>	<u>E(ox)/eV</u>	<u>E(red1)/eV</u>	<u>E(ox)-E(red)</u>	<u>E_{opt}</u>
2,2'-Bipyridine	+1.84 ^b	-2.57	4.41	4.32
2,2'-Biquinoline	+1.60 ^b	-2.10	3.70	~3.8

a - All potentials measured in 0.1M TBABF₄/acetonitrile vs a Ag/Ag⁺ reference electrode

b - Irreversible wave

Figure 4: Absorption Spectra of 2,2'-Biquinoline
and 2,2'-Bipyridine in Dichloromethane



Since the biquinoline ligand undergoes reduction prior to bipyridine it is apparent that we must obtain a spectrum of the biquinoline anion itself to enable us to interpret the absorption spectra of these reduced ruthenium-biquinoline complexes. This spectrum has been obtained in two ways, namely by chemical reduction of biquinoline by lithium metal in rigorously dry tetrahydrofuran and also by electrochemical reduction of the ligand, again in thf, at a platinum O.T.T.L.E. In the latter case electrochemical reduction was facilitated by the use of a lithium perchlorate (LiClO_4) electrolyte in place of TBABF_4 which appears to lower the potential required to reduce biquinoline by approximately 0.4 volts allowing the spectrum of Li^+biq^- to be collected as illustrated in figure 5.

Since we now possess the spectra of bipy^0 , bipy^- , biq^0 and biq^- we may proceed to collect and interpret the spectra of these mixed-ligand ruthenium complexes.

We have now established that the complex $[\text{Ru}(\text{bipy})_2(\text{biq})]^{2+}$ undergoes one reversible one-electron oxidation and three successive reversible one-electron reductions. The one-electron oxidised species has been generated at a platinum gauze; the spectrum obtained is illustrated in figure 6 with the observed bands listed in table 6.

Figure 5: Absorption Spectrum of Li^+biq^- in Tetrahydrofuran

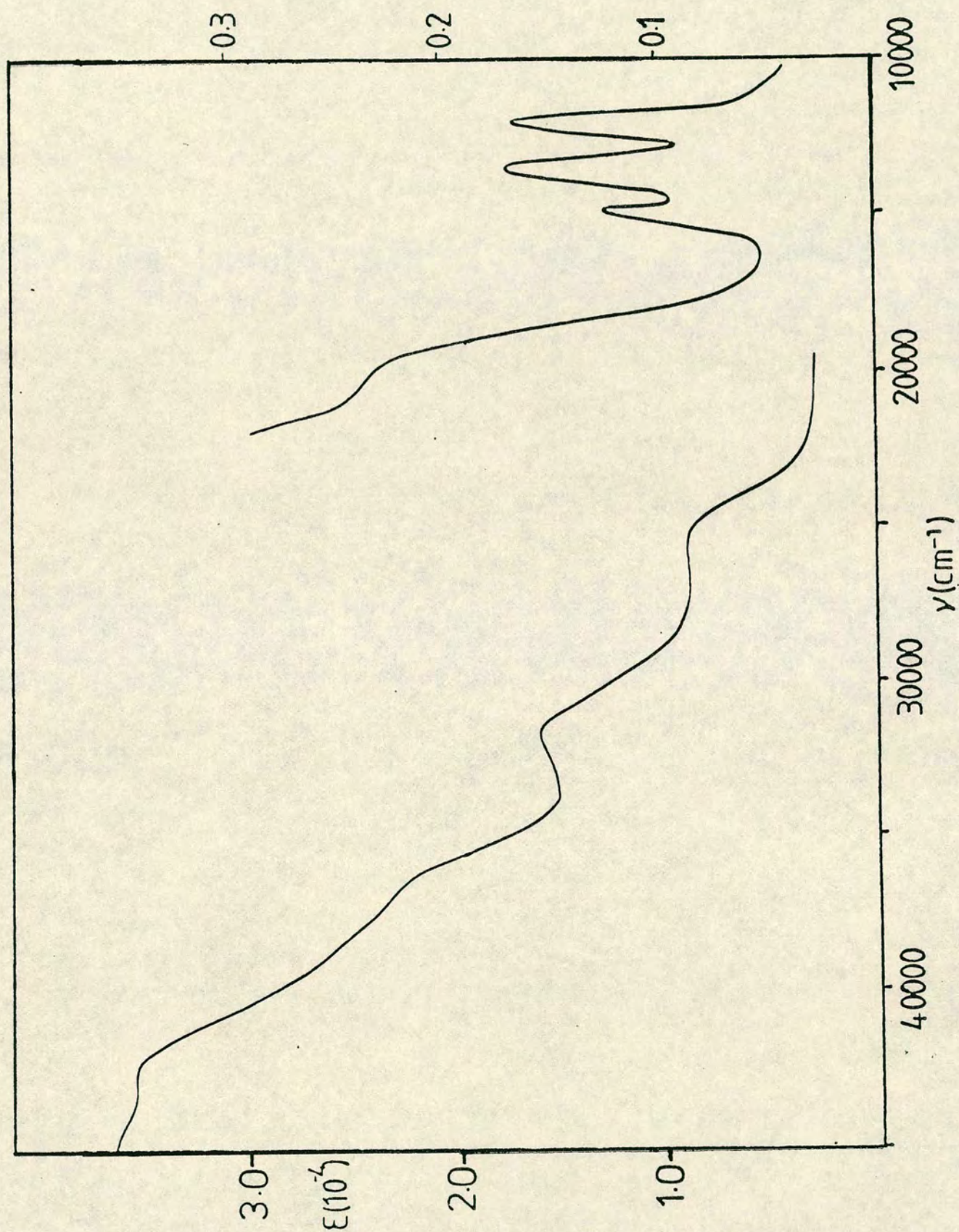


Figure 6: Absorption Spectra of $[\text{Ru}(\text{bipy})_2(\text{biq})]^{2+/3+}$ in Dichloromethane at Room Temperature

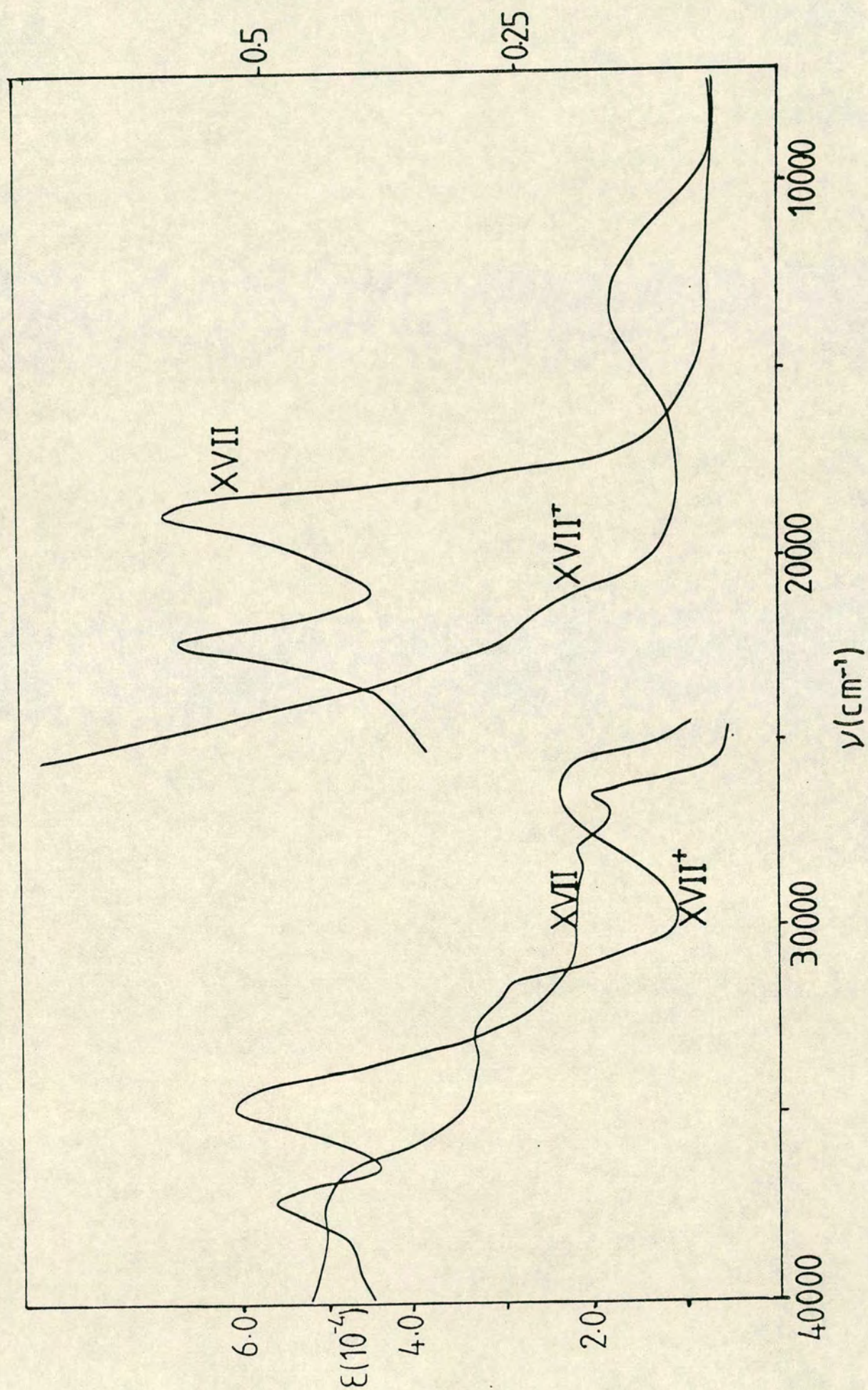


Table 6: Absorption bands in $[\text{Ru}(\text{bipy})_2(\text{biq})]^{2+/3+}$
in Dichloromethane. $\nu / 10^3 \text{cm}^{-1}$ ($\epsilon \times 10^{-4}$)

<u>Complex</u>	<u>$[\text{Ru}(\text{bipy})_2(\text{biq})]^{2+}$</u>	<u>$[\text{Ru}(\text{bipy})_2(\text{biq})]^{3+}$</u>
	19.0(0.61)	13.0(0.16)
	22.8(0.58)	22.0(0.24) ^a
	26.4(2.08)	26.0(2.52)
	27.8(2.35)	31.5(2.97) ^a
	34.6(6.18)	32.7(3.21) ^a
	37.3(5.52)	37.1(5.01) ^a
	39.0(4.58) ^a	

a - Observed as shoulders

In these mixed-ligand complexes we anticipate observing bands in the absorption spectrum of the ruthenium(II) species due to:

- $\pi \rightarrow \pi^*$ transitions in both the neutral bipyridine and biquinoline ligands.
- MLCT transitions from the ruthenium(II) centre to both biquinoline and bipyridine.

It is no surprise therefore that the spectrum of $[\text{Ru}(\text{bipy})_2(\text{biq})]^{2+}$ is considerably more complex than that of $[\text{Ru}(\text{bipy})_3]^{2+}$ and $[\text{Ru}(\text{biq})_3]^{2+}$. By comparison with the absorption spectra of the parent complexes we readily assign the bands in $[\text{Ru}(\text{bipy})_2(\text{biq})]^{2+}$ as shown in table 7.

Our assignment of the bands at 26 400 and 27 800 cm^{-1}

Table 7: Assignment of the Absorption Bands in
 $[\text{Ru}(\text{bipy})_2(\text{biq})]^{2+}$

<u>Band $\nu_{\text{max}}/10^3 \text{cm}^{-1}$</u>	<u>Assignment</u>
19.0	$\text{Ru(II)} d\pi \rightarrow \pi^*(11)\text{biq}^{\text{O}}$
22.8	$\text{Ru(II)} d\pi \rightarrow \pi^*(7)\text{bipy}^{\text{O}}$
26.4	$\text{Ru(II)} d\pi \rightarrow \pi^*(12)\text{biq}^{\text{O}}$
27.8	$\text{Ru(II)} d\pi \rightarrow \pi^*(8)\text{bipy}^{\text{O}}$
29.5	$\pi(10) \rightarrow \pi^*(11)\text{biq}^{\text{O}}$
34.6	$\pi(6) \rightarrow \pi^*(7)\text{bipy}^{\text{O}}$
37.3	$\pi(10) \rightarrow \pi^*(12)\text{biq}^{\text{O}}$

Table 8: Assignment of the Absorption Bands in
 $[\text{Ru}(\text{bipy})_2(\text{biq})]^{3+}$

<u>Band $\nu_{\text{max}}/10^3 \text{cm}^{-1}$</u>	<u>Assignment</u>
13.7	$(\text{L}(\text{biq}^{\text{O}}) \pi(10) \rightarrow \text{Ru(III)} d\pi$ $(\text{L}(\text{bipy}^{\text{O}}) \pi(6) \rightarrow \text{Ru(III)} d\pi$
22.0	$\text{L}(\text{bipy}^{\text{O}}) \pi(5) \rightarrow \text{Ru(III)} d\pi$
26.0	$\pi(10) \rightarrow \pi^*(11)\text{biq}^{\text{O}}$
31.5, 32.7	$\pi(6) \rightarrow \pi^*(7)\text{bipy}^{\text{O}}$
37.2	$\pi(10) \rightarrow \pi^*(12)\text{biq}^{\text{O}}$

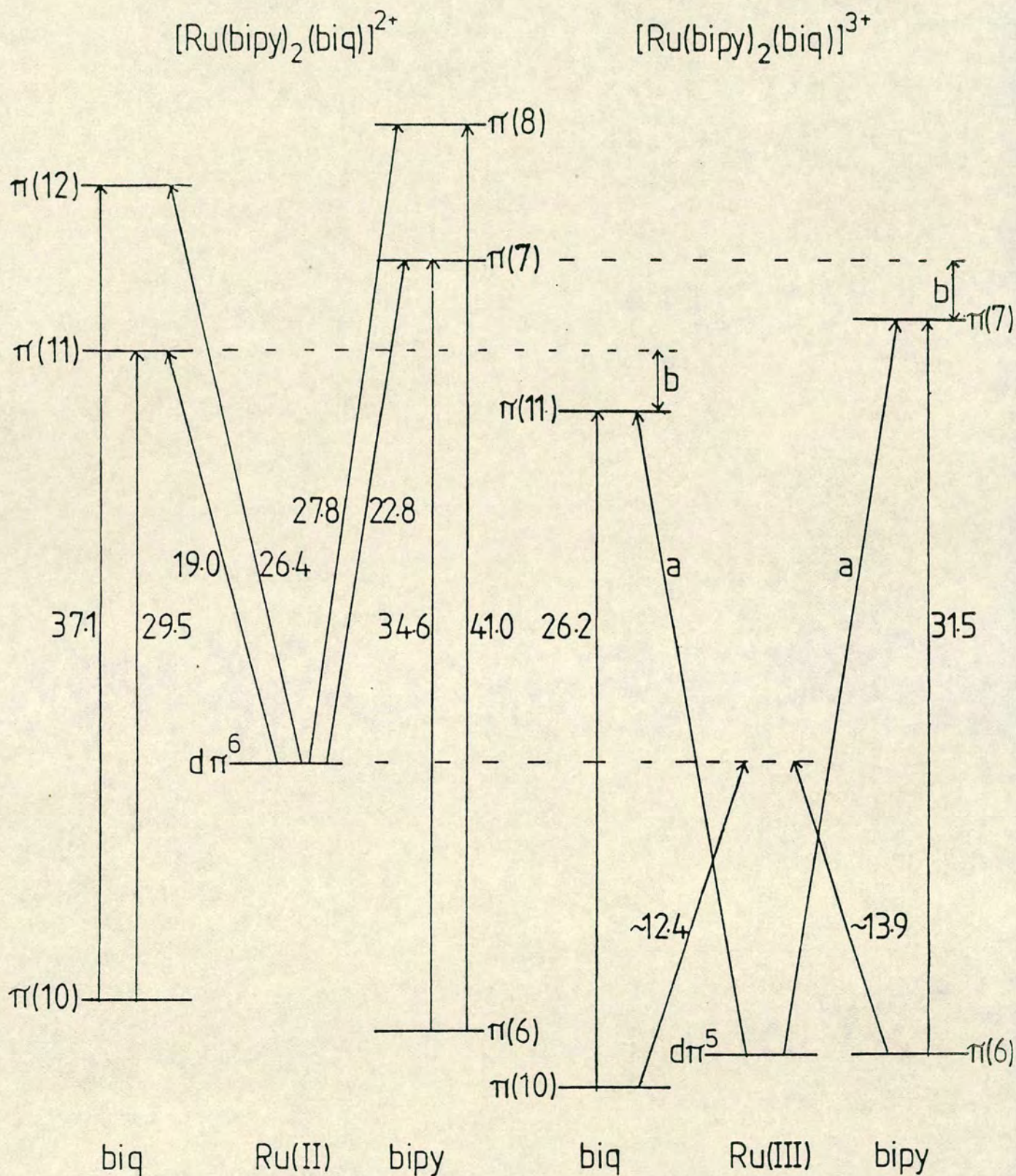
to metal-to-ligand charge-transfers from $\text{Ru(II)}d\pi$ to higher unoccupied ligand levels is in disagreement with Hester and Bugnons,²¹ assignment of this band to a $\pi(10) \rightarrow \pi^*(11)$ intraligand biquinoline transition. Although we are unable to electrochemically predict the energy of these higher energy metal-to-ligand charge-transfers, as shown in figure 7 our assignments are self-consistent since we are able to measure the $\pi(7)$ to $\pi(8)$ gap in coordinated bipyridine and the $\pi(11)$ to $\pi(12)$ gap in coordinated biquinoline from the parent complexes. Therefore we are able to independently predict these transition energies.

The conversion of $[\text{Ru}(\text{bipy})_2(\text{biq})]^{2+}$ to the oxidised species proceeds with isosbestic points, six in number being observed. The absorption spectrum of $[\text{Ru}(\text{bipy})_2(\text{biq})]^{3+}$ may be understood in terms of a Ru(III) metal centre surrounded by three neutral diimine ligands. Our assignment of the bands in the absorption spectrum of this species is shown in table 8,

On oxidation the familiar shift of the bands assigned to $\pi(6) \rightarrow \pi^*(7)\text{bipy}^0$ transitions to lower energy is noted. Similar behaviour is attributed to the biquinoline ligand, with the longest wavelength intraligand band again moving to lower energy.

Our electrochemical studies on the free ligands have shown the $\pi(6)$ level in bipyridine is stabilised by approximately 0.2 volts relative to the $\pi(10)$ level in biquinoline, however in the coordination complex these levels are found to be at similar energies. In the oxidised

Figure 7: Schematic Energy Level Scheme for
 $[\text{Ru}(\text{bipy})_2(\text{biq})]^{2+/3+}$



Note

a) Bands obscured

b) The $\pi(7)\text{bipy}^{\circ}$ and $\pi(11)\text{biq}^{\circ}$ levels are assumed to be stabilised by $2\,600\text{ cm}^{-1}$ on Ru(III) relative to Ru(II).

c) Figures listed are directly measured optical transitions.

complex a broad, weak band is observed in the near infra-red region, with a similar absorption present for $[\text{Ru}(\text{bipy})(\text{biq})_2]^{3+}$ (see later). As shown in figure 7 one component of this band may be assigned to a $\text{L}(\text{bipy})\pi(6) \rightarrow \text{Ru}(\text{III})\text{d}\pi^5$ charge-transfer band but an absorption due to a $\text{L}(\text{biq})\pi(6) \rightarrow \text{Ru}(\text{III})\text{d}\pi^5$ transition should also be observed at a similar, but lower, energy. We therefore suggest the width of this band must be due to overlying ligand-to-metal charge-transfer transitions.

A comparison with the visible absorption spectrum of $[\text{Ru}(\text{bipy})_3]^{3+}$, see chapter 1, allows us to assign the shoulder at $22\,000\text{ cm}^{-1}$ to a $\text{L}(\text{bipy})\pi(5) \rightarrow \text{Ru}(\text{III})\text{d}\pi^5$ transfer.

Examination of the reductive behaviour of $[\text{Ru}(\text{bipy})_2(\text{biq})]^{2+}$ revealed one wave at -1.205V , a much lower potential than the first reduction of $[\text{Ru}(\text{bipy})_3]^{2+}$, and two further waves at more extreme potentials. The energy level scheme shown in figure 7 makes it clear that a one-electron reduction of this complex should selectively populate the $\pi(11)$ biquinoline level and thus selectively modify the spectrum.

We predict that we would remove the strong absorption at $37\,000\text{ cm}^{-1}$ and the poorly resolved absorption at $29\,500\text{ cm}^{-1}$ which are assigned to intraligand biquinoline transitions. The strong charge-transfer band assigned to a $\text{Ru}(\text{II}) \rightarrow \text{biquinoline } \pi(12)$ transition is also noted to be removed on reduction whilst the intraligand $\pi \rightarrow \pi^*$ bipyridyl band is little affected.

It was also hoped that the bands attributed to

biquinoline in the visible region would be removed allowing clarification of the $\text{Ru(II)} \rightarrow \text{bipy}^{\text{O}}$ charge-transfer which remains, however the diffuse biquinoline anion spectrum intrudes.

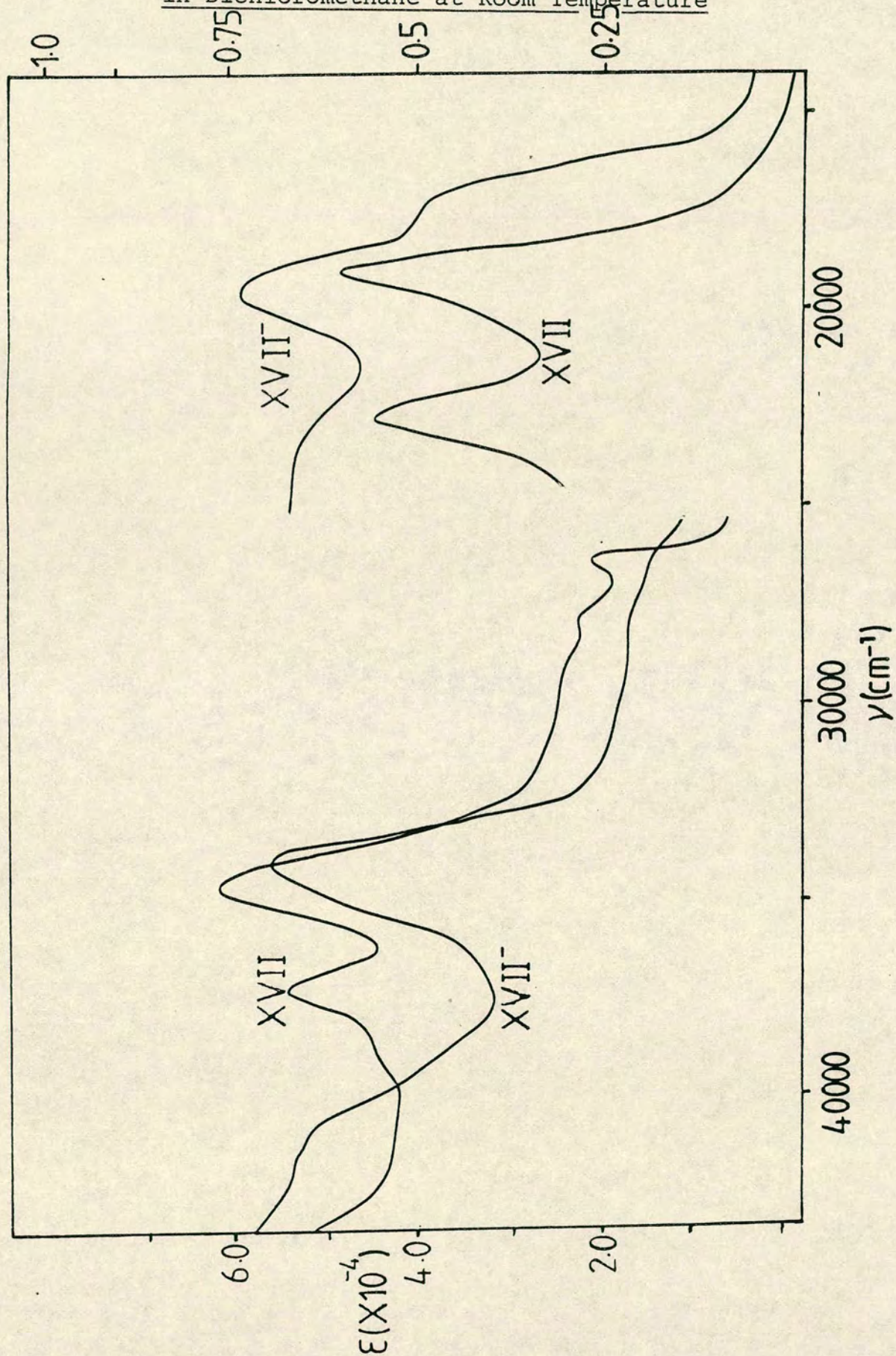
The one-electron reduction product, $[\text{Ru}(\text{bipy})_2(\text{biq})]^+$, may be prepared at a platinum O.T.T.L.E., and its absorption spectrum, shown in figure 8 is in good agreement with the spectrum reported by Hester.²¹ The absorption bands in this species are assigned in table 9 (by comparison with the spectrum of Li^+biq^-).

Table 9: Assignment of the absorption bands in
 $[\text{Ru}(\text{bipy})_2(\text{biq})]^+$

<u>Band $\nu/10^3 \text{cm}^{-1}$ ($\epsilon \times 10^{-4}$)</u>	<u>Assignment</u>
17.5sh(0.51)	
19.8 (0.72)	$\pi \rightarrow \pi^* \text{biq}^-$
23.6sh(0.67)	$\pi \rightarrow \pi^* \text{biq}^- + \text{Ru(II)} \rightarrow \text{bipy}^{\text{O}}$
34.0 (5.69)	$\pi(6) \rightarrow \pi(7) \text{bipy}^{\text{O}}$
41.0 (5.37)	$\pi \rightarrow \pi^* \text{biq}^-$
	$\pi(6) \rightarrow \pi(8) \text{bipy}^{\text{O}}$

That is the absorption spectrum of $[\text{Ru}(\text{bipy})_2(\text{biq})]^+$ may be readily interpreted in terms of the characteristically diffuse spectrum of the biquinoline anion together with the well-known bands due to the $\text{Ru(II)}(\text{bipy}^-)$ chromophore

Figure 8: Absorption Spectra of $[\text{Ru}(\text{bipy})_2(\text{biq})]^{2+}/+$
in Dichloromethane at Room Temperature



superimposed. Therefore the mono-reduced species may be formulated as $[\text{Ru(II)(bipy}^{\text{O}})_2(\text{biq}^{\text{•-}})]^+$. All attempts to generate and stabilise the further reduced species of this system only led to decomposition of the sterically hindered complex.

The complex $[\text{Ru(bipy)(biq)}_2]^{2+}$ also undergoes a reversible one-electron oxidation. This Ru(III) species may be prepared at a platinum O.T.T.L.E. at room temperature; the conversion proceeds with five isosbestic points being observed. The ultra-violet and visible absorption spectra of $[\text{Ru(bipy)(biq)}_2]^{2+/3+}$ are shown in figure 9 with the observed bands assigned in table 10.

As for the bis-bipyridyl complex this species exhibits an ultra-violet spectrum in the rest state and oxidised form which may be readily assigned. Examination of the near infra-red and visible region of the spectrum of $[\text{Ru(bipy)(biq)}_2]^{3+}$, however, does not lead to such a straightforward interpretation. It is possible to assign transitions from the ruthenium(II) centre to the $\pi(8)$ bipyridine and $\pi(11)$ and $\pi(12)$ biquinoline levels but the $\text{Ru(II)} \rightarrow \text{bipy}\pi(7)$ band is obscured in $[\text{Ru(bipy)(biq)}_2]^{2+}$.

On oxidation these $\text{Ru(II)} \rightarrow \text{ligand}$ bands are removed and in the near infra-red/visible region we observe two bands which are attributable to ligand to ruthenium(III) charge-transfers. The broad absorption, centred at $13\,200\text{ cm}^{-1}$, is considerably more intense than the analogous band in $[\text{Ru(bipy)}_2(\text{biq})]^{3+}$. This again suggests this absorption does not only contain a component due to a

Figure 9: Absorption Spectra of $[\text{Ru}(\text{bipy})(\text{biq})_2]^{2+/3+}$
in Dichloromethane at Room Temperature

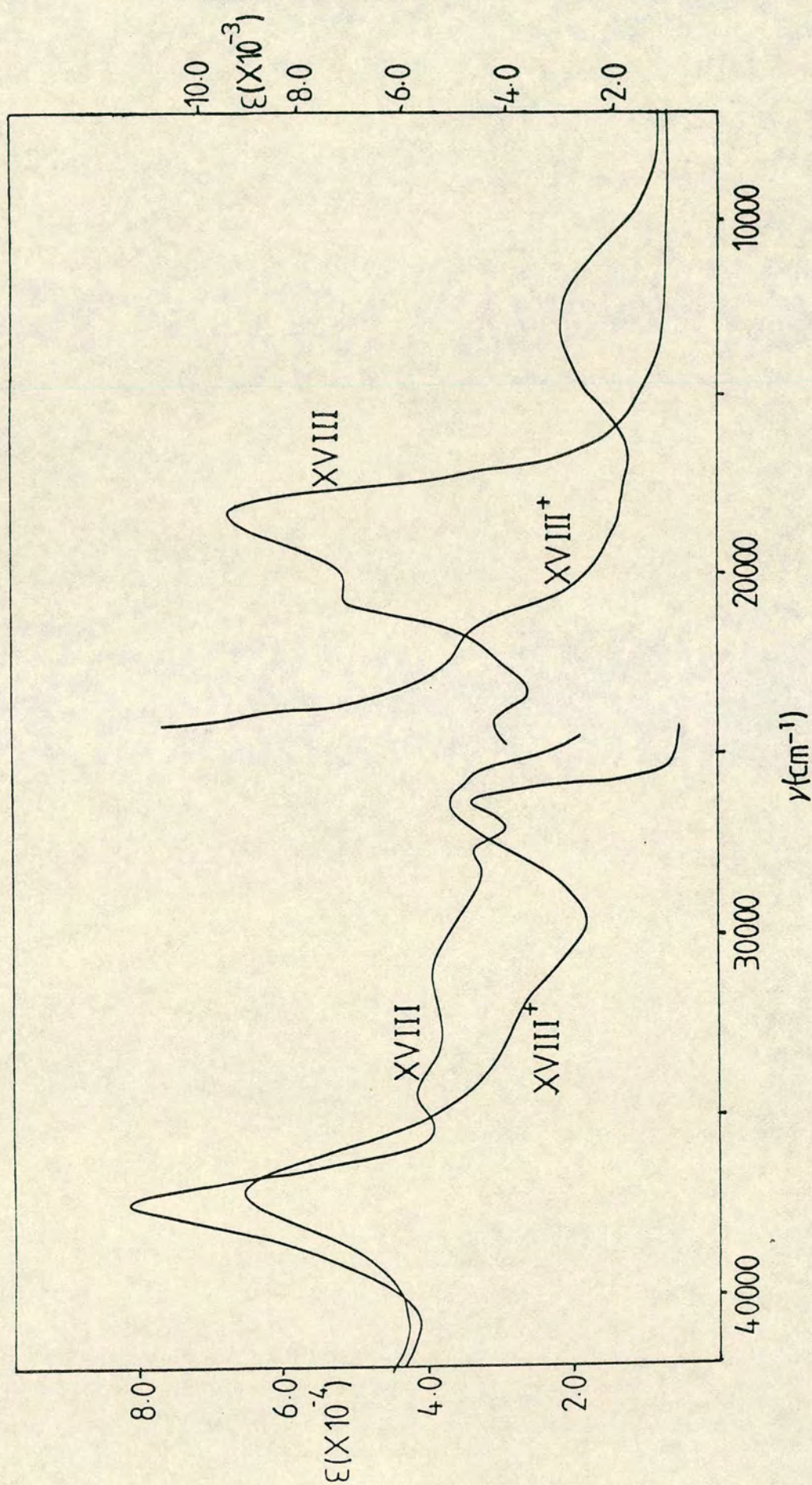


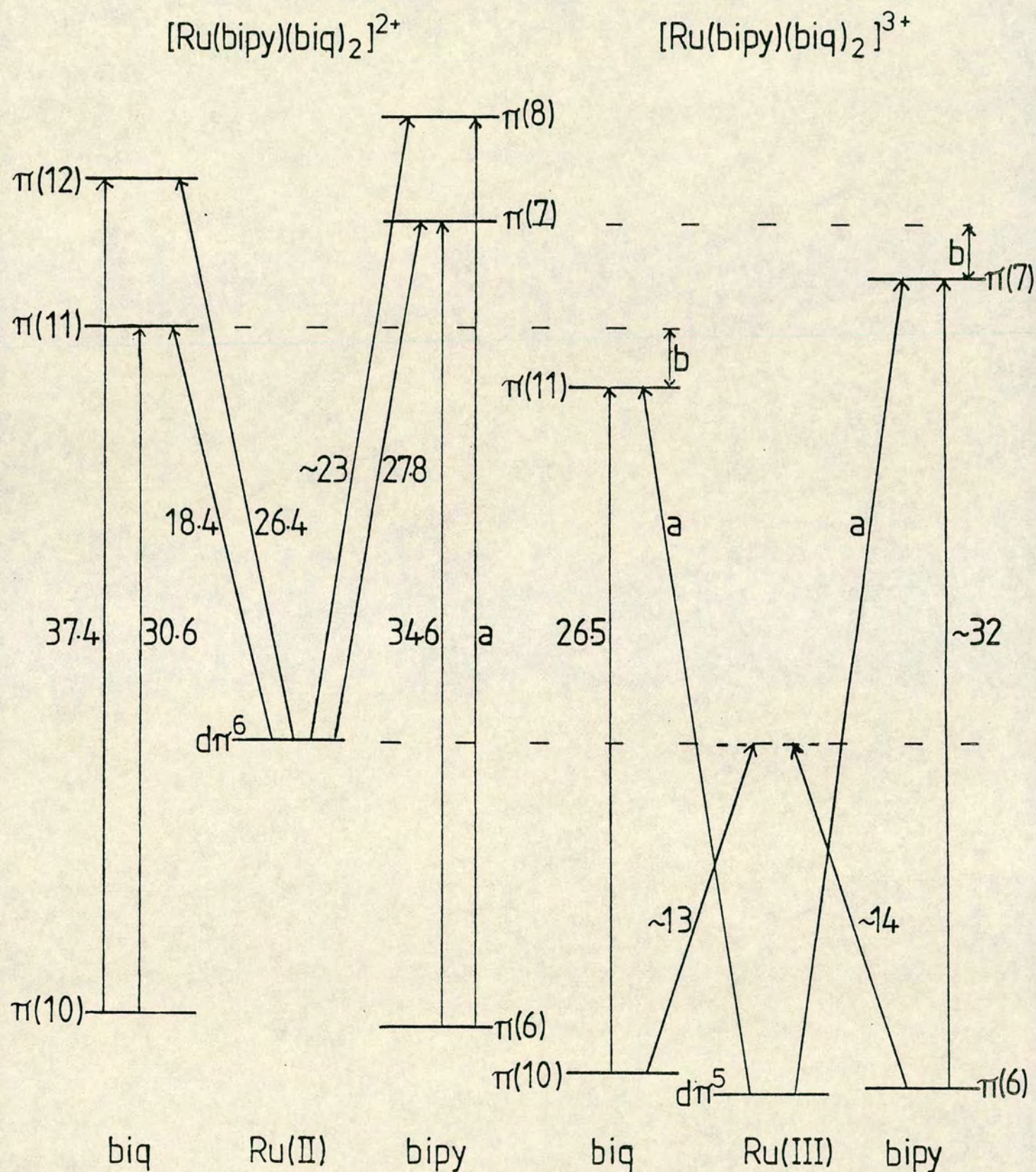
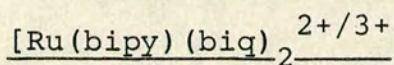
Table 10: Assignment of the absorption bands in $[\text{Ru}(\text{bipy})(\text{biq})_2]^{2+/3+}$ $\nu/10^3 \text{cm}^{-1}$ ($\epsilon \times 10^{-4}$)

Complex	Transition								$\frac{\text{bipy}\pi(6)}{\rightarrow \text{Ru(III)}}$
	$\frac{\pi(10) \rightarrow \pi(12)}{\text{biq}^0}$	$\frac{\pi(6) \rightarrow \pi(7)}{\text{bipy}^0}$	$\frac{\pi(10) \rightarrow \pi(11)}{\text{biq}^0}$	$\frac{\text{Ru(11)} \rightarrow}{\text{bipy}\pi(8)}$	$\frac{\text{Ru(11)} \rightarrow}{\text{biq}\pi(12)}$	$\frac{\text{Ru(11)}}{\text{bipy}\pi(7)}$	$\frac{\text{Ru(11)} \rightarrow}{\text{biq}\pi(11)}$	$\frac{\text{bipy}\pi(5)}{\rightarrow \text{Ru(III)}}$	$\frac{\text{biq}\pi(10)}{\rightarrow \text{Ru(III)}}$
$[\text{Ru}(\text{bipy})(\text{biq})_2]^{2+}$	37.4(8.07)	34.6(4.15)	30.6(3.92)	27.8(3.47)	26.4(3.39)	a	18.4(0.96)	-	-
$[\text{Ru}(\text{bipy})(\text{biq})_2]^{3+}$	37.2(6.54)	a	26.5(3.71)	-	-	-	-	21.8(0.45)	13.2(0.29)

a - Band obscured

b - Assuming the $\pi(5)-\pi(6)$ gap in bipyridine is similar to the $\pi(7)-\pi(8)$ gap.

Figure 10: Schematic Energy Level Scheme for



Note: a) Bands obscured

b) The $\pi(7)$ bipy^0 and $\pi(11)$ biq^0 levels are assumed to be stabilised by $2\,600\text{ cm}^{-1}$ on Ru(III) relative to Ru(II) .

c) Figures listed are directly measured optical transitions.

bipyridyl ligand $\pi(6)$ to Ru(III) charge-transfer but also some transition involving a biquinoline to ruthenium(III) charge-transfer. Our schematic molecular orbital scheme predicts the energy required for the $L(biq)\pi(10) \rightarrow Ru(III)$ transition is slightly lower than for the transition involving bipyridine.

By analogy with the spectrum of $[Ru(bipy)_3]^{3+}$ we assign the shoulder at $21\,800\text{ cm}^{-1}$ to a transfer from the $\pi(5)$ level in bipyridine to the ruthenium(III) centre.

At first glance an examination of a cyclic voltammogram of the reductive behaviour of $[Ru(bipy)(biq)_2]^{2+}$ appears to show two sets of two one-electron reductions, see figure 11 but actually the first three waves should be considered together. We know that the biquinoline ligand is more readily reduced than bipyridine therefore the first two reductions are biquinoline-based. However, the third reduction should be bipyridyl-based by comparison with its reduction potential with that of the $[Ru(bipy)_3]^{0/-}$ couple (see table 2).

In order to further examine this complex, which we recall to have an anomalous visible spectrum, we have generated these reduced species at a platinum O.T.T.L.E.

The ultra-violet and visible absorption spectra of the species $[Ru(bipy)(biq)_2]^{2+/+/0}$ are shown in figure 12. The assignments we propose for the bands observed in this complex are shown in table 11 and are consistent with the sequential reduction of the two separate biquinoline ligands.

The complex nature of the absorption spectra of

Figure 11: Cyclic Voltammogram of $[\text{Ru}(\text{bipy})(\text{biq})_2]^{2+}$
in Dichloromethane at Room Temperature

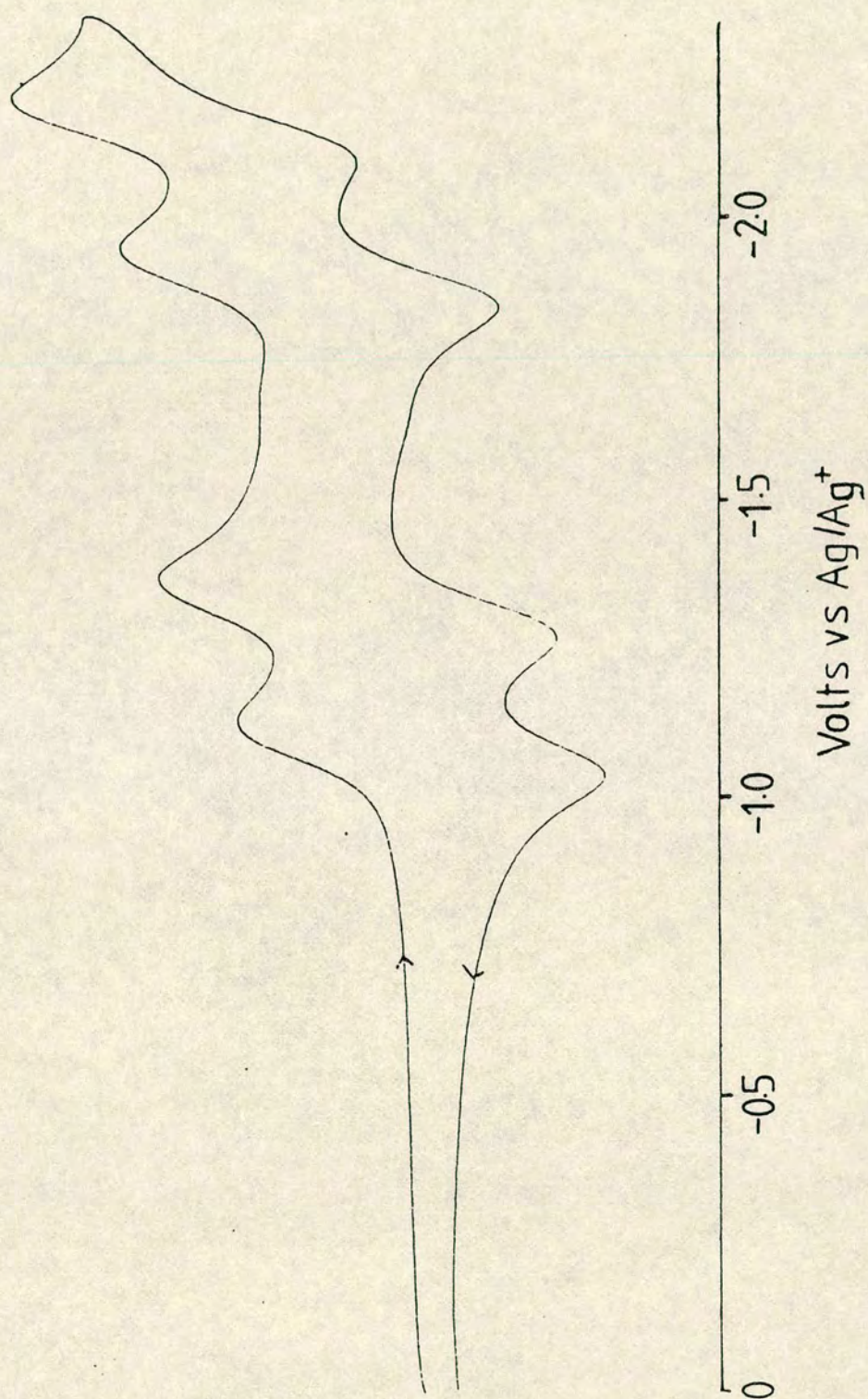


Figure 12: Absorption Spectra of $[\text{Ru}(\text{bipy})(\text{biq})_2]^{2+}/+/o$ in Dichloromethane at -30°C

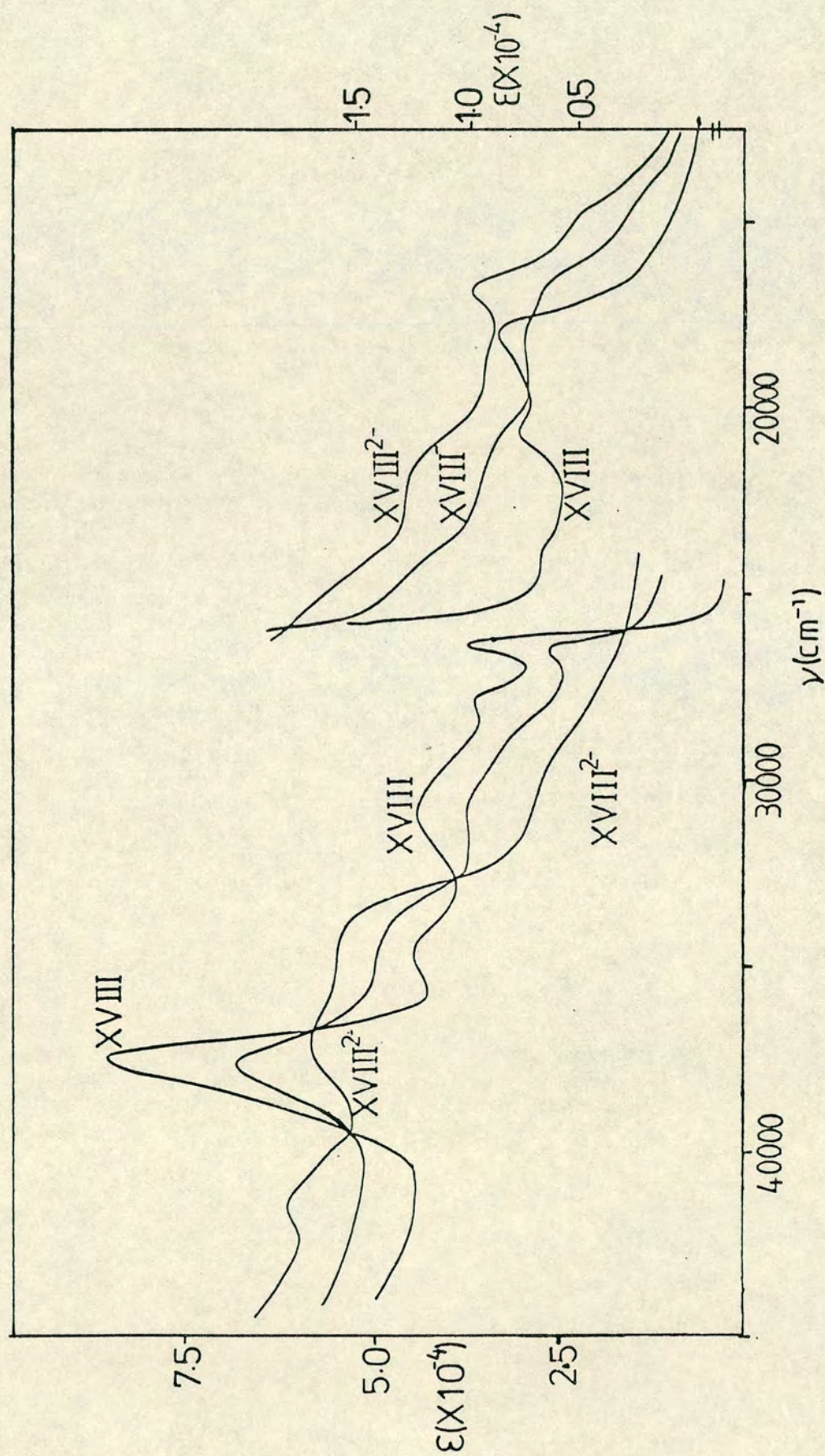


Table 11: Assignment of the Absorption Bands in [Ru(bipy)(biq)₂]^{+ / 0}

Complex	Transition									
	$\frac{\pi \rightarrow \pi^+}{\text{biq}^-}$	$\frac{\pi(6) \rightarrow \pi(8)}{\text{bipy}^0}$	$\frac{\pi(10) \rightarrow \pi(12)\text{biq}^0}{\pi(12)\text{biq}^0}$	$\frac{\pi(6) \rightarrow \pi(7)}{\text{bipy}^0}$	$\frac{\pi(10) \rightarrow \pi(11)\text{biq}^0}{\pi(11)\text{biq}^0}$	$\frac{\text{Ru(II)} \rightarrow \text{bipy}\pi(8)}{\text{bipy}\pi(8)}$	$\frac{\text{Ru(II)} \rightarrow \text{biq}\pi(12)}{\text{biq}\pi(12)}$	$\frac{\text{Ru(II)} \rightarrow \text{bipy}\pi(7)}{\text{bipy}\pi(7)}$	$\frac{\text{Ru(II)} \rightarrow \text{bip}\pi(11)}{\text{bip}\pi(11)}$	$\frac{\pi \rightarrow \pi^*}{\text{biq}^-}$
[Ru(bipy)(biq) ₂] ⁺	a	a	37.6(6.74)		30.4(3.41)	a	26.3(2.21)	b	a	15.0sh 17.0(0.67) 22.5(0.99)
[Ru(bipy)(biq) ₂] ⁰	28.9(2.51) 34.1(5.37) 41.7(5.82)	37.0(5.91)	-	a	-	a	-	b	-	15.2sh 17.0(1.03) 19.4(0.97) 22.5(1.27)
Li ⁺ biq ⁻	25.2(0.96) 31.8(1.74) 41.2(3.48)									12.0(0.18) 13.8(0.19) 16.0(0.12) 19.0(0.23)

Note: a - Band obscured
b - See text

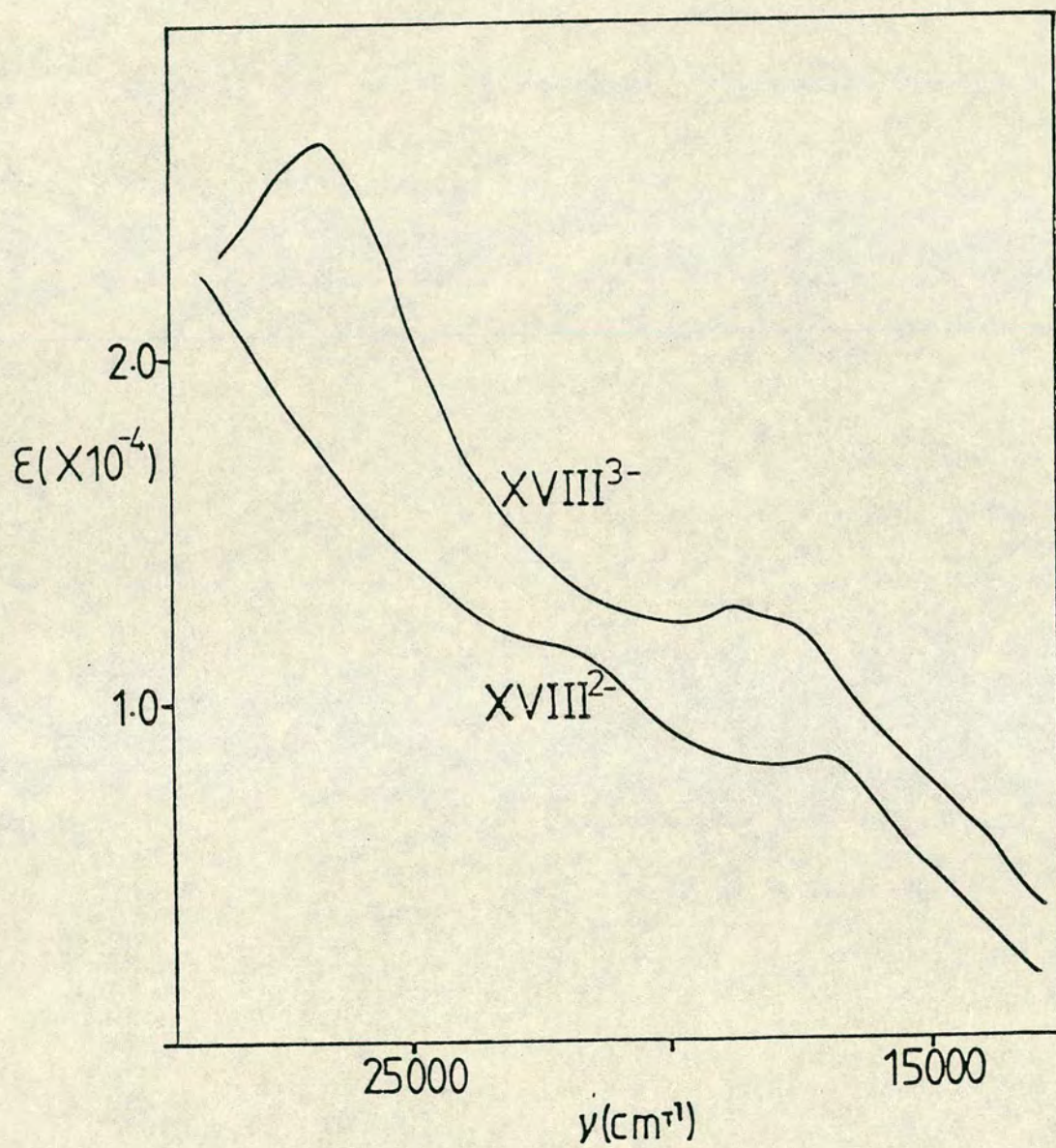
$[\text{Ru}(\text{bipy})(\text{biq})_2]^{+/\circ}$ means this data requires a more detailed description.

In the visible region of the spectrum a stepwise growth of the bands which characterise the $\text{biq}^{\cdot-}$ chromophore is observed. This broad, relatively intense absorption swamps the anticipated loss of the $\text{Ru}(\text{II}) \rightarrow \text{biq}^{\circ}$ charge-transfer band and does not appear to allow the observation of the $\text{Ru}(\text{II}) \rightarrow \text{bipy}^{\circ}$ transition, although the band at $22\,500\text{ cm}^{-1}$, assigned to $\pi \rightarrow \pi^* \text{biq}^{\cdot-}$, may contain some component of $\text{Ru}(\text{II}) \rightarrow \text{bipy}^{\circ}$. In the ultra-violet region however, a stepwise loss of the bands we have assigned to $\pi\pi^*$ biquinoline transitions is noted. It is noted that on the second reduction the bands characteristic of the $\pi(6) \rightarrow \pi^*(7)$ and $\pi(6) \rightarrow \pi^*(8)$ transitions in bipyridine coordinated to a ruthenium (II) centre may be more easily observed as the biq° chromophore disappears.

Several attempts to generate the three-electron reduced species $[\text{Ru}(\text{bipy})(\text{biq})_2]^{-}$ met with failure with the complex undergoing decomposition. However at -30°C in rigorously dry thf and in the presence of excess bipyridine and biquinoline it was possible to reversibly generate $[\text{Ru}(\text{bipy})(\text{biq})_2]^{-}$ at a platinum O.T.T.L.E. This absorption spectrum, shown in figure 13, reveals the growth of bands which we recognise as being characteristic of the $\text{bipy}^{\cdot-}$ chromophore. The presence of excess biquinoline and bipyridine means that almost the entire ultra-violet spectrum of XVIII^{3-} is masked by the $\pi\pi^*$ transition in the free ligands.

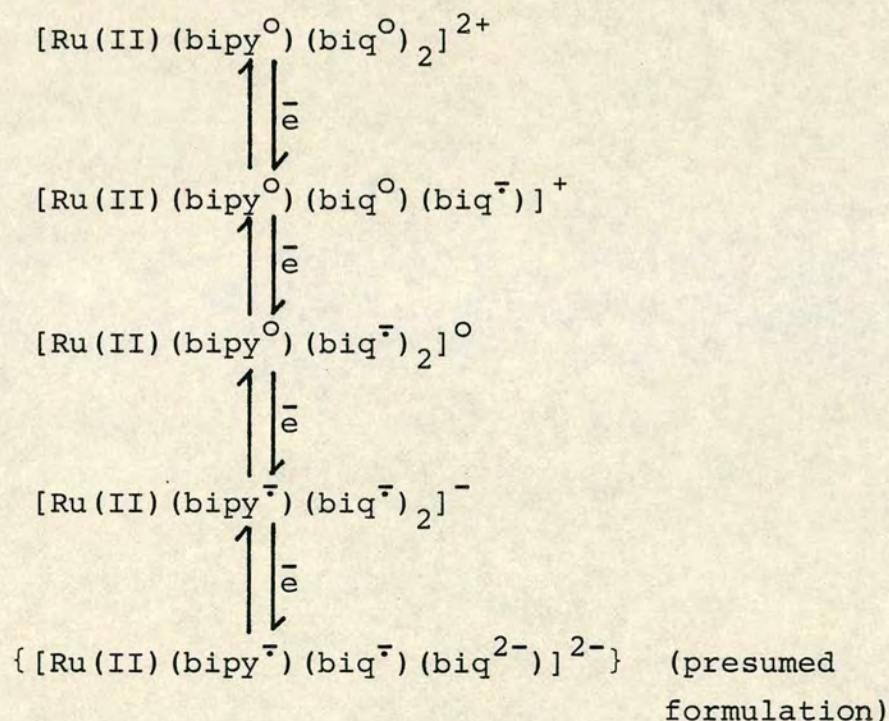
All attempts to generate the four-electron reduced

Figure 13: Absorption Spectra of $[\text{Ru}(\text{bipy})(\text{biq})_2]^{0/-}$
in Tetrahydrofuran at -30°C in the Presence of
Excess Bipyridine and Biquinoline



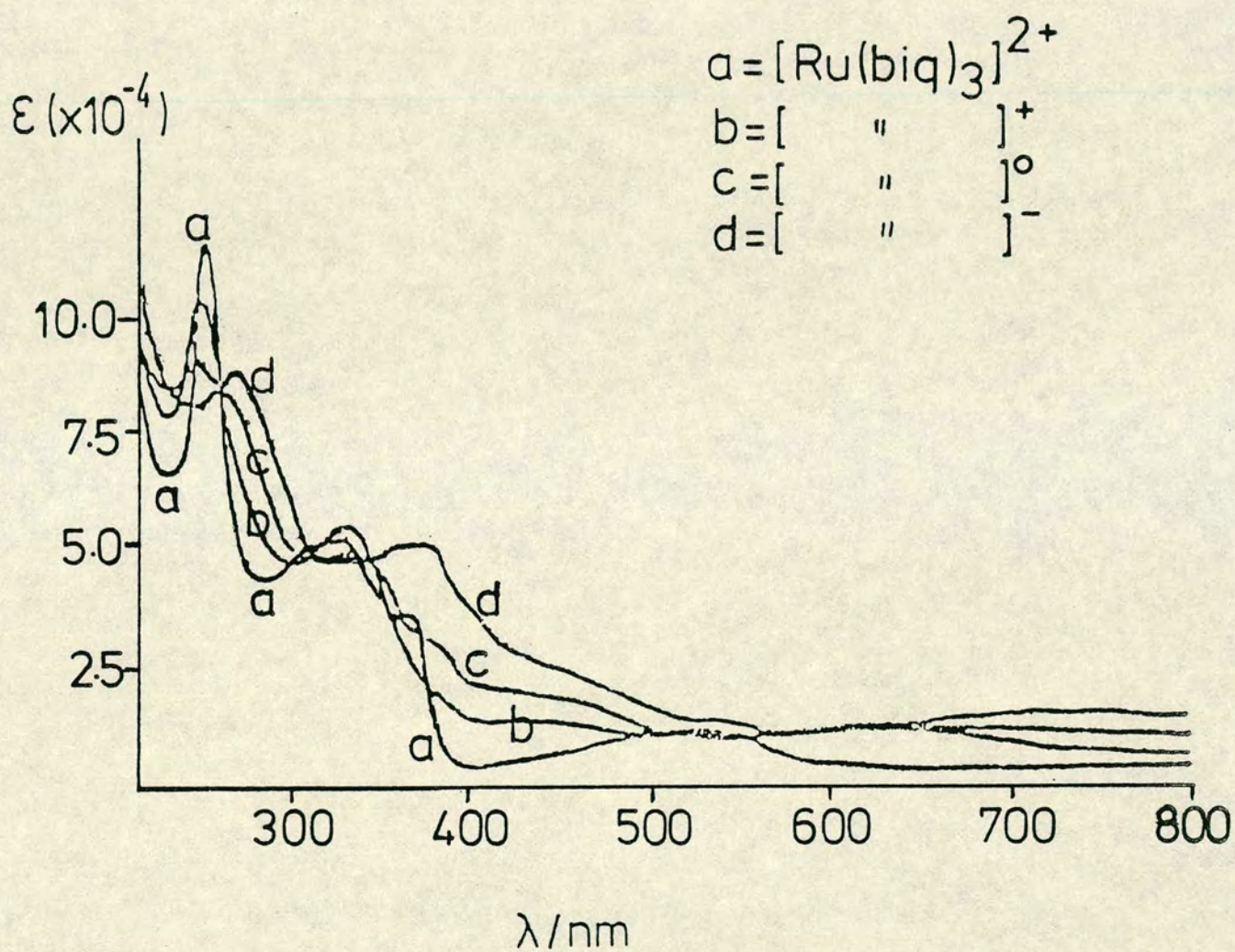
product $[\text{Ru}(\text{bipy})(\text{biq})_2]^{2-}$ at an O.T.T.L.E. failed however it is most reasonable to assign this reduction to the second one-electron reduction of one of the biquinoline ligands.

Our studies on this complex $[\text{Ru}(\text{bipy})(\text{biq})_2]^{2+}$, which appears to show an anomalous series of metal-to-ligand charge-transfer transitions, indicate that the redox behaviour of this species is in fact reconcilable with the localised-ligand model. That is the reduced species can be safely formulated as below:



Hester and Bugnon²¹ have reported a series of absorption spectra for the species $[\text{Ru}(\text{biq})_3]^{2+/+/0/-}$ as shown in figure 14. These spectra are now seen to be in agreement with the stepwise loss of bands characteristic of the biq^{O} chromophore, especially the well resolved $\pi(10) \rightarrow \pi(12)$

Figure 14: Absorption Spectra of $[\text{Ru}(\text{biq})_3]^{2+ / + / 0 / -}$
in Acetonitrile at Room Temperature



Reference 21. P. Bugnon and R.E. Hester;
Chem. Phys. Lett., 102, 537 (1983).

intraligand band at $37\,000\text{ cm}^{-1}$ and the discrete $\text{Ru(II)}d\pi \rightarrow \text{biq}^{\text{O}}\pi(12)$ band at approximately $26\,000\text{ cm}^{-1}$, accompanied by the stepwise growth of bands characteristic of the $\text{biq}^{\cdot-}$ chromophore.

In summary our work shows that although these sterically-strained biquinoline-containing Ru(II) complexes show unusual behaviour in their visible absorption spectra the oxidised and reduced forms may be readily understood in terms of separate Ru-bipyridine and Ru-biquinoline moieties.

The origin of this anomalous charge-transfer behaviour seems to lie in the steric interactions caused by the bulky biquinoline ligands. In $[\text{Ru}(\text{bipy})(\text{biq})_2]^{2+}$, for example, the two biquinoline ligands would appear to interact with the bipyridyl ligand which would then cause some distortion to occur.

On reduction of $[\text{Ru}(\text{bipy})(\text{biq})_2]^{2+}$ some distortion of the ligands is induced and, quite possibly, some extension of Ru-N bond lengths, which may relieve these steric interactions in the rest state complex. However as we have shown the metal-to-ligand charge-transfer transitions are generally masked by more intense intraligand bands in the one- and two-electron reduced systems.

It must be admitted however that all such structural/energetic considerations might have been expected to emerge in the ground-state E^{O} values and absorption spectra. An alternative possibility is that the probability/intensity of the metal-to-ligand charge-transfer transitions, rather than their position, is strongly modified, in a novel fashion, by the physical interference of bipyridine and biquinoline.

This could lead to the $\text{Ru(II)} \rightarrow \text{bipy}^{\text{O}}$ charge-transfer drastically losing intensity with a corresponding increase in the lower energy $\text{Ru(II)} \rightarrow \text{biq}^{\text{O}}$ band.

Experimental

The complexes $[\text{Ru}(\text{bipy})_2(\text{biq})](\text{PF}_6)_2$ and $[\text{Ru}(\text{bipy})(\text{biq})_2](\text{PF}_6)_2$ were prepared by the method of Belser and Zelewsky.²⁰

Purification of acetonitrile and dichloromethane and electrochemical and spectroelectrochemical techniques are as described in chapter 2.

Tetrahydrofuran was purified by distillation from sodium wire/benzophenone.²²

References

1. A. Jurvis, V. Balzani, P. Belser and A. von Zelewsky;
Helvetica Chim.Acta, 64, 2175 (1981).
2. P. Belser, A. von Zelewsky, A. Juris, F. Barigelletti,
A. Tucci and V. Balzani; Chem.Phys.Lett., 89, 101
(1982).
3. A. Juris, F. Barigelletti, V. Balzani, P. Belser and
A. von Zelewsky; Isr.J.Chem., 22, 87 (1982).
4. P. Belser, A. von Zelewsky, A. Juris, F. Barigelletti
and V. Balzani; Gazzetta Chimica Italiana; 113, 731
(1983).
5. F. Barigelletti, A. Juris, V. Balzani, P. Belser and
A. von Zelewsky; Inorg.Chem., 22, 3335 (1983).
6. P. Belser, A. von Zelewsky, A. Juris, F. Barigelletti
and V. Balzani; Chem.Phys.Lett., 104, 100 (1984).
7. D.M. Klassen, Inorg.Chem.; 15, 3166 (1976).
8. M.K. DeArmond; Accounts Chem.Res., 7, 309 (1974).
9. G.A. Crosby; Accounts Chem.Res., 8, 231 (1975).
10. T.J. Kemp; Progr.React.Kinetics, 10, 301 (1980).
11. M.K. DeArmond; Coord.Chem.Rev., 36, 325 (1981).
12. V. Belzani, F. Bolletta, M.T. Gandolfi and M. Maestri;
Topics Current Chem., 75, 1 (1978).
13. N. Sutin and C. Creutz; Pure Appl.Chem., 52, 2717
(1980).
14. G.A. Crosby; Advan.Chem.Serc., 150, 149 (1976).
15. G.A. Crosby, R.J. Watts and D.W.H. Carstens;
Science, 170 1195 (1970).

16. J.N. Demas and G.A. Crosby; J.Am.Chem.Soc., 93, 2841 (1971).
17. J. van Houten and R.J. Watts; J.Am.Chem.Soc., 98, 4853 (1976).
18. M.K. DeArmond, C.M. Carlin and W.L. Huang; Inorg. Chem.; 19, 62 (1980).
19. B.P. Sullivan, B.P. Salmon, T.J. Meyer and J. Peedin; Inorg.Chem.; 18, 3369 (1979).
20. P. Belser and A. von Zelewsky; Helv.Chim.Acta.; 63, 1675 (1980).
21. P. Bugnon and R.E. Hester; Chem.Phys.Lett., 102, 537 (1983).
22. D.J. Wersfold and S. Bywater; J.Chem.Soc., 5234 (1960).

Appendix 1

Near infra-red ($3500-7000\text{ cm}^{-1}$) studies on reduced transition metal bipyridyl complexes

As we have discussed in previous Chapters the reduced bipyridyl systems, and also a series of substituted bipyridyl systems, may all be understood in terms of a localised model. We have also shown that the absorption spectrum of each system may be interpreted in terms of discrete $M(\text{bipy}^0)$ and $M(\text{bipy}^{\bar{1}})$ chromophores. Such an interpretation of these reduced systems implies that any species containing co-existing bipyridine ligands in their resting and reduced oxidation states may effectively be treated as "Mixed-valence complexes" with the possibility of an inter-valence charge-transfer (IVCT) transition existing. Indeed a few mixed-ligand monomeric complexes have previously been described which exhibit an absorption band, in the near infra-red region, attributed to an inter-valence charge-transfer transition.^{1,2}

In 1967 Hush³ defined inter-valence charge-transfer as "An optical transition which involves the transfer of an electron from one nearly localised site to an adjacent one, the donor and acceptor being metal ions which possess more than one accessible oxidation state". Using the "Theory of Radiative and Radiationless Transfer", Hush provided explanations for the characteristic features of these bands and developed a method for the calculation of the degree of

electron delocalisation.

Robin and Day⁴ then used the calculated degree of delocalisation in order to classify the vast range of these mixed-valence complexes into three groups (I, II and III) as follows:

Class I. Such systems are deemed to be strongly localised with the inter-valence charge-transfer band typically observed at high energies, outwith the visible region, having a large band-width and being of low or negligible intensity e.g. GaCl_2 where half of the Ga ions carry a formal +1 charge and the other half carry a formal +3 charge.⁵

Class II. These systems are said to be intermediate in character with some delocalisation noted, whilst valences are still distinguishable. The inter-valence band is normally observed in the visible region, e.g. Prussian blue - the well known crystalline solid which contains both six-coordinate ferricyanide $[\text{Fe(III)-C-N}]$ and six-coordinate ferrocyanide $[\text{Fe(II)-C-N}]$ in a regular cubic array.⁶ Neither of these monomeric species alone gives rise to the intense blue colour of the complex which apparently arises from excitations involving Fe(II) to Fe(III) transitions.

Class III. These systems are completely delocalised. In such complexes, unlike class I or II systems it is not possible to discern the absorption spectra of the constituent ions. The term inter-valence charge-transfer is then no longer appropriate to transitions observed in these systems.

Further theoretical studies on such inter-valence absorptions have been described by Piepho, Schatz, Krausz

and Wong.^{7,8} It is apparent from figure 1 that an electron may be transferred from one centre to the other either by an optical transition (Eop) or indeed by traversing the thermal energy barrier (Eth). It has been shown^{3,7-9} that in strongly localised systems $E_{op}/E_{th} = 4$, however as the electronic coupling between the valence centres increases the Eop/Ea ratio also increases.

In, for example, $[\text{Ru}(\text{bipy})_3]^+$ and $[\text{Ru}(\text{bipy})_3]^0$ bipyridyl ligands thus exist side by side in different oxidation states (and accordingly with different geometries). In principle inter-valence charge-transfer may occur, with an electron hopping from one ligand to another under photo-stimulation as shown in figure 1.

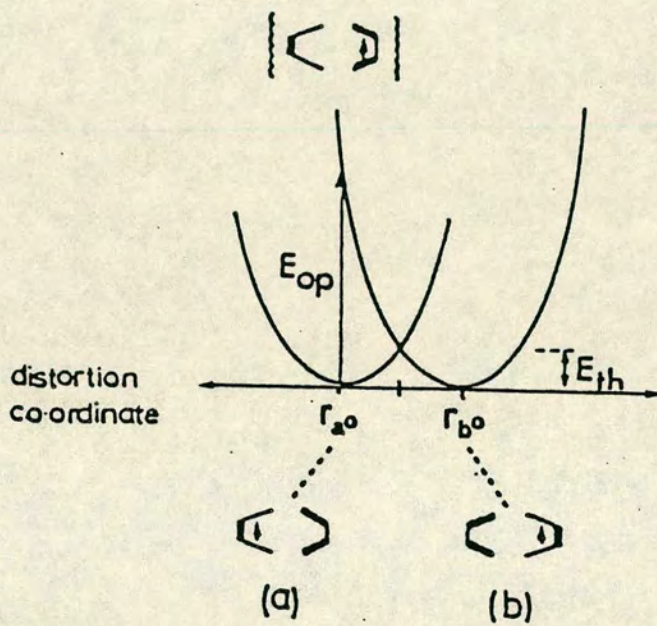
The valence isomers (a) and (b), in figure 1, are wholly equivalent but the instantaneous transfer process (Eop) creates (b) in a strained (vibrationally excited) level, from which it relaxes to its equilibrium geometry. Location of this weak I.V.C.T. band is experimentally very challenging, see figure 2, but probes the energy barrier to electron hopping and the nature of inter-ligand communication.

This behaviour was first observed in these types of systems for $[\text{Ru}(\text{bipy})_3]^{+/0}$, $[\text{Ru}(\text{bipy})_2(\text{py})_2]^+$, $[\text{Ir}(\text{bipy})_3]^{2+/+}$ and $[\text{Ir}(\text{bipy})_2(\text{bipy}')]$ ^{+ 10-13}. In each of these species containing both bipy^0 and bipy^- ligands a weak, diffuse band is observed at approximately $4\text{--}6\ 000\ \text{cm}^{-1}$ superimposed upon the background solvent/electrolyte absorptions (see table 1).

As shown in figure 1 a thermally stimulated charge-

Figure 1: Energy - Distortion Co-ordinate Diagram
Applicable for Valence Interchange in
Symmetric Complexes

Valence Interchange



E_{th} is the thermal
 energy barrier at
 the saddle-point

With negligible
 delocalization,
 E_{th} approaches $\frac{1}{4}E_{op}$

Table 1: Near infra-red absorption bands observed
in reduced transition metal bipyridyl
complexes

<u>Complex</u>	<u>Band maximum/cm⁻¹ (ε)</u>
$[\text{Ru}(\text{bipy})_3]^+ \text{ }^{10,11}$	4 500 (210)
$[\text{Ru}(\text{bipy})_3]^0 \text{ }^{10,11}$	4 500 (345)
$\text{cis-}[\text{Ru}(\text{bipy})_2(\text{py})_2]^+ \text{ }^{10,11}$	4 350 (121)
$\text{trans-}[\text{Ru}(\text{bipy})_2(\text{py})_2]^+ \text{ }^{10,11}$	4 090 (100)
$[\text{Ir}(\text{bipy})_3]^{2+} \text{ }^a$	6 000 (300)
$[\text{Ir}(\text{bipy})_3]^+ \text{ }^a$	6 000 (510)
$^b[\text{Ir}(\text{bipy})_2(\text{bipy}')]^+ \text{ }^{13}$	5 000 (216)

Notes

a - Present work

b - See chapter 4

transfer (Eth) may also occur. Indeed Motten, Hanck and DeArmond¹⁴ have attributed the temperature dependent line broadening observed in the e.s.r. spectrum of $[\text{Ru}(\text{bipy})_3]^+$, but not in the spectrum of $[\text{Ru}(\text{bipy})_3]^-$, to such a ligand-to-ligand transition and have estimated the thermal barrier (Eth) for $[\text{Ru}(\text{bipy})_3]^+$ to be approximately $1\,000\text{ cm}^{-1}$ in acetonitrile. This is in excellent agreement with the optical data with Eop/Eth ratio being slightly greater than the theoretical lower limit of 4 which implies some degree of excitation coupling is involved in this system which is in fact a requirement for the processes described above to occur.

A later study on the temperature dependent e.s.r. spectrum of $[\text{Ru}(\text{bipy})_3]^0$ has shown the thermal barrier in this case to be approximately 450 cm^{-1} ¹⁵. The optical I.V.C.T. band for $[\text{Ru}(\text{bipy})_3]^0$ is observed at $4\,500\text{ cm}^{-1}$. Hanck and coworkers have suggested that an increase in the exciton coupling is occurring in this system relative to $[\text{Ru}(\text{bipy})_3]^+$. Wong and co-workers⁸ have shown that the thermal barrier is dependent upon the extent of electronic coupling in the system under study whilst the optical energy required is independent of this term.

In the present study we have utilised spectrophotometers with the capability of detailed background subtraction in order to further study these bands. We have also chosen to study $[\text{Ir}(\text{bipy})_3]^{3+}$ and its reduced analogues in order to overcome solubility problems encountered whilst examining other complexes. Since these I.V.C.T. bands are very weak

Figure 2: Near infra-red spectrum of $[\text{Ir}(\text{bipy})_3]^{3+/2+}$
in 0.1M TBABF₄/CH₃CN

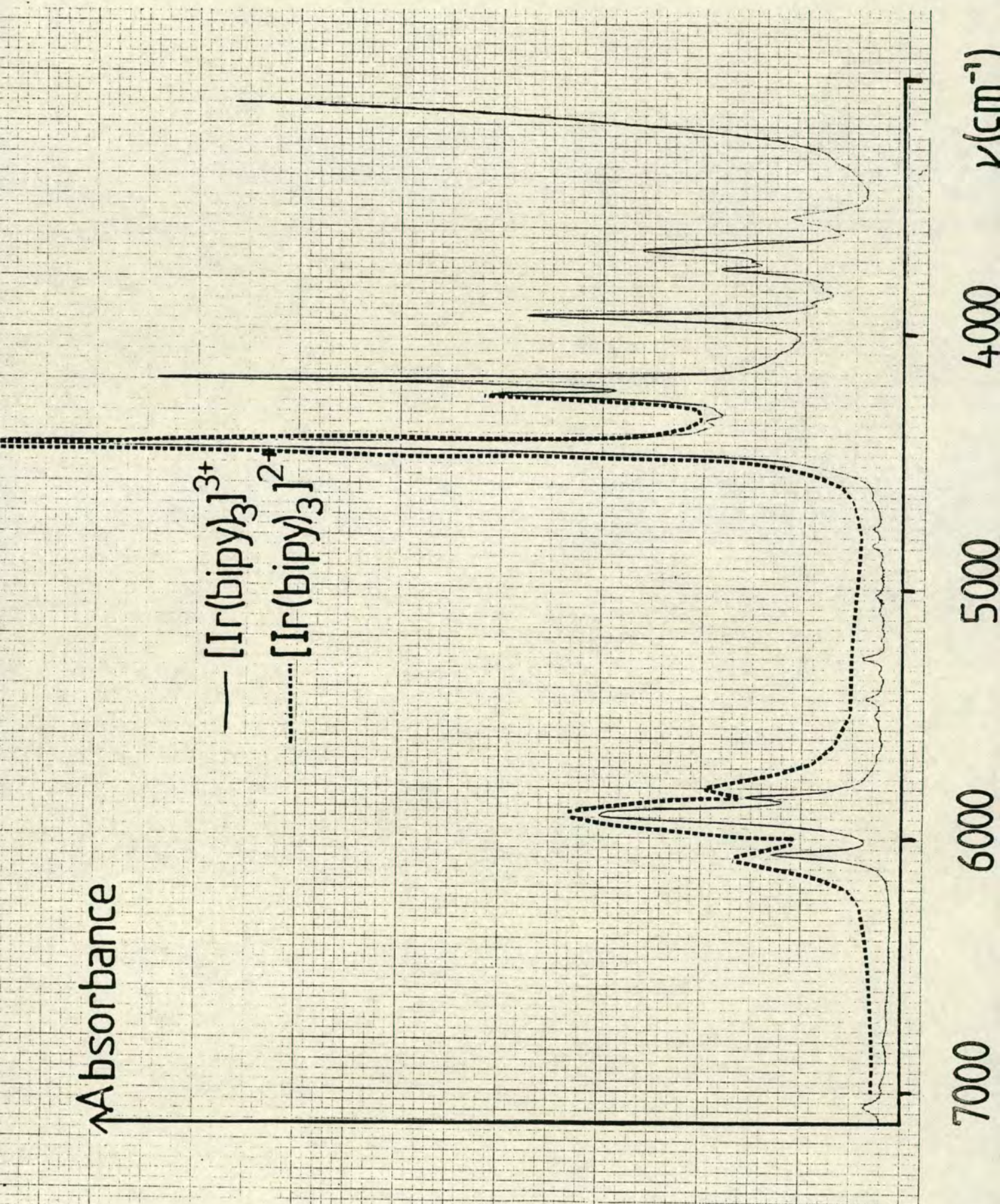
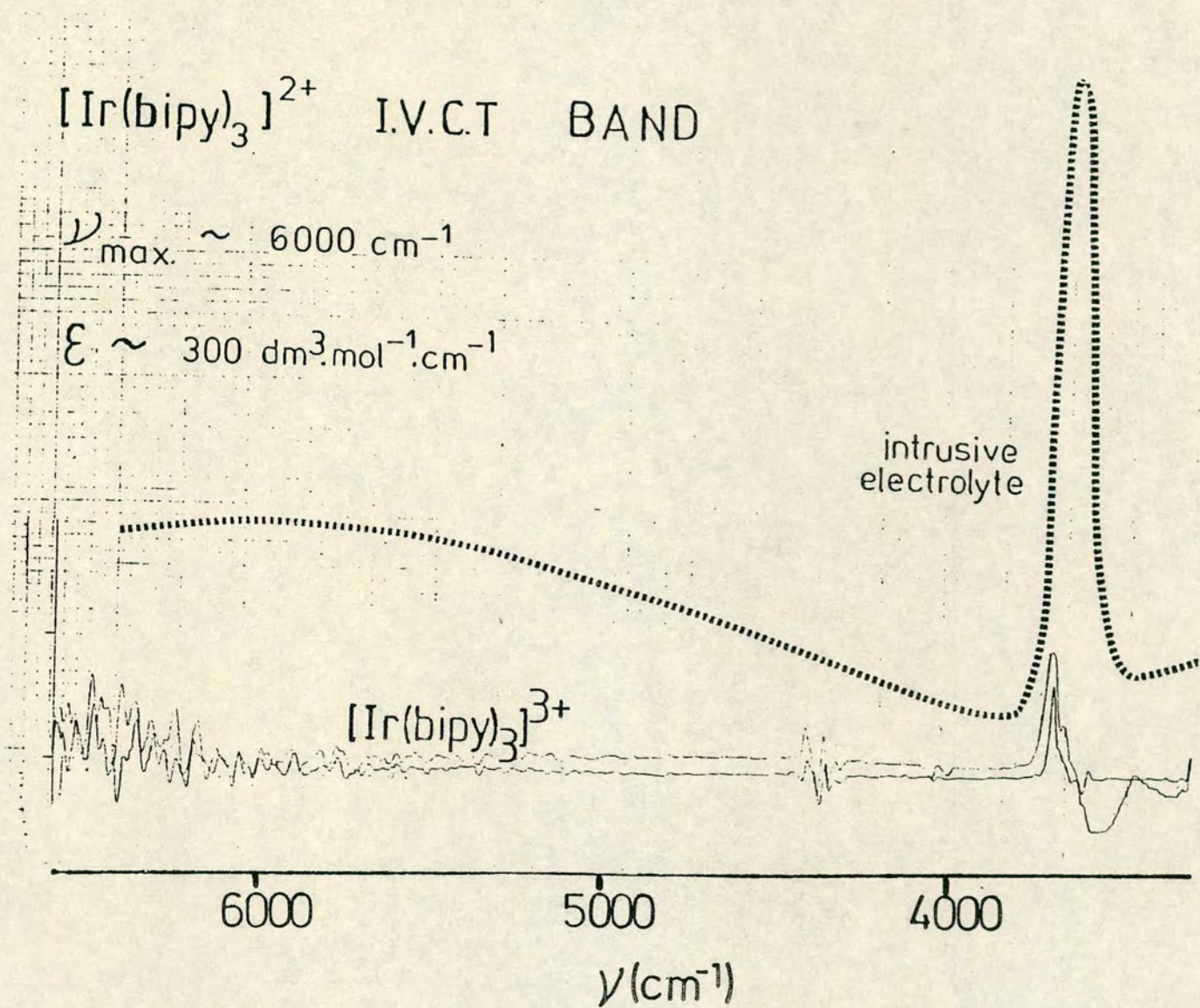


Figure 3: Near infra-red spectrum of $[\text{Ir}(\text{bipy})_3]^{3+/2+}$
with electrolyte/solvent contributions
subtracted



it is necessary to utilise solutions which are approximately one hundred times more concentrated than those normally required when studying the ultra-violet and visible regions. In our electrolyte/solvent media we have observed that $[\text{Ru}(\text{bipy})_3]^0$ is not sufficiently soluble to allow us to study its near infra-red spectrum in any great detail. However the reduced analogues of $[\text{Ir}(\text{bipy})_3]^{3+}$ which are anticipated to be "inter-valence active" are both charged and sufficiently soluble for further study.

The reduced species $[\text{Ir}(\text{bipy})_3]^{2+}$ was generated at a platinum O.T.T.L.E. with the near infra-red spectrum of this species shown in figure 3.

It is apparent that these weak inter-valence charge-transfer bands, when observed free from background solvent/electrolyte absorptions, are worthy of further study in order to examine their energy, intensity, temperature - and solvent-dependence against theoretical models.^{7-9,16}

Recently Hanck and coworkers¹⁷ have presented near infra-red data for a series of reduced tris(polypyridyl)-ruthenium(II) complexes ($[\text{Ru}(\text{pq})_3]^{+/0}$ and $[\text{Ru}(\text{biq})_3]^{+/0}$ where pq = 2-pyridylquinoline) and report the observation of an inter-valence charge-transfer band in these species.

Experimental.

Complex preparation, solvent purifications and spectroelectrochemical techniques used were as previously described in Chapters 2 and 3.

References

1. A. Vogler and H. Kunkely; J.Am.Chem.Soc., 103, 1559 (1981).
2. A. Vogler and H. Kunkely; Angew.Chem.Int.Ed.Engl., 21, 77 (1982).
3. G.C. Allen and N.S. Hush; Prog.Inorg.Chem., 8, 357
4. P. Day and M.B. Robin; Advan.Inorg.Chem.Radiochem., 10, 267 (1967).
5. D.B. Brown; 'Mixed Valence Compounds', Reidel, Dordrecht (1980).
6. A. Ludi and H.U. Gudel; Struct.Bonding, (Berlin), 14, 1 (1973).
7. S.B. Piepho, E.R. Krausz and P.N. Schatz; J.Am.Chem.Soc., 100, 2996 (1978).
8. K.Y. Wong, P.N. Schatz and S.B. Piepho; J.Am.Chem.Soc., 101, 2793 (1979).
9. N.S. Hush; Chem.Phys., 10, 361 (1975) and references therein.
10. L.J. Yellowlees; Ph.D. Thesis, University of Edinburgh (1982).
11. G.A. Heath, L.J. Yellowlees and P.S. Braterman; Chem.Phys.Lett., 92, 646 (1982).
12. V.T. Coombe, G.A. Heath, A.J. Mackenzie and L.J. Yellowlees; Inorg.Chem., 23, 3423 (1984).
13. P.S. Braterman, G.A. Heath, A.J. Mackenzie, B.C. Noble, R.D. Peacock and L.J. Yellowlees; Inorg.Chem., 23, 3425 (1984).

14. A.G. Motten, K.W. Hanck and M.K. DeArmond; Chem. Phys.Lett., 79, 541 (1981).
15. D.E. Morris, K.W. Hanck and M.K. DeArmond; J.Am. Chem.Soc., 105, 3032 (1983).
16. J.P. Launay and F. Babonneau; Chem.Phys., 67, 295 (1982).
17. C.D. Tait, D.B. MacQueen, R.J. Donohoe, M.K. DeArmond, K.W. Hanck and D.W. Wertz; J.Phys.Chem., 90, 1766 (1986).

Appendix 2List of Abbreviations Used

bipy	-	2,2'-bipyridine
biq	-	2,2'-biquinoline
phpy	-	2-phenylpyridine
py	-	pyridine
e.s.r.	-	electron spin resonance
n.m.r.	-	nuclear magnetic resonance
TBABF ₄	-	tetrabutylammonium tetrafluoroborate
CH ₃ CN	-	acetonitrile
CH ₂ Cl ₂	-	dichloromethane
thf	-	tetrahydrofuran
ϵ	-	extinction coefficient ($\text{l mol}^{-1}\text{cm}^{-1}$)
ν	-	wavenumber
p.p.m.	-	parts per million
I	-	$[\text{Ru}(\text{bipy})_3]^{2+}$
II	-	$[\text{Ir}(\text{bipy})_3]^{3+}$
III	-	$\text{cis-}[\text{Ru}(\text{bipy})_2\text{CO.Cl}]^+$
IV	-	$\text{cis-}[\text{Ru}(\text{bipy})_2\text{Cl}_2]$
V	-	$\text{cis-}[\text{Ru}(\text{bipy})_2\text{CO.MeCN}]^{2+}$
VI	-	$\text{cis-}[\text{Ru}(\text{bipy})_2(\text{MeCN})_2]^{2+}$
VII	-	$\text{cis-}[\text{Ru}(\text{bipy})_2\text{CO.py}]^{2+}$
VIII	-	$\text{cis-}[\text{Ru}(\text{bipy})_2\text{py.MeCN}]^{2+}$
IX	-	$\text{cis-}[\text{Ru}(\text{bipy})_2(\text{CO})_2]^{2+}$
X	-	$\text{cis-}[\text{Ru}(\text{bipy})_2\text{CO.H}]^+$
XI	-	$\text{cis-}[\text{Ir}(\text{bipy})_2\text{Cl}_2]^+$

XII	-	$\text{cis-}[\text{Ir}(\text{bipy})_2(\text{CF}_3\text{SO}_3)_2]^+$
XIII	-	$[\text{Cr}(\text{bipy})_3]^{3+}$
XIV	-	$[\text{Ir}(\text{bipy})_2\text{OH} \cdot (\text{bipy}')]^{2+}$
XV	-	$[\text{Ru}(\text{bipy})_2(\text{phpy})]^+$
XVI	-	$[\text{Ru}(\text{biq})_3]^{2+}$
XVII	-	$[\text{Ru}(\text{bipy})_2(\text{biq})]^{2+}$
XVIII	-	$[\text{Ru}(\text{bipy})(\text{biq})_2]^{2+}$
XIX	-	$\text{cis-}[\text{Ru}(\text{bipy})_2(\text{py})_2]^{2+}$
XX	-	$[\text{Ru}(\text{bipy})(\text{py})_4]^{2+}$

List of Courses Attended

Aspects of Structural Chemistry - Dr. C. Glidewell
(University of St.Andrews).

Current Research at Edinburgh - Professor Ebsworth,
Drs. Heath, Schroder and Welch.

Chemical Technology and Industrial Chemistry - Drs. A.J.
Nichol, L.H. Mustoe and R.S. Sinclair (Paisley
College of Technology).

Molecular Electronics - Professors R.W. Mann and
J.O. Williams (U.M.I.S.T.).

Microcomputers - Dr. A. Rowley and Mr. A. King,
(University of Edinburgh).

Activation of Small Molecules - Dr. M. Schroder
(University of Edinburgh).

Recent Developments in Electrochemistry - Drs. H.H.
Girault and G.A. Heath.

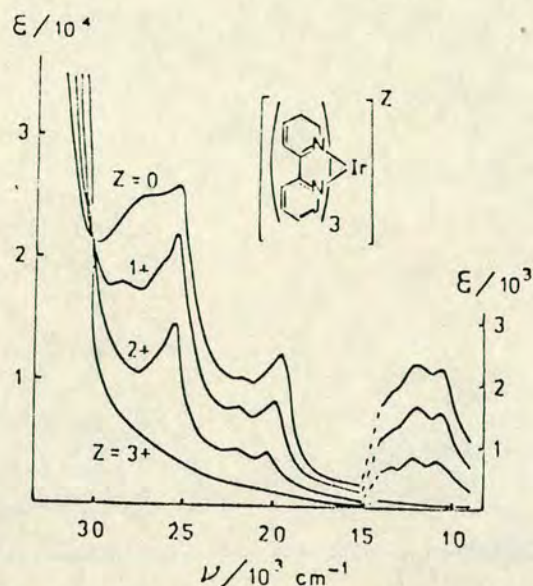
Homogeneous Catalysis - Dr. T.A. Stephenson.

2nd International Conference on the Chemistry of the
Platinum Group Metals - (University of Edinburgh).

30th I.U.P.A.C. Conference (1985) - (University of
Manchester).

University of Strathclyde Inorganic Club Conferences
1984, 1985, 1986.

Departmental and Research Seminars and Colloquia.

Figure 1. Absorption spectra for $[\text{Ir}(\text{bpy})_3]^{3+/2+/+/0}$.

Contribution from the Department of Chemistry,
University of Edinburgh, Edinburgh EH9 3JJ, U.K.

**Spectroelectrochemical Studies on Tris(bipyridyl)iridium
Complexes: Ultraviolet, Visible, and Near-Infrared
Spectra of the Series $[\text{Ir}(\text{bpy})_3]^{3+/2+/+/0}$**

Vyryan T. Coombe, Graham A. Heath,* Alan J. MacKenzie,
and Lesley J. Yellowlees*

Received July 15, 1983

Recently¹ we described the progression in absorption spectra for tris(bipyridyl)ruthenium(II), $[\text{Ru}(\text{bpy})_3]^{2+}$ (I^{2+}) and its reduced analogues, $[\text{Ru}(\text{bpy})_3]^+$ (I^+), $[\text{Ru}(\text{bpy})_3]^0$ (I^0), and $[\text{Ru}(\text{bpy})_3]^-$ (I^-). In each case we were able to assign all the observed bands in terms of characteristic electronic transitions involving noninteracting bpy^0 and bpy^- ligands (for I^+ and I^0) or discrete bpy^- ligands alone (I^-). We thus concluded that the complexes should be formulated with localized charge distributions, namely $[\text{Ru}^{\text{II}}(\text{bpy}^0)_3]^{2+}$, $[\text{Ru}^{\text{II}}(\text{bpy}^0)_2(\text{bpy}^-)]^+$, $[\text{Ru}^{\text{II}}(\text{bpy}^0)(\text{bpy}^-)_2]^0$, and $[\text{Ru}^{\text{II}}(\text{bpy}^-)_3]^-$. Parallel spectroelectrochemical studies on substituted Ru^{II} -bipyridyl complexes have recently appeared.²

Tris(bipyridyl)iridium(III) $[\text{Ir}(\text{bpy})_3]^{3+}$ (II^{3+}), in common with I^{2+} , is a low-spin d^6 complex. However, the tervalent complex II^{3+} has relatively facile ligand reductions, and, remarkably, six successive one-electron steps are observed. The pattern of electrode potentials for II^{3+} was noted by DeArmond et al.³ to suggest a localized-charge model for the reduced complexes II^{2+} , II^+ , etc. We now report confirmation of this interpretation using the spectroelectrochemical methods found to be definitive for I^{2+} .

There are marked differences in the electronic spectra of isoelectronic $[\text{Ru}(\text{bpy})_3]^{2+}$ (I^{2+}) and $[\text{Ir}(\text{bpy})_3]^{3+}$ (II^{3+}). Whereas for I^{2+} the visible spectral region is dominated by a metal-to-ligand charge-transfer (MLCT) transition, the first

prominent absorption band of II^{3+} is an intraligand $\pi\pi^*$ transition at $32\,200\text{ cm}^{-1}$,⁴ the visible and near-infrared regions of the absorption spectrum being entirely featureless. The spectra of the intermediate complexes, I^+ and I^0 , are complicated in the visible region due to superposition of the $\text{Ru}^{\text{II}}-\text{bpy}^0$ MLCT transition and characteristic bpy^- intraligand transitions. Thus we anticipated that $[\text{Ir}(\text{bpy})_3]^{3+}$ and its reduced analogues would prove helpful in clarifying the visible spectral region, as the bpy^- intraligand transitions should emerge from a featureless background.

Results and Discussion

The reduced complexes $[\text{Ir}(\text{bpy})_3]^{2+/+/0}$ were generated in turn in an optically transparent thin-layer electrode (OTTLE) cell, at -1.30 , -1.45 , and -1.60 V , respectively, vs. an aqueous Ag/Ag^+ reference electrode, and their spectra were measured in situ from 3500 to $33\,000\text{ cm}^{-1}$. In each case, after observation of the corresponding steady-state spectrum, the potential was set at -0.6 V and the spectrum was noted to return exactly to that of II^{3+} in its original concentration, thus establishing that no decomposition had occurred. In these circumstances, with strict exclusion of air, the entire series of iridium complexes proved neither solvent nor temperature sensitive, with invariant spectra in purified acetonitrile (at 30 and -40°C), N,N -dimethylformamide, and dimethyl sulfoxide. Although $[\text{Ir}(\text{bpy})_3]^-$ (II^-) is stable on a voltammetric time scale, it apparently decomposed on electroanalysis. After generation of II^- and attempted regeneration of II^{3+} at either 15 or -40°C , the original spectrum was not recovered, and further characterization of II^- (or II^{2-} and II^{1-}) was not pursued.

The successive spectra for $[\text{Ir}(\text{bpy})_3]^{3+/2+/+/0}$ show crucial features in common with those for the ruthenium series. We see progressive growth of bands characterizing bpy^- and matching loss of the bpy^0 bands as the system is further reduced. A striking feature of Figure 1 is the maintenance of a pseudoisosbestic point relating four independent species. Thus, throughout the course of these reductions only the net interconversion of effectively isolated $\text{Ir}^{\text{III}}(\text{bpy}^0)$ and $\text{Ir}^{\text{III}}(\text{bpy}^-)$ chromophores is detected. This unequivocal observation justifies the consideration of extinction coefficients *per* ligand chromophore (see below) and establishes that the complexes should be formulated as shown in Table I. Assignment of

(1) Heath, G. A.; Yellowlees, L. J.; Brateman, P. S. *J. Chem. Soc., Chem. Commun.* 1981, 287. Elsewhere,^{1,4,10} we have used symbols differently for such redox sequences, e.g., I , I^- , I^{2-} , I^{3-} for $[\text{Ru}(\text{bpy})_3]^{3+/2+/+/0}$, respectively.

(2) (a) Elliot, C. M.; Hershenhart, E. *J. Am. Chem. Soc.* 1982, 104, 7519. (b) Bugnon, P.; Hester, R. E., personal communication.

(3) Kahl, J. L.; Hanck, K. W.; DeArmond, K. *J. Phys. Chem.* 1978, 82, 540.

(4) DeArmond, M. K.; Carlin, C. M.; Huang, W. L. *Inorg. Chem.* 1980, 19, 62.

Table I. Absorption Spectra of Tris(bipyridyl) Complexes of Ruthenium(II) and Iridium(III): $\nu/10^3 \text{ cm}^{-1}$ ($\epsilon/10^4 \text{ L mol}^{-1} \text{ cm}^{-1}$)

complex	transitions					
	$\pi \rightarrow \pi^*, \text{bpy}^0$	$L \rightarrow \text{MCT}, \text{bpy}^-$	$\pi \rightarrow \pi^*, \text{bpy}^-$	$M \rightarrow L, \text{bpy}^0$	$\pi \rightarrow \pi^*, \text{bpy}^-$	$\pi \rightarrow \pi^*, \text{bpy}^-$
$[\text{Ru}^{\text{II}}(\text{bpy}^0)_3]^{2+} (\text{I}^{2+})$	35.0 (7.06)			22.1 (1.37)		
$[\text{Ru}^{\text{II}}(\text{bpy}^0)_2(\text{bpy}^-)]^+ (\text{I}^+)$	34.2 (5.12)		29.2 (1.74)	21.1 (1.25)	19.9 (1.35)	13.0 (0.09)
					18.9 (1.28)	11.5 (0.10)
						10.2 (0.09)
$[\text{Ru}^{\text{II}}(\text{bpy}^0)(\text{bpy}^-)_2]^0 (\text{I}^0)$	33.8 (4.00)		29.0 (2.50)	20.8 (sh)	19.5 (1.48)	12.9 (0.16)
					18.4 (1.46)	11.4 (0.19)
						10.1 (0.18)
$[\text{Ru}^{\text{II}}(\text{bpy}^-)_3]^- (\text{I}^-)$			29.8 (3.82)		18.9 (1.56)	11.1 (0.26)
					18.0 (1.58)	9.9 (0.27)
$[\text{Ir}^{\text{III}}(\text{bpy}^0)_3]^{3+} (\text{II}^{3+})$	32.2 (4.50)					
$[\text{Ir}^{\text{III}}(\text{bpy}^0)_2(\text{bpy}^-)]^{2+} (\text{II}^{2+})$	32.5 (3.89)	obscured	25.6 (1.44)		22.2 (0.46)	13.4 (0.07)
					20.4 (0.44)	12.2 (0.08)
						10.8 (0.08)
$[\text{Ir}^{\text{III}}(\text{bpy}^0)(\text{bpy}^-)_2]^+ (\text{II}^+)$	32.8 (3.66)	28.6 (1.79)	25.4 (2.18)		22.0 (0.79)	13.1 (0.13)
					10.0 (0.83)	12.0 (0.16)
						10.7 (0.16)
$[\text{Ir}^{\text{III}}(\text{bpy}^-)_3]^0 (\text{II}^0)$		27.2 (2.51)	25.4 (2.54)		21.9 (1.04)	13.1 (0.19)
					19.6 (1.22)	11.9 (0.24)
						10.7 (0.23)

the various absorption bands follows directly from this. Table I also gives the absorption spectral data for the ruthenium series, including complete hitherto unpublished results for the near-infrared bands.

The visible spectral region around $20\,000 \text{ cm}^{-1}$ is indeed much simplified in the iridium complexes, compared to that of the corresponding (isoelectronic) ruthenium systems, because of the absence of a MLCT band. The growth of the visible $\pi\pi^*$ bpy^- band upon reduction of II^{3+} is unambiguous, and the progression in intensity may be readily quantified. The measured extinction coefficient of the band at $20\,000 \text{ cm}^{-1}$ for $[\text{Ir}(\text{bpy}^0)_2(\text{bpy}^-)]^{2+}$ (II^{2+}) compares well with the similar absorption in $\text{Na}^+ \text{bpy}^-$,⁵ and increases linearly from II^{2+} to II^0 .

The higher energy $\pi\pi^*$ bpy^- band observed here at $25\,500 \text{ cm}^{-1}$ is sharp and strongly resembles the analogous band in $\text{Na}^+ \text{bpy}^-$.⁵ This is in accord with our earlier suggestion that the corresponding absorption in $[\text{Ru}(\text{bpy})_3]^{+2/0-}$, which is considerably broadened, includes a $M \rightarrow L$ (bpy^-) transition.¹

The near-infrared band also increases linearly in strength according to the number of bpy^- ligands. The values of the extinction coefficients per reduced ligand agree closely with those for $\text{Na}^+ \text{bpy}^-$ and for the ruthenium complexes, as does the structure within the band itself.

The simultaneous presence of discrete bpy^0 and bpy^- ligands in II^{2+} and II^+ should be directly demonstrated by ligand-ligand intervalence charge-transfer (IVCT) transitions, as identified in isoelectronic I^+ and I^0 .⁶ We have confirmed that such a band is present in the absorption spectra of II^{2+} ($\nu = 3840 \text{ cm}^{-1}$, $\epsilon = 170 \text{ L mol}^{-1} \text{ cm}^{-1}$) and II^+ ($\nu = 3840 \text{ cm}^{-1}$, $\epsilon = 300 \text{ L mol}^{-1} \text{ cm}^{-1}$) in *N,N*-dimethylformamide and acetonitrile, but absent as expected in II^{3+} and II^0 , which contain only bpy^0 and bpy^- ligands, respectively.

The series II^{3+} to II^0 , like the series I^{2+} to I^- , is best described by the localized model. The iridium system in fact clarifies the visible and near-ultraviolet spectra as there are no low-energy charge-transfer bands to mask the bpy^- transitions. These observations put beyond doubt the character of the re^3x -active orbitals of these and many other d^6 bipyridyl complexes. Electrons entering such orbitals are effectively trapped on the individual ligands, with negligible communication between the neighboring chelate rings. The thermal barrier to transposition of the electron is calculated to be approximately 1000 cm^{-1} ($1/4 h\nu_{\text{IVCT}}$).⁷

These spectroelectrochemical studies establish general diagnostic criteria for the presence of coordinated bpy^- . Exact band positions will depend on the central metal charge and on the nature of the accompanying ligands, but complexes thought to contain reduced, charge-localized, bipyridyl ligands must show (i) a near-infrared band near $10\,000 \text{ cm}^{-1}$ containing three peaks (or shoulders) separated by approximately 1000 cm^{-1} ($\epsilon \sim 10^3/\text{ligand}$), (ii) a visible doublet band near $20\,000 \text{ cm}^{-1}$ ($\epsilon \sim 5 \times 10^3/\text{ligand}$), and (iii) a near-ultraviolet band near $25\,000 \text{ cm}^{-1}$ ($\epsilon \sim 15 \times 10^3/\text{ligand}$). For example, the rich absorption spectra⁵ of the series $[\text{Fe}(\text{bpy})_3]^{2+/+/-}$ may be fully analyzed in terms of the familiar pattern of localized ligand-based reductions. In contrast, Schwarz and Creutz recently employed these criteria explicitly to establish that under pulse radiolysis $[\text{Rh}(\text{bpy})_3]^{3+}$ is reduced to unstable $[\text{Rh}^{\text{II}}(\text{bpy}^0)_3]^{2+}$, rather than $[\text{Rh}^{\text{III}}(\text{bpy}^0)_2(\text{bpy}^-)]^{2+}$.⁸

It is notable that I^+ and II^{2+} are strictly analogous, with a common $M(d\pi^6)/(\text{bpy}^0)_2(\text{bpy}^-)$ configuration, whereas the optically excited states I^* and II^* differ fundamentally. Metal-centered oxidations of $[\text{Ru}(\text{bpy})_3]^{3+}$ and $[\text{Os}(\text{bpy})_3]^{2+}$ occur at modest potentials, but oxidation of $[\text{Ir}(\text{bpy})_3]^{3+}$ is inaccessible due to the increased core charge on iridium. Thus the additional nuclear proton drastically lowers the d-orbital manifold (more than the increased central ion charge stabilizes the ligand levels) so that in II^{3+} and II^* the $d\pi$ -levels fall below the ligand HOMO level. The contrasting natures of the equilibrated I^* and II^* states (MLCT and $L\pi\pi^*$, respectively) are confirmed by photoemission spectroscopy.⁹

Much attention focuses on I^* since $[\text{Ru}(\text{bpy})_3]^{3+}$ has been widely discussed as a prototype dye for photovoltaic cells. Flash photolysis absorption spectra^{10,11} and resonance Raman studies¹² on I^* establish independently that an asymmetric charge distribution applies to the emitting state, I^* , as well, viz. $^*[\text{Ru}^{\text{III}}(\text{bpy}^0)_2(\text{bpy}^-)]^{2+}$. Electrode potential correlations for numerous tris(bipyridyl)metalates have demonstrated that the ligand-orbital energies are strongly determined by central ion valency and surprisingly insensitive to d^n population.¹³ Thus, in some respects $[\text{Ir}^{\text{III}}(\text{bpy}^0)_2(\text{bpy}^-)]^{2+}$ provides a better electronic structural model than $[\text{Ru}^{\text{II}}(\text{bpy}^0)_2(\text{bpy}^-)]^+$ for the ligand array in I^* .

(8) Schwarz, H. A.; Creutz, C. *Inorg. Chem.* 1983, 22, 707.

(9) DeArmond, M. K.; Carlin, C. M. *Coord. Chem. Rev.* 1981, 36, 325.

(10) Braterman, P. S.; Harriman, A.; Heath, G. A.; Yellowlees, L. J. *J. Chem. Soc., Dalton, Trans.* 1983, 1801.

(11) Lachish, U.; Infelta, P. P.; Gratzel, M. *Chem. Phys. Lett.* 1979, 62, 317.

(12) Bradley, P. G.; Kress, N.; Hornberger, B. A.; Dallinger, R. F.; Woodruff, W. H. *J. Am. Chem. Soc.* 1981, 103, 7441.

(13) Heath, G. A.; Yellowlees, L. J. to be submitted for publication.

(5) Mahon, C.; Reynolds, W. L. *Inorg. Chem.* 1967, 6, 1297.

(6) Heath, G. A.; Yellowlees, L. J.; Braterman, P. S. *Chem. Phys. Lett.* 1982, 92, 646.

(7) Hush, N. S. *Prog. Inorg. Chem.* 1967, 8, 391.

Experimental Section

$[\text{Ir}(\text{bpy})_3](\text{BF}_4)_3$ was prepared by following a published method for $[\text{Ir}(\text{bpy})_3](\text{NO}_3)_3$,¹⁴ except that fluoroboric acid replaced nitric acid in the later stages, and the compound was then chromatographed repeatedly on Sephadex LH-20 as previously described.¹⁵ The analytically pure product (λ_{max} 32 200 cm^{-1} , $\epsilon = 4.5 \times 10^4 \text{ L mol}^{-1} \text{ cm}^{-1}$), was checked by voltammetry (group of three equally intense reductions) and ^{13}C NMR (five resonances only) and showed no trace of the very common and persistent byproduct "hydroxytris(bipyridyl)iridium(III)"¹⁶ ($\lambda_{\text{max}} = 32\,500 \text{ cm}^{-1}$, $\epsilon = 3.6 \times 10^4 \text{ L mol}^{-1} \text{ cm}^{-1}$) or any other impurity.

Spectroelectrochemical data were collected as before,^{1,6} by using a Metrohm E506 potentiostat and an OTTLE cell located directly in the beam of a Beckman 5270 spectrophotometer.

Acknowledgment. We thank Napier College of Commerce and Technology, Edinburgh, for access to this spectrometer, Johnson Matthey for a generous loan of iridium salts, and the SERC for financial support.

Registry No. Ir^{3+} , 16788-86-6; Ir^{2+} , 71818-70-7; Ir^+ , 91549-50-7; Ir^0 , 91549-51-8.

- (14) Flynn, G. M.; Demas, J. N. *J. Am. Chem. Soc.* 1974, 96, 1959.
 (15) Kahl, J. L.; Hanck, K.; DeArmond, K. *J. Inorg. Nucl. Chem.* 1979, 41, 495.
 (16) (a) Nord, G.; Hazell, A. C.; Hazell, R. G.; Farver, O. *Inorg. Chem.* 1983, 22, 3429. (b) Braterman, P. S.; Heath, G. A.; MacKenzie, A. J.; Noble, B. C.; Peacock, R. D.; Yellowlees, L. *J. Inorg. Chem.*, following paper in this issue.

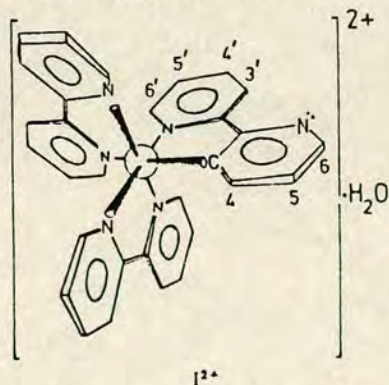
Contribution from the Departments of Chemistry, University of Glasgow, Glasgow G12 8QQ, U.K., and University of Edinburgh, Edinburgh EH9 3JJ, U.K.

Solution Structure and Properties of the (2,2'-Bipyridinyl- C^3, N)bis(2,2'-bipyridine- N, N')iridium(III) Hydrate Ion, "Pseudo- $[\text{Ir}(\text{bpy})_3(\text{OH})]^{2+}$ "

Paul S. Braterman,[†] Graham A. Heath,^{*†} Alan J. MacKenzie,[†] Brian C. Noble,[†] Robert D. Peacock,^{*†} and Lesley J. Yellowlees[†]

Received August 8, 1983

We report here comprehensive spectroscopic and electrochemical evidence that the pseudo-hydroxytris(2,2'-bipyridine)iridium(III) dication (Ir^{2+}) should be formulated with a 2,2'-bipyridinyl(1-)- C^3, N' ligand.



The species " $[\text{Ir}(\text{bpy})_3 \cdot \text{H}_2\text{O}]^{3+}$ " (Ir-H^{3+}) has properties very different from those of $[\text{Ir}(\text{bpy})_3]^{3+}$, including reversible deprotonation to Ir^{2+} .¹ Both coordinatively aquated (with one monodentate bpy) and "covalently hydrated" structures have

Table I. ^1H NMR Assignments for the C-Metalated Ring^{a,c}

solvent	H_4	H_5	H_6
$\text{Me}_2\text{SO}-d_6$	6.60	7.09	8.44
$\text{Me}_2\text{CO}-d_6$	6.85	7.10	8.47
$\text{MeOH}-d_4$	7.33	7.52	8.70

^a All δ values recorded at 360.13 MHz. ^b In MeOH , $J_{4,5} = 7.8$, $J_{5,6} = 5.3$, and $J_{4,6} = 1.3$ Hz. ^c Four further solvent-sensitive multiplets (at δ 7.66, 8.23, 8.37, and 8.73 in $\text{MeOH}-d_4$) complete the assignments to the unique ligand for H_4 , H_5 , H_6 , and H_7 , respectively.

been advanced.² Recently, however, Ir-H^{3+} was suggested with considerable insight to be related to $[\text{Ir}(\text{bpy})_3]^{3+}$ by rotation, ortho C-metalation (displacing H^+), and N-protonation of a single aromatic ring, accompanied by H-bonded association of H_2O .³

Uncertainties remain because of the following: (i) Exact Ir/o -phenanthroline analogues of Ir^{2+} and Ir-H^{3+} have been reported,⁴ although the suggested rearrangement is impossible for this rigid ligand. (ii) While the low-resolution X-ray data of Ir-H^{3+} establish that all three bipyridyl ligands are chelated and roughly planar, the identities of the donor atoms (N or C) are not clearly distinguished.³ Also the position of the presumed water molecule, on which the inference of C-metalation was based, is very poorly defined.^{3a} Thus, for example, C-metalation of two rings could not be excluded. (iii) Published ^1H and ^{13}C NMR spectra confirm low molecular symmetry but have not been satisfactorily assigned, even for salient features relating to the modified ligand.^{2,5}

The 200- and 300-MHz ^1H NMR spectra of Ir^{2+} (which we have studied as its BF_4^- salt) are complex, but the maximum number of 23 separately detectable aromatic resonances are observed. We find that systematic comparison in $\text{MeOH}-d_4$, $\text{Me}_2\text{CO}-d_6$, and $\text{Me}_2\text{SO}-d_6$ allows convincing identification of the doublet-of-doublet signals for each of the three protons in the uniquely attached ring (Figure 1a). These resonances are distinguished by their particular solvent sensitivity, presumably due to dipolar interactions of the neighboring uncoordinated nitrogen atom, and their mutual coupling is confirmed by double-resonance techniques (see Table I).

In the 90-MHz ^{13}C NMR spectrum of Ir^{2+} in $\text{Me}_2\text{SO}-d_6$ (Figure 1b,c), we find signals representing 30 nonequivalent carbon atoms. Most strikingly, in a spectroscopic mode specific for non-H-bearing carbon atoms,⁶ seven single resonances persist. Six of these resonances, in the range 154–162 ppm with respect to Me_4Si , correspond to the ring–ring bridging positions (cf. 155.7 ppm in $[\text{Ir}(\text{bpy})_3]^{3+}$), while the seventh, standing apart at 140 ppm, is clearly due to the unique, presumably iridium-bound, carbon atom.

Electrochemical studies provide new insight into the electronic nature of the complex. Cyclic voltammetry of Ir^{2+} in dimethyl sulfoxide or acetonitrile shows two closely spaced

- (1) Watts, R. J.; Harrington, J. S.; Van Houten, J. *J. Am. Chem. Soc.* 1977, 99, 2179.
 (2) Serpone, N.; Ponterini, G.; Jamieson, M. A.; Bolleta, F.; Maestri, M. *Coord. Chem. Rev.* 1983, 50, 209.
 (3) (a) Wickramasinghe, W. A.; Bird, P. H.; Serpone, N. *J. Chem. Soc., Chem. Commun.* 1981, 1284. (b) Nord, G.; Hazell, A. C.; Hazell, R. G.; Farver, O. *Inorg. Chem.* 1983, 22, 3429. This report of the X-ray crystal structure of Ir^{2+} itself, as the perchlorate hydrate salt, appeared after submission of our paper. Although donor atom identity must still be inferred from circumstantial evidence relating to the detailed molecular geometry, the new analysis clearly indicates the correctness of the proposal for Ir–C bonding put forward in ref 3a and the present work.
 (4) Kahl, J. L.; Hanck, K. W.; DeArmond, K. *J. Phys. Chem.* 1979, 83, 2611.
 (5) Kahl, J. L.; Hanck, K. W.; DeArmond, K. *J. Inorg. Nucl. Chem.* 1979, 41, 495.
 (6) The appropriate "quaternary-carbon-only" pulse sequence was suggested to the Edinburgh NMR laboratory by Dr. D. M. Doddrell of Griffith University, Queensland, Australia.

[†] University of Glasgow.
^{*} University of Edinburgh.

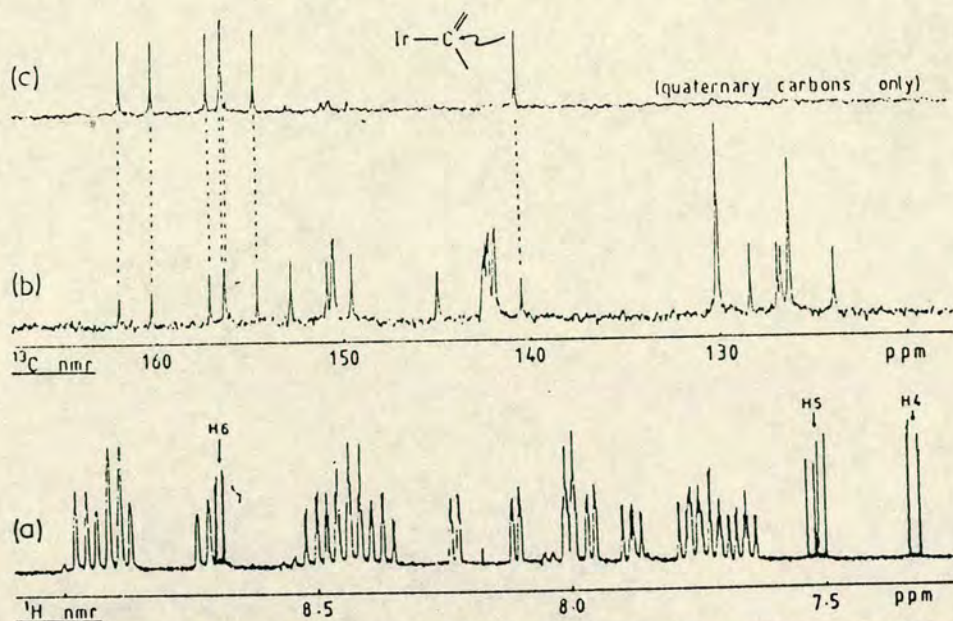


Figure 1. NMR spectra of Ir^{3+} in MeOH-d_4 : (a) ^1H spectrum (360.13 MHz; line sharpened); (b) proton-decoupled ^{13}C spectrum (90.56 MHz); (c) proton-decoupled ^{13}C spectrum (90.56 MHz) for quaternary carbons only.

reversible reduction waves at -1.03 and -1.23 vs. SCE and two further waves, reversible and quasireversible, at -1.86 and -2.21 V, respectively. These reductions, also reported by Kahl et al.,⁷ are characteristic of two and only two ordinary bipyridine ligands chelated to Ir(III) . Moreover, the measured electrode potentials imply⁸ the simultaneous presence of an effectively monoanionic neighboring ligand, represented by the chelated bipyridinyl group. Thus we note the first reduction potential is intermediate between that of $[\text{Ir}(\text{bpy})_3]^{3+}$ (-0.82 V) and $[\text{Ir}(\text{bpy})_2\text{Cl}]^+$ (-1.20 V), and the system is elegantly modeled by the further reductions of $[\text{Ir}(\text{bpy})_2(\text{bpy}^-)]^{2+}$ at -1.00 and -1.20 V. Ir^{2+} also shows a new irreversible two-electron oxidation wave ($E_p = +0.95$ V), which we associate with the C-metalated ligand. It should be noted that the voltammetric behavior of Ir^{2+} is in marked contrast with Kahl's $[\text{Ir}(\text{phen})_2(\text{phen}')(\text{OH})]^{2+}$ (where phen represents bidentate and phen' monodentate *o*-phenanthroline), for which three early reductions are reported.⁴

The electronic spectra of Ir^{2+} , Ir^+ , and Ir^0 have been compared by using an optically transparent thin-layer electrolysis cell. Ir^{2+} and Ir^+ (but not Ir^0) both show the well-known⁹ $\pi(6) \rightarrow \pi(7)$ transition of coordinated bpy around $33\,000\text{ cm}^{-1}$, with appropriately reduced intensity compared to $[\text{Ir}(\text{bpy})_3]^{3+}$.¹⁰ Equally, Ir^+ and Ir^0 (but not Ir^{2+}) show the characteristic absorptions of coordinated bpy^- near $11\,000$, $20\,000$, and $26\,000\text{ cm}^{-1}$ in accordance with the now familiar pattern of localized reductions in $(d\pi)^0$ bpy complexes.^{10,11} In addition, Ir^+ (but not Ir^0 or Ir^{2+}) shows a band at 5000 cm^{-1} ($\epsilon = 220\text{ mol}^{-1}\text{ dm}^3\text{ cm}^{-1}$) characteristic of ligand-ligand ($\text{bpy}^- \rightarrow \text{bpy}$) intervalence charge transfer.¹²

Ir^{2+} has been resolved into its optical isomers and shows an exciton couplet around $33\,000\text{ cm}^{-1}$ readily assigned to a *cis*- $\text{M}(\text{bipy})_2$ moiety.⁹ Reduction to Ir^0 , followed by reoxidation to Ir^{2+} , does not cause any loss of optical activity. These ob-

servations are, of course, consistent with successive ligand-based reductions at a kinetically inert Ir(III) center.

Collectively, these data demonstrate clearly that "pseudo- $[\text{Ir}(\text{bpy})_3(\text{OH})(\text{BF}_4)_2]$ " contains a deprotonated N,C-bound ligand that is indeed physically and electronically unique and remains distinct from the accompanying normal bipyridine ligands in nonaqueous solution.¹³

Acknowledgment. We thank Drs. D. Reed, D. R. Rycroft, and I. H. Sadler for their considerable contribution in recording the high-resolution NMR spectra, and G.A.H. acknowledges the generous loan of iridium salts by Johnson Matthey to support this work.

Registry No. $\text{Ir}^{2+}(\text{BF}_4)_2$, 91467-35-5; Ir^+ , 91467-36-6; Ir^0 , 91467-37-7.

- (13) New ^1H and ^{13}C NMR data for the related protonated species Ir-H^{3+} , viz. $[\text{Ir}(\text{bpy})_2(\text{C}_{10}\text{H}_8\text{N}_2)](\text{ClO}_4)_2$, have established the nature of Ir-H^{3+} : Spellane, P. J.; Watts, R. J.; Curtis, C. J. *Inorg. Chem.* 1983, 22, 4060.

(7) Kahl, J. L.; Hanck, K. W.; De Armand, K. *J. Phys. Chem.* 1978, 82, 540.

(8) Such structure/ E° correlations will be discussed in full elsewhere: Heath, G. A.; Yellowlees, L. J., manuscript in preparation.

(9) Mason, S. F. *Inorg. Chim. Acta Rev.* 1968, 2, 89.

(10) Coombe, V. T.; Heath, G. A.; MacKenzie, A. J.; Yellowlees, L. J., *Inorg. Chem.*, preceding paper in this issue.

(11) Heath, G. A.; Yellowlees, L. J.; Brateman, P. S. *J. Chem. Soc., Chem. Commun.* 1981, 287.

(12) Heath, G. A.; Yellowlees, L. J.; Brateman, P. S. *Chem. Phys. Lett.* 1982, 92, 646.